# OSTEOBLAST TRANSCRIPTOME AND FUNCTION OF EXTRACELLULAR MATRIX PROTEIN GENES IN SKELETAL FORMATION OF ZEBRAFISH

**RATISH RAMAN**

Thesis submitted in partial fulfilment of the requirements for the degree of Doctor of Philosophy in Sciences

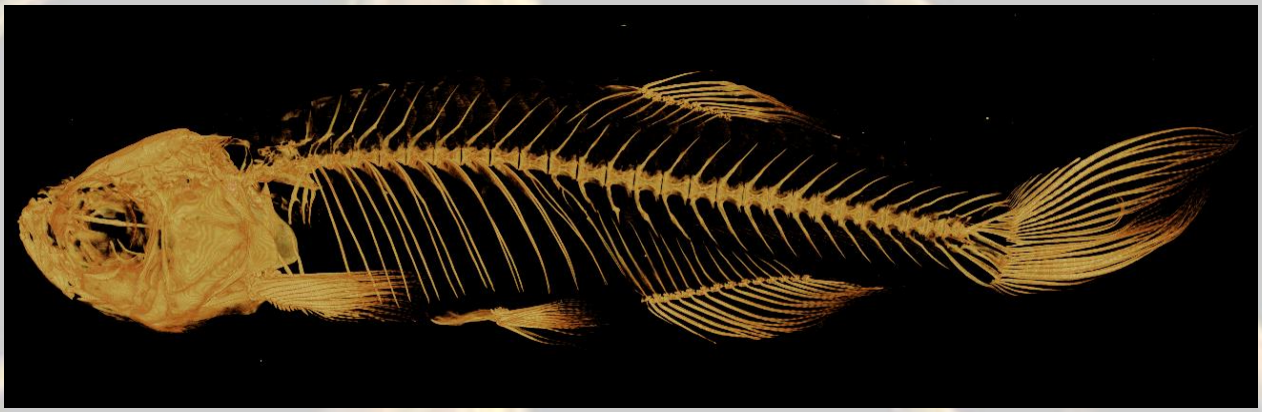

**Laboratory of Organogenesis and Regeneration**

**GIGA-Research Center**

**Faculty of Sciences**

**University of Liege**

**Supervised by: Dr. Marc Muller**

**Academic year 2023-2024**

H2020 Marie Sklodowska-Curie Actions Innovative Training Network No 766347

# OSTEOBLAST TRANSCRIPTOME AND FUNCTION OF EXTRACELLULAR MATRIX PROTEIN GENES IN SKELETAL FORMATION OF ZEBRAFISH

**RATISH RAMAN**

Thesis submitted in partial fulfilment of the requirements for the degree of Doctor of Philosophy in Sciences

Laboratory of Organogenesis and Regeneration

GIGA-Research Center

Faculty of Sciences

University of Liege

Supervised by: **Dr. Marc Muller**

Academic year 2023-2024

H2020 Marie Skłodowska-Curie Actions Innovative Training Network No 766347

# *SOURCE OF FUNDING*

H2020 Marie Sklodowska-Curie Actions Innovative Training Network No. 766347

# *COLLABORATORS*

H2020 Marie Skłodowska-Curie Actions Innovative Training Network No 766347

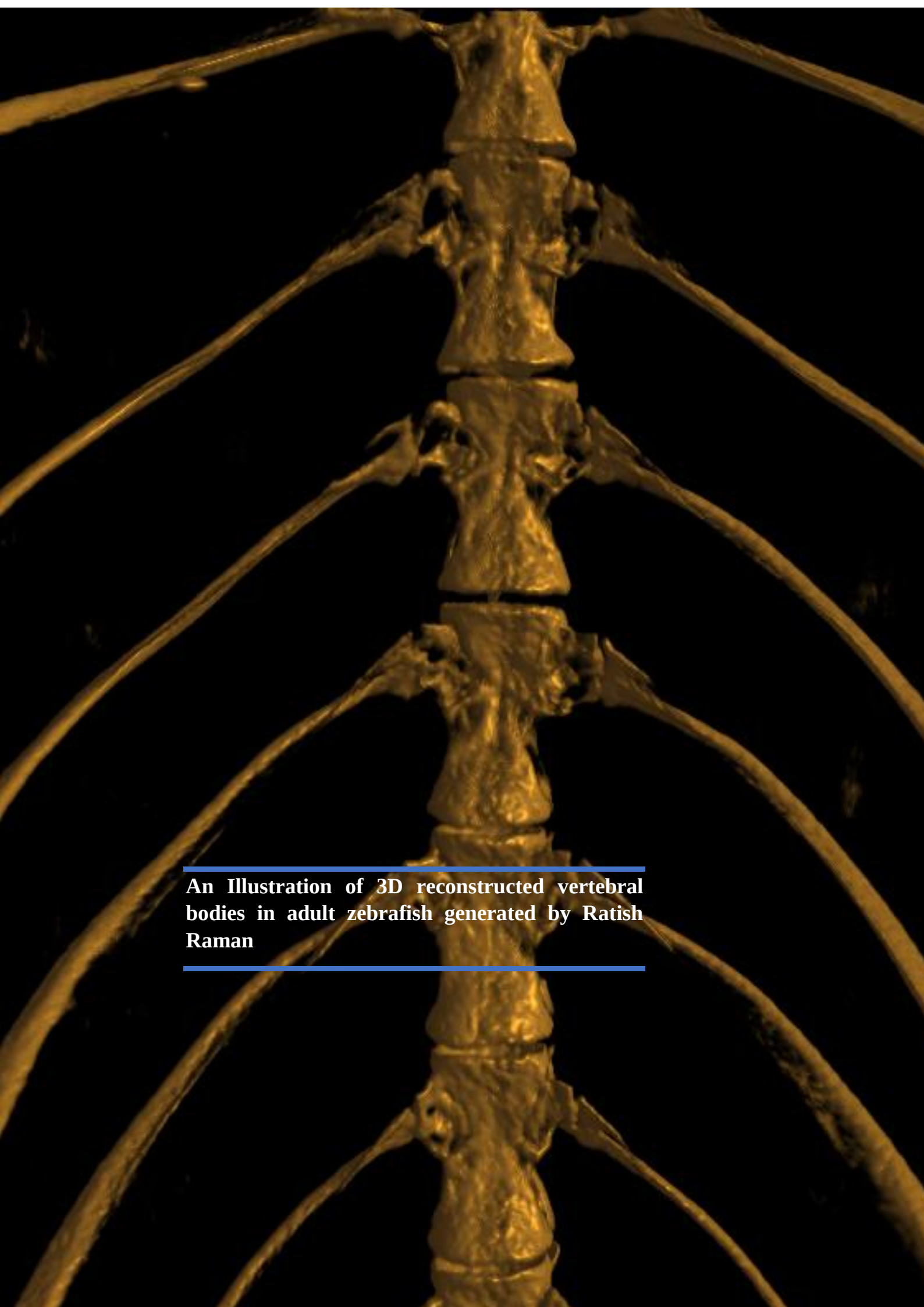

**An Illustration of 3D reconstructed vertebral bodies in adult zebrafish generated by Ratish Raman**

# *ACKNOWLEDGEMENTS*


## General Acknowledgements

I would like to thank all the members of the jury, Prof. Dequiedt, Prof. Gavaia, Prof. Tylzanowski, Dr. Peers, Pr. Dr. Henrotin, and Prof.Thiry for their guidance and evaluation of my work. Your kind advice helped me improve the quality of the present manuscript. I am truly grateful for your expertise and valuable time in assessing my thesis.

I also express my gratitude to the members of my thesis committee who followed my work through the years. Dr. Frederich, Dr. Peers, Pr. Dr. Henrotin, and Dr. Thiry, I thank you not only for your advice and guidance from the beginning of the thesis but also for your immense support.

I am grateful to Dr. Marc for giving me the opportunity to pursue my doctoral thesis in your laboratory. You have allowed me to work and evolve in a lab with a great atmosphere. Moreover, you taught me to work with a great model that is the zebrafish efficiently. I thank you for your guidance.

## Remerciements personnels

I would sincerely like to express my gratitude to all co-workers, co-authors, collaborators, and GIGA platforms who have helped me throughout my PhD and contributed to this work.

My first and very special vote of thanks and heartfelt gratitude goes to you, Marc, my supervisor/ promoter and true Doktorvater. I will be forever grateful that you selected me as an Early-Stage Researcher (ESR) to work in the MSCA-ITN project- "BioMedAqu" with you; you taught me so much in so many ways. Our interactions during late nights after research socials, a few of those have been thought provoking and inspiring to me where we have discussed science in detail that includes some key principles and concepts (do you remember the Kickoff Meeting at Gran Canaria – the night before the ESR presentation??). You have been a true scientific father to me, and especially during the COVID-19 pandemic when I wasn't able to see my family, you have been the source of strength and a beacon of hope. We developed a great understanding and rapport to work and discuss the project progress, skype was our friend then and continues to be even now. Apart from science, you have introduced me to rock music and our frequent visits along with lab colleagues to "SPIRIT OF 66" club will forever remain fresh in mind. I am also thankful that along with you, I got the opportunity to attend our BioMedAqu meetings and a few international conferences and above all you have also been very supportive of sending me to various international training courses outside of the BioMedAqu project that were helpful for my research topic. Observing you on how you interact with people from the scientific community or fellow professors, deal with collaborators and research partners, I have been able to establish and reinforce the faith on the art of being patient, smart, being kind, generous, being dedicated and hardworking, these qualities that are the virtues one must hold on to and never give up. Thank you for always being there and meeting me with open arms, always cheering me during my ups and downs, spreading your passion for Biochemistry and zebrafish development - skeletal research and toxicology, passing on your wisdom in science and life teachings, your interests in international politics and many more interesting facets that you possess, you have truly inspired me during my PhD journey all these years.

Thank you, Prof. Yves Henrotin, my co-supervisor for giving me the opportunity to work on the findings from your startup /spin off from University of Liege "ARTIALIS" that helped me to take forward the research to the best of my ability. Our many interactions that have been brief and short during my thesis committee or during WOODIES held in Brussels in 2019 to commemorate World Osteoarthritis Day or during BioMedAqu summer school Liege where you shared your valuable insights about scientific startups and spoke about how you started ARTIALIS were indeed insightful. I am indeed grateful to you.

Thank you so much Sing-E Lee, my project manager from the BioMedAqu project. I still remember very distinctly my first day of joining Marc's Lab -Laboratory of Organogenesis and Regeneration (LOR) and having tea together, which happened to be our thing every day. Both of us joined around the same time under Marc. Thank you for your great spirit not only at work but also during BBQ at your place or Christmas dinner or socials during BioMedAqu summer schools. You have been a source of immense joy and support. My sincere regards to your family -Thibault, kids: Ming and Sebastian who have greeted me always with a smiling "namaste" every time I have been at your place.

I would like to take this opportunity to thank my immediate lab colleagues from Laboratory of Organogenesis and Regeneration (LOR) for all the good times and for making wonderful memories that, would remain with me for the rest of my life.


My sincere thanks to our zebrafish facility manager Helen. You have always been there for me and helped me around in the lab when in need. My orientation to the zebrafish facility and lab, the know-how and getting around the facility with ease and confidence all of these wouldn't have been so smooth had it not be for you and your immense knowledge of working with zebrafish. Thank you so much once again.

Thank you also to the zebrafish group at GIGA the ZDDM, the amazing enthusiastic PI's Dr. Marianne Voz, Prof Bernard Peers and Dr. Isabelle Manfroid who have been such wonderful PIs and I am very fortunate to have got the chance to interact with you and work alongside your team members. I also had great time in interacting with Lydie Flasse and Stephanie Herkenne who joined in later as senior scientists and shared their experiences in research which was insightful. I would like to mention Jojo (small jordane), Virginie the two amazing technicians who were there during my initial phases when starting to work in the lab, thanks guys. My lab colleagues Renaud Nivelle, Dinh Duy Thanh, Jeremie Zappia, Claudio

Carril, My Hanh Tranh, Gustavo G.L, Laura M, Marco Morbidelli, Colin, Chiara G, Deborah, Blondie-Jordane, Caroline D, Ann-Sophie, Arnaud L, Anna Rosa Lopez, David B, Claudia and Alice, I would like to thank you for the wonderful times in the lab and for your valuable interactions and especially our Christmas Dinner with the zebrafish Groups and BMGG team that enriched my stay even more. I would like to say a big thank you to the team of Prof. Ingrid Struman, the Protein Team headed by Patricia for amazing time during meetings of BMGG lab organization or Christmas dinners or celebration of publications or grant application success and the valuable interactions during social gatherings that have been the most enriching experiences during my stay at GIGA Research Center. All of you are and were so friendly and approachable that I never felt out of place in reaching out to any one of you in need of assistance. Thank you so much to each and everyone.

I would like to extend my heartfelt thanks and gratitude to the Marie-Curie Project BioMedAqu and the team that includes my promoter who was also the coordinator for this project and the other PIs who are partners in this project for guiding all of us, sharing your expert knowledge in the field of skeletal biology and moulding all of us (ESRs). The experiences gathered during the summer schools that were organized, the trainings and the secondments have been instrumental in shaping me and all of us as an expert in the field of skeletal research whether in zebrafish and/or aquaculture thereby it has broadened my knowledge during this doctoral research project in the European Union Horizon 2020 funded MSCA-ITN project.


I would like to take this opportunity to thank Rajan Uncle who has been a mentor to me. He has held my hand and guided me through the most challenging phases of my career. To all the late nights where you have stood alongside me, had immense faith in me, you gave me the confidence when I had very little, you have answered the silliest questions and taught me basics of statistics. I would like to extend my heartfelt gratitude, thanks to you and Padma aunty. To all my teachers and Professors right from Kindergarten to 10th grade at Our Lady of Perpetual Succor High School (O.L.P.S.) to High School (11$^{TH}$ AND 12$^{TH}$ Grade) at S.K. Somaiya College to bachelor's at K.J. Somaiya College of Sci. & Comm. to master's at

Ramnarain Ruia College and summer internship at (BARC – Bhabha Atomic Research center), I wish to extend my sincere thanks to all of you. I wish to thank my course coordinator Lena Åslund at Uppsala University for Medical Masters with specialization in Molecular Medicine, to my batch mates, to the lab supervisors, to Lief Andersson for accepting me as a summer intern in his group, especially to my supervisor Mårten Larsson and my master's thesis supervisor Tatjana for all your guidance and support. I would like to convey my sincere thanks to Ivan Bedzhov at Max Planck Institute for Molecular Biomedicine for giving me an amazing research project to gain experience, for your valuable time, support and having immense faith in me.

My foundation, my pillar and my strength, that is my family. I wouldn't be here had it not been for the immediate 5 core members -My grandmother (paati) who means the world to me, amma (mom), appa (dad), Jyothi (aunt) and Chittapa (uncle) for providing me with the best of education and raising me to be a responsible human being. I am very thankful and grateful to all of you. To my relatives from both Maternal and Paternal side, I have represented all of you in a word art "Tree of Life" to convey how much you all mean to me. I have managed to include all names of the people belonging to the Mahadevan-Sundaram-Krishnamoorthy (MSK) family. I have to say a big thank you to each and every one of you, especially my cousins for being there for me during my troubled times and also during the most amazing / wonderful moments.

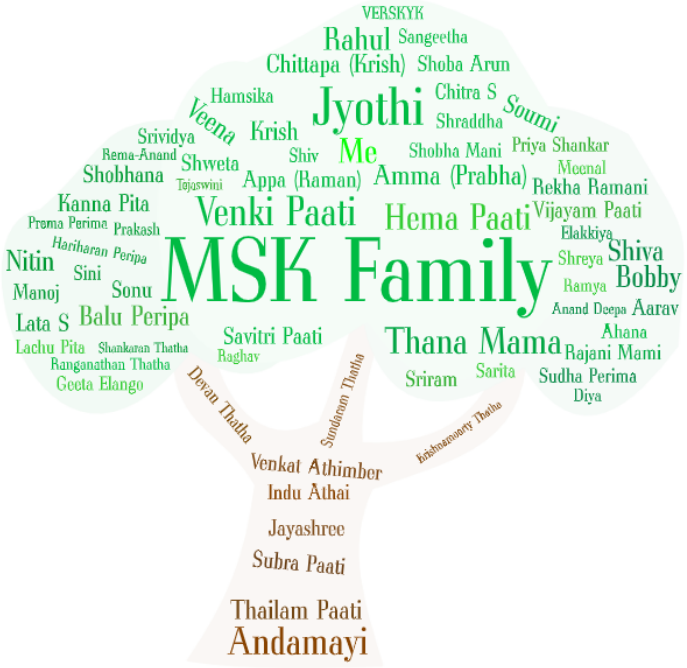

Growing up my mum and my aunt told me “Never forget your real friends for they are the ones who carry you through life”. This brings me to express my love and gratitude to my friends who are my lifeline. I would like to say a big thank you to all of you for putting up with me and never getting bored of me! – (ranting over failed experiments or sharing my dreams or wish during our gathering or even worse listening to my research work) haha xD I am joking…. Just as the interior of the ball is an intertwined meshwork that holds itself in place and shape, you all are my close-knit network without whom I wouldn’t be able to be the person I am. I will forever be grateful that you all have accepted me as who I am. I couldn’t have asked for anything better than this amazing friendship where you all are like a family to me and the mutual understanding that we all share. So, thank you all from the bottom of my heart.

I dedicate my thesis to my beloved grandmother, Smt. A.S. Venkitambal Sundaram.

For, each man can do best and excel in only that thing of which he is passionately fond, in which he believes, as I do, that he has the ability to do it, that he is in fact born and destined to do it….

-Dr. Homi Jehangir Bhabha

# Table of Contents

SUMMARY ..... 20

ABBREVIATIONS ..... 22

LIST OF PUBLICATIONS ..... 24

I. INTRODUCTION ..... 27

1. SKELETAL TISSUES ..... 29
1.1. Cartilage ..... 29
1.2. Bone Development ..... 32
1.3. Bone formation /Ossification; Different types of bones and ossification ..... 37
1.4. Factors affecting bone formation. ..... 41
2. THE ZEBRAFISH MODEL SYSTEM ..... 47

2.1. Cartilage and bone development in zebrafish ..... 49
2.2. Zebrafish Axial Skeleton ..... 57
3. TOOLS FOR STUDYING ZEBRAFISH SKELETOGENESIS ..... 62

3.1. Types of ossification in zebrafish and cell types. ..... 67
3.2. Mineralization of the bone matrix in zebrafish ..... 69
4. BMP SIGNALING ..... 71

5. OSTEOARTHRITIS (OA) ..... 74

5.1. Spinal OA ..... 77
5.2. Zebrafish model of OA ..... 79
6. BONE ECM PROTEINS AND THEIR IMPORTANCE ..... 80

6.1. Collagens ..... 81
6.2. Fibulins ..... 84

II. OBJECTIVES OF THIS STUDY ..... 91

III. RESULTS ..... 95

1. Osteoblast transcriptome and function of the ECM proteins Col10a1a and Fbln1. 97
2. Function of Efemp1 in zebrafish skeletal development: ..... 133
3. Effect of probiotics on skeletal development and health in the zebrafish model. 153

IV. DISCUSSION & CONCLUSIONS ..... 175

1. Various osteoblast populations in developing zebrafish. ..... 177
2. Inactivation of genes coding for extracellular matrix proteins. ..... 180
3. Col10a1a ..... 181
4. Fbln1 ..... 182
5. Efemp1 ..... 184
6. Dietary supplements for improving skeletal health. ..... 186

V. BIBLIOGRAPHY ..... 189

# *SUMMARY*

SUMMARY- ENGLISH

Osteoblast differentiation has been studied using a variety of systems, ranging from osteosarcoma cell lines to differentiating mesenchymal stem cells to KO mice, resulting in the description of a set of transcription factors and regulatory pathways that are involved in this process. Small teleost model systems like zebrafish are increasingly used to study vertebrate skeletal development and zebrafish mutants and transgenic lines are very useful models for studying human pathologies such as osteoporosis, osteopetrosis and osteoarthritis.

Understanding osteoblast differentiation and their function in bone matrix deposition and mineralization is central to the comprehension of bone development and of various bone pathologies. It is, therefore, crucial to not only follow the expression of some landmark transcription factors or extracellular matrix (ECM) proteins, but to also investigate the status of signalling pathways and factors regulating these processes. This can only be achieved by assessing the entire transcriptome of these cells. Zebrafish larvae offer the unique opportunity to directly access osteoblasts from the entire body without specific dissection. The aims are to study the osteoblast transcriptome of developing zebrafish and to investigate the role of the *efemp1*, *fbln1*, and *col10a1a* genes, coding for ECM proteins, in zebrafish skeletal development.

To gain insights into the mechanisms of osteoblast differentiation in the early development stage, we isolated cells from the transgenic reporter line *Tg(sp7:sp7-GFP)* at 4 days post-fertilization. Based on their differential GFP fluorescence, we identified two subpopulations of which we conducted transcriptomic profiling. Our data revealed that these two subpopulations are clearly distinct and that they differentially express many genes involved in skeletal development. The expression profile of these two populations clearly identifies them as osteoblastic cells, at present we consider the low fluorescence P1 population as pre-osteoblastic cells and the highly fluorescent P2 population as intermediate, functional osteoblasts.

ECM proteins are of crucial importance for cartilage and bone tissues. Based on their differential expression profile in these subpopulations, we generated mutants of the ECM protein coding genes *col10a1a*, *fbln1* and *efemp1* to examine their functions. Our results show that mutation of *col10a1a* results in decreased mineralization, while mutation of *fbln1* results in increased mineralization and a missing operculum. Mutation of *efemp1* results in increased mineralization and reduced intervertebral space, providing a model for spinal osteoarthritis. Furthermore, we investigated the effects of two probiotics on bone matrix synthesis and mineralization. We discovered that probiotic treatment is able to promote bone formation and to prevent the effects of inhibiting BMP signalling, with *Bacillus subtilis* being the more potent.

Collectively, these insights provide valuable cues that may contribute to improve understanding the roles of ECM proteins and probiotics in development, growth, and health of the bone skeleton.

RESUME-FRANCAIS

La différenciation des ostéoblastes a été étudiée à l'aide de divers modèles, allant des lignées cellulaires d'ostéosarcomes aux cellules souches mésenchymateuses jusqu'aux souris KO, aboutissant à la description d'un ensemble de facteurs de transcription et de voies de régulation impliqués dans ce processus. Des modèles de petits téléostéens, comme le poisson zèbre, sont de plus en plus utilisés pour étudier le développement du squelette des vertébrés, les mutants du poisson zèbre et les lignées transgéniques ce sont avérés très utiles pour étudier les pathologies humaines telles que l'ostéoporose, l'ostéopétrose ou l'arthrose.

Comprendre la différenciation des ostéoblastes et leur fonction dans le dépôt et la minéralisation de la matrice osseuse est essentiel à la compréhension du développement osseux et de diverses pathologies osseuses. Il est donc crucial non seulement de suivre l'expression de certains facteurs de transcription ou de protéines de la matrice extracellulaire (ECM), mais également d'étudier l'état des voies de signalisation et des facteurs régulant ces processus. Ceci ne peut être réalisé qu'en évaluant l'ensemble du transcriptome de ces cellules. Les larves de poisson zèbre offrent l'opportunité unique d'accéder directement aux ostéoblastes du corps entier sans dissection spécifique, car elles ne se différencient pas au sein de la moelle osseuse. Les objectifs sont d'étudier le transcriptome des ostéoblastes du poisson zèbre en développement et d'étudier le rôle des gènes *efemp1*, *fbln1* et *col10a1a*, codant pour des protéines de l'ECM, dans le développement du squelette du poisson zèbre.

Pour mieux comprendre les mécanismes de différenciation des ostéoblastes au début du développement, nous avons isolé des cellules de la lignée rapporteuse transgénique *Tg(sp7:sp7-GFP)* à 4 jours après la fécondation. Sur base de leur fluorescence GFP différentielle, nous avons identifié deux sous-populations dont nous avons effectué un profilage transcriptomique. Nos données ont révélé que ces deux sous-populations sont clairement distinctes et qu'elles expriment de manière différentielle de nombreux gènes impliqués dans le développement du squelette. Le profil d'expression de ces deux populations les identifie clairement comme des cellules ostéoblastiques. Nous considérons actuellement la population P1 à faible fluorescence comme des cellules précurseurs de type squelettique et la population P2 hautement fluorescente comme des ostéoblastes intermédiaires fonctionnels.

Les protéines ECM revêtent une importance cruciale pour les tissus cartilagineux et osseux. Sur base de leur profil d'expression différentielle dans ces sous-populations, nous avons généré des mutants des gènes codant pour les protéines ECM *col10a1a*, *fbln1* et *efemp1* afin d'examiner leurs fonctions. Nos résultats montrent que la mutation de *col10a1a* entraîne une diminution de la minéralisation, tandis que la mutation de *fbln1* entraîne une augmentation de la minéralisation et un opercule manquant. La mutation de *efemp1* entraîne une minéralisation accrue et une réduction de l'espace intervertébral, fournissant ainsi un modèle d'arthrose vertébrale. De plus, nous avons étudié les effets de deux probiotiques sur la synthèse et la minéralisation de la matrice osseuse. Nous avons découvert que le traitement probiotique est capable de favoriser la formation osseuse et de prévenir les effets de l'inhibition de la signalisation BMP, *Bacillus subtilis* étant le plus efficace.

Collectivement, ces informations fournissent des indices précieux qui peuvent contribuer à améliorer la compréhension du rôle des protéines de la matrice extracellulaire et des probiotiques dans le développement, de la croissance et de la santé du squelette osseux.

# *ABBREVIATIONS*

**A**

ALPL/alpl: alkaline phosphatase

AC: articular cartilage

ARS: Alizarin red staining

**B**

BMP/bmp: Bone Morphogenic protein

BMPR: Bone Morphogenic protein receptor

BMD: Bone Mineral Density

BSP: Bone Sialoprotein

**C**

Ca: Calcium

CNCC: Cranial Neural Crest Cells

COL/Col: Collagen

**D**

DAF-FM-DA: Diaminofluorescein-FM Diacetate

dpf: days post fertilization

**E**

ECM: extracellular matrix

EMT: Epithelial to Mesenchymal Transition

ERK pathway: extracellular

**F**

FGF/fgf: fibroblast growth factor

**G**

GAG: Glucosaminoglycans

GFP: green fluorescence protein

GH: growth hormone

**H**

Hh/hh: Hedgehog

hpf: hours post fertilization

**I**

IGF1: insulin like growth factor 1

Ihh/ihh: Indian hedgehog

IVD: intervertebral disc

IVL: intervertebral ligament

**J**

JNK: c-Jun N-terminal kinase

**M**

MAPK: mitogen-activated protein kinases

MMPs: matrix metall oproteinases

MO: morpholino

mg: miligram

mM: milimolar

mRNA: messenger ribonucleic acid

Mu/mu: mutant

m-CSF: macrophage colony stimulating factor

MSC: mesenchymal stem cell

**K**

KO: knockout

**N**

NCC: neural crest cell

ng: nanogram

NFK-β: nuclear factor kappa-light-chain enhancer of activated B cells

Nkx: NK homeobox

NSCs: notochord sheath cells

NO: nitric oxide

**O**

OA: osteoarthritis

Osx/osx: osterix

OCN - bone γ-carboxyglutamic acid

Protein or BGP

**P**

P: Phosphorus

Pdgf: Plateled derived growth factor

pg: picogram

PTH: Parathyroid hormone

**R**

RUNX2/runx2: Runt-Related Transcription Factor 2

RT-PCR: reverse transcriptase polymerase chain reaction

**S**

SCI: spinal cord injury

Smad: Mothers against decapentaplegic homolog

Shh: Sonic hedgehog

Sox: SRY (sex determining region Y) Box

Sp7: specific protein 7

**T**

Tcf: ternary complex factor

TH: Thyroid hormone

TGFβ/tgfβ: Transforming growth factor beta

TIMP/Timp: tissue inhibitors of metalloproteinase

TNAP: Tissue Nonspecific Alkaline Phosphatase

TMD: Tissue mineral density

**V**

VC: vacuolated cells

VL: Vertebral Length

V.Th: Vertebral Thickness

Vegf/vegf: vascular endothelial growth factor

**W**

WNT/wnt: Wingless-related integration site

wt: wild type

**#**

3D: three dimensions

µ-CT: micro-computed tomography

µg: microgram

# *LIST OF PUBLICATIONS*

The following is a list of works published during the course of the doctorate.

Publications issued from this thesis:

- **Osteoblast transcriptome in developing zebrafish and extracellular matrix proteins *Col10a1a* and *Fbln1* playing a key role in skeletal development and homeostasis.**

  **Ratish Raman**, Mishal Antony, Renaud Nivelle, Arnaud Lavergne, Jérémie Zappia, Gustavo Guerrero-Limon, Caroline Caetano da Silva, Priyanka Kumari, Jerry Maria Sojan, Christian Degueldre, Mohamed Bahri Ali, Agnes Ostertag, Corinne Collet, Martine Cohen-Solal, Alain Plenevaux, Yves Henrotin, Jörg Renn and Marc Muller. Biomolecules. 2024 Jan 23;14(2):139. doi: 10.3390/biom14020139. PMID: 38397376; PMCID: PMC10886564.

  Link: https://www.mdpi.com/2218-273X/14/2/139

- **A zebrafish mutant in the extracellular matrix protein gene *efemp1* as a model for spinal osteoarthritis.**

  **Ratish Raman**, Mohamed Ali Bahri, Christian Degueldre, Caroline Caetano da Silva, Christelle Sanchez, Agnes Ostertag, Corinne Collet, Martine Cohen-Solal, Alain Plenevaux, Yves Henrotin, and Marc Muller. Animals (Basel). 2023 Dec 24;14(1):74. doi: 10.3390/ani14010074. PMID: 38200805; PMCID: PMC10778253.

  Link: https://pubmed.ncbi.nlm.nih.gov/38200805/

- **Probiotics Enhance Bone Growth and Rescue BMP Inhibition: New Transgenic Zebrafish Lines to Study Bone Health.**

  **Ratish Raman***, **Jerry Maria Sojan***, Marc Muller, Oliana Carnevali and Jörg Renn. Int J Mol Sci. 2022 Apr 26;23(9):4748. doi: 10.3390/ijms23094748. PMID: 35563140; PMCID: PMC9102566.

  Link: https://pubmed.ncbi.nlm.nih.gov/35563140

  (*) both authors have equally contributed to this manuscript.

Additional co-authored publications:

- **wnt11f2 Zebrafish, an Animal Model for Development and New Insights in Bone Formation.**

  Caroline Caetano da Silva, Agnes Ostertag, **Ratish Raman**, Marc Muller, Martine Cohen-Solal and Corinne Collet. Zebrafish. 2023 Feb;20(1):1-9. doi: 10.1089/zeb.2022.0042. PMID: 36795617; PMCID: PMC9968865.
  Link: https://pubmed.ncbi.nlm.nih.gov/36795617/

- **Empirical Evaluation of Deep Learning Approaches for Landmark Detection in Fish Bioimages.**

  Navdeep Kumar, Claudia Di Biagio, Zachary Dellacqua, **Ratish Raman**, Arianna Martini, Clara Boglione, Marc Muller, Pierre Geurts and Raphaël Marée. In: Karlinsky, L., Michaeli, T., Nishino, K. (eds) Computer Vision – ECCV 2022 Workshops. ECCV 2022. Lecture Notes in Computer Science, vol 13804. Springer, Cham. https://doi.org/10.1007/978-3-031-25069-9_31
  Link: https://link.springer.com/chapter/10.1007/978-3-031-25069-9_31

- **WNT11, a new gene associated with early onset osteoporosis, is required for osteoblastogenesis.**

  Caroline Caetano da Silva, Thomas Edouard, Melanie Fradin, Marion Aubert-Mucca, Manon Ricquebourg, **Ratish Raman**, Jean Pierre Salles, Valérie Charon, Pascal Guggenbuhl, Marc Muller, Martine Cohen-Solal and Corinne Collet. Hum Mol Genet. 2022 May 19;31(10):1622-1634. doi: 10.1093/hmg/ddab349. PMID: 34875064; PMCID: PMC9122655.
  Link: https://pubmed.ncbi.nlm.nih.gov/34875064/

- **3D biomimetic platform reveals the first interactions of the embryo and the maternal blood vessels.**

  Niraimathi Govindasamy, Hongyan Long, Hyun-Woo Jeong, **Ratish Raman**, Burak Özcifci, Simone Probst, Sebastian J Arnold, Kristina Riehemann, Adrian Ranga, Ralf H Adams, Britta Trappmann and Ivan Bedzhov. Dev Cell. 2021 Dec 6;56(23):3276-3287.e8. doi: 10.1016/j.devcel.2021.10.014. Epub 2021 Nov 5. PMID: 34741805.
  Link: https://pubmed.ncbi.nlm.nih.gov/34741805/

# I. INTRODUCTION

# 1. SKELETAL TISSUES

The arrangement and distribution of cartilage, bones, and muscles that organize the musculoskeletal system take place during embryonic development. This system provides form, support, strength and movement to the body by integrating the following components: - skeletal tissue which provides structural support and forms the mechanical framework, while - muscular tissue generates force and - tendons transmit this force during muscle contraction to the skeleton (Murchison et al., 2007; Schilling et al., 1996b; Walker, 1991). Tendons and ligaments are dense, fibrous connective tissues where the former connects muscle to the bone while the latter connects bone to bone (Birk and Trelstad, 1986; Chen and Galloway, 2014). Therefore, together the bones, cartilage, muscles, joints, tendons, and ligaments make up the skeletal tissue. Both cartilage and bones are specialized connective tissues that are made of cells embedded within the extracellular matrix (ECM). The characteristic differences between the two tissues are defined by the cells, their nature and the varied proportion of components of their ECM (McKee et al., 2019).

## 1.1. Cartilage

Cartilage is formed from condensed mesenchyme that is mostly derived from the mesoderm germ layer. This process of forming cartilage is termed chondrification or chondrogenesis and the cells that form cartilage are called chondrocytes (Goldring, 2012a). Cartilage is a strong, semi-rigid supporting tissue that is avascular and can resist compression forces, making it flexible. The mechanical properties of this connective tissue are basically due to the water content that constitutes around 90%, along with the preponderance in the ECM of collagen fibers, elastic fibers, glycosaminoglycans (Asanbaeva et al., 2007) such as chondroitin sulphates, and proteoglycans. The predominant collagen present in the cartilage ECM is collagen type II, while the collagens type IX, X and XI are present in lower amounts (Boyan et al., 2018; Mayne, 1989). Cartilage is also present at the ends of the bones forming articular cartilage (AC) to form articulating surfaces, providing joints with low-friction, tough, durable, bearing material (Akkiraju and Nohe, 2015; Asanbaeva et al., 2007). It has been reported that cartilage has a very low turnover rate, resulting in an extremely low regenerative capacity of this connective tissue, making it difficult to repair and replace (Bielajew et al., 2020).

It has been quite a challenge to establish the link between the different types of cartilage that are present in vertebrates, as well as their varied molecular and biochemical aspects. Cartilage can be categorized into four kinds; matrix-rich cartilage, cell-rich cartilage, vesicular cartilage, and acellular cartilage, that might have evolved either independently or diversified from a single type of connective tissue (Cole and Hall, 2004). Histologically, there are three major types of cartilage, namely hyaline, elastic and fibrous /fibrocartilage found in mammals (**Fig. I-1**). They can be distinguished based on their physical characteristics and matrix components and can also be identified histologically (Parvizi and Kim K., 2010).

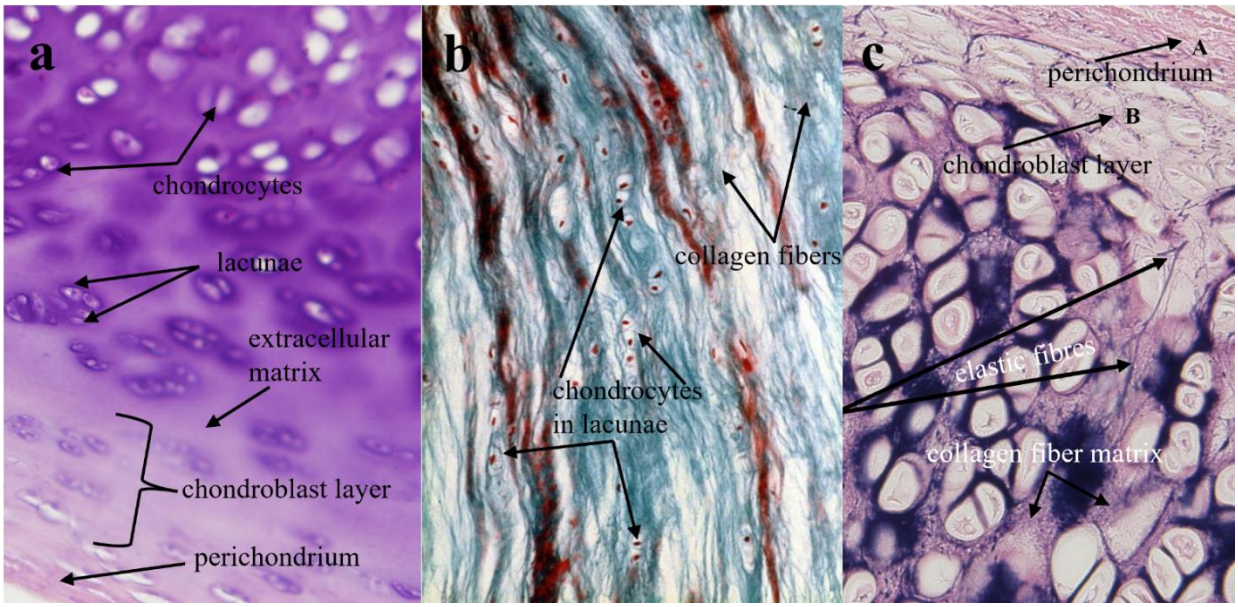


**Figure I-1. Histological sections of different types of cartilage tissues; hyaline, fibrous and elastic cartilage**. (a) Hyaline cartilage is distinguished by the presence of chondrocytes residing within lacunae and enveloped by an extracellular matrix. The chondrocytes exhibit a tendency to aggregate into isogenic clusters. (b) Fibrous cartilage is characterized by a substantial accumulation of collagen fibers, with chondrocytes residing within lacunae that are more extensively distributed. (c) Elastic cartilage is characterized by a substantial presence of elastic fibers within a collagen fiber matrix. Figure I-1a & c adapted from (https://cell.byu.edu/pdbio325-tissue-biology/hyaline-elastic-and-fibro-cartilage) and Figure I-1b adapted from (https://www.pinterest.com/pin/fibrocartilage-description-cells-in-fluidgel-matrix-function-supports-protects-absorbs-shock-location-between-bony--341288477996091100/).

Hyaline cartilage is the most predominant cartilage type found in the human body, it is mainly composed of isogenous chondrocytes or chondrones that are sitting in their lacunae, hydrated aggregates of proteoglycans, GAGs, extracellular fluid within the meshwork of collagen II, that is mostly covered by an outer fibrous membrane called perichondrium (**Fig. I-1a**). The main function of hyaline cartilage is to provide resistance against bending, compression, and impact. During embryogenesis and endochondral bone formation, hyaline cartilage is also known to serve as the precursor to bone. It is mostly found in the nasal septum, the epiphyseal growth plate, most ventral parts of the ribs, tracheal rings, and larynx. It can also be found in the lining of synovial joints in adult vertebrates (Hall, 2015).

Fibrous cartilage / fibrocartilage is the strongest type of cartilage in comparison to the other two types. It is primarily characterized by the presence of large amounts of thick and dense collagen type I and II fibrils along with alternating layers of hyaline cartilage matrix (**Fig. I-1b**). Fibrocartilage is found in intervertebral discs, costochondral joints, sacroiliac joints, pubic symphysis, meniscus and around tendons and ligaments (Maynard and Downes, 2019b).

Elastic cartilage consists of elastic fibers (made up of elastin and associated fibrils) that are woven into collagen fibrils, primarily collagen type II and aggregating proteoglycans in the cartilaginous matrix. They are also surrounded by a perichondrium (**Fig. I-1c**). It is found in the ear, especially in the pinna and eustachian tube, epiglottis and in the larynx. The

presence of high amounts of elastin provides elastic cartilage with structural support, elasticity, and flexibility in these tissues (Lee and Burke, 2021; Naumann et al., 2002).

The metabolic activities of chondrocytes are amended by many factors present within their chemical and mechanical environment. Among these, the most important factors are the pro-inflammatory cytokines and growth factors that have anabolic and catabolic effects and have a crucial role in the degradation and synthesis of matrix macromolecules that exert their effects on ECM metabolism (Fortier et al., 2011; Goldring et al., 2008; Kapoor et al., 2011). These growth factors and peptides, along with the chondrocytes are crucial in forming an arrangement that is often referred to as the template or "the cartilage anlage" required for the development of long bones (Pazzaglia et al., 2019), a process referred to as endochondral ossification (**Fig. I-2**).

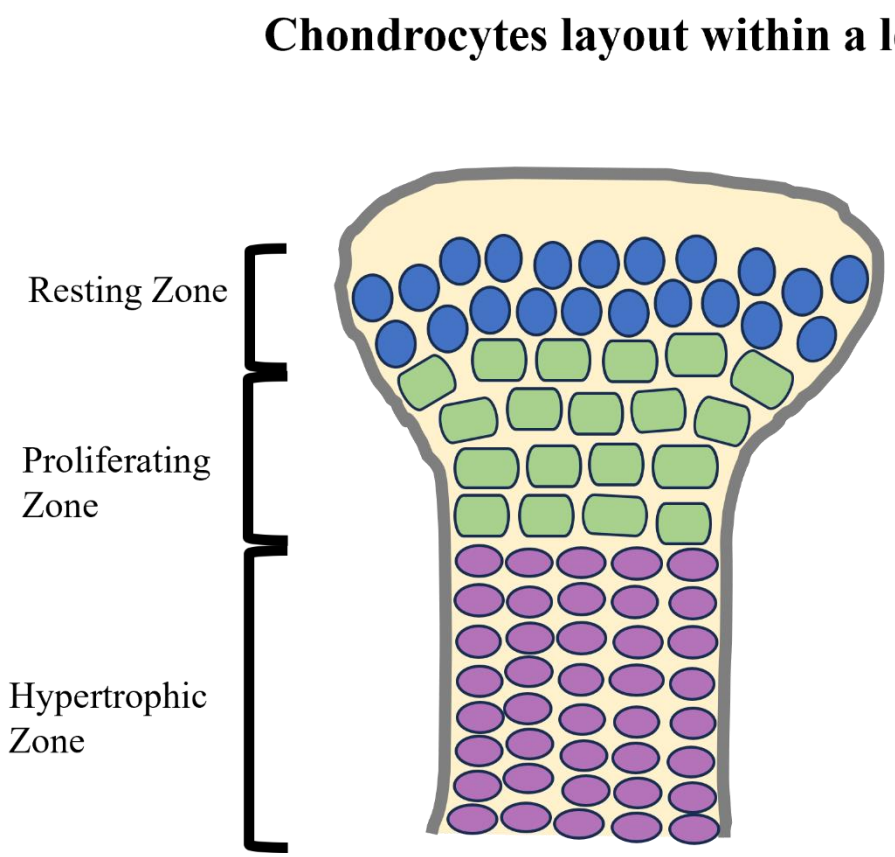


**Figure I-2 The layout of chondrocytes inside the long bone.** Simplified schematic representation showing the layout of chondrocytes in different zones inside the long bones (Chen et al., 2021).

The chondrocytes present at the center of the cartilage anlagen go through proliferation, followed by differentiation, hypertrophy or cell death, exclusive cell morphologies, and metabolic activities, as illustrated above in (**Fig. I-2**). The two mechanisms attributed to cartilage growth are interstitial growth and appositional growth (Asanbaeva et al., 2007; Myers and Ateshian, 2014). Interstitial growth is marked by cell division of the chondrocytes

followed by synthesis of the extracellular matrix and thereafter expansion of cartilage matrix from within the tissue, thus resulting in the increase in length. Appositional growth is identified by differentiation of chondroblasts or perichondral cells followed by synthesis of the extracellular matrix and expansion of the girth/width of the cartilage.

## 1.2. Bone Development

Unlike other tissues, bone is a unique type of connective tissue that is mineralized physiologically. The process of extracellular matrix deposition followed by mineralization is referred to as ossification or osteogenesis, resulting in a tissue that, in contrast to the cartilage, is a strong, vascular, and semi-rigid connective tissue which is termed as bone. Histologically, bone tissue is mainly divided into two types: compact bone and spongy bone (**Fig. I-3**). The compact bone exhibits a recurring arrangement of structural units known as osteons, which consist of concentric rings of lamellae encircling the central canal, commonly referred to as the Haversian canal. In contrast, spongy or cancellous bone is characterized by a reticular structure composed of numerous interconnected bony struts or a lacy network of bone, creating multiple tiny cavities that are occupied by marrow.

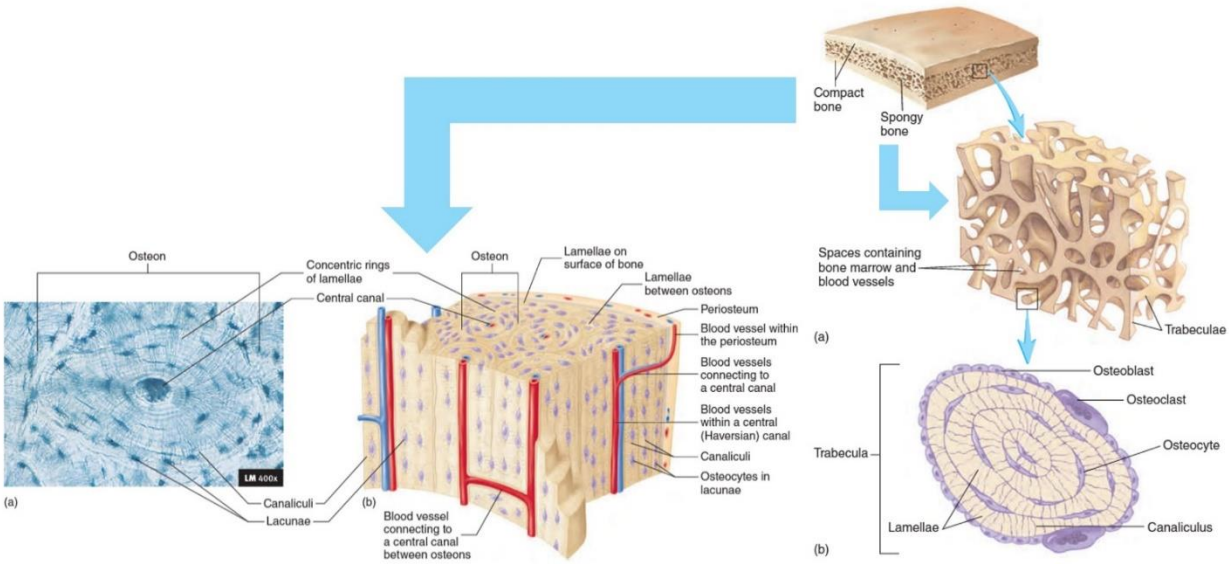


**Figure I-3. Types of Bone Tissue.** Bone is divided into two major types; compact bone and spongy bone. (https://arccwaite.files.wordpress.com/2018/12/seeleys-essentials-of-anatomy-and-physiology-9th-edition.pdf/chapter_6).

Bones are of great significance for the human body to provide skeletal support, form, strength (Birk and Trelstad, 1986), and movement to the body (Chen and Galloway, 2014), it serves as a home for hematopoiesis and a reservoir for calcium and other important minerals (de Baat et al., 2005). They are composed of cellular components, the mineralized matrix

component, and the nonmineralized matrix component. The cellular components of bone consist of three main cell types; bone forming cells (osteoblasts), bone resorbing cells (osteoclasts) and bone sensing cells (osteocytes) (**Fig. I-4**) (Mohamed, 2008), (Florencio-Silva et al., 2015).

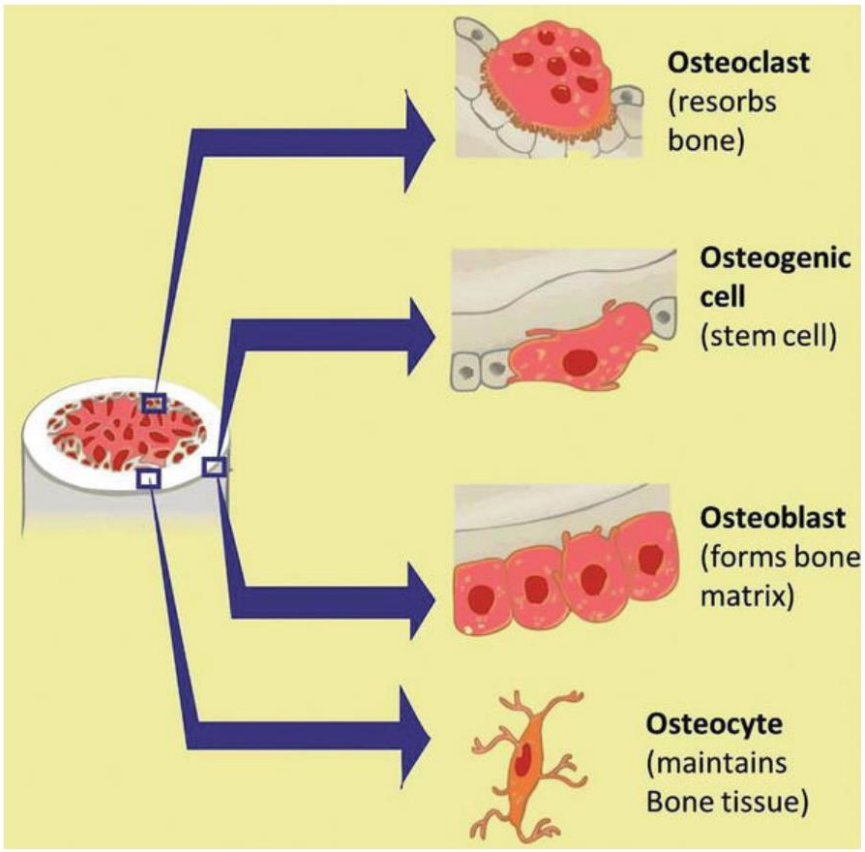


**Figure I-4. Cellular components of the bone.** Diagrammatic representation of cellular components that make up the bone. (https://www.intechopen.com/chapters/64747).

The bone extracellular matrix is mainly composed of type I collagen, along with other collagens and non-collagenous proteins such as osteocalcin (OCN=BGLAP), osteopontin (SPP1)(Malaval et al., 2008), osteonectin (SPARC) and alkaline phosphatase (Clarke, 2008). Once enmeshed into the bone ECM, osteoblasts cease dividing and eventually mature/differentiate into osteocytes that have a star-shaped morphology with extensions called canaliculi that assist in joining and interconnecting with neighboring osteocytes (Dallas et al., 2013). Thus, osteocytes serve as mechano-sensors and master regulators of bone remodeling by secreting factors that keep the activities of both osteoblasts and osteoclasts in check (Dallas et al., 2013).

### 1.2.1. Osteoblasts

Osteoblasts are bone forming cells that differentiate from pluripotent mesenchymal stem cells (MSCs) (in the bone marrow of long bones in mammals), going through a

maturation process where transcription factors like Osterix (SP7) and Runt related factor 2 (RUNX2) play actuating roles as reviewed by (Karsenty and Wagner, 2002)(see also below). The osteoblasts can be categorized into well-defined stages of increasing hierarchy based on their degree of specification towards the skeletal lineage; osteoprogenitors, preosteoblasts, committed osteoblasts and mature osteoblasts (**Fig. I-5**) (Florencio-Silva et al., 2015).

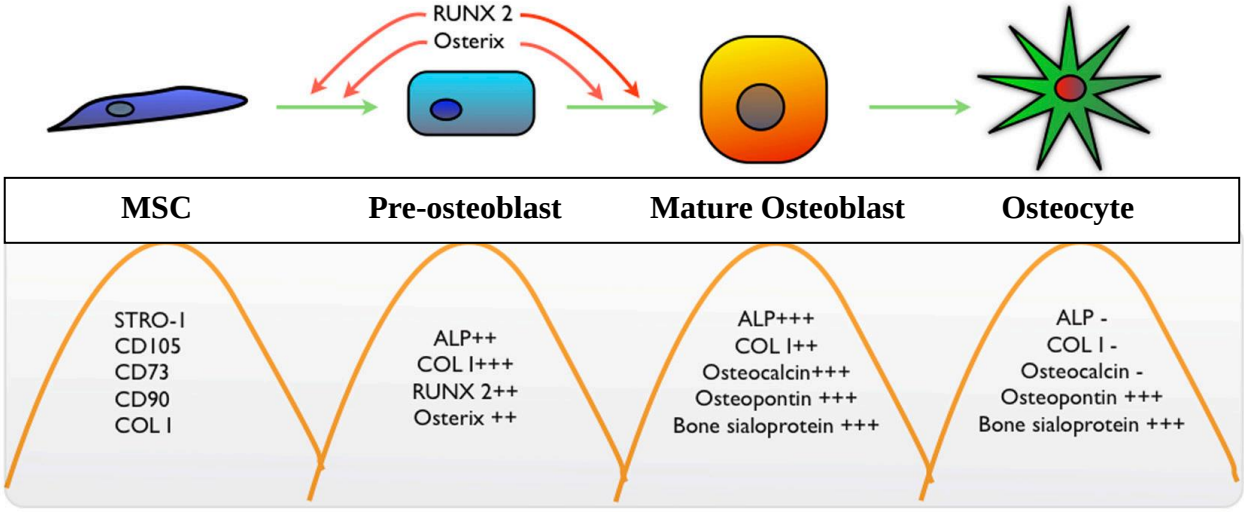


**Figure I-5. Overview of osteoblast differentiation pathways.** Simplified illustration depicting the key proteins that are expressed during osteoblast differentiation (Miron and Zhang, 2012).

The commitment to an osteoprogenitor cell fate is marked by the expression of the transcription factor SOX9 that also directs cell differentiation towards a chondrocyte cell fate (Lefebvre and Dvir-Ginzberg, 2017). The subsequent differentiation of osteoprogenitor cells to the preosteoblast cell lineage is characterized by the expression of RUNX2 in the osteoprogenitor cell (Bruderer et al., 2014; Komori, 2010). The subsequent expression of SP7/OSX in preosteoblasts signifies the commitment to form osteoblasts, as a result of WNT-β catenin signaling. It is the expression of SP7 and RUNX2 that defines the cell's commitment to form osteoblasts (Yoshida et al., 2012).

Ultimately, RUNX2 and SP7 induce the expression of alkaline phosphatase (ALPL), BGLAP, and bone sialoprotein (BSP), thus marking the cell's differentiation into a mature osteoblast (Schlesinger et al., 2020). These proteins are present on bone surfaces and are pledged to be very important for the deposition of the nonmineralized/unmineralized bone matrix called osteoid. The osteoid then eventually undergoes hardening by means of hydroxyapatite (inorganic salts of calcium and phosphate) deposition, thereby conferring stiffness and rigidity which help to withstand compression forces, and yet remain flexible (Franz-Odendaal et al., 2006; Schlesinger et al., 2020). This process of hardening is referred to as mineralization.

### 1.2.2. Osteoclasts

The process of forming osteoclasts is termed osteoclastogenesis. In contrast to osteoblasts, osteoclasts are multinucleated cells derived from hematopoietic stem cells and belong to the monocyte-macrophage lineage, that mature via the signaling by RANK-L and macrophage colony stimulating factor (M-CSF) (**Fig. I-6**) (Karsenty and Wagner, 2002).

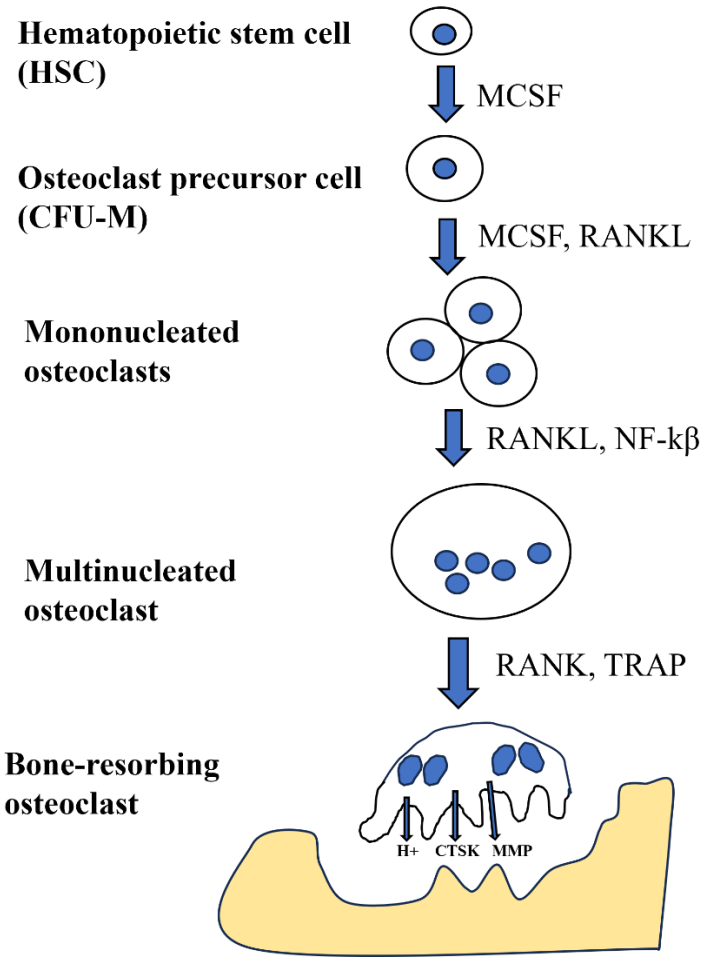


**Figure I-6. Schematic representation of osteoclastogenesis.**

Both proteins are generated by bone marrow stromal cells and by osteoblasts, M-CSF is required for osteoclast precursors to proliferate, while RANK-L is essential for differentiation of precursor osteoclast cells to mature osteoclasts (Nakamura et al., 2012). This cell type is basically responsible for degrading mineralized tissue that is termed as bone resorption. Bone resorption is a two-step process: initiation along with dissolution of the mineralized matrix, followed by enzymatic degradation of the organic matrix. The mechanism starts with the adhesion of the mature osteoclast to the mineralized bone matrix, leading to osteoclast activation and the formation of a tight-sealing zone that encloses the resorption lacuna (Chen et al., 2018). This zone encircles a membrane area/region that arises as the result of acidification and secretion of lysosomal and proteolytic enzymes (cathepsin K and matrix metalloproteinases) between the cell and the bone surface, thereby releasing the mineral

components (Calcium (Ca) and Phosphorus (P)) and digesting the organic matrix of the bone (Nakamura et al., 2012). Thus, the balance of bone formation to resorption is a tightly controlled program that ensures uniformity in bone mass regulated not only by osteocytes and osteoblasts but also physiologically regulated by factors such as osteoprotegerin (OPG) or interferon Gamma (IFN-γ) that inhibit RANK-L, thereby affecting osteoclast differentiation (**Fig. I-7**) (Dallas et al., 2013; Detsch and Boccaccini, 2015; Pirraco et al., 2010).

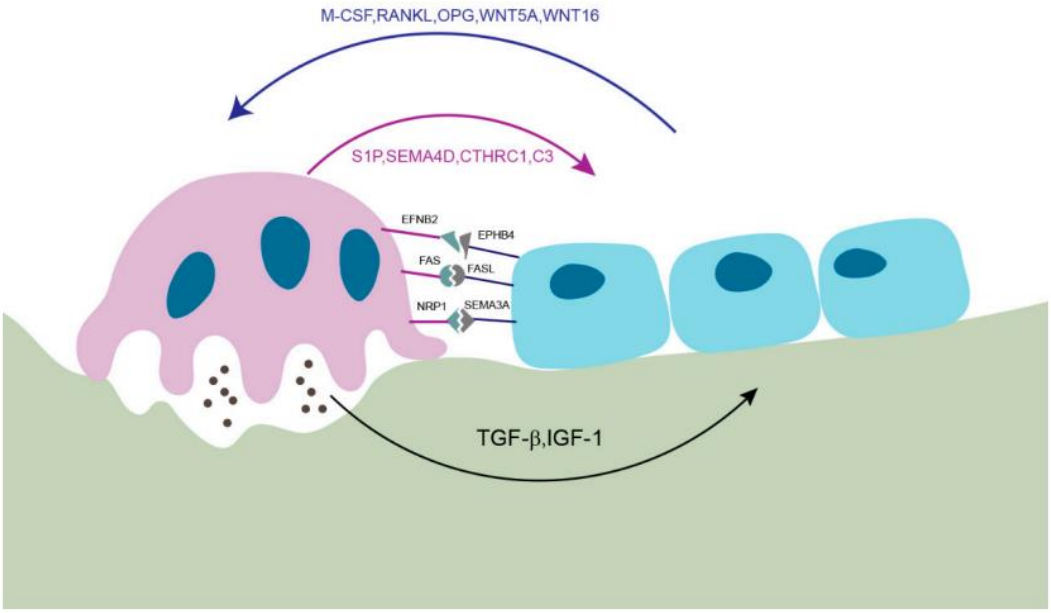


**Figure I-7. Interaction between osteoblast-osteoclast.** Scheme of bone remodeling, a dynamic process that involves osteoblast-osteoclast communications which are essential for bone remodeling during bone homeostasis. (Kim et al., 2020).

After the completion of bone resorption, the osteoclasts undergo apoptosis, usually triggered by high concentrations of extracellular calcium, Fas-ligand secreted by osteoblasts, the reduction of pro-survival cytokines including M-CSF and RANK-L, which have been indicated as a few of the possible mechanisms (**Fig. I-7**) (Chen et al., 2018; Clarke, 2008; Detsch and Boccaccini, 2015). Both osteoblasts and osteoclasts cooperate to actuate bone growth, thickness of the cortical layer and structural arrangement of the lamellae (Mohamed, 2008; VanPutte et al., 2013). The internal structure of the bone continues to change to meet the functional requirements, and these noticeable differences arise due to the activity of osteoclasts and osteoblasts. The balance between the activity of osteoblasts and osteoclasts is required for maintaining normal bone homeostasis (Setiawati and Rahardjo, 2008). However, this balance is skewed with age and in postmenopausal women, the osteoclast activity overtakes and surpasses the activity of osteoblasts, leading to an increased bone resorption and overall weaker, brittle bones as observed in osteoporosis.

## 1.3. Bone formation /Ossification; Different types of bones and ossification

Ossification/ bone formation is a highly regulated and complex process involving formation and maintenance of bone that can be divided into two major ways/types, namely intramembranous ossification and endochondral ossification (Akter and Ibanez, 2016; Cashman and Ginty, 2003; VanPutte et al., 2013).

### 1.3.1. Endochondral Ossification

Endochondral ossification occurs in vertebrates where bone tissue is formed from a cartilage intermediate (**Fig. I-8**). It is the main mechanism behind the bone growth in the long bones of the body, such as the femur, tibia, and humerus (Breeland et al., 2022)(**Fig. I-2**).

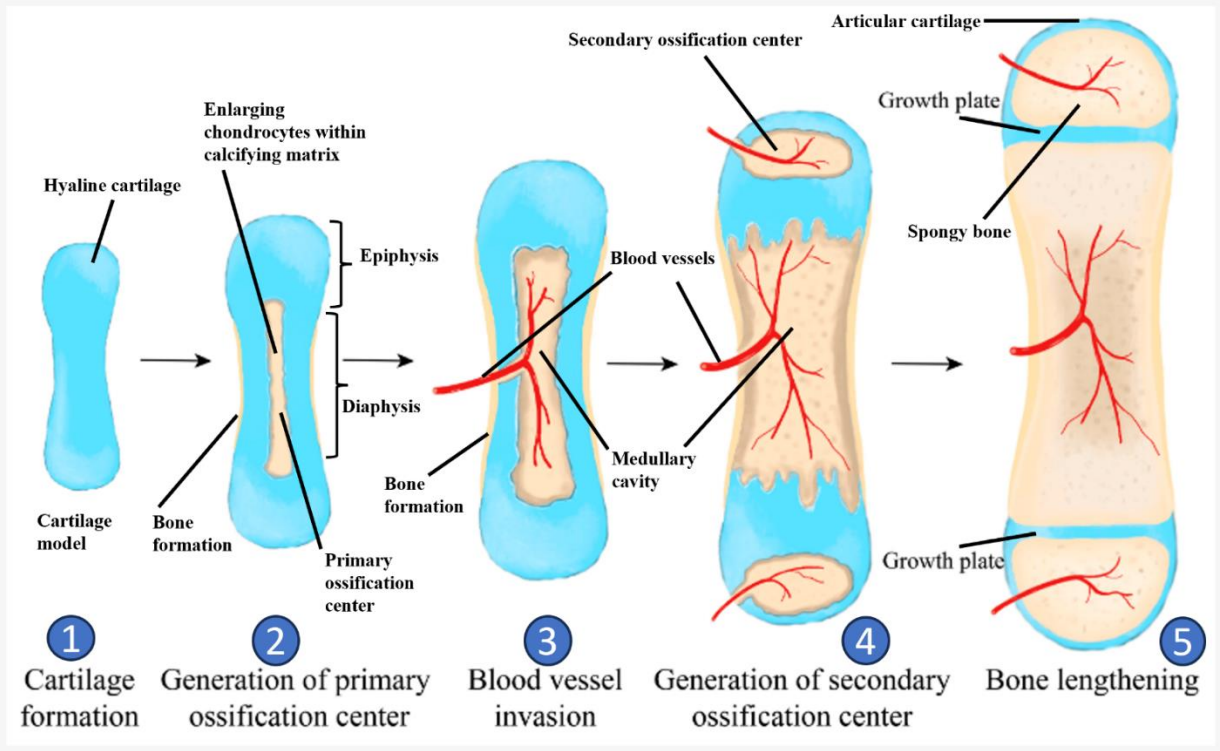


**Figure I-8. The stages of the endochondral ossification process in long bones.** 1. Bone collar is formed around a cartilaginous scaffold/model. 2. The degeneration of mature chondrocytes results in the formation of a perforated trabecula cavitation. 3. The infiltration of blood vessels and bone cells results in the process of mineralization and the formation of the primary ossification centers, located in the center of the bone. 4. In long bones, the secondary ossification centers are situated at the ends of the bone. The growth plates are situated between the epiphysis and metaphysis of long bones, hence facilitating longitudinal bone growth. 5. The first ossification step is completed. The figure is adapted from (Zhang et al., 2023).

Endochondral ossification begins during embryonic development, when a hyaline cartilage model is formed in the shape of the bone that will eventually form. This replacement of cartilage with mineralized bone tissue in long bones over time is an intricate process that is triggered by the differentiation of proliferating chondrocytes within the cartilage framework to a non-proliferative hypertrophic state (Kiernan et al., 2018). Depending upon the location of mineralization, it is categorized into two types; perichondral and endochondral ossification. Both endochondral and perichondral ossification are crucial for the development of long bones (Setiawati and Rahardjo, 2008). Perichondral ossification takes place at the outer edge of the cartilage model, usually inside the cartilage template that is present before the long bones are formed during embryonic development. This process entails the conversion of perichondrium, which is a compact layer of connective tissue that covers the cartilage, into an ossified ring enclosing the cartilage structure. The perichondrium harbors progenitor cells that undergo differentiation to give rise to osteoblasts secreting the bone matrix and giving rise to the periosteal bone collar, a covering of bone that surrounds the cartilage surface, as seen in **(Fig. I-9a)** (Kronenberg, 2003; Mackie et al., 2008). This is followed by invasion of osteoblast progenitors, osteoclasts, blood vessel endothelial cells and hematopoietic cells from the perichondrium into the hypertrophic cartilage. The hypertrophic chondrocytes are not resorbed as previously thought (Karaplis, 2008; Mackie et al., 2008), but rather they de-differentiate to later form trabecular osteoblasts, stromal cells, or adipocytes (Chagin and Chu, 2023; Haseeb et al., 2021). According to some estimates, up to 83% of intramedullary osteoblasts are believed to derive from chondrocytes, while about one-third to one-half of trabecular osteoblasts originate from chondrocytes (Long, 2022). Additional influx occurs of osteoblast progenitors that differentiate into trabecular bone-forming cells, while hematopoietic and endothelial cells establish bone marrow that forms a primary ossification center (POC), see **(Fig. I-9a)**. Thus, MSCs become osteoblasts via two modes of differentiation routes (Jing et al., 2017). The osteoblast progenitors differentiate into osteoblasts in the perichondrium to form cortical bone around the cartilage anlage (Aghajanian and Mohan, 2018). The primary ossification center expands during embryonic development and the establishment of secondary ossification centers (SOCs) **(Fig. I-9b)** takes place at one or both ends of the developing bone, thus resulting in the development of the epiphyseal growth plate cartilage accountable for longitudinal growth of the bones (long bones), see **(Fig. I-8 & 9b)** (Long and Ornitz, 2013).

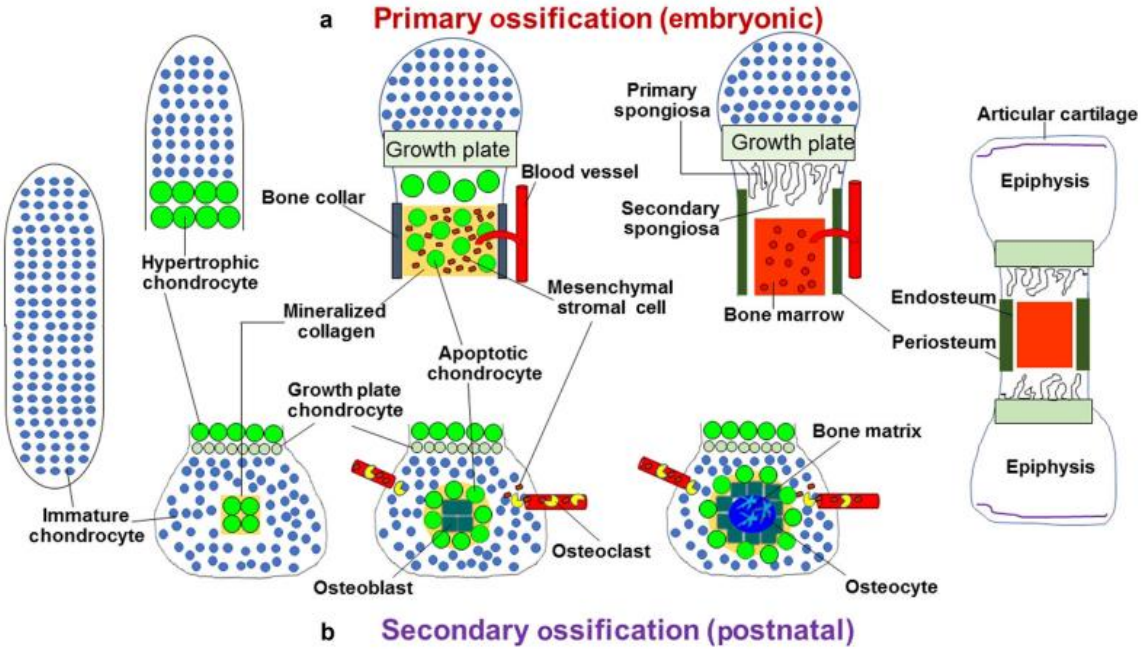


**Figure I-9.** Schematic representation of endochondral ossification process depicting the primary ossification and secondary ossification. Figure sourced from (Aghajanian and Mohan, 2018)

Secondary endochondral ossification proceeds very similarly as shown in **(Fig. I-9b)**. Primary and secondary ossification centers differ in terms of their timing. Following birth, secondary ossification initiates at post-natal in rodents on day 7–8 in the middle section of the bone and enlarges outwards contributing to expansion of bone width, while the primary ossification is essentially the longitudinal growth of the bone (Long and Ornitz, 2013). The resulting long bone has the outer shell made of compact bone, the cortical bone, organized in a Haversian system as described in (**Fig. I-3**) (Martini et al., 2018). The organization of osteocytes and the bone matrix in a highly structured manner ensures the strength and ability of cortical bone to undergo repair and remodelling. The extensive vascular network of cortical bone enables it to effectively withstand mechanical stresses and meet the metabolic requirements of bone tissue (Fratzl and Weinkamer, 2007), as discussed in **(section 1.2 )**.

### 1.3.2. Intramembranous Ossification

Intramembranous ossification results in the formation of bone that is formed directly from mesenchymal cells, without the presence of a cartilage template (**Fig. I-10**) (Maynard and Downes, 2019b). The resulting bone tissues are flat bones that are found on the skull and other bones such as the clavicle.

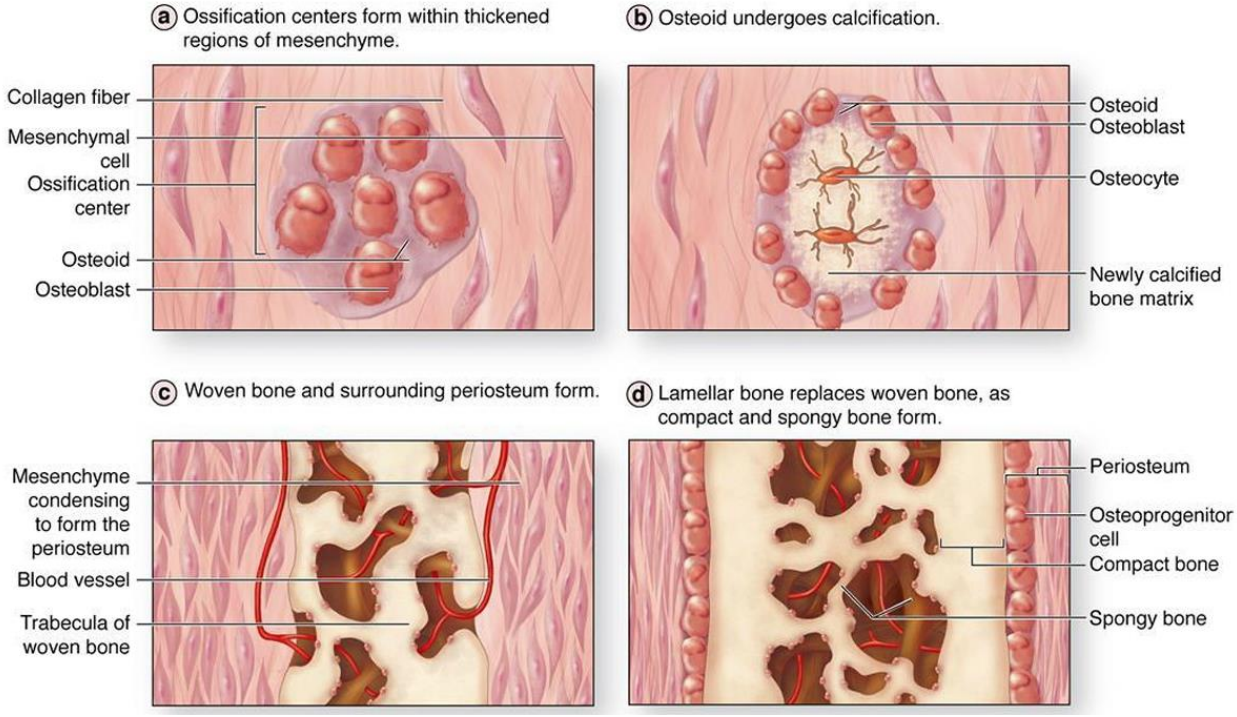


**Figure I-10. Schematic representation of intramembranous bone formation.** a. Mesenchymal cells within the derma differentiate into osteoblasts and form ossification centers. b. Osteoblasts secrete bone osteoid, and osteoblasts captured into this matrix differentiate into osteocytes. c. Osteoid is laid down between embryonic blood vessels forming a random network of trabeculae. d. Bone becomes compact on the outer part and red bone marrow develops centrally of the bone. (https://arccwaite.files.wordpress.com/2018/12/seeleys-essentials-of-anatomy-and-physiology-9th-edition.pdf/chapter_6).

Intramembranous ossification takes place during skull growth and is also observed in the sphenoid and mandible, despite the presence of endochondral components. This means that both endochondral and intramembranous growth processes take place within the same bone (Setiawati and Rahardjo, 2008). The formation of bone tissue is sometimes categorized as either periosteal or endosteal ossification depending upon its location (Cashman and Ginty, 2003). Periosteal bone exclusively arises from intramembranous ossification, while endosteal bone can originate either intramembranously or through endochondral ossification, depending upon the specific location and the process of formation (Dennis et al., 2015). The process of intramembranous ossification (**Fig. I-10**) commences with the proliferation and differentiation of mesenchymal cells into osteoblasts that produce and secrete an extracellular matrix made up of collagen and other proteins, that eventually mineralizes to form the hard, calcified bone tissue (Karaplis, 2008). The osteoblasts go on to secrete the extracellular matrix that is termed osteoid, mineralize it, and become entrapped within the matrix, forming osteocytes that make

up the spongy bone tissue (Breeland et al., 2022). The osteoblasts continue to deposit bone matrix, forming layers of bone tissue on top of each other. As the bone tissue thickens, blood vessels begin to penetrate the bone and the bone tissue becomes vascularized. This results in woven bone which then becomes surrounded by the periosteum made of two layers. The inner layer generates more and more osteoblasts that accumulate on the surface, secreting matrix that thickens to form the compact bone layer thus surrounding the existing spongy bone tissue (Provot et al., 2013). In comparison to spongy bone, the compact bone is denser, stronger, and does not contain a red bone marrow cavity but it rather provides support and protection (Seeman, 2008). Periosteal ossification is important for the growth and expansion of bones, it refers to the creation of bone tissue by the periosteum, that covers the outer surface of bones. The periosteum contains a large number of osteoprogenitor cells, which undergo differentiation into osteoblasts and, by appositional development, lead to an augmentation in the diameter of bones, resulting in enhanced strength (Cashman and Ginty, 2003; Karaplis, 2008). Finally, osteoblasts and osteoclasts work together to remodel the periosteal bone, in order to adapt to mechanical strains and help in the maintenance and restoration throughout an individual's life (Florencio-Silva et al., 2015; Karsenty and Wagner, 2002).

## 1.4. Factors affecting bone formation.

The process of ossification is an important process for the development and maintenance of the skeletal system in vertebrates. Bone formation is regulated by several different factors, including transcription factors, signaling pathways, extracellular matrix proteins, and other regulatory molecules. Impairments in this process can lead to skeletal disorders, for example, cleidocranial dysplasia (Balioğlu et al., 2018), a disorder characterized by the failure of normal clavicle formation. Mutations in genes involved in important processes can result in skeletal anomalies that include bone disorders, such as osteogenesis imperfecta and osteopetrosis (Kornak and Mundlos, 2003). These mutations generally manifest as either craniosynostosis, resulting from premature fusion of sutures, or as enlarged fontanels that result when two skull bones delay closure or fail to appose correctly (Ko Min, 2016; Kornak and Mundlos, 2003). To give some examples, mutations in FGFR1, 2, or 3, have been shown to cause craniosynostosis (Ciurea and Toader, 2009; Ko Min, 2016). FGFRs have been reported to regulate cranial suture fusion and animal studies have pointed out that mutations in FGFRs lead to abnormal signal transduction which affects midface and cranium (Purushothaman et al., 2011). Defects in WNT signaling have been linked to bone disorders (Yang, 2012), for instance an inactivating mutation of LRP5 causes osteoporosis pseudoglioma syndrome (OPPG) that is characterized by early onset osteoporosis with low bone mineral density and blindness (Levasseur et al., 2005), while mutation or overexpression of WNT ligands could also cause abnormalities in osteogenesis (Day et al., 2005; Hill et al., 2005). LRP5 is known to be responsible for encoding a co-receptor of the WNT signaling pathway, which plays a role in regulating bone mineral density (BMD) and activation of LRP5 stimulates bone formation (Gong et al., 2001). The loss-of-function of LRP5 leads to an inability to transmit signals downstream of the WNT canonical pathway causing suppression of WNT signaling, hindering appropriate formation of bone, leading to reduced bone mineral density (BMD) and resulting in the development of osteoporosis at an early stage of life (Cui

et al., 2011; Gong et al., 2001). Recently, it was reported that more severe manifestation of early-onset osteoporosis (EOOP) is linked to a recessive form of LRP5, in combination with an additional mutation in either DKK1 or WNT3A (Caetano da Silva et al., 2021) Intracellular mediators of the WNT signaling pathway, such as β-Catenin, also affect osteogenic differentiation of mesenchymal stem cells (MSCs), as conditional deletion of the β-catenin gene in early osteogenic progenitors arrested terminal differentiation of MSCs into osteoblasts, thus resulting in excessive chondrocyte formation (Kim et al., 2013a; Rodda and McMahon, 2006). Thus, signaling pathways categorized based on their initiation by various signaling ligand families, such as Hedgehog (HH), Wingless and int-1 (WNT), NOTCH, Transforming Growth Factor-beta (TGF-β), Bone Morphogenic Protein (BMP), and Fibroblast Growth Factor (FGF) are critical in osteogenic differentiation (discussed below). These signaling pathways transduce their signals and interact with key transcription factors like SOX9, RUNX2, OSX, TWIST1, and MSX2 that are crucial for bone development, and they have been shown to regulate both the ossification processes, as depicted in (**Fig. I-11**).

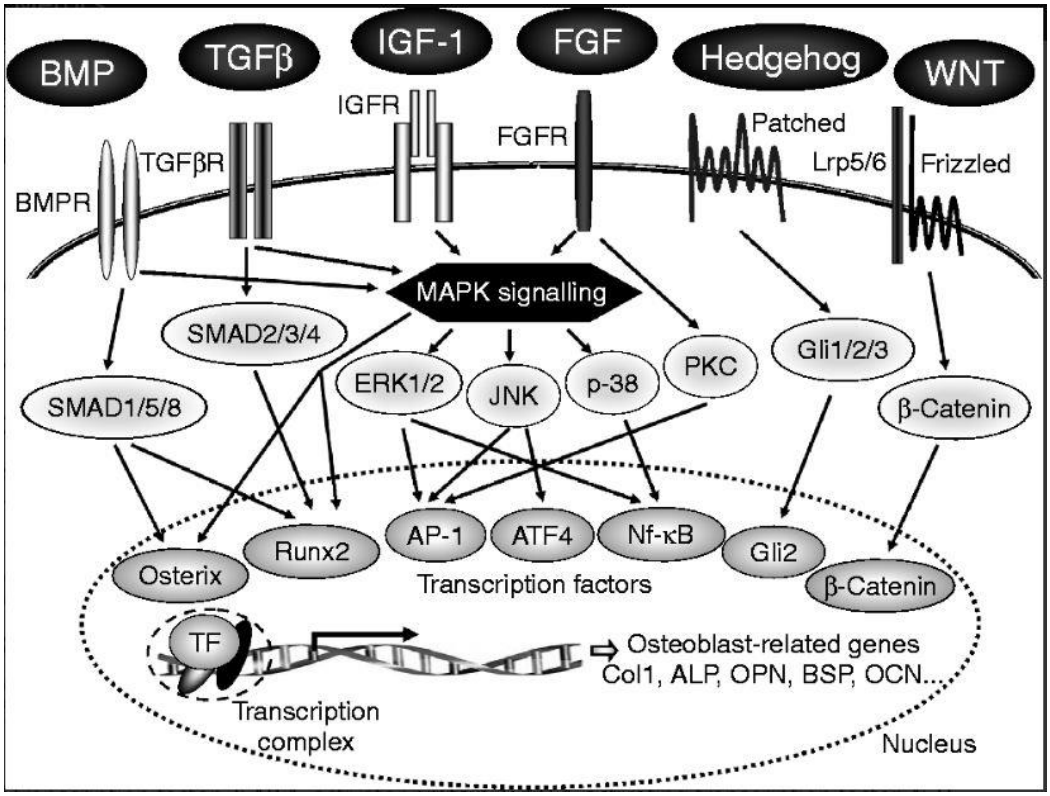


**Figure I-11. Signal-transduction pathways are involved in the regulation of osteoblast differentiation and bone formation.**

Hedghehog (HH) signaling has been shown to be involved in several developmental processes of different tissues and there are 3 homologs of HH found in mammals: sonic (SHH), Indian (IHH) and desert (DHH)(Carballo et al., 2018). Both SHH and IHH have been shown to be involved in skeletal development (Ohba, 2020). SHH promotes the epithelial-mesenchymal transition of the sclerotome and the skeletogenic mesenchyme and regulates differentiation of the cranial neural crest cells (cNCC) derived skeletal structures and digit patterning in the appendicular skeleton (Chiang et al., 1996; Fan et al., 1995; Hu et al., 2003;

Jeong et al., 2004; Riddle et al., 1993). IHH is involved in the endochondral ossification process (Ingham and McMahon, 2001) , it is found to be expressed in pre- and early hypertrophic chondrocytes in the growth plate (Maeda et al., 2007) where it plays an important role in regulating proliferation and differentiation of chondrocytes, required for subsequent osteoblast differentiation (Ohba, 2016). Mutations in *IHH* have been linked to syndactyly with craniosynostosis and acrocapitofemoral dysplasia (Bosse et al., 2000; Hellemans et al., 2003), while mutations in *SHH* lead to congenital hand deformities and severe craniofacial alternations, neurological syndromes, polydactyly, and syndactyly (Abramyan, 2019; Umair et al., 2018). The TGFβ / BMP belong to a superfamily along with Activins and Growth and Differentiation Factors (GDFs) primarily involved in TGFβ and BMP signaling (Feng and Derynck, 2005). In mice, double knockout for *Tgfβ2* and *Tgfβ3* causes impaired frontal and parietal bones respectively, while deletion of *Tgfβ2* in the germline leads to mild defects in the ossification and cranial formation (Florisson et al., 2013; Sanford et al., 1997). TGFβ signaling has been shown to play an important role in promoting condensation and differentiation of mesenchymal cells, inducing proliferation of chondrocytes and inhibit terminal differentiation of chondrocytes (Furumatsu et al., 2009; Mueller and Tuan, 2008). Similarly, BMPs are critical for mesenchymal differentiation and for proliferation and maturation of chondrocytes (Culbert et al., 2014; Li et al., 2003). BMP signaling is extremely important for osteoblast development, as knocking out *Bmp2* and *Bmp4* disrupted osteoblast differentiation and resulted in reduced bone mass in mouse (Kamiya and Mishina, 2011; Wu et al., 2016a). Additionally, there have been reports indicating that RUNX2 has the ability to impact the expression of BMPs (Choi et al., 2005; James et al., 2006; Phimphilai et al., 2006). A recent report conducted on patient having cleidocranial dysplasia (CCD) carrying a rare heterozygous deletion in *RUNX2* gene, influenced BMP4 expression, while treatment with BMP4 rescued the osteogenic capacity of the affected bone marrow mesenchymal stem cells (Liu et al., 2022). On exploring the role of RUNX2 in BMP signaling in these patients, it was shown that RUNX2 regulates osteoblast differentiation via the BMP 4 signaling pathway by inhibiting the BMP antagonist CHRDL1 (Liu et al., 2022). Thus, BMPs together with RUNX2 are important regulators of osteoblast differentiation (Salazar et al., 2016). Also, mutations in the BMP Type I receptor (ACVR1/ALK2) cause a condition called *Fibrodysplasia ossificans progressiva* (FOP) that leads to heterotopic endochondral ossification (Culbert et al., 2014). Additionally, TGFβ/BMP signaling can be negatively regulated by intracellular antagonists like SMAD 6/7, extracellular antagonistic ligands such as NOGGIN and BMPER, inner nuclear membrane proteins, intracellular ubiquitin ligases and transcriptional repressors whose disfunction causes craniofacial malformations, affects joints, or leads to fractures or skeletal disorders/anomalies (Doyle et al., 2012; Gong et al., 1999; Lehmann et al., 2007; Zong et al., 2015).

The WNT pathway has also been reported to be involved in promoting chondrocyte hypertrophy, for instance absence of WNT5A has been shown to delay chondrocyte hypertrophy which affects bone formation and WNT5A/B is essential for transition of chondrocytes to hypertrophy (Hartmann and Tabin, 2000; Yang et al., 2003). Activation or inhibition of WNT signaling have been associated with alterations of bone mass (either increase or decrease, respectively) (Bennett et al., 2007; Day et al., 2005; Hill et al., 2005; Hu et al., 2005). Mutations in *WNT1* have been linked to early onset of osteoporosis and *osteogenesis imperfecta* (Lu et al., 2018). BMP and WNT signaling together have been shown

to regulate the development and remodeling of several organs and tissues; for example, studies employing mesenchymal cell lines have resulted in both synergistic and antagonistic outcomes when examining the relationship between BMP and WNT signaling in osteoblasts (Kamiya et al., 2010; Kamiya et al., 2008; Mbalaviele et al., 2005). Both pathways play a crucial role in the regulation of osteoblast differentiation and bone formation (Maes et al., 2010).

The FGFs or fibroblast growth factors and their receptors are known to be involved in formation of most tissues, including bone development, and act as important regulators during the earliest stages of development and organogenesis (Ornitz and Marie, 2015). Studies suggests that syndromes of craniosynostosis in humans have been directly linked to mutations in fibroblast growth factor receptors (Degnin et al., 2010) like *FGFR1, FGFR2* and *FGFR3*(Ciurea and Toader, 2009; Teven et al., 2014; Wilkie, 1997). Several FGFs, like *FGF2, FGF4, FGF9, FGF18,* and *FGF20* are expressed during early stages of intramembranous bone formation (Britto et al., 2001; Lazarus et al., 2007; Liu et al., 2002; Ohbayashi et al., 2002; Rice et al., 2000). Studies have shown that FGFR-mediated activation of ERK1/2, PLCγ/PKCα and PI3K/Akt signaling pathways leads to modulation of cell proliferation, differentiation and apoptosis of osteoblasts, which affects bone formation (Ornitz and Marie, 2015). FGF2 ectopic expression in mice causes macrocephaly and coronal synostosis (Holmes et al., 2018), while complete KO of *Fgf18* in mice leads to craniofacial defects and delayed ossification (Xie et al., 2014). *Fgf9* has been shown to be expressed in the calvarial mesenchyme (Kim et al., 1998) and *Fgf18* is found in mesenchymal cells and in differentiating osteoblasts (Ohbayashi et al., 2002; Reinhold and Naski, 2007), while both *Fgf9* and *Fgf18* are expressed in the perichondrium and periosteum (Hung et al., 2007; Liu et al., 2002; Ohbayashi et al., 2002), and *Fgf2* is expressed in the chondrocytes (Gonzalez et al., 1996). Mice lacking *Fgf2* display a significant reduction in bone mass with no observable changes in growth plate structure or function (Montero et al., 2000).

All of these signaling pathways are crucial during the development, osteoblast differentiation and in the ossification process (Ornitz and Marie, 2015; Provot et al., 2013; Yang, 2012). Their combined action governs the expression and function within the differentiating skeletal cells of the transcription factors, such as SOX9, RUNX2 and SP7 that are required for cartilage and bone development (**Fig. I-11**) (**Fig. I-5**) (Bruderer et al., 2014; Oh et al., 2014). The SOX9 transcription factor belongs to the SRY family and it is required for chondrogenesis (Akiyama, 2008). The *SOX9* gene is considered as the master gene for chondrocyte differentiation, it is mutated in skeletal dysplasia including campomelic dysplasia characterized by endochondral ossification abnormalities (Kiernan et al., 2018; Maes and Kronenberg M., 2016). Further, SOX9 is known to regulate the expressions of SOX5 and SOX6 and to directly activate collagen II, all chondrocyte differentiation markers (Lefebvre and Dvir-Ginzberg, 2017). SOX9 also induces expression of collagen X in hypertrophic chondrocytes (Leung et al., 2011). Studies have shown that *Sox9* is essential for maintaining the identity of chondrocytes and its downregulation is essential for progression of hypertrophy in mice (Dy et al., 2012). Interactions between various signaling pathways like IHH, PTH-related peptide (PTHLH), BMP, Wnt and FGF play an important role in regulating a balance between chondrocyte proliferation and hypertrophy (Chen et al., 2021; Minina et al., 2002).

RUNX2 is a transcription factor belonging to the RUNX family and is considered crucial for osteoblast commitment and differentiation (Komori, 2011). It is expressed in osteoblast progenitors, in immature and in early mature osteoblasts (Bruderer et al., 2014). RUNX2 is essential for the differentiation of early mesenchymal stem cells into osteoblasts and it controls the expression of various genes like collagen I, bone sialoprotein (BSP), osteopontin (OP) and osteocalcin (OC) (Komori, 2010; Marie, 2008; Oh et al., 2012). It is important for both intramembranous and endochondral ossification processes during skeletogenesis, since germline deletion of *Runx2* impedes the formation of mature, mineralized bone and is extremely lethal (Komori et al., 1997; Otto et al., 1997). Studies have shown that the expression of RUNX2 is observed in proliferating chondrocytes, in pre-hypertrophic chondrocytes and in the perichondrium during endochondral bone development (Inada et al., 1999; Kim et al., 1999).

The transcription factor SP7 (OSX) regulates osteoblast differentiation and bone formation (Nakashima et al., 2002). It has been reported that SP7 expression is essential for the RUNX2-positive cells to differentiate into mature and functional osteoblasts and osteocytes (Zhou et al., 2010; Zou et al., 2006). Patients lacking the *SP7* gene suffer from a moderate form of *osteogenesis imperfecta* and harbor bone fractures, delayed tooth development and show mild skeletal deformities (Lapunzina et al., 2010).

Other transcription factors, such as MSX2 and DLX5, also play a crucial role during the differentiation of osteoblasts during the formation of cranial bones by interacting with RUNX2 (Rice and Rice, 2008) and, as mentioned above, numerous regulatory factors, including signaling pathways such as TGFβ, BMP, Wnt, FGF and HH are essential in influencing bone formation by regulating cell differentiation and survival in a spatiotemporal fashion (Dailey et al., 2005; Lenton et al., 2005; Opperman, 2000; Rice and Rice, 2008). Hormonal signals also play an important role in the regulation of bone formation. For example, growth factors like insulin-like growth factor 1 (IGF1) (Guntur and Rosen, 2013), or thyroid hormone (TH) can stimulate bone formation by promoting mesenchymal cell differentiation and bone matrix production (Bassett and Williams, 2016). Thyroid hormone and growth hormone play an equally important role in the regulation of bone formation via WNT signaling and BMP signaling pathways (Williams, 2013). It has been shown that TH activates *COL1* and *BGLAP* expression in osteoblasts and inhibits osteoclast formation in humans and mouse (Bassett and Williams, 2016) (Zaitune et al., 2019).

Parathyroid hormone (PTH) is known as the key regulator of calcium and phosphate homeostasis in the body, one of the factors that play a role in regulating bone formation (Lombardi et al., 2020). Studies conducted *in vitro* have reported that the proliferation and differentiation of osteoblasts are stimulated by PTH, through increased expression of *BMP2* and other growth factors essential for differentiation of osteoblasts (Zhang et al., 2011). PTH is also known to exert its effect on osteoclast differentiation and bone resorption by stimulating the expression of *RANKL*, causing the calcium to be released into the blood stream (Wein, 2017), and thus maintaining normal calcium levels in the blood (Kahil et al., 2020). Parathyroid hormone stimulates production of Vitamin D, which assists in enhancing calcium and phosphorus absorption from the intestine (Christakos et al., 2011). Thus, both calcium and vitamin D are involved in a feedback loop that is tightly regulated by the

secretion of PTH. Therefore, overall, the process of ossification in vertebrates is influenced by a complex interplay of genetic, hormonal, mechanical, and environmental factors.

# 2. THE ZEBRAFISH MODEL SYSTEM

Using model systems to study and understand vertebrate development, as well as to assist in solving unanswered questions in biomedical research, is becoming very common. Zebrafish (*Danio rerio*) emerged as one the most valuable model organism used in biological research. It is a teleost tropical freshwater fish (Dooley and Zon, 2000) and has become a very well-established animal model for studies in developmental biology, when compared with the most widely used model systems, the rat (*Rattus norvegicus*), the mouse (*Mus musculus*) and others (Dooley and Zon, 2000). It has also become an excellent model system for the study of muscle and skeletal development in vertebrates (Ackermann and Paw, 2003). One important advantage is that fertilization and embryonic development take place outside of the body, in contrast to mammals where these processes occur *in utero*. Early developmental stages are easily accessible in the zebrafish embryo as the chorion, a membrane surrounding the egg and the embryo, and the embryo itself are transparent (Ackermann and Paw, 2003; Dooley and Zon, 2000). The zebrafish has a completely sequenced, annotated genome comprised of 25 chromosome pairs (Howe et al., 2013). It is impressive that about 70% of the human protein-coding genes are known to have at least one homolog in the zebrafish (Howe et al., 2013). Also, all the main organs are formed within 24 hours post fertilization (hpf) and the larvae hatch around 2-3 days post fertilization (dpf). At 26 hpf, the heart starts to beat, initiating blood circulation, and pigmentation begins to show up between 30 to 72 hpf (Kimmel et al., 1995; Lister, 2002). Even though there are other established simple animal models such as *Drosophila melanogaster* and *Caenorhabditis elegans*, employed for studying many biological processes (Cooper, 2000; Dooley and Zon, 2000), these organisms are not suitable for addressing questions related to development and functions of vertebrate specific features like multi-lineage hematopoiesis, notochord, skeletogenesis and neural crest cells, as they are invertebrates (Cooper, 2000). The embryonic development in zebrafish has been described and characterized in detail, thus facilitating the analysis and comparison of abnormal development during diseases like muscular dystrophy, tuberculosis, and cancer, to name just a few (Bassett et al., 2003; Kimmel et al., 1995; Swaim et al., 2006). The zebrafish therefore has become an important model, alongside mice and rats, as many mutant/variant genes have been found in genetic screens to cause conditions similar to human diseases (Dooley and Zon, 2000). Osteogenesis and anomalies of mineralized tissues are one of the areas of intense investigations in the mammalian field, but different from other areas of organ formation, tissue morphogenesis and developmental biology, zebrafish has been somewhat a late entrant as a model organism in the area of bone research (Apschner et al., 2011). Zebrafish, which offers genetic mutants, facilitates a wide range of studies aimed at examining the signaling pathways involved in bone development, caudal fin regeneration, screening for osteoactive compounds, performing transcriptomics, *in vivo* cell tracking using transgenic reporter lines, drug treatments, and the discovery of therapeutic tools for bone diseases (**Fig. I- 12**).

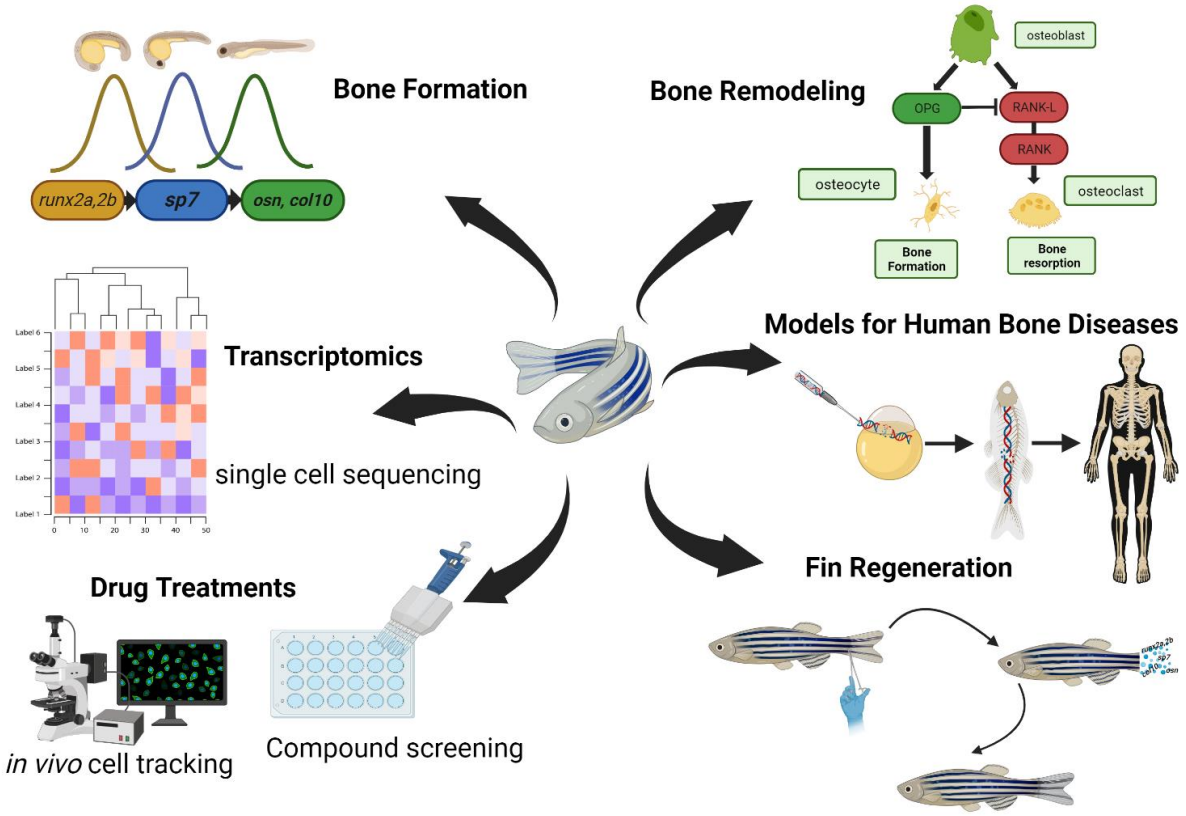


**Figure I-12. Zebrafish applications in skeletal biology.** Examples of applications of the zebrafish model in the field of skeletal research includes modeling for human bone diseases by generating mutants, staining for cartilage and skeletal elements, large scale compound screening of osteoactive compounds and drug treatments, in vivo cell tracking using *Tg* reporter line and performing transcriptomic studies at various stages during development. Images created with BioRender.com.

## 2.1. Cartilage and bone development in zebrafish

### 2.1.1. Craniofacial development

Zebrafish and other teleosts have skeletal structures that are made up of both bone and cartilage. It is very important to understand the development and maintenance of teleost bone and cartilage in order to better comprehend the evolution of the skeletal system and skeletal anomalies for developing necessary therapeutic interventions.

The skull of fish, especially zebrafish, is far more complicated than that of other model creatures like frogs, birds, and mammals in terms of the number of bones, diversity of skeletal types, and articulations. For example, there are 74 cranial bone elements in adult zebrafish in comparison to the mammalian skull with merely 22 (Cubbage and Mabee, 1996), as shown in the schematic representation of a zebrafish skull from larvae to juvenile (**Fig. I- 13**).

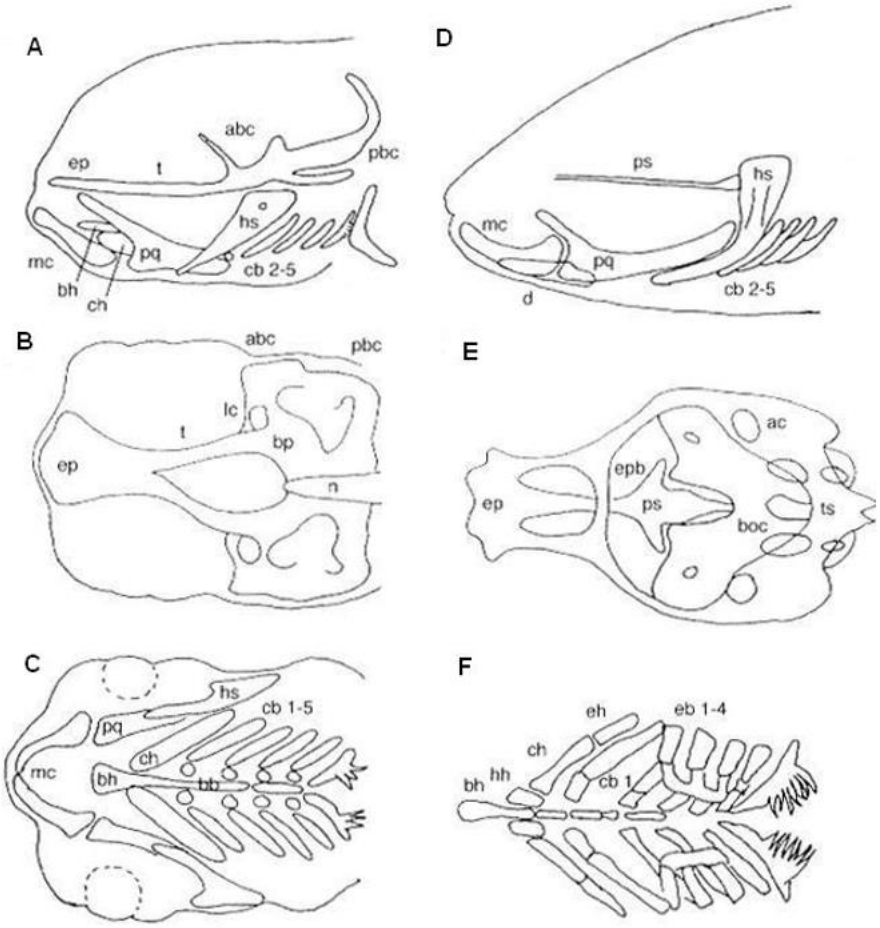


**Figure I-13. Schematic representation of zebrafish skull in larval and juvenile stages.** The larval stages are shown in figures and juvenile stages are shown in figures (D-F). (A, C, D, F) showing the viscerocranium and (B, E) the neurocranium. The elements are: anterior basicranial commisure (abc), auditory capsule (ac), basibranchials (bb), basihyal (bh), basioccipital, basal plate (bp), ceratobranchials, ceratohyal (ch), dentary (d), epibranchial (eb), epihyal (eh), ethmoid plate (ep), epiphysial bar (epb), hypohyal (hh), hyosymplectic (hs), lateral commissure (lc), Meckel's cartilage (mc), notochord (n), posterior basobranchial

commissure (pbc), palatoquadrate (pq), parasphenoid (ps), trabeculae (t), tectum synopticum (ts). (Nuesslein-Volhard, 2002).

The development of the chondrocranium and the patterning of pharyngeal segments in zebrafish has been very well documented and described in detail both in mutant and wild type organisms (Neuhauss et al., 1996; Schilling and Kimmel, 1997; Schilling et al., 1996b). The craniofacial anatomy of zebrafish is made of the neurocranium (**Fig. I-13. B, E**) (supports the brain and sensory systems) and the viscerocranium (**Fig. I-13. A, C, D, F**) (playing a role as feeding and respiratory apparatus), both of which are composed of cartilaginous elements that are replaced by bone and a few intramembranous skeletal elements which support the gill cover (Mork and Crump, 2015). Many of these bones, especially those forming the cranial vault, are cartilaginous (Lettice et al., 1999) in the beginning and eventually ossify much later after the embryonic period to form the osteocranium (Nuesslein-Volhard, 2002).

The pharyngeal skeleton in zebrafish is derived embryonically mainly from neural crest, while the muscles are derived from mesoderm (Noden, 1991; Schilling and Kimmel, 1994). The patterning of the pharyngeal segments is consistent with their hindbrain rhombomeric origin (**Fig. I-14. A-B**), which translates into a segmentally organized set of cartilages, bones, and muscles (**Fig. I-15. A-C**) (Schilling and Kimmel, 1997). In the course of the development of the chondrocranium, the cranial neural crest cells (cNCCs) migrate laterally and ventrally before differentiating into a lineage of chondrocytes that proceeds to form osteogenic or osteoblast-like cells that secrete the bone matrix and undergo ossification (Huysseune, 2000). As this differentiation proceeds simultaneously at the cellular level, at each stage the cells express different genes or markers that code for transcription factors or ECM proteins (**Fig. I-16**).

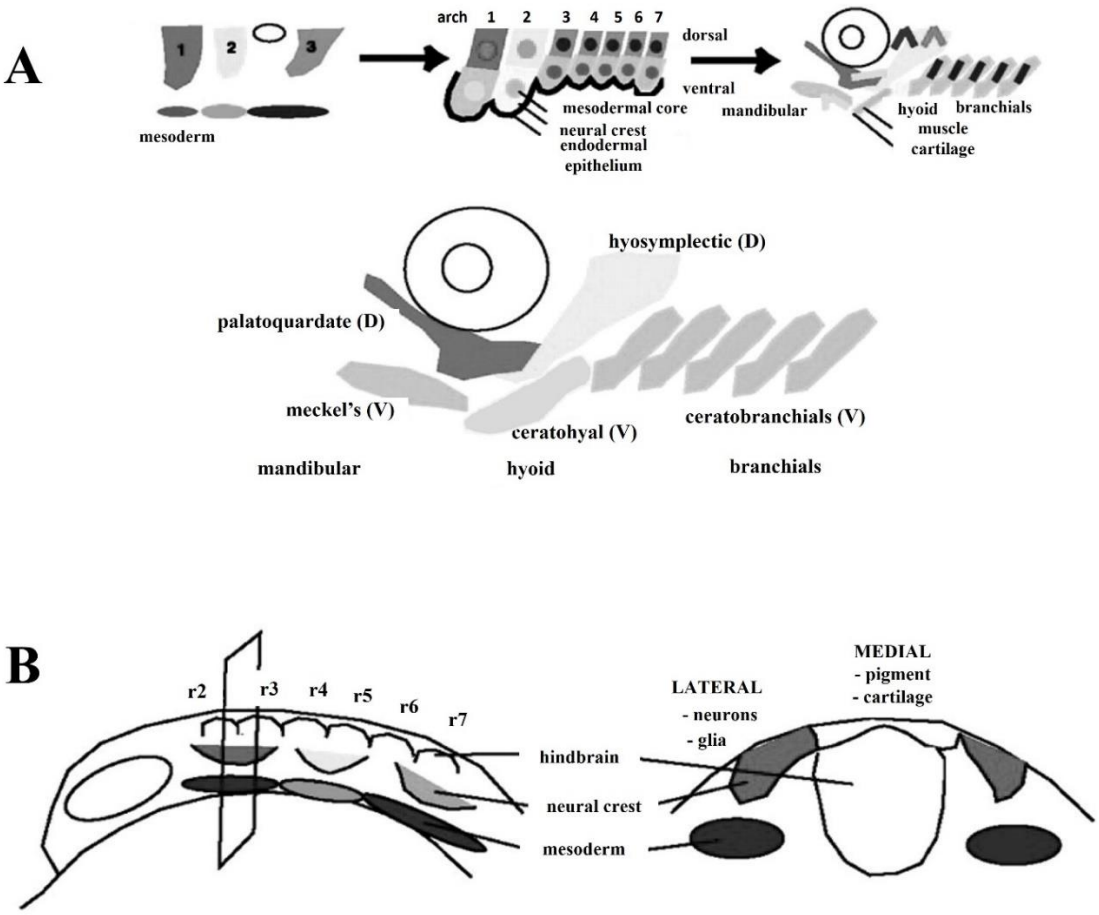


**Figure I-14. Schematic representation of the different components and patterning of the pharyngeal skeleton in zebrafish.** (A) The figure shows neural crest cells, mesodermal and endodermal components of the zebrafish head. The shading of elements inside a segment corresponds to the following: mandibular, 1 (derived from neural crest and mesoderm); hyoid, 2 (derived from neural crest and mesoderm); branchials, 3-7 (derived from neural crest and mesoderm). The figure briefly describes a schematic picture of the initial stages of development, namely during mid-somitogenesis, wherein the formation of head segments commences in a vertebrate embryo of a general kind. Neural crest cells undergo ventral migration into the pharyngeal arches by three distinct migratory streams, labeled as streams 1-3. During the advanced phases of embryonic development, the pharyngeal segments undergo further division into distinct dorsal and ventral regions. Within these regions, a cylinder composed of neural crest cells surrounds mesodermal cores, which are in turn enveloped by epithelial tissue. In the larval stages of zebrafish development, each arch consists of segment-specific cartilages that originate from neural crest cells, as well as muscles that originate from mesoderm cells. (B) This figure illustrates the schematic depiction of a zebrafish embryo at an early stage, specifically at mid-somitogenesis, when the migration of neural crest cells commences. The hindbrain of the embryo is divided into several segments known as rhombomeres, ranging from r2 to r7. Neural crest cells exhibit migratory behavior as they relocate to specific parts of the mesoderm inside distinct arches, which is contingent upon their segmental origins in close proximity to the hindbrain. A diagram illustrating the transverse section is shown, thereby depicting the spatial distribution of the lateral neural crest responsible for generating neuronal and glial cell lineages, as well as the medial crest cells responsible for forming cartilage and pigment. (Yelick and Schilling, 2002).

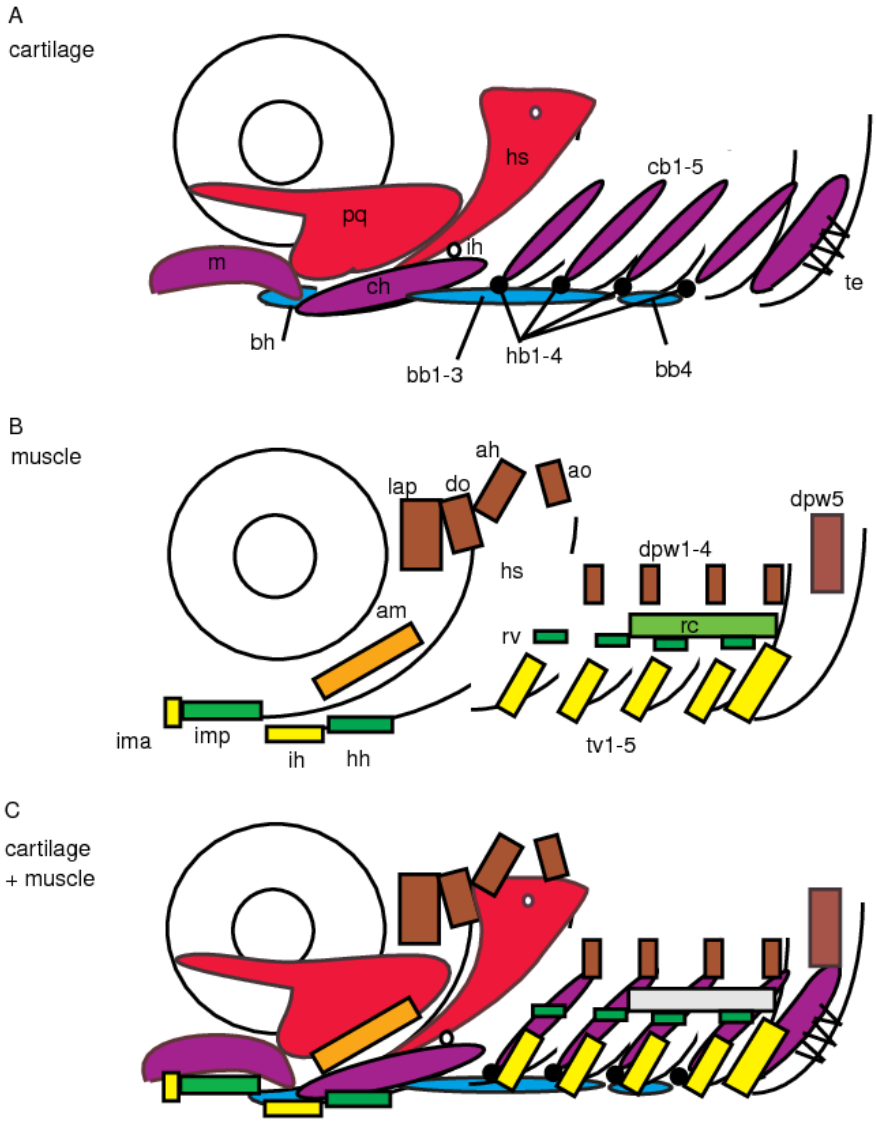


**Figure I-15. The summary of segmental homologies observed in the cranial cartilages and muscles of zebrafish larvae.** (A) Schematic lateral view of the pharyngeal skeleton at 96 hours. Homologous structures exhibit analogous coloration patterns, with the basi structure displaying a blue hue, the hypo structure appearing black, the cerato structure exhibiting a purple shade, and the epi structure presenting a red coloration. (B) The cranial muscles can be categorized into four groups based on their coloration: the dorsal muscles are brown, the intermediate muscles are green, the ventral muscles are yellow, and the putative dorsal muscles are orange. (C) The combination of A and B. (Schilling and Kimmel, 1997).

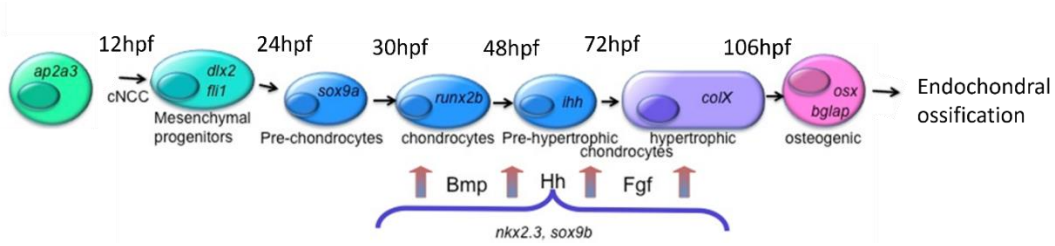


**Figure I-16. Schematic representation of cranial neural crest cell (cNCC) differentiation in zebrafish.** During chondrogenesis, the different cartilaginous elements arise from cNCCs. The progenitors differentiate and express various genes like *hox2a* and *ap2α3* that are very essential for the specification of arch segmentation. Followed by the expression of *dlx2a*, the cells start to migrate, and those cells start to express genes important for chondrogenesis such as *runx2b*, *sox9a*, *col2a1*. The chondrocytes will proliferate to give rise to hypertrophic chondrocytes that will become osteogenic or osteoblast like cells and undergo endo- or peri-chondral ossification. In addition, the influence from signaling pathways (Bmp, Fgf and Hh) is crucial for the patterning of the pharyngeal skeleton in the craniofacial area (Muller et al., 2010).

The anterior portion of the larval neurocranium, which includes the ethmoid plate, paired trabeculae, and a portion of each bilateral otic capsule, is formed by cranial neural crest cells (cNCCs), while the posterior and medial components are derived from mesoderm and develop around the cranial end of the notochord (**Fig. I-17. A-C**). The ethmoid plate can serve as a model for the mammalian hard palate in that both derive from two groups of anterior maxillary cNCCs which migrate and fuse at the midline to form the roof of the mouth (Mork and Crump, 2015). Genetic mutations or misexpressions in critical genes that regulate the growth and migration of the cNCCs lead to impairment of the midline fusions and to unfused (cleft) palate both in mammals and in fish (Bush and Jiang, 2012; Eames et al., 2013; Swartz et al., 2011; Wada et al., 2005). Interestingly, similar observations have been documented in the midline region in mutant zebrafish for Bmp pathway components, Sonic hedgehog (Shh), Plateled-derived growth factor (Pdgf), or in genes like *irf6* whose phenotypes range from complete lack of the anterior neurocranium to unfused plates, presence of two parallel rods, or a single rod instead of an entire complete plate, similar to mammalian cases (Carroll et al., 2020; Eberhart et al., 2008; Raterman et al., 2020; Wada et al., 2005). Both the more dorsal palatoquadrates, which articulate with the posterior end of the Meckel's to form the jaw joint, and the ventrally positioned bilateral Meckel's cartilages, which unite at the midline and serve as the lower jaw in the larva, are derived from the mandibular arch.

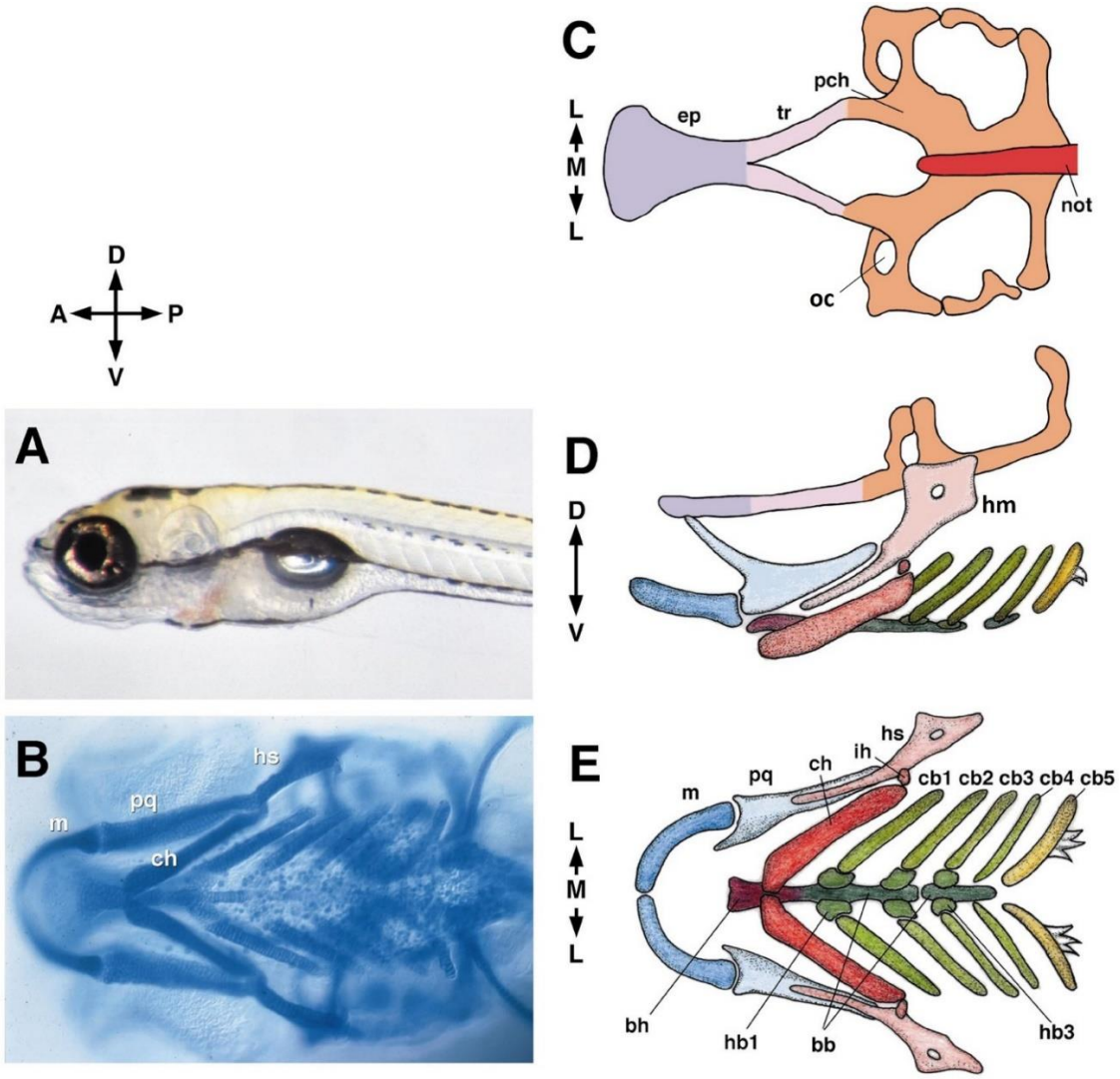


**Figure I-17. 5dpf (days post fertilization) picture of young zebrafish larva in lateral position and the head cartilaginous skeleton layout.** (A) zebrafish larva 5 days old in lateral view (anterior to the left). (B) Alcian Blue stained image of head cartilage in ventral view. (C-E) are pictographic representations of the head cartilage in various views. (C) The cartilage elements of the neurocanium and the notochord in a dorsal view. (D) The lateral view of the pharyngeal skeleton. (E) The ventral view of 5dpf zebrafish larva showing the pharyngeal arches. A, anterior; bb, basibranchial; bh, basihyal; cb, ceratobranchial; ch, ceratohyal; D, dorsal; ep, ethmoid plate; hb, hypobranchial; hs, hyosymplectic; ih, interhyal; L, lateral; M, medial; m, meckels; not, notochord; oc; otic capsule; P, posterior; pch, parachordal; pq, palatoquadrate; tr, trabecula; V, ventral. (Kimmel et al., 2001).

A smaller interhyal cartilage forms the hyoid joint, joining the hyosymplectic and the ceratohyal (**Fig. I-17. A & D**). At the midline, the unpaired basihyal cartilage is in touch with each ceratohyal (**Fig. I-17. B & E**). The neurocranium is joined to the anterior portion of the otic cartilage by the hyosymplectic, (**Fig. I-17. A & D**). This attaches the jaw skeleton to the rest of the head (Kimmel et al., 1998).

The viscerocranium derives mainly from cNCCs and contains the jaw, branchial arches, and teeth, as shown in figures; (**Fig. I-13 A, C, D** and **F**) and (**Fig. I-15**). Their origins have been studied extensively, highlighting its importance for development and survival in zebrafish, and have been shown to originate from the embryonic pharyngeal arches (Kague et

al., 2012; Mork and Crump, 2015). The seven pharyngeal arches of the zebrafish embryo make up the viscerocranium, where the first and the second pharyngeal arch, i.e., the mandibular and the hyoid arch, serve as supportive structures of the jaw (**Fig. I-17. B & D** and **Fig. I-18. A**) (Schilling and Kimmel, 1997). The remaining third to seventh pharyngeal arches are called branchial arches that form the supporting structures of the gills and the teeth (**Fig. I-17. B & E**) (Schilling and Kimmel, 1997). Multiple skeletal components develop along each of the arches' dorsal-ventral axis, each of the seven pharyngeal arches have separate dorsal and ventral sets of cartilages and muscles (Schilling and Kimmel, 1994; Schilling et al., 1996a). Advancing posteriorly, arches 3–7 create unpaired basibranchials at the ventral midline, which in turn connect to paired ventrolateral rod–shaped ceratobranchial cartilages attached to tiny hypobranchials (Vandewalle et al., 1998). The delicate, heavily branched gill tissues are supported by the ceratobranchials and arch 7 gives rise to several ossified pharyngeal teeth. The arches are patterned by signals from the surrounding epithelia as well as by NCC-intrinsic information carried over from their neuroepithelial origins. For example, the transcription factors of the *Hox* family determine the major anterior-posterior and dorsal-ventral axes, as well as precisely which parts of each arch need to produce cartilage or bone to establish a domain-specific generalized skeletal plan (Lovely et al., 2016; Prince et al., 1998). Despite differences in the precise shapes and numbers of arch-derived skeletal elements in various animals, the general functions of these pathways in patterning the pharyngeal arches prior to skeletal development have proven to be highly conserved across vertebrates in mice and in zebrafish (Medeiros and Crump, 2012).

Due to the similarities between the fish and the mammals, it is possible to use the sophisticated genetic tools available in the zebrafish system to find novel genes that may influence these skeletal homologs in both systems. Most of the genes and their roles are conserved across species. For example, the anterior portion of the neurocranium, which mimics the mammalian palate, and the cranial vault, are unambiguous homologs between zebrafish and mammals (Swartz et al., 2011; White et al., 2021). The zebrafish skull has skeletal joints, including fibrous joints (such as skull sutures) and articular joints in the mouth, similar to mammalian skulls (**Fig. I-18. B**) (Topczewska et al., 2016). *nkx3.2*, also known as *bapx1*, belongs to the NK2 class of homeobox genes (Lettice et al., 2001). Its mutation in zebrafish results in an open mouth condition that is caused by loss of the jaw joint (Waldmann et al., 2021). Mutations in the Endothelin-1 pathway cause significant alterations to the anterior lower face of mice and zebrafish. These alterations include reductions and transformations of the Meckel's cartilage and the ceratohyals in zebrafish *edn1* mutants (Miller et al., 2000) and a dramatically reduced mandible in *Edn1* mouse mutants (Kurihara et al., 1994). In addition, mutations in EDN1 key target genes such as *Dlx5/6* cause the lower jaw to be transformed into upper jaw and lead to repatterning of the skull in mutant mice a (Depew et al., 2002).

The skeletal elements and the various joints that we observe during the larval stages are comparatively more robust and increased in size in adults due to the growth and developmental changes. This is clearly illustrated in the figure below where we show comparison of joints in different locations (ranging from hyoid joint to jaw joints to skull sutures to joints connecting the vertebral bodies and in pectoral fins) in larval stage and in adults (**Fig.18. A & B**) (Askary et al., 2016; Smeeton et al., 2017).

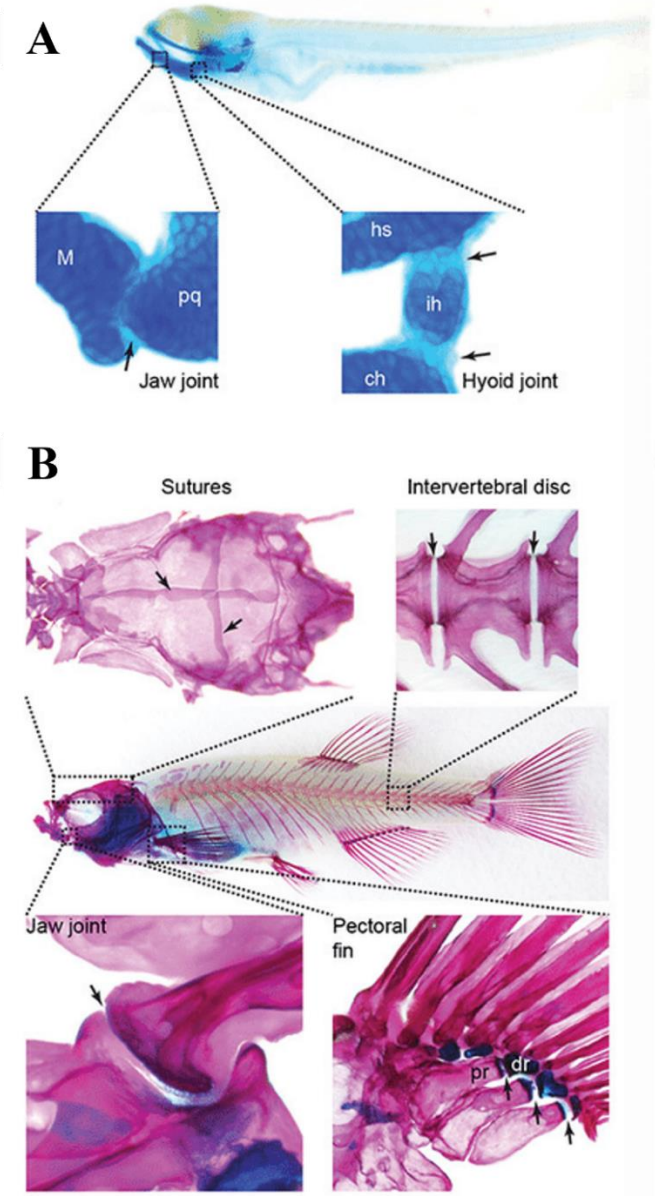


**Figure I-18. A comparative view of skeletal joints in 5dpf zebrafish and older zebrafish.** (A) Shows the alcian blue stained young zebrafish larva highlighting the cartilaginous joints; the jaw joint (between meckels (m) and palatoquadrate (pq) and the bipartite hyoid joint between hyosymplectic (hs), interhyal (ih), and ceratohyal (ch) cartilage). (B) Alcian blue (cartilage) and alizarin red (bone) co-stained adult zebrafish showing many types of joints; sutures of the skull, intervertebral joints, the synovial joints in the jaw and pectoral fin; distal radial (dr) and proximal radial (pr). The figure is adapted from (Smeeton et al., 2017).

## 2.2. Zebrafish Axial Skeleton

The axial skeleton of fish consists of the vertebral column and the dorsal, anal, and caudal median fins, while the paired pectoral and pelvic fins are found ventro-laterally in the abdominal area (**Fig. I-19**) (Cubbage and Mabee, 1996). In terms of development and basic anatomy, zebrafish and humans are quite similar but there are differences in the axial and appendicular skeleton that can be observed during embryological and developmental studies and also by radiographic analysis (Fisher et al., 2003; Hirasawa and Kuratani, 2015).

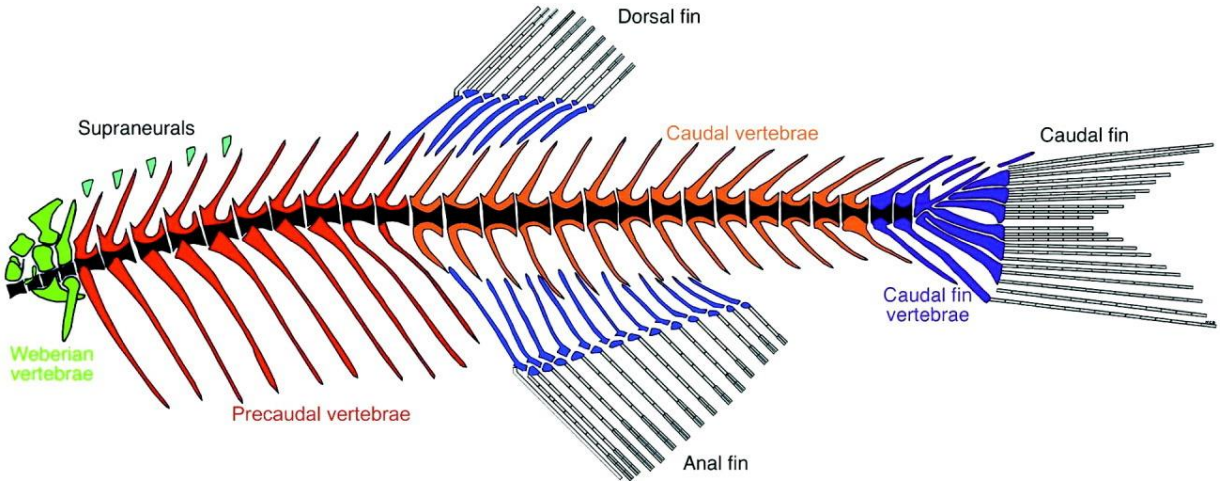


**Figure I-19. Pictographic representation of zebrafish adult axial skeleton.** The Weberian apparatus is indicated in green, while supraneurals are indicated in light green, the vertebra centra are in black. The precaudal vertebrae are shown in red, caudal vertebrae are in orange color, while the caudal fin vertebrae are in purple and the dorsal, anal fin endoskeletons are shown in blue. The centra, neural arches and spines, parapophyses, and ribs make up the precaudal vertebrae, that are anteriorly regionalized as the Weberian vertebrae called the Weberian apparatus. Centra, dorsal neural arches and neural spines, and ventral hemal arches and hemal spines make up the caudal vertebrae. It is important to note that posterior to the Weberian apparatus begins the precaudal vertebrae until vertebra 14. Thereafter, from vertebra 15 onwards through 28, they make up the caudal vertebrae. The three caudal vertebrae, especially the most posterior one, are adapted to support the caudal fin. The last precaudal and/or first caudal vertebra, which lacks a haemal spine and has prolonged, unfused hemal arches or parapophyses, is frequently referred to as a "transitional" vertebra (Cubbage and Mabee, 1996). Figure from (Bird and Mabee, 2003).

### 2.2.1. Vertebral column

In terms of spinal morphology, humans have 33 vertebrae, but zebrafish have 30 to 32. The zebrafish vertebral column is made up of a Weberian apparatus made up of four vertebrae between the swim bladder and the ear, 10 abdominal vertebrae (also known as precaudal vertebrae or trunk vertebrae) that are articulated with rod-shaped rib segments, 14 caudal vertebrae, and three caudal fin vertebrae (**Fig. I-19**) (Bird and Mabee, 2003). Like the mammalian spinal canal, the spinal cord in zebrafish travels through the neural arches that extend dorsally from each vertebra, also there are haemal arches on the ventral sides of the caudal vertebrae that encompass the caudal artery and vein (Bagnat and Gray, 2020).

Each zebrafish vertebral body is composed of a vertebral centrum that has a very distinct hourglass-shaped three-dimensional (3D) morphology, plus neural and haemal arches (**Fig. I-20. A**) (Dietrich et al., 2021b). In contrast to mammalian vertebrae, the cavities within zebrafish vertebral bodies do not carry red bone marrow, since hematopoiesis occurs in the kidney (Song et al., 2004). Instead, they are filled with adipose tissue and packed with vacuolated notochord cells, wherein each vertebra has trabecular struts that encircle the narrow centers (Bensimon-Brito et al., 2012) (**Fig. I-20.B**). Similar to mammals, spinal bones in zebrafish are interconnected by soft tissue (the intervertebral disc), allowing mobility and extending the range of locomotion (Galbusera and Bassani, 2019). It is also important to note that the nucleus pulposus and fibrocartilaginous cartilage that make up the intervertebral disc (McKee et al., 2019) in mammals is absent in zebrafish, instead a ring-shaped ligament (intervertebral ligament) connects the outermost circular margins of two neighboring vertebrae, thereby distinguishing the intervertebral soft tissue (**Fig. I-20.B**) (McKee et al., 2019). The zebrafish spine is loaded axially due to compressive forces from swimming through water and direct muscle forces conveyed by tendons linked to the vertebrae (Suniaga et al., 2018).

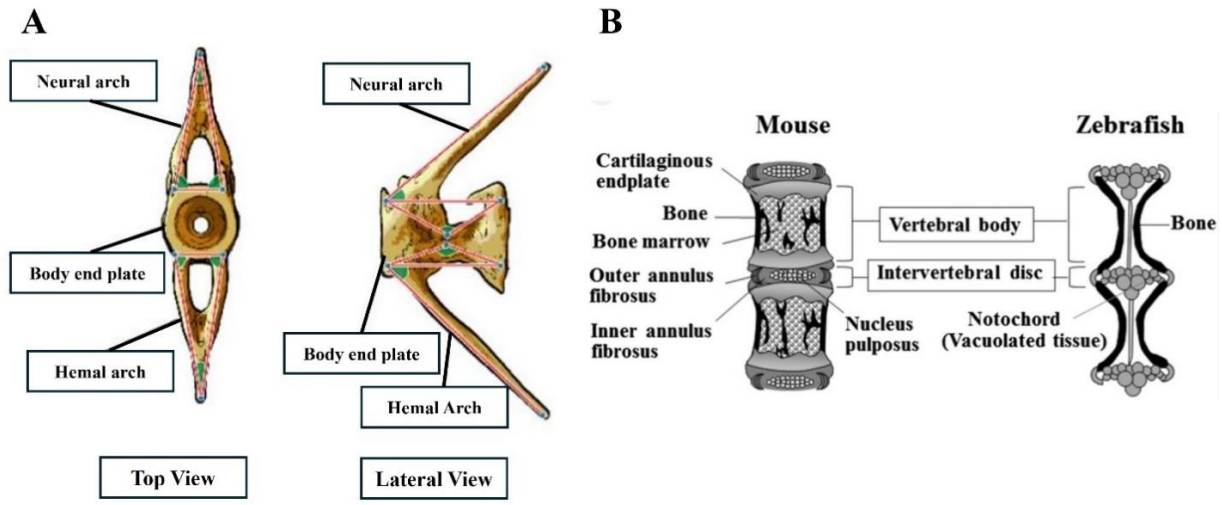


**Figure I-20. Illustration of precaudal vertebral body from adult zebrafish and a comparative view of mouse and adult zebrafish vertebral bodies.** (A) Shows the precaudal vertebral body in top and lateral (side) views and its parts consisting of neural arch, body end plate and haemal arch. (B) Highlights the differences between mouse and adult zebrafish vertebrae. Nucleus pulposus and annulus fibrosus make up the intervertebral discs in mice that lie between the vertebral bodies. The vertebral bodies of mice are packed with spongiosa. In zebrafish, the corresponding intervertebral structures are made of vacuolated tissues, that are situated between lumens and are encircled by bone. The figure is adapted from (https://doi.org/10.1101/2020.07.10.197533) and (Guo et al., 2018).

Although mineralization of the axial skeleton only starts at later stages (8-9 dpf), most of the processes of axial patterning begin quite early during the development in zebrafish, at 10.5hpf when the first somite arises (Kimmel et al., 1995). This sets the ball rolling for segmentation, which progresses antero-posteriorly in a gradual fashion giving rise to pairs of somites every 30 minutes till the segmentation is completed, consisting of 30 pairs of somites at 24hpf. This segmentation pattern shows muscle precursors in the segmented plate that have been induced by signals derived from the notochord until the notochord is surrounded by segmented pairs of somites (Stickney et al., 2000). This process is highly controlled and is similar to somite formation in other vertebrate species, each somite then forming the myotome (muscle precursors) and the sclerotome (vertebral column precursor). In amniotes, the sclerotome is a population of mesenchymal cells that are generated from the ventral somite and migrate to surround axial midline structures, and then differentiate into cartilage and bone. This results in the development of the vertebral column. In zebrafish embryos (anamniote), although there are specific single cells that are known to give rise to both myotome and sclerotome cells, a lineage of single cells in the ventral somite has been demonstrated to form sclerotome cells (Stickney et al., 2000). Simultaneously, on the molecular level, expression of specific genes influences the segmentation, such as the Hox family of genes. The morphological diversity and axial position of the various types of vertebrae occurs due to positional cues coming from regional *Hox* gene expression, as was revealed in mouse and chicken studies (Mallo et al., 2010; Pineault and Wellik, 2014).

The developing zebrafish notochord is made up of stacked cells that are of two types: vacuolated cells (VC) and an outer monolayer of chordoblasts that are referred to as notochord epithelium cells or the notochordal sheath cells (NSCs) as shown in (**Fig. I-21**) (Pogoda et al., 2018b).

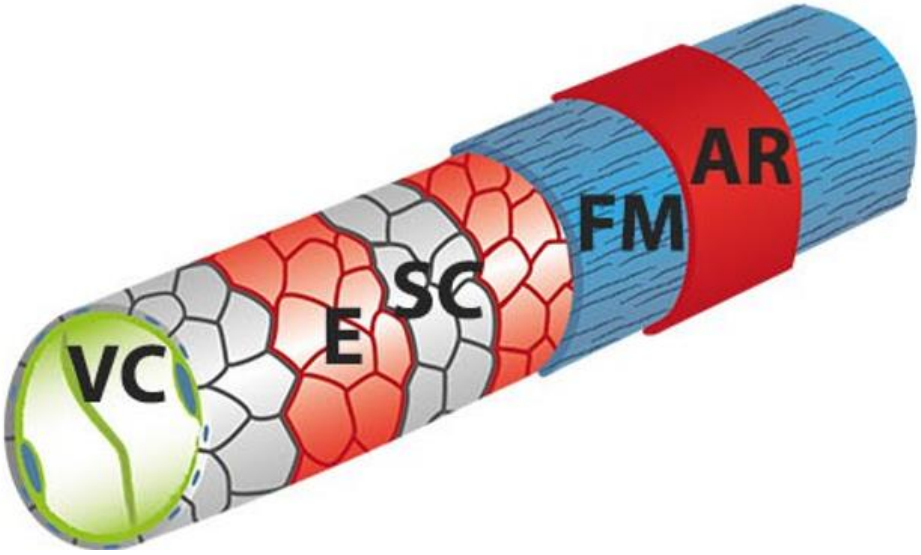


**Figure I-21. A simplified graphical layout depicting the zebrafish notochord.** The innermost cells of the notochord are the vacuolated cells (VC) and the alternating pattern of grey cells, which are *entpd5a* negative, are the notochordal sheath cells (SC) followed by red cells which become *entpd5a* positive at 6 dpf (E). The sheath cells are surrounded by a fibrous matrix (FM) that undergoes mineralization in *entpd5a* positive areas and can be detected by alizarin red staining (AR). It is important to note that the segmental expression of *entpd5a* in notochord sheath cells indicates the sites of chordacentra mineralization. The zebrafish notochordal sheath cells

have been shown to form alternating domains consisting of mineralizing domains (*entpd5a* positive) and non-mineralizing domains (grey cells), also called the "other cartilage-like domains". Figure adapted from (Lleras Forero et al., 2018).

In zebrafish, the vertebral body precursors (centra) do not develop through an intermediary cartilage stage. Instead, the early larval notochord directly secretes the bone matrix that makes up the centra, via the mineralization of the notochordal sheath, a collagen 2-based matrix deposed by the outer cells /chordoblasts. This bone lacks osteoblasts (Bensimon-Brito et al., 2012) (Fleming et al., 2004). Mineralization of the notochordal sheath requires Entpd5a that is crucial for bone formation which then aids in the recruitment of *sp7*+ osteoblasts in the mineralized domain (*entpd5a*-positive cells) (**Fig. I-21**), whereas the *entpd5a*-negative domain/ the cartilage-like domain could somehow contribute to the specification of intervertebral discs (Wopat et al., 2018). These segments of the mineralized notochord sheath, which are referred to as chordacentra, are subsequently encircled by a bone structure known as autocentra that is composed of somite-derived scleroblasts which do not have a cartilaginous foundation (Arratia et al., 2001; Bensimon-Brito et al., 2012; Grotmol et al., 2003; Inohaya et al., 2007). It is important to note that in zebrafish, even though segmentation clearly operates, disruption of the paraxial segmentation does not affect the normal segmentation of the chordacentra; their mineralization takes place independently, under the influence of axial notochord sheath cells (Fleming et al., 2004; Lleras Forero et al., 2018).

### 2.2.2. Fins

The majority of fish have two sets of fins: two pairs of abdominal fins, which prefigure the paired limbs in vertebrates, and a group of midline fins along the anterior to posterior body axis known as the unpaired or median fins (Cubbage and Mabee, 1996). The dorsal, anal, and caudal fins, as well as their bony internal support elements and external supports, are all part of the median fin rays (**Fig. I-22**) (Siomava and Diogo, 2018).

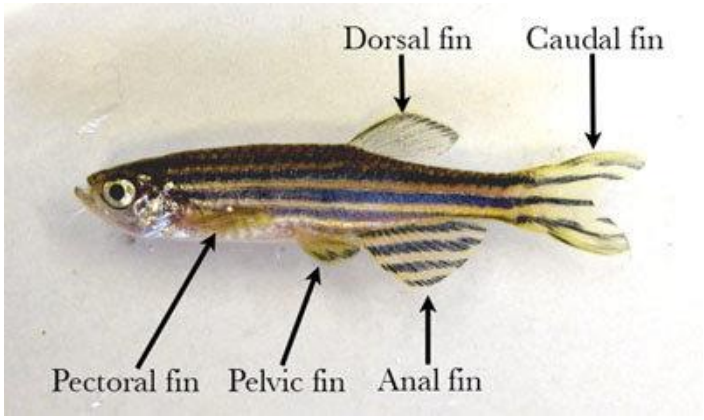


**Figure I-22.Photograph of adult male zebrafish showing the different fins.** The abdominal fins are also called the pectoral fins and the pelvic fins are paired, whereas the anal fin, dorsal fin and caudal fins are unpaired. (Gupta and Mullins, 2010).

In zebrafish, the potential contribution of the trunk neural crest to the caudal fin has been reported and investigated (Kague et al., 2012). The caudal fin is the first fin to develop in zebrafish, followed by the anal and finally the dorsal fin radials and the fin rays. It has been reported that the exoskeleton and endoskeleton of both the dorsal and anal fins develop bi-directionally (Bird and Mabee, 2003). The positioning of the dorsal and anal fins has not been clearly documented in zebrafish, but the influence of the *hox* and *tbx* gene expression has been reported in sharks (Freitas et al., 2006). Moreover, the influence of *hox* family gene expression and other factors like retinoic acid (Spoorendonk et al., 2008) haven been linked in early stages of development to the formation of the pectoral fins owing to their striking similarity to tetrapod limbs. *Wnt*, *Shh* and *Fgf* signaling pathways also play an important role in patterning of the appendage/limb development (Gibert et al., 2006; Grandel et al., 2000; Le Pabic et al., 2022a; Mercader et al., 2006).

# 3. TOOLS FOR STUDYING ZEBRAFISH SKELETOGENESIS

Zebrafish is a great candidate for the screening of various novel osteogenic and/or mineralogenic compounds or for investigating the effect of drugs or inhibitors as the skeletal structures, can be easily assessed through whole-mount/live staining methods (**Fig. I-23**). Different ways to visualize cartilage and mineralized skeletal structures during early developmental stages are available in zebrafish. Alcian blue stains the cartilage glycoproteins and sulfated glycosaminoglycans (**Fig. I-23. A**) (Gavaia et al., 2000; Walker and Kimmel, 2007), Alizarin Red-S (ARS) visualizes ossified bone matrix / mineralized skeletal structures in fixed embryos (**Fig. I-23. B**) or live staining zebrafish larvae using 4-amino-5-methylamino-2'-7'-difluorofluorescein diacetate (DAF-FM-DA), detecting nitric oxide (NO) (Kojima et al., 1999; Lepiller et al., 2007), could reveal developing bone elements and, weakly cranial cartilages (**Fig. I-23. C**) (Renn, 2014). Additionally, the mineralized skeletal elements can be visualized in living specimens using live ARS stain (**Fig. I-23. D**), and also by calcein that labels calcified skeletal structures (Du et al., 2001).

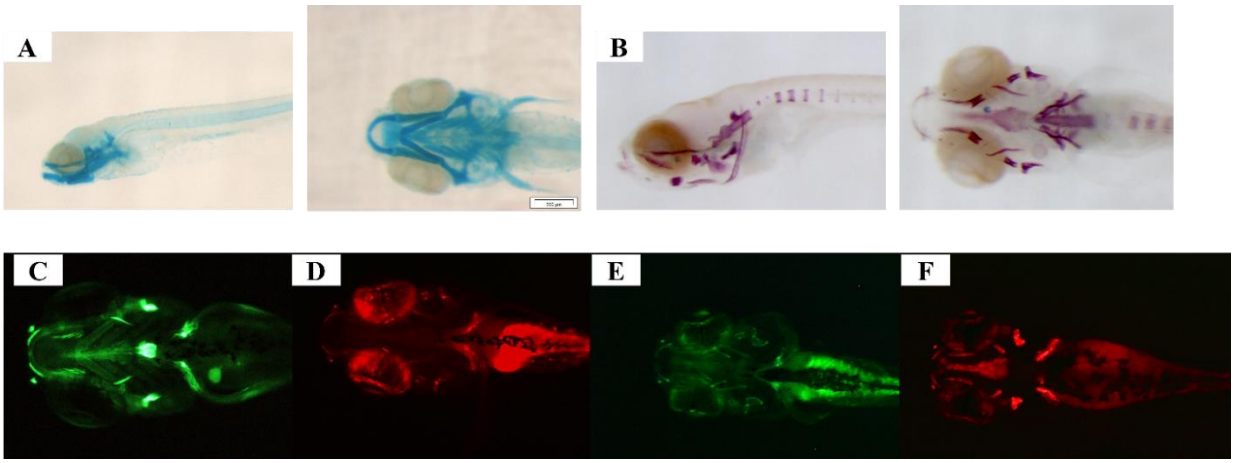


**Figure I-23. Different methods to visualize zebrafish bone and cartilage during early developmental stages.** (A) Cartilage elements can be visualized by alcian blue staining in developing zebrafish larvae at 5 dpf in both lateral and ventral positions. (B) Developing bone elements can be visualized by alizarin red (ARS) staining on fixed embryos at 10 dpf in lateral and in ventral views. (C) DAF-FM-DA live stain at 4 dpf detects NO in developing bone elements and also weakly stains the cranial cartilage elements. (D) Mineralized skeletal structures can be visualized by live ARS stain in living specimen. The image shown in panel (D): is of 4 dpf zebrafish larvae. (E, F) Using *Tg* reporter lines one can also visualize the developing skeletal elements at various stages of zebrafish development live in either green or red fluorescence for example at 4 dpf. (E) *Tg* reporter line (*Tg(sp7:sp7-GFP)*) where GFP expression is driven by the zebrafish endogenous *osx*/*sp7* promoter gene, a marker for osteoblasts and (F) *Tg* reporter line (*Tg(Ola.Sp7:mCherry)*) where mCherry expression is driven by the medaka *osx*/*sp7* gene promoter.

In addition to the state of the art staining techniques for skeletal and cartilage structures, there are several transgenic reporter lines that have been generated in several research labs to label skeletal lineages at different stages using specific bone marker genes (Hammond and Moro, 2012). These lines enable studies in living animals at the cellular level with increased

morphological resolution, as the expression of fluorescent proteins is driven by or under the control of bone-related promoters. To highlight a few, *Tg(1.7col2a1a:mCherry-caax)* labels chondrocytes (Dale and Topczewski, 2011), preosteoblasts are labelled in *Tg(runx2:GFP)* (Kague et al., 2012), intermediate osteoblasts are revealed in lines where the transgene expression is driven by an *sp7*/*osx* promoter, such as *Tg(sp7:sp7-GFP)* (Sojan et al., 2022), *Tg(Ola.sp7:NLS-GFP)zf132*, *Tg(sp7:EGFP)b1212* (DeLaurier et al., 2010b; Spoorendonk et al., 2008), *Tg(Ola.sp7:mCherry)* (Windhausen et al., 2015), *Tg(osterix:GFP)* (DeLaurier et al., 2010b). Mature osteoblasts are labeled in *Tg(ocn:GFP)* (Knopf et al., 2011) and osteoclasts in *Tg(Ctsk:YFP)* (Sharif et al., 2014). The *Tg(col10a1a:col10a1a-GFP)* is a transgenic line where the expression of a fusion protein between Col10a1a and GFP is driven by the endogenous *col10a1a* zebrafish promoter, which then binds to and visualizes unmineralized and mineralized bone matrix by GFP fluorescence (Sojan et al., 2022). A table listing the available transgenic reporter lines as of 2020 is shown below (**Table 1**)**.** Using these lines in conjunction with live staining methods (Calcein, Alizarin red, or DAF-FM-DA) enables to visualize and monitor skeletal development and cell maturation dynamically in a live setting, advancements in microscopic imaging techniques (confocal, light sheet) open the way to tracking the cells in real time at various specific stages, thus making these resources relevant to be employed in studying zebrafish skeletal development.

| Cell type | Gene/pathway | Transgenic line |
|---|---|---|
| Neural crest-derived skeletal cells | *sox10* | Tg*(sox10:GFP)*$^{ba5}$ |
| | *sox10* | Tg*(sox10:kaede)*$^{zf393}$ |
| | *sox10* | Tg*(sox10:mRFP)*$^{vu234}$ |
| | *sox10* | Tg*(-4725sox10:Cre)*$^{ba74}$ |
| | *sox10* | Tg*(−4.9sox10:egfp)*$^{ba2}$ |
| | *fli1* | Tg*(fli1:EGFP)*$^{y1}$ |
| Cartilaginous cells | *foxp2* | Tg*(foxp2-enhancerA:EGFP)*$^{zc42}$ |
| | *col2a1a* | Tg*(Col2a1aBAC:mcherry)*$^{hu5910}$ |
| | *col2a1a* | Tg*(-1.7col2a1a:EGFP-CAAX)*$^{nu12}$ |
| | *col18a1* | Tg*(16Hsa.COL18A1-Mmu.Fos:EGFP)*$^{zf215}$ |
| Preosteoblasts | *cyp26b1* | Tg*(cyp26b1:YFP)*$^{hu5786}$ |
| | *cyp26b1* | *Tg(cyp26b1:YFP)*$^{hu7426}$ |
| Branchial arches and notochord cells | *cyp26a1* | Tg*(cyp26a1:eYFP)*$^{nju1/+}$ |
| Intervertebral disc cells | *shhb* | Tg*(-5.2shhb:GFP)*$^{mb1}$ |
| | *twist* | Tg*(Ola.twist1:EGFP)*$^{ca104}$ |
| Early osteoblasts | *osx/sp7* | Tg*(sp7:EGFP)*$^{b1212}$ |
| | *osx/sp7* | Tg*(Ola.sp7:mCherry)*$^{zf131}$ |
| | *osx/sp7* | Tg *(Ola.sp7:NLS-GFP)*$^{zf132}$ |
| | *osx/sp7* | Tg*(osterix:mCherry-NTRo)*$^{pd46}$ |
| | *osx/sp7* | Tg*(osx:Kaede)*$^{pd64}$ |
| | *osx/sp7* | **Tg*(osx:CFP-NTR)*** |
| | *osx/sp7* | Tg*(osx:H2A-mCherry)*$^{pd310}$ |
| | *osx/sp7* | Tg*(osterix:Lifeact-mCherry)*$^{°u2032}$ |
| | *col10a1* | Tg*(Col10a1BAC:mCitrine)*$^{hu7050}$ |
| | *col10a1* | Tg*(-2.2col10a1a:GFP)*$^{ck3}$ |
| | *runx2* | Tg*(Hsa.RUNX2-Mmu.Fos:EGFP)*$^{zf259}$ |
| | *runx2* | Tg*(RUNX2:egfp)* |
| Mature osteoblasts | *osc/bglap* | Tg*(Ola.bglap.1:EGFP)*$^{hu4008}$ |
| | *entpd5a* | Tg*BAC(entpd5a:YFP)*$^{hu5939}$ |
| | *entpd5a* | *TgBAC(entpd5a:Kaede)*$^{hu6867}$ |
| | *col1a1* | Tg*(col1a1:EGFP)*$^{zf195}$ |

| | | |
|---|---|---|
| | *rankl* | **Tg*(rankl:HSE:CFP)*** |
| | *notch1a* | Tg*(Ola.sp7:N1aICD)*$^{cy31}$ |
| Osteoclasts | *ctsk* | Tg*BAC(ctsk:Citrine)*$^{zf336}$ |
| | *ctsk* | Tg*(ctsk:YFP)* |
| | *ctsk* | Tg*(ctsk:DsRed)* |
| | *ctsk* | **Tg*(CTSK-DsRed)*** |
| | *ctsk* | Tg*(Ola.ctsk:EGFP)*$^{zf305}$ |
| | *ctsk* | **Tg*(ctsk:mEGFP)*** |
| | *trap* | **Tg*(TRAP:GFP)*** |
| | *trap* | Tg*(trap:GFP-CAAX)*$^{u2031}$ |
| Bmp responsive cells | Bmp pathway | Tg*(Bre:GFP)*$^{p77}$ |
| | Bmp pathway | Tg*(bre:egfp)*$^{pt510}$ |
| | Bmp pathway | Tg*(BMPRE:EGFP)*$^{ia18}$ |
| β-catenin activated cells | Wnt pathway | Tg*(7xTCF-Xla.Siam:GFP)*$^{ia4}$ |
| | Wnt pathway | Tg*(7xTCFXla.Siam:nlsmCherry)*$^{ia5}$ |
| | Wnt pathway | Tg(*hsp70l:wnt8a-GFP*)$^{w34}$ |
| | Wnt pathway | Tg(*hsp70l:dkk1-GFP*)$^{w32}$ |
| | Wnt pathway | Tg(*myl7:EGFP*)$^{twu34}$ |
| Stress responsive cells | UPR pathway | Tg*(ef1α:xbp1δ-gfp)*$^{mb10}$ |
| | UPR pathway | Tg(Hsa.*ATF6RE:*d2GFP)$^{mw85}$ |
| | UPR pathway | Tg(Hsa.*ATF6RE:*eGFP)$^{mw84}$ |

**Table 1. Table showing the list of *Tg* reporter lines developed and available to utilize for investigating skeletal development in zebrafish** (Tonelli et al., 2020).

It also very convenient to visualize and study in detail the architecture of the adult zebrafish skeleton with the help of state-of-the-art imaging techniques, such as X-Ray and micro–computed tomography (µ-CT) as depicted in (**Fig. I-24. A-B**) (Boerckel et al., 2014; Hur et al., 2017). Using µ-CT scans of the zebrafish spine, 3D morphometric parameters, such as vertebral body length (VL), bone volume, bone volume per tissue volume, vertebral cross-sectional thickness (V.Th), and eccentricity (i.e., roundness) can be extracted (**Fig. I-24. D**) (Fiedler et al., 2018; Hur et al., 2017; Watson et al., 2020a). This helps to understand the overall skeletal wellbeing of the fish. Moreover, instead of calculating bone mineral density (BMD), its equivalent tissue mineral density (TMD) is calculated, measuring the amount of mineral in bone tissue per unit volume (Kwon et al., 2019). These parameters aid in evaluating changes in the vertebral morphology in zebrafish skeletal mutants that could be due to aging, disease/anomalies or altered musculoskeletal activity.

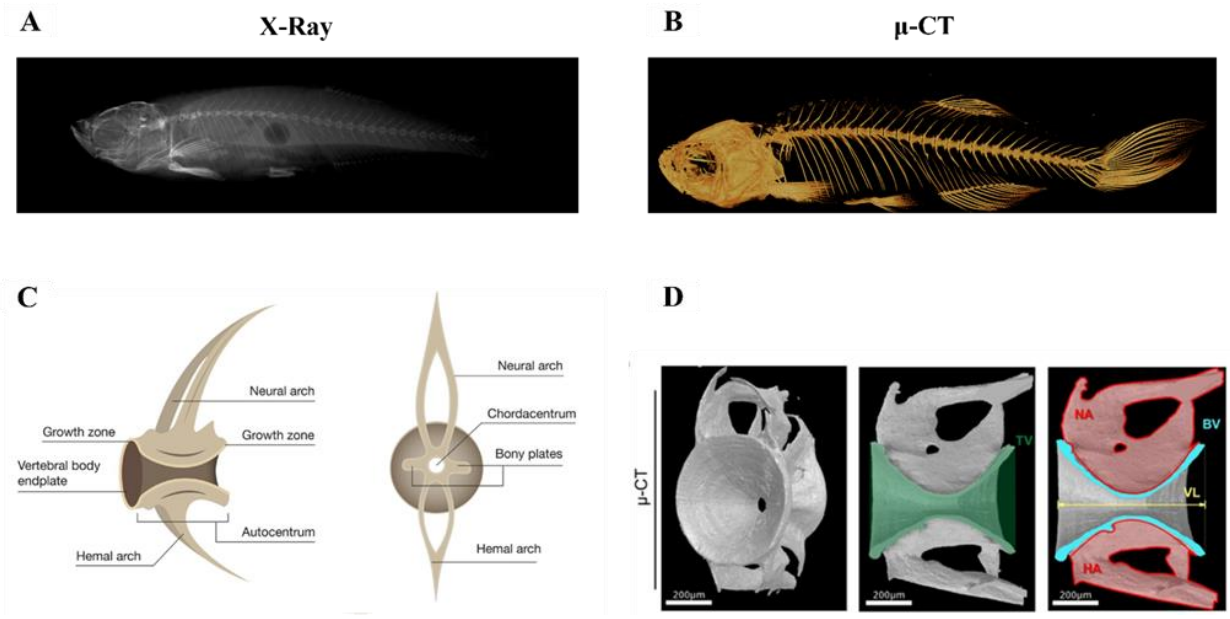


**Figure I-24. Different modalities that can be employed to study and analyze the zebrafish bone structure.** (A) X-ray image showing the zebrafish adult skeleton, that is generally used for an explorative investigation to identify the region of interest or the volume of interest. (B) µ-CT image on the entire adult zebrafish skeleton. (C) Schematic representation of a single vertebral body in lateral position (left) and transverse cross section (right). The image shows the typical hour-glass shape of the autocentrum that forms the core of the vertebral body. (D) The structural parameters that can be measured on the sagittal cross sections of the vertebrae: tissue volume, bone volume, vertebral length (VL) and vertebral thickness (VTh). Figure adapted from (Vimalraj et al., 2021).

## 3.1. Types of ossification in zebrafish and cell types.

The zebrafish bones develop through endochondral, intramembranous, or perichondral ossification (**Fig. I-25. A-B**) (Tonelli et al., 2020).

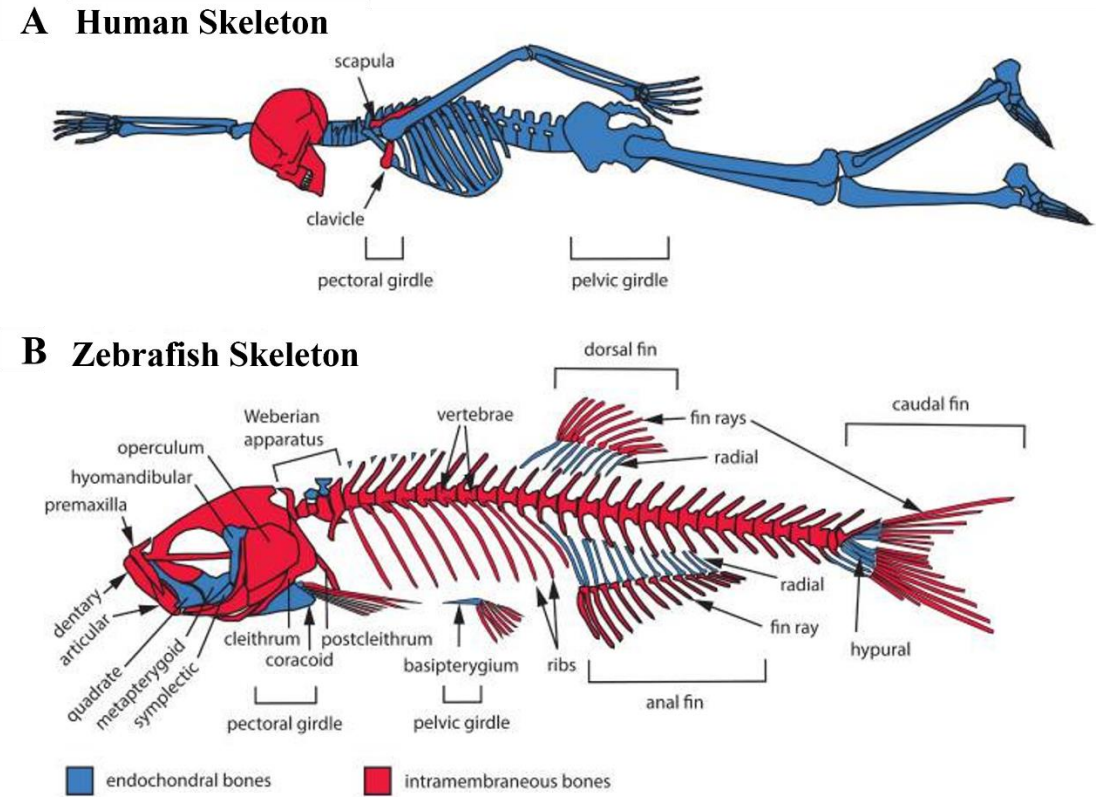


**Figure I-25. Overview of different types of ossification observed in zebrafish in a comparative view alongside humans.** (A) Adult human skeleton in its entirety. In the human skull, intramembranous bones, such as those of the calvaria (the top region of the neurocranium), predominate in terms of surface area. On the other hand, endochondral bones primarily inhabit the cranial base. All the bones that make up the trunk and appendicular skeletons are endochondral, with the exception of certain parts of the clavicle and the scapula. (B) Adult zebrafish skeleton. The primary kind of ossification observed in the zebrafish skeleton is intramembranous ossification. Example elements such as the cranial roof, cleithrum, opercles, and most of the vertebrae are formed by this process. On the other hand, only a few parts are created through endochondral ossification, in which a cartilage template is gradually replaced by bone, including the neural arches of vertebrae 1 to 5. In the lower zebrafish jaw, perichondral ossification takes place on a chondral surface without changing the cartilage template. Perichondral ossification begins with the transition of perichondrium into periosteum and therefore is also considered as a type of intramembranous ossification. Whereas the zebrafish vertebral centrae directly mineralize from the notochord sheath, (a layer around the notochord), following an intramembranous ossification, whereas this is completely different in mammals where the vertebrae are formed through a cartilage intermediate (Le Pabic et al., 2022a).

The zebrafish skeleton / bone have more or less the same skeletal cells as those found in mammals: chondrocytes, osteoblasts, osteoclasts (Dietrich et al., 2021b) and osteocytes (Witten and Huysseune, 2009). In addition, the genes that regulate skeletal development are evolutionarily conserved across vertebrates. A considerable proportion of the zebrafish bone

surface is covered by osteoblasts, whose shape is highly variable and dependent on their location (Tonelli et al., 2020). There are three overlapping stages in the differentiation of osteoblast, each characterized by a specific marker gene. Preosteoblasts express *runx2a* and *runx2b* that characterize the early stage, the intermediate stage is characterized by *sp7*/*osterix* (*sp7*) expression and lastly mature stage osteoblasts express late differentiation marker genes, including predominantly *bglap*/*osteocalcin* (*ocn*), osteonectin (*osn*), *spp1*, *collagens* and other bone matrix genes (Brown et al., 2009; Valenti et al., 2020). In particular *bglap* (bone gamma-carboxyglutamate protein or osteocalcin) is a small osteoblast-secreted protein that is widely accepted as the marker for matrix-secreting mature osteoblast (Gavaia et al., 2006).

Both *runx2* genes are expressed in cartilage and bone primordia at 24hpf, while at 36 hpf, *sp7*/*osx* expression starts in the entire skeletal system alongside the *runx2* pre-osteoblast marker genes (Valenti et al., 2020). Conservation is high between the zebrafish and human SP7 protein, reaching 92% in the zinc finger domain responsible for targeting DNA regions for transcriptional regulation (Liu et al., 2020; Nakashima et al., 2002). Moreover, *SP7* is one of the highly conserved "bone genes" across species, it is a zinc finger transcription factor exclusively expressed by osteoblasts that is essential for differentiation and maturation of osteoblasts and the formation of osteocytes (Wang et al., 2021). Sp7 acts downstream of the Runx2 factors, its expression is regulated by the Shh pathway (Avaron et al., 2006) and controls the transcription of several bone matrix genes like *bglap*, collagen1a (*col1a)*, and alkaline phosphatase (*alpl*) (Huang et al., 2007). Mutation of the *sp7* gene leads to delayed osteoblast differentiation, increased proliferation of early osteoblasts and increased *BMP* signaling which causes defects in bone growth, irregular skull bones and mineralization (Chen et al., 2019; Kague et al., 2016). In addition, *sp7* mutation results in significant downregulation of genes such as *bglap, spp1, col1a1a, col1a1b* and *sost*, all involved in bone and chondrocyte development (Niu et al., 2017). The *col10a1a* gene, encoding the type X collagen alpha chain, was also significantly downregulated in the zebrafish *sp7* mutant (Niu et al., 2017), in contrast to what is observed the *Sp7* null mutant mouse (Nakashima et al., 2002). Actually, in zebrafish, *col10a1a* is expressed in immature osteoblasts (Kim et al., 2013b; Li et al., 2009)overlapping with the expression of *sp7* and other bone matrix genes (Avaron et al., 2006) unlike what is observed in mammals.

Osteoblasts that surround themselves with bone matrix eventually transform into osteocytes, as zebrafish have cellular bones, unlike other teleosts such as medaka. Osteoblasts that stay on the bone surface facing the periosteum can either become inactive bone-lining cells or experience apoptosis. However, when there is a requirement for mature osteoblasts in case the population dwindles (either due to natural turnover or to a regenerative process requiring fresh recruitment, *e.g.* amputation), new osteoblasts are generated (Knopf et al., 2011). Osteoblasts then downregulate the mature osteoblast marker *bglap*, followed by upregulation of the pre-osteoblast marker *runx2b*, resulting in cell proliferation before giving rise to immature osteoblasts that express *sp7*, repopulate and relocate to the region of injury to start the process of regeneration (Sehring et al., 2022; Stewart and Stankunas, 2012). These dedifferentiated osteoblasts have been reported to remain lineage-restricted and to re-differentiate to osteoblasts during regeneration (Sousa et al., 2011).

There are several genes and signaling pathways that play an important role during the intermediate and late stages of osteoblast differentiation. For example, *Tcf7* has been shown

to be a mediator of the *WNT* signaling pathway and *cvl2* a mediator of the *BMP* pathway; both are expressed in all bone precursors and in developing dermal and cranial bones (Valenti et al., 2020). Hedgehog (*Hh*) signaling is another crucial pathway that regulates the osteogenic differentiation and the mineralization process, partially through inhibiting the process of autophagy (Hu et al., 2019) which itself inhibits the expression of osteoblast related genes such as *sp7*, *bmp2* and *col10a1a* (Bae et al., 2016; Nakamura et al., 2015). Additional studies indicate that genes like *akt2*, *sparc*, *dlx*, *shox*, *bmp1a* and the collagen family of genes like *col1a1a*, *col1a1b* and *col1a2* also have their role in bone development, development of the inner ear and the pharyngeal cartilage, osteoblast differentiation, bone matrix deposition and mineralization during skeletal development in zebrafish (Gistelinck et al., 2016; Levi et al., 2022). The detailed importance of the *BMP* signaling pathway in skeletal development of zebrafish is described in a section below.

Mononucleated and multinucleated osteoclasts are responsible for zebrafish bone resorption (Witten et al., 2001). Although mononucleated osteoclasts are present in the early stages of development and are associated with shallow resorption patterns, multinucleated osteoclasts create resorption lacunae, which are typically described for mammalian osteoclasts in later life (Witten and Huysseune, 2009). The interplay and balance between bone formation and resorption is a key factor in bone remodeling for the maintenance of a healthy skeleton.

## 3.2. Mineralization of the bone matrix in zebrafish

The bone matrix secreted by the mature osteoblasts consists of a soft matrix that is predominantly composed of Collagen I, other collagens and non-collagenous proteins that eventually hardens due to incorporation of hydroxyapatite to result in hardened vertebrate bone. Mutations in several collagen genes cause skeletal abnormalities in zebrafish, indicating their importance in the formation of bone matrix (Eyre and Weis, 2013). Proteins such as Osteopontin, Osteocalcin (Bglap), Matrix Gla protein (Mgp) (Gavaia et al., 2006), alkaline phosphatase (Alpl) (Miyake et al., 1997; Shibata et al., 1997) and bone sialoprotein (Bsp) (Malaval et al., 2008) are present in the bone matrix that bind to the hydroxyapatite crystals, thereby regulating the mineralization process (Shibata and Yokohama-Tamaki, 2008). Mgp is a vitamin K-dependent protein that inhibits hydroxyapatite crystal formation, *Mgp* null mice display ectopic mineralization of arteries that leads to rupture followed by early death in the initial two months (Luo et al., 1997).

Even though the macromolecular and elemental composition of bone matrix are identical in mammals and zebrafish, some degree of difference in mineralization has been observed. In contrast to tetrapods, whose (Calcium) Ca and (Phosphorus) P based bone matrix depends on the dietary intake of P and Ca, zebrafish absorb Ca through their gills from their Ca-rich environment (Dietrich et al., 2021b). However, P is acquired through diet, and low P and high P can have detrimental effects on skeletal development and affect mineralization in zebrafish (Costa et al., 2018). Interestingly, reduction of P levels in the diet results in an excess of non-mineralized matrix (Cotti et al., 2020), that can later mineralize upon restoration of a normal P diet. Similar results were observed in salmon (Drábiková et al., 2021). It is believed that locally, in the osteoblast and its microenvironment, phosphatases such as phosphatase orphan 1 (Phospho1) or tissue-nonspecific alkaline phosphatase (Tnap/Alpl) are crucial for the initiation of mineralization (Stewart et al., 2006). Alpl is an

enzyme that promotes hydroxyapatite crystal formation (Yagami et al., 1999). Mutations in the human *ALPL* gene has been shown to cause hypophosphatasia (Whyte, 2017), a rare hereditary disorder characterized by a wide range of systemic symptoms, such as mineralization defects of bones and teeth, premature loss of teeth and craniosynostosis (Whyte, 2017). Recently, it was shown that knockdown of *alpl* and/ or Alpl chemical inhibition in zebrafish cause decreased mineralization, impaired cartilage and bone development, and neuronal defects (Chen et al., 2017; Ohlebusch et al., 2020). Hence, in fish, phosphate is essential for normal skeletal mineralization and maintenance of bone health.

One of the most important factors that determines bone mineralization and extracellular phosphate is encoded by the interplay between the Entpd5, Tnap/Alpl and Enpp1 proteins, that govern the levels of extracellular phosphate and pyrophosphate, as described in (**Fig. I-26)**.

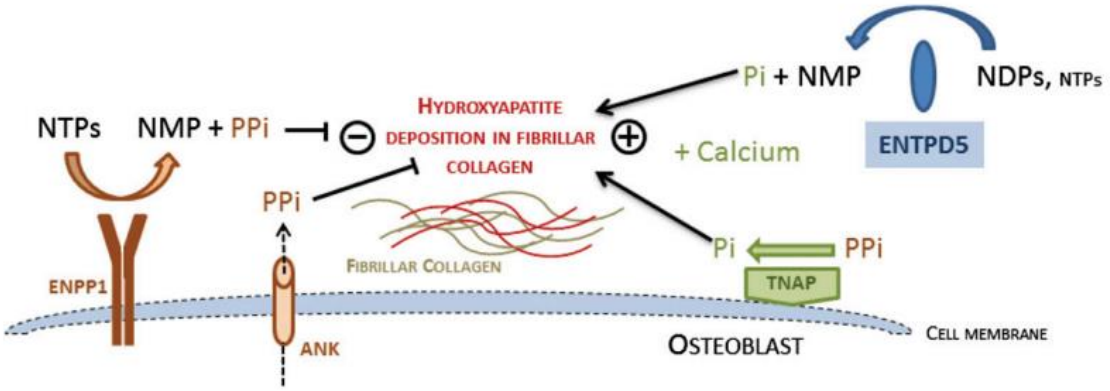


**Figure I-26. Importance of the *entpd5*, *enpp1*, *tnap*, and *ank* genes in extracellular phosphate concentration and bone mineralization.** Pyrophosphate is produced from NTPs through the action of Enpp1 and is also exported from cells through the Ank transmembrane channel. The biomineralization process that takes place on the fibrillar collagen matrix, is inhibited by pyrophosphate. This inhibition is counteracted by the tissue-nonspecific alkaline phosphatase (TNAP)-mediated hydrolysis. The free phosphate thus generated is crucial for proper mineralization. ENTPD5 significantly contributes to the generation of sufficiently high amounts of free phosphate, via hydrolyzing nucleotide diphosphates (NDPs) (and, to a lesser extent, also NTPs). The essential role of TNAP for the process of mineralization has been demonstrated in mammals (Yadav et al., 2011). The role of both ENTPD5 in mammals and the relative contributions of TNAP in teleosts are yet to be determined. Evidence in zebrafish show that the absence of Enpp1 activity in the dragonfly (*dgf*) mutant embryos causes a decrease in the amount of pyrophosphate, resulting in a shift in the phosphate/pyrophosphate balance towards higher phosphate levels, which leads to an increase in (ectopic) mineralization. On the contrary, mutations in the *entpd5a* gene results in lower phosphate levels in the nobone (*nob*) mutants, shifting the balance in favor of the pyrophosphate which ultimately results in no mineralization (Huitema et al., 2012). This interplay between the proteins involved in maintaining the extracellular phosphate concentration and bone mineralization was elucidated by studying the zebrafish genes, however it implies to all the vertebrates.

# 4. BMP SIGNALING

Bone morphogenetic proteins (BMPs) belong to the Transforming Growth Factor beta (TGF-β) superfamily that play an important role in many biological processes (Jiramongkolchai et al., 2016), however their role in all the processes related to skeletal morphogenesis is widely recognized (Chen et al., 2004b). As their name suggests, they were discovered and isolated as proteins that influence and have a role in cartilage and bone formation. BMPs are the largest subfamily of the TGF-β family, and their amino acid sequences are highly conserved from invertebrates (insects) to vertebrates (humans) (Newfeld et al., 1999). Based on their structural and sequence homology, the more than 20 BMP ligands have been classified into various groups, several of which are capable of signaling either as homodimeric or heterodimeric proteins, wherein heterodimeric forms show increased osteoinduction activity, except for BMP-3 and BMP-15 that were shown to act as monomers (Israel et al., 1996; Koosha and Eames, 2022). These ligands are acting in autocrine, paracrine, or endocrine fashion by binding to a heterotetrameric receptor complex composed of two BMPRI and two BMPRII transmembrane serine/threonine kinase receptors, thereby activating the type II receptor, as depicted below (**Fig. I-27. A**). This in turn cross-phosphorylates certain serine and glycine residues in the GS domain of the type I receptor. Interestingly type I receptors contain a segment of around 30 residues that is rich in serine and glycine, which is located between the transmembrane and kinase domains (Jsbrand and Kramer, 2016), the GS domain (Leung and Peng, 2003). Phosphorylation of the GS domain is a crucial in the transmission of signals by these serine/threonine kinase receptors. (Miyazono and Shimanuki, 2008) The crystallographic analysis of the intracellular domain of TβR-I demonstrated that the inactive state of the TβR-I kinase is sustained through a physical interaction between the GS domain, the N-terminal lobe, and the activation loop of the kinase (Huse et al., 1999). Intracellularly, BMP signaling is transduced by a canonical Smad route and a non-canonical p38 pathway (Kim and Choe, 2011). It has also been shown that the activated BMPRs phosphorylate TAK1 in the noncanonical route, which attracts TAB1 and triggers a p38 MAPK signaling cascade that phosphorylates p38 enabling it to enter the nucleus which influences the expression of *Runx2*, *Dlx5*, and *Sp7* in pre-osteoblasts to boost their transcriptional activity (Grafe et al., 2018). Activated BMPRs phosphorylate and activate receptor-specific Smad1, 5, and 8 (R-Smads), which attract and bind Smad4 (co-Smad) to form heteromeric complexes that translocate into the nucleus, thereby initiating the transcription of its target genes by binding to the promoter and the cofactors (Derynck and Zhang, 2003; Massagué et al., 2005). BMP-activated Smad complexes regulate the expression of important osteogenic genes and recruit transcription factors such as Hoxc-8, FAST-1, OAZ, Runx2, AP-1, and STAT3 during chondrocyte maturation (Johansson et al., 1997; Tsumaki et al., 2004). Smad 6 and Smad 7 are regarded as inhibitory Smads (I-Smads) that compete with R-Smads to bind the type I receptor and thus prevent it from phosphorylating or binding to co-Smads and stop it from binding to R-Smads. Apart from I-Smads, extracellular inhibitors such as Noggin, Chordin, and Follistatin are known to block receptor activation by binding to BMP ligands, thus inhibiting BMP signaling (Lowery and Rosen, 2018). In addition, intracellular inhibitors like Smurfs suppress phosphorylation of R-Smads, thereby blocking BMP signaling (**Fig. I-27. B**).

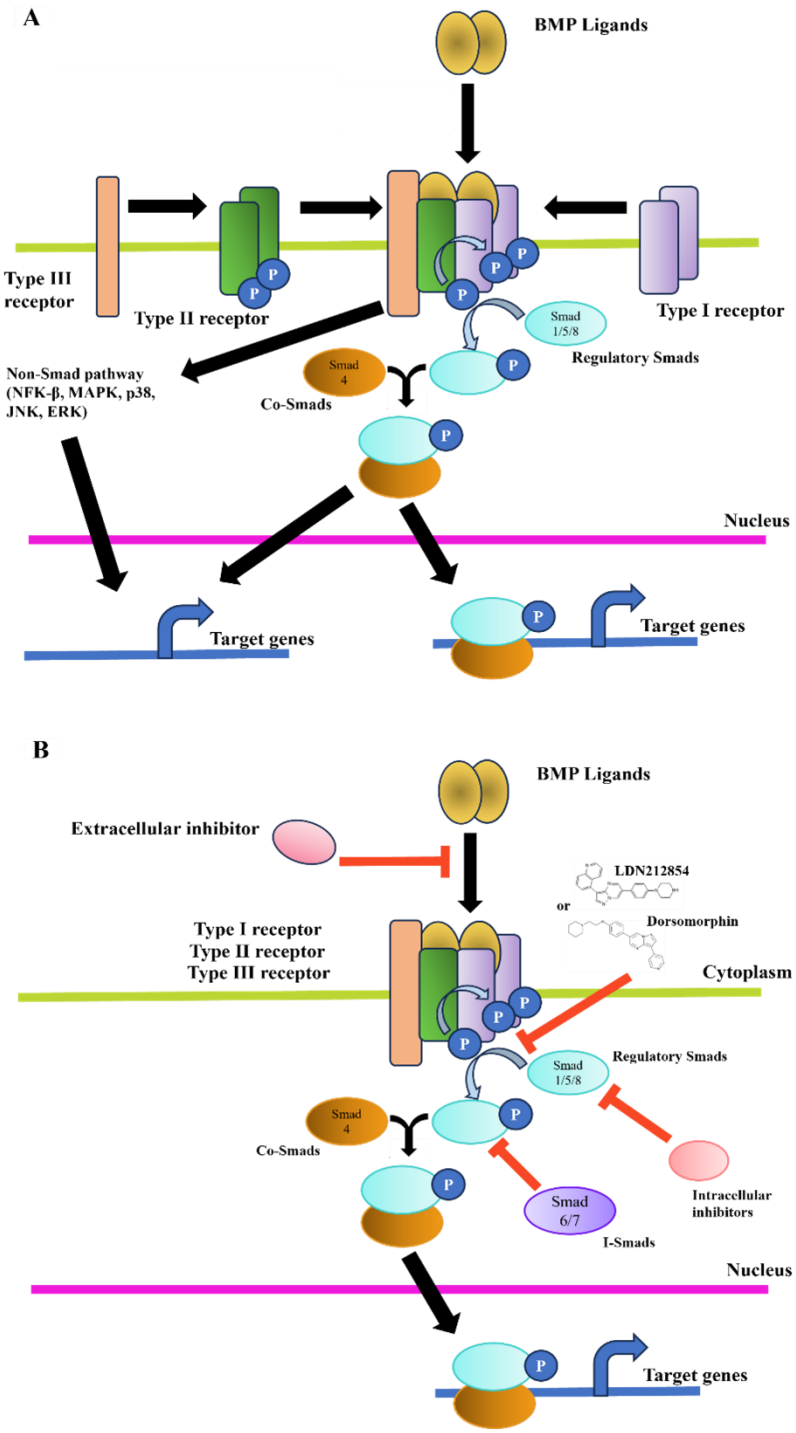


**Figure I-27. Schematic illustration of BMP signaling pathway and the inhibitors. (A) BMP signaling pathway.** The secreted BMP ligand binds to BMPR (receptor complex), leading to the active kinase domain of the Type II receptor to phosphorylate the receptors type I and III respectively. The Smad pathway is activated by phosphorylating the regulatory Smads (R-Smads 1/5/8) by the type I receptor. The activated R-Smads (1/5/8) couple with co-Smad (Smad4) so as to translocate to the nucleus to commence the process of transcription of specific target genes. Upon dimerization, the activation of type I and type II receptors can result in the stimulation of other intracellular transduction signals, which are not dependent on the R-Smads such as the ERK, MAPK, P38M JKN and NFK-β. **(B) BMP signaling inhibitors.** Extracellular inhibitors can form a compound with BMP ligand, hence obstructing its ability to bind to its receptor. Smurf 1/2 (Intracellular inhibitors) and Smad 6/7 (I-Smad) can inhibit the process of phosphorylation of Smad 1/5/8 and their subsequent binding to the co-factor Smad 4. Small molecule inhibitors such as Dorsomorphin (DM), DMH1, K02288 and LDN212854 are small molecules that competitively block the kinase activity of BMP type I receptor.

The drug dorsomorphin, a small molecule inhibitor, was the first BMP type I receptor inhibitor that was discovered in a large compound screening conducted in zebrafish, by disrupting the dorso-ventral patterning during early development in zebrafish (Yu et al., 2008). Exposure to dorsomorphin leads to embryonic dorsalization that mimics the effect caused by BMP antagonists like Noggin, Chordin, or Follistatin (Yan and Wang, 2021). It has been shown that the heterocyclic core of dorsomorphin interacts with the ATP binding site in the kinase domain of the BMP type I receptors (Yu et al., 2008), thus inhibiting the kinase activity (**Fig. I-27. B**) (Bai et al., 2017). Several other BMP inhibitors have been since then discovered, such as K02288, LDN193189, or LDN212854 that display significantly better selectivity for specific BMP receptors than dorsomorphin in lower dosages (Boergermann et al., 2010; Jiramongkolchai et al., 2016; Mohedas et al., 2013; Sanvitale et al., 2013).

In the zebrafish embryo, BMPs play well-established roles in driving the differentiation of ectodermal cells and mediating dorsal patterning to establish the dorsal-ventral axis (Medeiros and Crump, 2012), while also having a very important role in skeletogenesis (Salazar et al., 2016). For example, BMP-activated Smads increase the expression of crucial osteogenic genes and they assist in recruiting several transcription factors such as Runx2, Osterix/Sp7, and Sox9 (Chen et al., 2012). Bmps are involved in cartilage and bone development, where many of the Bmp family of proteins like Bmp2a, 2b, Bmp4, Bmp5 and Bmp7 are found to be secreted in the pharyngeal region (Holzschuh et al., 2005). Expression of the BMP extracellular inhibitor Chordin reduced deposition of bone matrix resulting from defect in the maturation of bone matrix secreting cells and down regulation of *runx2a*, *runx2b*, *sox9a*, *sox9b* and *col10a1a* expression (Smith et al., 2006). Additionally, it has been reported that BMP signaling is essential between 48-72 hpf and 72-96 hpf for bone mineralization in the head skeleton (Dalcq et al., 2012), while inhibition of BMP signaling predominantly affects the osteoblast function and not the proliferation or terminal differentiation ability of osteoblast (Windhausen et al., 2015). Disruptions of TGF-/BMP signaling have been associated to several bone diseases, such as tumor metastasis, brachydactyly type A2, and osteoarthritis (Wu et al., 2016b). Signaling pathways also interact with each other, for example studies have shown that *Ihh* expression is induced by BMP signaling, and both signals work together to govern cartilage formation by inducing the proliferation of chondrocytes (Minina et al., 2001).

# 5. OSTEOARTHRITIS (OA)

Osteoarthritis (OA) is a degenerative joint disease that falls under the skeletal anomaly category and is one of the most prevalent: OA continues to affect tens to millions of people irrespective of their age and sex worldwide (James et al., 2018). OA is predominantly a joint disease, it occurs mainly in synovial joints of the knee, hips, wrist joints of the hand, elbow, shoulder joints and ankle joints. The most commonly affected joint is the knee joint (Wallace et al., 2017). In 2016, a study conducted across India reported that almost 45% of females above 65 years of age show symptoms of knee OA, while 70% of females over 65 years of age show radiological evidence of knee OA (Pal et al., 2016). In Europe, a 2019 study conducted on the incidence of knee OA revealed approximately 576/100,000 cases in females and around 419/100,000 cases in males (Stewart, 2021). Hence, it is clear that OA as a progressive joint disease will be of increasing concern in the years to come.

OA is a chronic, progressive joint-related disorder that is characterized by articular cartilage (AC) degeneration, synovial inflammation, and changes in the periarticular and subchondral bone (Yuan et al., 2014). Therefore, OA is reportedly considered to be a degenerative cartilage disease similar to rheumatoid arthritis wherein the cartilage, synovium, bone and bone marrow, menisci, ligaments, muscles, and neural tissues are involved in the complex onset and progression (Lories and Luyten, 2011). Thus, progression of OA is a process that is due to abnormal remodeling and functional failure of joints (Loeser et al., 2012). In a healthy knee, the bone–cartilage interface is composed of a deep layer of calcified articular cartilage and the subchondral bone plate and trabecular bone underneath, separated by the tidemark. As a result, the bone–cartilage interface is a complex functional unit that is located at the heart of both the function and pathology of the joint. Within the confines of this particular setting, various components engage in cooperative and synergistic interactions with one another (Goldring, 2012b). Compared to a healthy knee joint (**Fig. I-28**), the joint of an OA patient displays a degradation of the articular cartilage that results in the destruction of the bone/cartilage interface which in normal circumstances acts as a protective layer, followed by subchondral bone remodeling that leads to neoangiogenesis and neurogenesis, thereby leading to the influx of inflammatory markers and attracting immune cells into the surrounding area which causes synovial inflammation and fibrosis (Goldring, 2009).

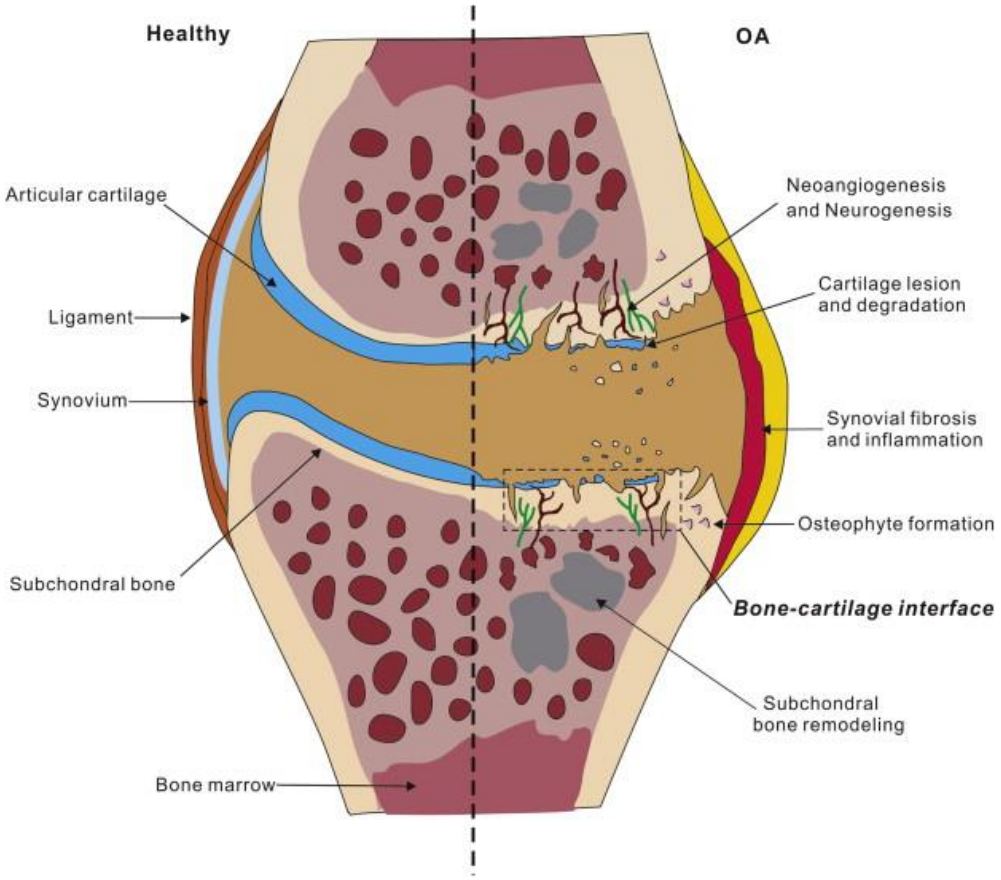


**Figure I-28. Highlighting the characteristic differences between healthy and OA knee joints.** The intimate contact between bone and cartilage tissue in a healthy individual knee is shown on the left (L) while the knee of a patient with OA, wherein alterations in either of the two tissues affecting other components, is shown on the right (R) (Yuan et al., 2014).

It is increasingly recognized that there is an intimate physical relationship between subchondral bone and joint cartilage, suggesting the possibility of biochemical and molecular crosstalk across the interface which is imbalanced in OA situation (Yuan et al., 2014; Zhou et al., 2020) as depicted in the **(Fig. I-28)**. Because of this, one can propose that there is an impenetrable barrier to soluble molecules and functional interaction formed by the calcified cartilage/bone interface, that would be shifted in the case of OA (Goldring and Goldring, 2010). This bone-cartilage interface/biochemical unit appears to play a significant role in both the beginning stages of OA and during later stages. Increased vascular communication, fissures, and microcracks throughout the bone/cartilage interface point to the possibility that this junction could now act as a transport conduit, facilitating molecular transport and molecular crosstalk between cartilage and subchondral bone in OA (Goldring, 2012b). Hence, this leads to the generation of mediators from both tissues, which then move from one zone to another, ultimately impacting and altering the homeostasis of the surrounding tissues. In addition to these significant alterations, OA is typically characterized by the creation of ectopic bone, which leads to the development of osteophytes that contribute to the progressing OA (Felson et al., 2005). Thus, subchondral bone thickening, formation of osteophytes or ectopic bone formation and increased bone turnover are causing alterations in composition and biochemical properties leading to progressive deterioration of the joint (Mansell and

Bailey, 1998; Mansell et al., 1997). In conclusion, the participation of a number of factors is collectively relevant to OA processes.

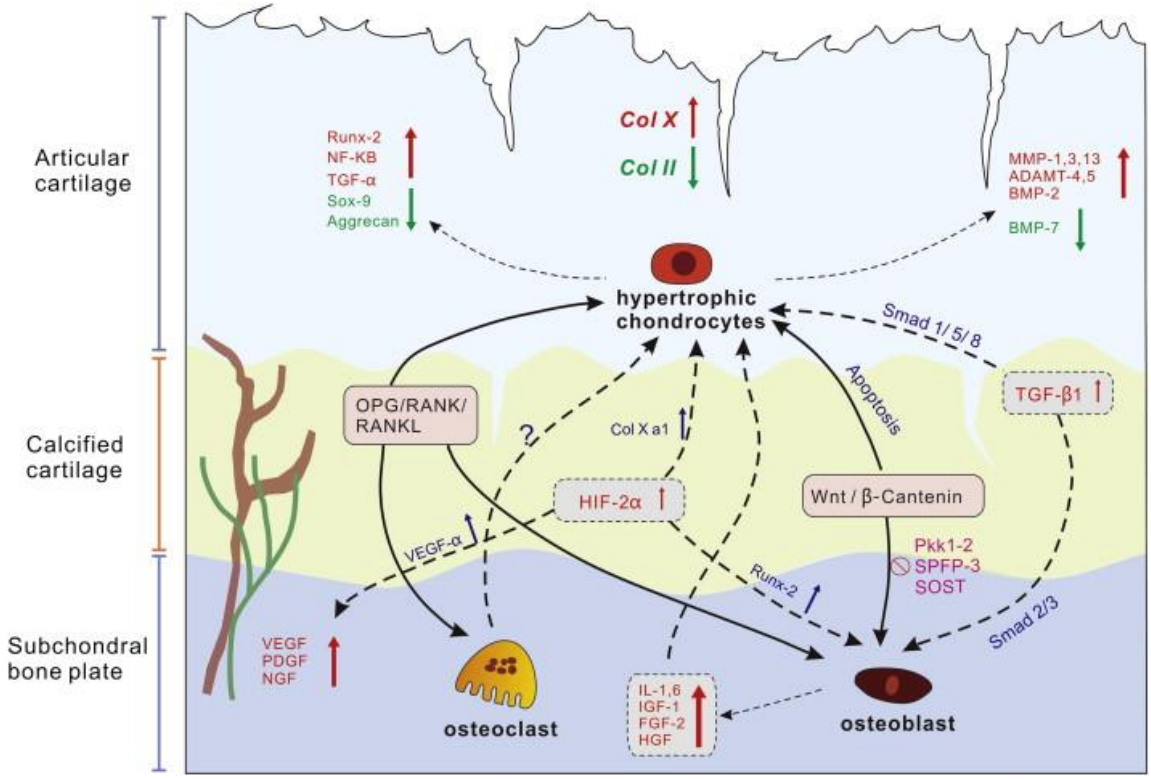


**Figure I-29. Molecular interactions at the Bone-Cartilage Interface during OA.** The damage caused by cartilage degradation and increased subchondral bone remodeling results in an imbalance of molecular interactions, thereby contributing to aberrant crosstalk (Yuan et al., 2014).

The molecular interactions in the bone-cartilage interface provide insight into the specific processes that underlie the influence of critical signaling pathways on the cartilage-bone pathophysiology that occurs in OA. A number of proteinases are responsible for the degradation of proteoglycans and the destruction of the collagenous framework, namely matrix metalloproteinases MMP-1, MMP-13, MMP-3 (Stromelysin-1), ADAMTS-4, and aggrecanase-1 (Troeberg and Nagase, 2012; Wu et al., 1991). *Cathepsin B* and other physiological activators, as well as tissue inhibitors of matrix metalloproteinases (TIMPs), are known to regulate MMP activity, whose imbalance might result in an imbalance between these components (Kostoulas et al., 1999). When the AC is subjected to repeated mechanical insults, this causes an increase in the production of MMPs, which is then followed by cartilage matrix degradation that is found to be particularly pronounced in the superficial layer of the AC (Buckwalter et al., 2013; Lin et al., 2004). At the molecular level, activation of transcriptional regulators such as RUNX2 and ligands such as FGF2 causes terminal differentiation of hypertrophic chondrocytes that express type X collagen in the early stages of osteoarthritis and control the expression of MMPs and ADAMTS (Akkiraju and Nohe, 2015; van der Kraan and van den Berg, 2012; Wang et al., 2004). During OA, *BMP2* mRNA levels are also found to be upregulated, again causing terminal differentiation of chondrocytes, and ultimately leading to an increase in the secretion of ColX and MMP-13

(Chawla et al., 2022). During the progression of OA, several inflammatory cytokines like *IL-1β*, *TNF-α* and *IL-6* have been shown to be upregulated causing cartilage homeostasis to be disrupted and leading to MMP mediated cartilage degradation (Kapoor et al., 2011) (**Fig. I-29**). Moreover, it has been shown that these inflammatory cytokines induce the expression of nuclear factor-kB (*NF-kB*) dependent hypoxia inducible factor (HIF-2α) that could lead to enhanced AC destruction (Rigoglou and Papavassiliou, 2013; Saito et al., 2010; van de Loo et al., 1995; Wehling et al., 2009). Hence, it appears that the damage caused to AC leads to a cascade of events whose activation results in an irreversible damage to the cartilaginous tissue in OA. Even though, the chondrocytes actively secrete collagen type II and proteoglycans upon detection of ECM loss, an imbalance generated between the ratio of ECM production to proteolytic enzyme secretion eventually causes a near complete degradation of this tissue (Akkiraju and Nohe, 2015). This results in abnormal/ incomplete osteoblast differentiation causing osteophyte formation due to fibroblastic differentiation causing joint stiffening/hardening or fibrosis (Hashimoto et al., 2002; Remst et al., 2015).

Furthermore, abnormal expression of growth factors such as TGF-β and BMP-2 has been reported that also contributes to the progression and worsening of the OA condition, resulting in the development of osteophytes, in addition to an upregulation of other inflammatory responses that are secreted by synovial macrophages (Uchino et al., 2000; van Beuningen et al., 1998). During the progression of OA, an imbalance is observed between a majority of signaling pathways, such as TGF-β1, BMP2/4/7, Wnt5a, Insulin Growth Factor 1 (IGF-1) and Fibroblast Growth Factor 2 (FGF-2) within OA cartilage. Moreover, an imbalanced bone turnover has been linked to OA, due to an increased ratio of RANKL to OPG as observed in rabbit OA subchondral bone and in human OA cartilage in comparison to normal or healthy cartilage (Akkiraju and Nohe, 2015), increasing osteoclast differentiation and activation.

## 5.1. Spinal OA

Though OA occurs mainly in the articular joints around different parts of the body, OA also occurs in the spine (Laplante and DePalma, 2012). Indeed, although the primary function of the intervertebral discs in the spine is to protect the spinal cord, provide flexibility and mobility, they also help in equal distribution of weight (weight bearing) or mechanical load (Laplante and DePalma, 2012; Sarzi-Puttini et al., 2005). Spinal OA in humans causes chronic lower back pain that gradually develops over time into a debilitating condition leading to discomfort and restricted motion (Goode et al., 2013; Goode et al., 2019). Due to the high risk of degeneration with increasing age, the three joint complexes that are found in the spinal cord—two facet joints, also known as zygapophyseal joints, and one intervertebral disc joint—are possible sources of back pain (Flowers et al., 2018; Goode et al., 2019; Goode et al., 2017). The degeneration of the cartilage surface causes the formation of vertebral osteophytes (bone spurs), followed by inflammation of the facet joints, which causes narrowing of the intervertebral disc space (Gellhorn et al., 2013)(**Fig. I-30**).

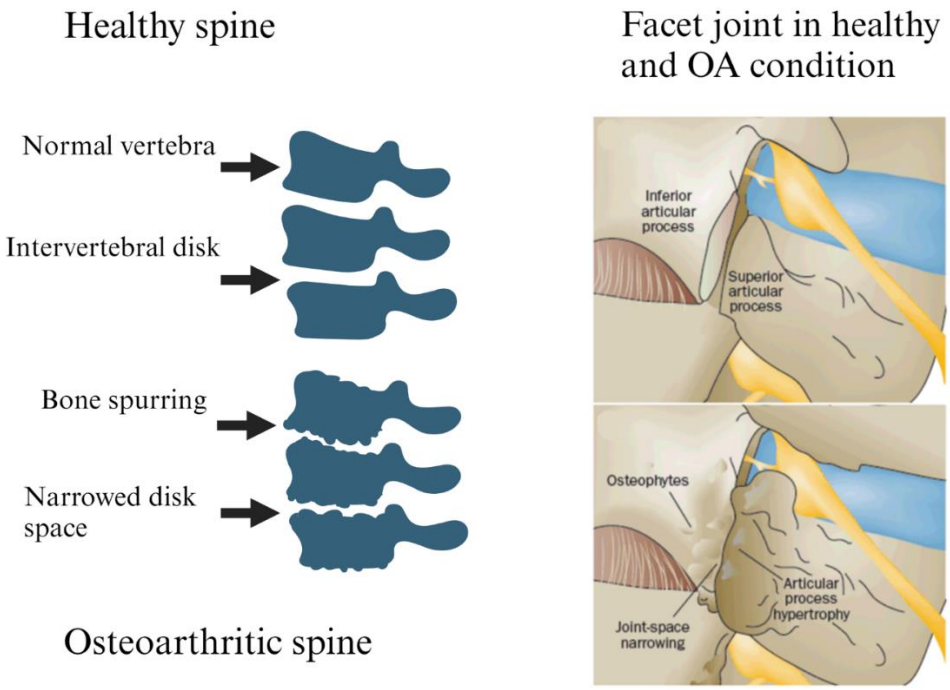


**Figure I-30. Normal Spine vs OA spine and Normal facet joints and advanced facet joint osteoarthritis.** OA spine reveals marked differences on comparing to healthy spine such as increased bone spurring and narrowed disk space. In OA spine, we can observe similar features in facet joints of the vertebra. Made with BioRender and adapted from (Gellhorn et al., 2013).

The etiology of OA is multifactorial; it includes genetic predisposition, age, sex, epigenetics, dietary habits, lifestyle, and ethnicity. In addition, one could add muscle strength, physical activity, excessive heavy-lifting sports, and work-related habits as potential factors involved in OA development (Musumeci et al., 2015) (Weinberg et al., 2017). Even though radiological diagnosis using X-RAY, CT, and PET-CT along with tissue biopsy remain at one's disposal for detecting OA (Murray et al., 2017), today screening for some of the relevant proteins such as ColX and other inflammatory markers in the blood serum can help in early prognosis of OA (Goode et al., 2017).

## 5.2. Zebrafish model of OA

For better comprehension regarding the development and progression of OA, several *in vivo* model systems such as rats, mice, rabbits, guinea pigs, sheep, horses and dogs are used, as well as cultured primary cells from affected joints (Kuyinu et al., 2016). Over the course of the past few years, several studies have been published demonstrating that zebrafish is an ideal model system for orthopedic research (Busse et al., 2020; Lawrence et al., 2018a; Waldmann et al., 2021). Indeed, in addition to skeletal anomalies like osteogenesis imperfecta or osteoporosis, the zebrafish has been garnered for research on the pathogenesis of osteoarthritis (Mitchell et al., 2013; van der Kraan, 2013; Zappia et al., 2023). It is possible to study spontaneously occurring osteoarthritis caused by genetic factors (in mutants generated in genes associated with OA in humans) in addition to looking at injury-induced OA, which would recapitulate the development of osteoarthritis due to sports, accidents, or professional overload. Older histological observations conducted in fishes (zebrafish, stickleback and lampreys) have shown the presence of “euarthroidal” joints that have similar features of mammalian synovial joints (Haines, 1942). Two cartilaginous joints in the head of the zebrafish have been the subject of extensive research (Askary et al., 2015; Miller et al., 2003): The jaw joint located between the Meckel's cartilage and the palatoquadrate, and the bipartite hyoid joint located between the ceratohyal, interhyal, and hyosymplectic cartilages (**Fig. I-18A**) (Smeeton et al., 2017). Both the pharyngeal jaw joint and the joints of the fins in zebrafish have a structure that is analogous to that of the synovial-like lubricating knee joint found in mice and humans (**Fig. I-18B**) (Askary et al., 2016). In addition, like all other vertebrates, zebrafish have intervertebral structures that can deteriorate with age (Hayes et al., 2013). However, in adult zebrafish these structures are devoid of cartilage(Hayes et al., 2013) as explained in **(section 2.2.1)** (**Fig. I-20B**) (Williams et al., 2019). It is indeed critical to note since zebrafish differ in structure of intervertebral joints and also in terms of mechanical loading of the vertebral column is axial in fish, similar to humans and as opposed to quadripedal land mammals.

# 6. BONE EXTRACELLULAR MATRIX PROTEINS AND THEIR IMPORTANCE

Extracellular matrix (ECM) is the most prevalent type of connective tissue that is present in almost all types of cellular microenvironment and is of extreme importance for tissue development (Henke et al., 2019). The ECM is a three-dimensional structure that is non-cellular and is secreted into the extracellular space by cells that is made up of a particular set of proteins as well as polysaccharides (Lin et al., 2020). The extremely diverse composition and nature of ECM enables it to perform numerous functions, ranging from supporting cells, regulating cell communication, cell survival, migration, proliferation, and differentiation (Bonnans et al., 2014; Mouw et al., 2014). In addition to regulating cell motility, ECM is also necessary for growth, development, wound healing, and fibrosis that results in ECM components being secreted into the existing matrix and aggregating with it (Olczyk et al., 2014; Wight and Potter-Perigo, 2011). The production of various forms of ECM proteins has been shown to contribute to the organization of multicellular tissues that revolve around cell to cell and cell to matrix interactions, such as angiogenesis, cardiac remodeling, vascular morphogenesis, and skeletal development (Alberts et al., 2002). Depending on the tissue, the ECMs are different based on the specific requirements of the tissue, thus each type of tissue has its own distinct composition and topology (Frantz et al., 2010). For instance, the ECM of skeletal tissues (bone and cartilage) are unique and, although cartilage and bone matrices are distinct, both are predominately composed of collagen fibrils (Gentili and Cancedda, 2009). Unlike cartilage, bone requires a high degree of mineralization since it is essential for making the structure rigid yet flexible, whereas cartilage contains aggrecan, a large proteoglycan which distributes the weight and provides durability (Murshed, 2018; Velleman, 2000). The bone ECM is made up of two major components, one inorganic (mineral) made up of hydroxyapatite, while the organic component is noticeably more diverse and is made up of mainly 90% of collagen type I and 10% of non-collagenous proteins. The osteoblasts are primarily responsible for ECM protein synthesis prior to the mineralization process (Mansour et al., 2017).

There are four distinct categories of non-collagenous proteins: the γ-carboxyglutamate-containing proteins, the glycoproteins, the proteoglycans, and the small integrin-binding ligands N-linked glycoproteins (SIBLINs) (Paiva and Granjeiro, 2017). Numerous ECM proteins are glycoproteins that are classified into two or several classes based on related domain structures and / or functions, the larger class comprises of relatively large molecules like laminins, fibronectin, and elastin, while the second family consists of several classes of smaller ECM proteins that were identified and have been reported to modulate cellular functions (Mouw et al., 2014). A recent addition to this family includes the *fibulins* (de Vega et al., 2009). The ECM also consists of other important components such as integrins, growth factors (GFs) and a group of matrix metallo-proteinases (MMPs) (Akkiraju and Nohe, 2015).

## 6.1. Collagens

Collagen is the most abundant protein that can be found in the body, it is accumulated within the ECM of connective tissues such as cartilage, bone, skin and tendons (Deshmukh et al., 2016). There are around 42 genes in humans that code for α-chains, and there are 28 different types of collagen (Ricard-Blum, 2011). Collagen is structured into fibrils so that it can fulfill its role in maintaining the structural integrity of tissues. Collagen types I, II, III, V, XI, XXIV, and XXVII are the fibril-forming collagens (**Fig. I-31)** that are characterized by a long uninterrupted triple helix-forming domain, characterized by a large number of Gly-X-Y repeats, flanked by small globular non-fibrillar domains at the end of the molecule (Exposito et al., 2010).

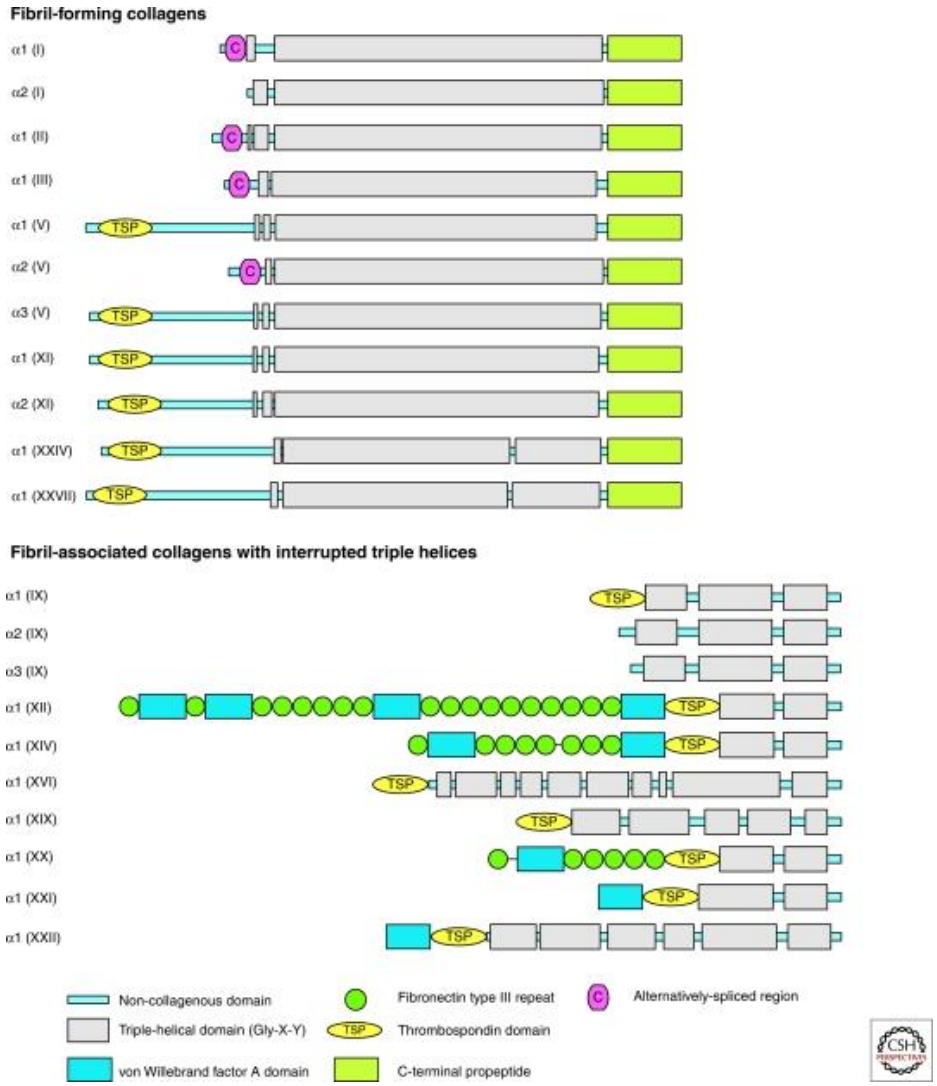


**Figure I-31. Structural organization of collagens, showing fibril-forming collagens**. Domain composition and supramolecular assemblies of collagens. (Ricard-Blum, 2011).

Collagen types I, II, and III are the most abundant fibril-forming collagens in vertebrates. Collagen type I is the most abundant and ubiquitously expressed kind of collagen.

It is made up of a heterotrimer of two a1-chains and one ß-chain (112(I)), that confers their crucial load-bearing, tensile strength, and mechanical stress resistance capabilities to many tissues including bone (Naomi et al., 2021). Different configurations contribute in their own unique way to the various qualities possessed by the tissues. In tendons, the fibrils of type I collagen are placed in parallel to form bundles, whereas in skin, the organization is more random, generating a complex network of interlaced fibrils (Gelse et al., 2003). In bone, type I collagen mostly occurs with either type III or type V collagen while forming fibrils (Birk et al., 1988; Fleischmajer et al., 1990), which have been demonstrated to play a vital role in the process of mineralization to form hard connective tissue, such as bones and teeth (Wojtas et al., 2020). In contrast, collagen types IV, VI, VIII, and X are all considered to be network-forming collagens (**Fig. I-32)** (Karsdal et al., 2013).

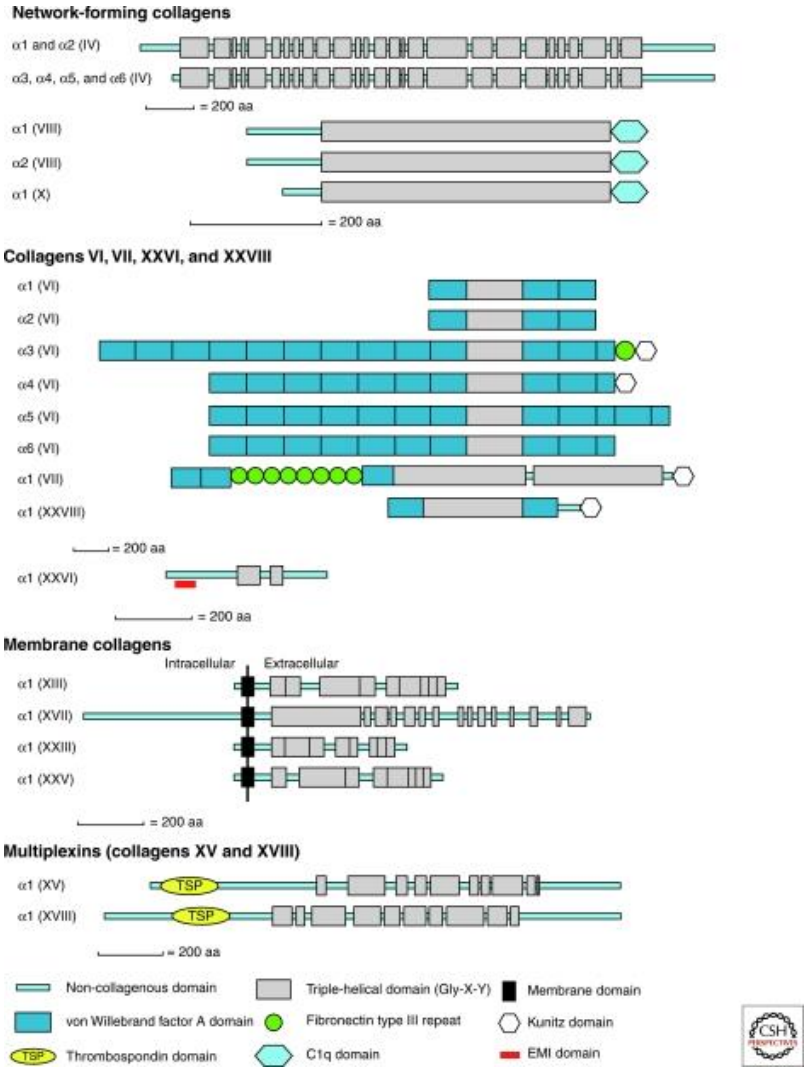


**Figure I-32. Structural organization of collagens, showing network-forming collagens.** Domain composition and supramolecular assemblies of collagens. (Ricard-Blum, 2011).

The majority of hyaline cartilage is made up of type II collagen, which can also be found in the vitreous body of the eye, the corneal epithelium, the notochord, in the intervertebral discs, and embryonic epithelial-to-mesenchymal transitions (Kague et al.)

(Ricard-Blum, 2011). Skeletal disorders, such as osteoarthritis and rheumatoid arthritis, are mostly associated with the degradation of type II collagen (Bay-Jensen et al., 2011). In all of the body's tissues, the epithelium and the stroma are separated by a particular type of extracellular matrix (ECM) known as the basement membrane (BM), which is primarily composed of type IV collagen. It has a big C-terminal NC1 globular domain, an N-terminal 7S domain, and a core triple helix that is approximately 25% longer than those seen in fibrillar collagens, and the Gly-X-Y repeat is frequently interrupted which leads to high flexibility (Knupp and Squire, 2005). Type VI collagen is a heterotrimeric molecule that has the isoform 123(VI). It consists of a short triple helix that is bordered by two extended globular domains, and it is present, albeit in a variable manner, in practically all organs. Collagen type VI molecules are known to have a distinct beaded appearance, and they interact with collagen type I and fibronectin (Engvall et al., 1986), whereas in higher vertebrates collagen X can be found in cartilage (Shen, 2005).

### 6.1.1. Collagen type X / Col-X/ Col10

Collagen X (Col10) is a short chain collagen that is localized to hypertrophic cartilage and at the chondro-osseus junction in the hematopoietic stem cell niche in mammals (Jacenko et al., 2002). It is made up of a homotrimer comprising three a1(X) chains, a triple helix of 463 aa, flanked by a highly conserved COOH-terminal non-collagenous domain (NC1) of 161 aa and a short (38 aa) non-helical amino terminus (NC2) (Shen, 2005). Similar to type VIII collagen, type X collagen trimers assemble into hexagonal matrices in vitro (Kwan et al., 1991; Ricard-Blum, 2011), and supramolecular aggregates of type X collagen form in the territorial matrix of hypertrophic chondrocytes in vivo (Schmid and Linsenmayer, 1990). Col10a1 gene from mice was shown to have a high degree of similarity with chicken, bovine, and human collagen X gene sequences when compared using combined nucleotide and deduced amino acid sequences . This suggests that the gene has been conserved throughout evolution (Ninomiya et al., 1986; Shen, 2005; Thomas et al., 1991). Col10A is widely regarded as a marker gene for hypertrophic chondrocytes across species ranging from humans to mice (Zheng et al., 2003). More than 30 mutations have been characterized for the human *COL10A1* gene, of which the most common and extensively studied condition is Schmid metaphyseal chondrodysplasia (Gudmann and Karsdal, 2016; Richmond et al., 1993). This type of osteochondrodysplasia is characterized by short-limbed small stature, normal facial structure, but extensive metaphyseal dysplasias of the long and short tubular bones (Richmond et al., 1993). Research carried out on mice has shown that complete inactivation of the *Col10a1* gene does not result in a significant phenotype; rather aberrant bone architecture and cox vara is only seen upon expression of altered versions of the gene, indicating that abnormal COL10A1 disrupts ECM function (Jacenko, 1998). In humans, mice, and sheep, ectopic chondrocyte hypertrophy that is characterized by elevated expression of Col 10 is thought to be a characteristic of osteoarthritis (OA) (van der Kraan and van den Berg, 2012). A biomarker C-10C is being used to screen patients with collagen degradation in OA, that measures / detects considerably higher quantities of collagen type X fragments in the serum of patients with OA, in addition to other candidates (He et al., 2014; Lotz et al., 2013).

Due to the partial duplication of its genome, the zebrafish has two copies of the *col10a1* gene, named *col10a1a* and *col10a1b*. In zebrafish, *col10a1a* is expressed in the osteoblasts, in addition to the expected hypertrophic chondrocytes (Eames et al., 2012). At 4, 5, and 6 dpf, the expression of *col10a1a* is seen in skeletal elements such as the dentary, maxilla, ethmoid plate, opercle, and cleithrum, as well as in the pharyngeal teeth, while the expression of *col10a1b* was detected only in teeth at 4 and 6dpf, respectively (**Fig. I-33)** (Debiais-Thibaud et al., 2019).

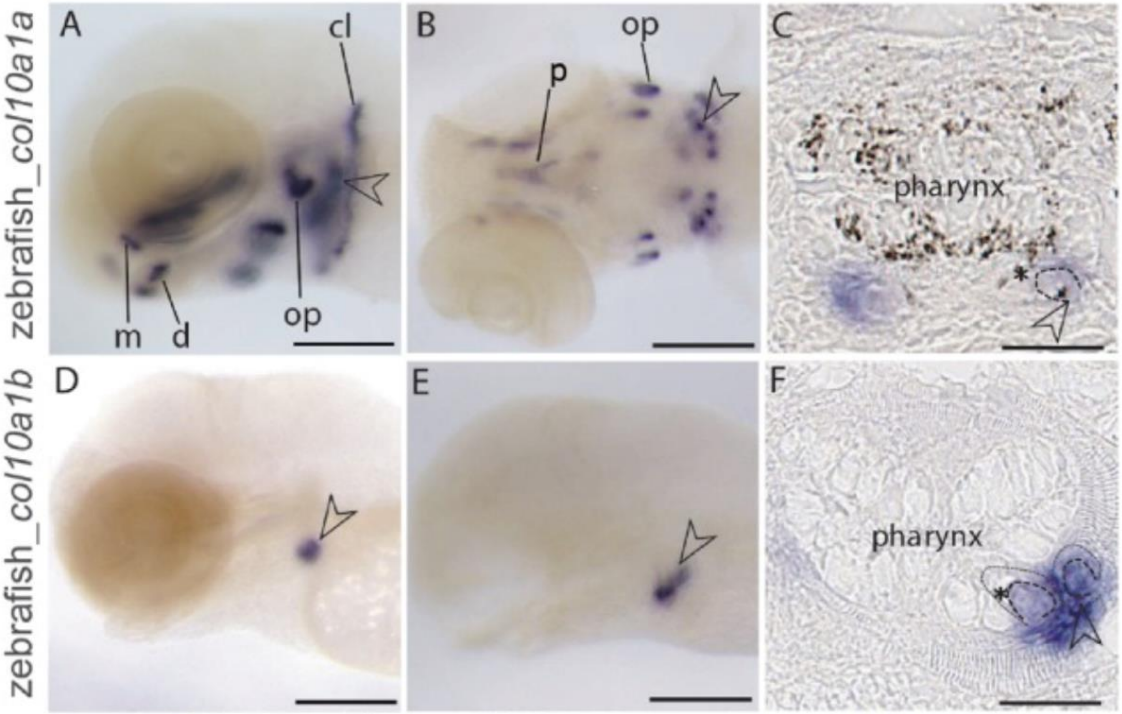


**Figure I-33. Expression of *col10a1a* and *col10a1b* in zebrafish at various stages using in situ hybridization.** Panels (A, B) Expression of *col10a1a* in whole-mount zebrafish larvae at 4 and 6 dpf. (D, E) Expression of *col10a1b* in whole-mount zebrafish larvae at 4 and 6 dpf respectively. (C, F) Expressions of *col10a1a* and *col10a1b* post in situ in paraffin sections of zebrafish larvae at 5dpf. arrowheads point to ameloblasts of developing teeth; cl- cleithrum; d- dentary; m- maxilla; op- opercle; p- parasphenoid. This Figure was sourced from (Debiais-Thibaud et al., 2019) and adapted.

## 6.2. Fibulins

Fibulins have only very recently been identified as a family of proteins that are found in the extracellular matrix, as a part of the smaller ECM proteins that help influence cellular behavior and functions (de Vega et al., 2009). Fibulins are a type of glycoproteins that are secreted by cells and are associated with basement membranes, elastic fibers, and other matrices throughout the body (Argraves et al., 2003). The fibulins share a common specific C-terminal fibulin-domain, and they contain a varying number of modules that are similar to

epidermal growth factor (EGF) (**Fig. I-34)** (de Vega et al., 2009; Mahajan et al., 2021). Furthermore, the seven members of the family have binding domains similar to those of other basement membrane proteins, such as tropoelastin, fibrillin, fibronectin, and proteoglycans, which take part in assembling a variety of supramolecular structures (Vogel and Hedgecock, 2001).

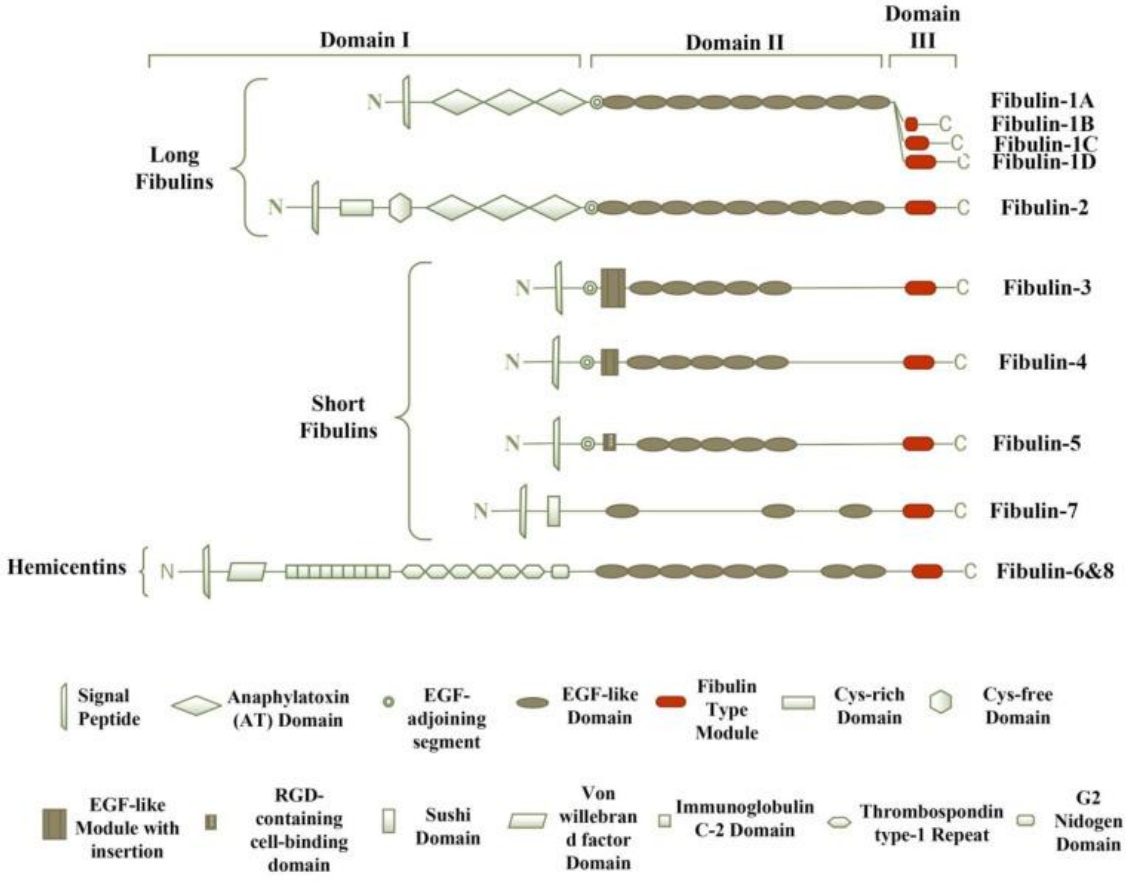


**Figure I-34. Domain structures of proteins belonging to the *fibulin* family.** The eight members of the family share a similar modular structure, consisting of I, II, and III domains. The C terminus of domain III contains a sushi motif, whereas the core of domain II is composed of EGF-like motifs. These motifs are found in domains II and III of all *fibulins*. The N-terminal domain I of the *fibulin* family varies in size and motif composition (Mahajan et al., 2021).

It has been demonstrated that *fibulins* play a role in the development of supramolecular ECM complexes as well as their continued stability. Due to the role that they play in the production and upkeep of the extracellular matrix, *fibulins* have been linked to a variety of pathological processes, including tissue organogenesis (Mahajan et al., 2021), vasculogenesis (Albig et al., 2006), fibrogenesis (Liu et al., 2019), and cancer (Fontanil et al., 2019; Zhang et al., 2020). Recent research using in vitro systems, mouse models, and human genetic disorders has led to a better understanding of the roles that fibulins play in the body (Argraves et al., 2003) (Chu and Tsuda, 2004).

### 6.2.1. Fibulin1 or Fbln1

The first member of the fibulin family, Fbln1 has a molecular weight that ranges from 90 to 100 kDa and it is also known as BM-90 (Argraves et al., 1989). There is evidence for the expression of fibulin-1 in basement membranes, connective tissues, and matrix fibers (Kluge et al., 1990; Roark et al., 1995). It has been shown in mouse that *Fbln1* RNA is expressed in presomitic mesoderm, somites, rhombomeres 2, 4, 6/7, in pharyngeal arches 1-4, and the expression of *Fbln1* in rhombomeres is identical to neural crest cells (NCC) marker *Crabp1* gene (Cooley et al., 2008). In the developing mouse embryo, the expression of *Fbln1* was found to be high in the mesenchymal cells of developing organs like the kidney, lung, and intestine, as well as in meninges that surround the spinal cord (Zhang et al., 1996). An *in vitro* expression analysis in human corneal fibroblasts using microarray revealed the expression of *FBLN1* and *FBLN2,* along with their binding partners, such as fibronectin, nidogen-1, aggrecan, fibrilin-1, endostatin, laminin alpha-2 chain, and ADAMTS-1 (de Vega et al., 2009; Timpl et al., 2003). In avian embryos, early expression of *FBLN1* has been observed during the first 23 hours of development in the embryonic midline, in the elastin fibers surrounding structures of the midline, and in the areas undergoing epithelial to mesenchymal transition, including the developing myotomes, neural crest, and endocardial cushions (Spence et al., 1992; Visconti et al., 2003). High levels of *FBLN1* expression are seen in tissues that are transitioning from epithelial to mesenchymal states during development, such as endocardial cushion tissue, developing myotomes, neural crest, tooth, and hair follicles (Zhang et al., 1996). Furthermore, it has been reported that both *Fbln1* and *Fbln2* are expressed in the developing cartilage in mice (Zhang et al., 1996). During the process of embryo development, FBLN1 interacts with FGF8, which is essential for the survival of neural crest cells (NCCs) and the embryo (Fresco et al., 2016). In a recent study conducted in rats, temporospatial expression pattern of *FBLN1* was investigated after spinal cord injury (SCI). The results showed a significant increase in the FBLN1 protein levels by immunoblotting, while double immunofluorescence detected the expression in neurons and microglia cells (Xu et al., 2015). All these observations indicate a role for FBLN1 in organogenesis, migration, cell-cell and cell-matrix interactions.

On the functional level, it is reported that the ECM of developing limb digits also contains FBLN1, and haploinsufficiency of a *FBLN1-D* variant is caused by the chromosomal translocation t(12;22) that leads to limb malformation called synpolydactyly in humans (Debeer et al., 2002). *Fbln1* KO mice have malformed cranial nerves, thymic hypoplasia, thinning of the wall of cardiac ventricles, abnormalities of the aortic arch artery, and defects of the ventricular septae (Mahajan et al., 2021). In addition, there is evidence that *Fbln1*$^{-/-}$ embryos (E17.5) displayed pharyngeal gland abnormalities, followed by decreased ossification of most cranial bones such as, frontal, parietal, tympanic ring, nasal, premaxillary bones, reduction in skull bones, NCC derived elements of the cartilages of the throat are reduced compared to WT embryos. Therefore, suggesting a role for *Fbln1* in the formation of structures that derive from the neural crest, since NCCs are essential to the development of all of these tissues (Cooley et al., 2008). Concerning skeletal development, mice lacking *Fbln1* had decreased mineralization of both the membranous and the endochondral bones, had smaller calvarial bone volume and a reduced expression of the protein SP7. In addition, it was shown that FBLN1 acts as a positive modulator of the BMP2-mediated induction of *Sp7*

expression (Cooley et al., 2014). Moreover, researchers have found evidence of increased *FBLN1* expression in both ovarian and breast carcinomas (Fontanil et al., 2019; Zhang et al., 2020).

Very little is known about the function of the *fbln1* gene in zebrafish. Its expression at early developmental stages was shown in somites and fin mesenchymal cells within the inter-epidermal space of the fin fold at 16hpf and 48hpf (**Fig. I-35)**, together with the *hemicentin2* (*hmcn2*) gene, another member of the Fibulin family (Feitosa et al., 2012). Morpholino knock-down of both these genes, but not each one alone, resulted in blistering in the trunk and moderately affected fin folds, indicating that there is a close interaction between Hmcn2 and Fbln1 that is essential for the migration of mesenchymal cells. Additional research needs to be carried out to shed light on the significance of these genes in the development of cartilage and bone in zebrafish.

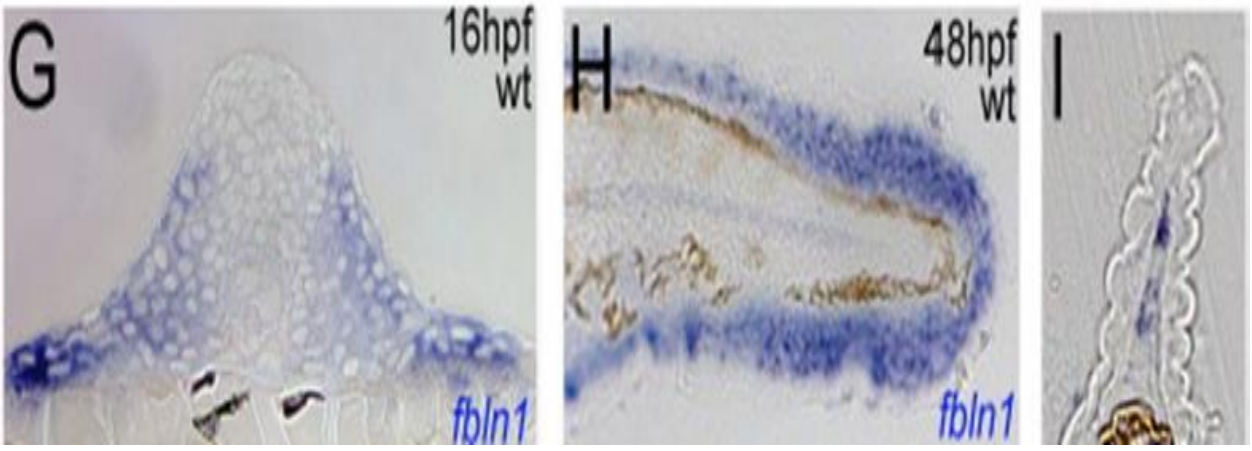


**Figure I-35. Expression of zebrafish *fbln1* at various stages with *in situ* hybridization.** At 16 hpf and 48 hpf, *fibulin1* is expressed in fin mesenchymal cells within the inter-epidermal space of the fin fold of zebrafish (Feitosa et al., 2012).

### 6.2.2. Fibulin3/Efemp1

Fibulin3/Fbln3 is another member of the Fibulin family, which is also called Efemp1 (EGF containing fibulin extracellular matrix protein 1). It is a short Fibulin protein molecule with 5 EGF-like domains (**Fig. I-34)** (de Vega et al., 2009). In humans, EFEMP1 has been shown to be distributed throughout the body and expressed along with FBLN4 in heart, lungs, placenta, and skeletal muscle (Giltay et al., 1999). In developing mouse embryos, *Efemp1* was shown to be highly upregulated in a wide variety of tissues, among which skeletal regions including the developing cartilage, bone, and condensing mesenchyme suggesting its role in shaping the skeletal parts of the body (Ehlermann et al., 2003). Mice lacking *Efemp1* have a decreased bone density (Mahajan et al., 2021).

*Fbln3* is expressed in the superficial zone of articular cartilage in healthy humans and mice, this level declines with increasing age in both species (Hasegawa et al., 2017). It has been shown that suppression of *Fbln3* by siRNA caused *SOX-9*, collagen II and aggrecan expression to significantly increase in AC, while overexpression of *Fbln3* inhibited chondrogenesis in MSC, suggesting that it plays an important role in governing the differentiation of adult progenitor cells. It has been reported that decline of FBLN3 expression during ageing could be an indication for an early event in OA (Hasegawa et al., 2017). An examination of the secretome of sclerotic and non-sclerotic (healthy) osteoblasts collected from OA subchondral bone indicated that sclerotic osteoblasts secrete significantly higher amounts of 3 fragments derived from FBLN3, Fib3-1, Fib3-2 and Fib3-3 (**Fig. I-36**)(Sanchez et al., 2018).

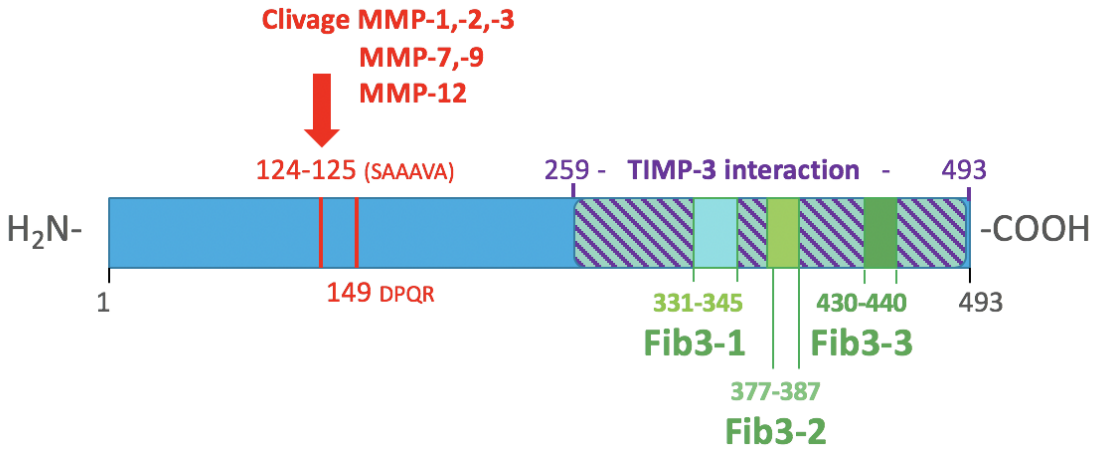


**Figure I-36. 3 fragments of *FBLN3* along with interaction partners.** The three *FBLN3* fragments are depicted within the complete sequence of the FBLN3 protein, also showing the domains II (blue) and III (hatched blue-violet), and putative interaction and cleavage sites (Sanchez et al., 2018).

Furthermore, the FBLN3 fragments Fib-3.1 and Fib-3.2 were found to be increased in the urine and serum of OA patients, indicating that they could be used as potential biomarkers for screening OA patients to monitor early changes in the subchondral bone metabolism (Henrotin et al., 2012). Other studies reported a close relationship between FBLN3 and tissue inhibitor of metalloproteinases 3 (TIMP-3) that plays a role in the pathogenesis of osteoarthritis (OA). The relationship between FBLN3 and TIMP-3 has been studied in the context of macular degeneration in the past, where it has been shown that there is dramatic accumulation and overlap of TIMP-3 and EFEMP1 expression between retinal pigment epithelia and Bruch membrane in patients with AL and AMD (Klenotic et al., 2004a). These proteins also colocalize *in vivo* in human placenta sections and form a complex *in situ* (Kevorkian et al., 2004; Sahebjam et al., 2007). Based on these observations, it seems likely that *FBLN3* is involved in the process of regulating the shaping of tissues in the body. Mice lacking *Efemp1/ Fbln3* experience premature aging as well as herniation, but they do not suffer from macular degeneration (Mahajan et al., 2021). The fact that the absence of *Efemp1* produces a phenotype that is quite different from that of *Fbln4* or *Fbln5* is evidence that *Fbln3/ Efemp1* is a functionally distinct member of the *Fibulin* family that plays a more

localized role in the biology of elastic fibers (Papke and Yanagisawa, 2014) (McLaughlin et al., 2007). In contrast, a point mutation in the *FBLN3* gene resulting in an R345W substitution can cause *Malattia Leventinese* or Doyne honeycomb retinal dystrophy (Marmorstein et al., 2007). We are still lacking detailed information about the role and function of *efemp1/fbln3* gene in zebrafish.

# II. OBJECTIVES OF THIS STUDY

This thesis has been developed in the framework of Marie Sklodowska-Curie Innovative Training Network (MSCA-ITN) Project BioMedAqu (H2020, MSCA-ITN No. 766347). The main goal of this research training network was to develop novel skills and expertise by integrating studies on skeletal biology in humans and biomedical research models such as zebrafish and medaka with the studies on farmed fish (aquaculture).

Understanding osteoblast differentiation and their function in bone matrix deposition and mineralization is central to the comprehension of bone development and of various bone pathologies. It is crucial to not only follow the expression of some landmark transcription factors or ECM proteins, but to also investigate the status of signaling pathways and factors regulating these processes. Our perspective was given by the observation that osteoarthritic patients present defects in their joint cartilage, but also in the underlying subchondral bone plate. Mechanistic and diagnostic studies of this condition often focus on cartilage or bone ECM proteins, as laid out in **(section 5)**. Our assumption was that the proteins affected in OA patients would play a role in skeletal formation and homeostasis, and that we could contribute to a better understanding of this role by investigating their homologs in the zebrafish model.

These considerations led to the formulation of two major questions for this thesis: - a general, and preliminary question was to unravel the transcriptomic profile of zebrafish osteoblasts at an early developmental stage (the very onset of the first bone elements formation in the head at 4 dpf) with a focus on ECM proteins; -the second question was whether genes that encode bone ECM proteins have an important role in skeletal development.

Thus, the main objectives of this thesis were:

1- **To determine the zebrafish osteoblast-specific transcriptome at 4dpf using a transgenic reporter line carrying fluorescent osteoblasts (*Tg(sp7:sp7-GFP)*).**

The first objective would be addressed by employing transgenic line where the expression of the fluorescent protein GFP is driven by the endogenous zebrafish *sp7* gene promoter. GFP-positive osteoblast cells were isolated from this line to perform RNA sequencing and transcriptomic analysis on the isolated cells.

2- **To elucidate the role of three extracellular matrix protein genes;** *col10a1a, fbln1* and *efemp1* **in zebrafish skeletal development.**

The second objective was addressed by generating KO mutants for three genes of interest; *col10a1a, fbln1* and *efemp1*. The effects of these mutations were investigated on cartilage and bone formation in 5dpf and 10dpf larvae, and in adults using µ-CT analysis.

3- **To investigate the effects of probiotics in the presence or absence of a BMP inhibitor on early skeletal growth using transgenic reporter zebrafish lines.**

This third objective arose from first results obtained within the BioMedAqu project indicating that probiotics treatment could be beneficial for skeletal health. A collaboration was initiated to use transgenic zebrafish reporter lines fluorescent in skeletal structures to further extend these findings.

# III. RESULTS

# 1. Osteoblast transcriptome and function of the ECM proteins Col10a1a and Fbln1.

Preliminary Notice: This section presents the main results covering objectives **1,** and **2**.

Currently zebrafish are extensively employed for investigating skeletal development and skeletal anomalies. To achieve this objective, it is important to comprehend the process of osteoblast differentiation and function, expression of signaling molecules and transcription factors. Small model systems such as zebrafish make it easier to observe and follow the development of skeletal structures *in vivo* real time using *Tg* reporter lines. We used the fluorescent reporter line *T (sp7:sp7-GFP)* generated in our lab that labels the osteoblasts to isolate *sp7* expressing GFP+ osteoblasts, and to analyze their transcriptome at 4dpf. Based on the GFP fluorescence intensity, we isolated two subpopulations of osteoblasts. RNA-Seq analysis of these two distinct osteoblast populations revealed several genes presenting different expression patterns. Subsequently, we selected two specific genes, *col10a1a* and *fbln1* that code for extracellular matrix proteins to study their function by generating inactivating mutants.

These results are summarized in a manuscript entitled “The Osteoblast Transcriptome in Developing Zebrafish Reveals Key Roles for Extracellular Matrix Proteins Col10a1a and Fbln1 in Skeletal Development and Homeostasis” Biomolecules. 2024 Jan 23;14(2):139. doi: 10.3390/biom14020139

The supporting information can be downloaded at:
https://www.mdpi.com/article/10.3390/biom14020139/s1

*Article*

# The osteoblast transcriptome in developing zebrafish reveals key roles for extracellular matrix proteins Col10a1a and Fbln1 in skeletal development and homeostasis.

**Ratish Raman [1], Mishal Antony [1], Renaud Nivelle [1], Arnaud Lavergne [2], Jérémie Zappia [3], Gustavo Guerrero-Limon [1], Caroline Caetano da Silva [4], Priyanka Kumari [5], Jerry Maria Sojan [6], Christian Degueldre [7], Mohamed Bahri Ali [7], Agnes Ostertag [4], Corinne Collet [4,8], Martine Cohen-Solal [4], Alain Plenevaux [7], Yves Henrotin [3], Jörg Renn [1] and Marc Muller [1,*]**

[1] Laboratory for Organogenesis and Regeneration (LOR), GIGA Institute, University of Liège, 4000 Liège, Belgium
[2] GIGA Genomics Platform, B34, GIGA Institute, University of Liège, 4000 Liège, Belgium
[3] MusculoSKeletal Innovative Research Lab, Center for Interdisciplinary Research on Medicines, University of Liège, Liège, Belgium
[4] INSERM U1132 and Université de Paris-Cité, Reference Centre for Rare Bone Diseases, Hospital Lariboisière, F-75010 Paris, France
[5] Laboratory of Pharmaceutical and Analytical Chemistry, Department of Pharmacy, CIRM, Sart Tilman, Liege, Belgium
[6] Department of Life and Environmental Sciences, Università Politecnica delle Marche, via Brecce Bianche, 60131 Ancona, Italy
[7] GIGA CRC In vivo Imaging, University of Liege, Sart Tilman, Liege, Belgium
[8] UF de Génétique Moléculaire, Hôpital Robert Debré, APHP, F-75019 Paris, France
* Correspondence: m.muller@uliege.be; Tel.: +32 473993074.

**Citation:** To be added by editorial staff during production.

Academic Editor: Firstname Lastname

Received: date
Revised: date
Accepted: date
Published: date



**Abstract:** Zebrafish is now widely used to study skeletal development and bone related diseases. To that end, understanding osteoblast differentiation and function, the expression of essential transcription factors, signaling molecules, and extracellular matrix proteins is crucial. We isolated Sp7-expressing osteoblasts from 4 days old larvae using a fluorescent reporter. We identified two distinct subpopulations and characterized their specific transcriptome as well as their structural, regulatory, and signaling profile. Based on their differential expression in these subpopulations, we generated mutants for the extracellular matrix protein genes *col10a1a* and *fbln1* to study their functions. The *col10a1a*$^{-/-}$ mutant larvae display reduced chondrocranium size and decreased bone mineralization, while in adults a reduced vertebral thickness and Tissue Mineral Density, and fusion of the caudal fin vertebrae were observed. In contrast, *fbln1*$^{-/-}$ mutants showed an increased mineralization of cranial elements and a reduced ceratohyal angle in larvae, while in adults a significantly increased vertebral centra thickness, length, volume, surface area, and Tissue Mineral Density was observed. In addition, absence of the opercle specifically on the right side was observed. Transcriptomic analysis reveals up-regulation of genes involved in collagen biosynthesis and down-regulation of Fgf8 signaling in *fbln1*$^{-/-}$ mutants. Taken together, our results highlight the importance of bone extracellular matrix protein genes *col10a1a* and *fbln1* in skeletal development and homeostasis.

**Keywords:** zebrafish; osteoblast; transcriptome; gene expression; *col10a1a*; *fbln1*; FGF8, ECM; skeletal development; vertebra

## 1. Introduction

Bone formation and homeostasis is a highly regulated process, whose better understanding will provide insights into diagnosis and therapeutic interventions to be developed for the welfare of an aging human population suffering from skeletal pathologies like osteoporosis, osteopetrosis, osteoarthritis, and age-/sports-related injuries. The two cell types critical for bone formation are the chondrocytes secreting the cartilage extracellular matrix (ECM) and the osteoblasts that are responsible for building new bone tissue (Long, 2012). Cartilage and bone cell fate is governed by the foremost regulator RUNX2 (Komori, 2017), whereas SP7 promotes osteoblast commitment in early osteoblast progenitors (DeLaurier et al., 2010a; Nakashima et al., 2002). Together with these two cell types, osteocytes form the cellular component of the bone skeleton, ultimately responsible for deposition, mineralization and maintenance of the bone ECM. The ECM forms the non-cellular component of the bone tissue, comprising the organic component made up of predominantly collagens and non-collagenous proteins, and the inorganic component consisting of calcium phosphate apatite and trace elements (Lin et al., 2020).

Despite being a late entrant in bone research, the zebrafish (*Danio rerio*) has recently become a powerful model for skeletal biology, due to its conserved genetic and functional characteristics compared to mammals and its numerous technical and experimental advantages (Apschner et al., 2011; Hammond and Moro, 2012; Le Pabic et al., 2022b). The most studied skeletal structures during early development are the cranial bones, as they are the first to undergo ossification and are of particular interest for the study of craniofacial disorders (Staal et al., 2018). Similar to terrestrial vertebrates, the skeleton of zebrafish contains bones of both dermal and chondral origins, which form from neural crest-derived cells relatively early in the course of development (Paudel et al., 2022; Schilling and Kimmel, 1994). In later stages and in adults, the vertebral column and fin rays are extensively studied (Tonelli et al., 2020). Individual structures of the skeleton are formed either by osteoblasts derived from mesenchymal cells, without a previous cartilage matrix (intramembranous), or through endo- or peri-chondral ossification building up onto a preformed cartilage extracellular matrix (ECM) previously secreted by chondrocytes (Apschner et al., 2011; Verreijdt et al., 2002). Both the key regulators and signaling pathways controlling skeletal development are highly conserved between mammals and teleosts (Caetano da Silva et al., 2023; Dietrich et al., 2021a; Li et al., 2009). Indeed, zebrafish osteoblasts express specific genes (Nie et al., 2021), often orthologs of their mammalian counterparts, such as those for the transcription factors Runx2 (*runx2a* and *runx2b*) and for Sp7 (*sp7*). The *sp7* gene is the earliest regulator and marker for osteoblasts in zebrafish (Niu et al.).

The ECM plays a crucial role in the formation of the skeleton, not only as a protein backbone for the mineralization to form the bone tissues, but also through its regulatory interactions with the bone cells.

The first zebrafish model for osteogenesis imperfecta (the *chihuahua* mutant) has a dominant mutation in the *col1a1a* gene, illustrating how modifying a major component of the bone ECM is able to affect skeletal development (Fisher et al., 2003) and how such a model can help to better understand bone mineralization (Cotti et al., 2022). Other collagens have been shown to affect skeletal formation, such as Col2a1a, Col11a2 (Bergen et al., 2019), or Col8a1a (Gray et al., 2014). COL10A1 is interesting, as it is expressed in hypertrophic chondrocytes in fish and mammals, but only zebrafish (and other teleosts) express it in osteoblasts (Kim et al., 2013b; Renn et al., 2013; Simões et al., 2006). It is a nonfibrillar collagen forming a homotrimer of three identical chains. In mammals, COL10A1 plays a significant role in endochondral bone development due to its specific expression in hypertrophic chondrocytes, mainly in the calcifying zone of growth plate cartilage (Gudmann and Karsdal, 2016). It is also expressed in the calcified zone of knee articular cartilage, where increased hypertrophy and COL10 expression are well documented in osteoarthritis (He et al., 2014). In humans, missense, nonsense and frame-shift mutations in the *COL10A1* gene cause Schmid type metaphyseal chondrodysplasia (SMCD) (Bateman et al., 2005; van der Kraan and van den Berg, 2012). In mice, the presence of abnormal COL10A1 resulting from dominant acting mutations in the *Col10a1* gene affects trabecular bone and causes *cox vara*, reduced thickness of the growth plate resting zone and articular cartilage, altered bone content and atypical distribution of matrix components within growth plate cartilage (Kwan et al., 1997) (Jacenko et al., 1993). In zebrafish, however, the significance of this additional expression is unknown.

Genes coding for non-collagenous ECM proteins were also identified. The *bglapl* gene is often used as a marker for mature or late osteoblasts (Rutkovskiy et al., 2016). Other genes, such as *spp1* (Venkatesh et al., 2014) or *gpc4* (Ling et al., 2017), were shown to be required for bone formation, in part by interacting with extracellular signaling proteins involved in WNT, BMP, or HH pathways that are crucial for skeletal formation. Another family of ECM proteins is the Fibulin family, glycoproteins that are found in basement membranes, fibers, and proteoglycan aggregates (Mahajan et al., 2021) in many locations where they play a role in organogenesis by stabilizing the ECM through their interactions with binding partners (Kobayashi et al., 2007). Its founding member, FBLN1 was shown to be required for bone mineralization in a mouse KO model (Cooley et al., 2014). Indeed, *Fbln1* KO results in defects in neural crest cell patterning, leading to anomalies of the aortic arch arteries, thymus, thyroid, cranial nerves, hemorrhages in the head and neck, and finally increased mortality (Cooley et al., 2008; Singh et al., 2006). Furthermore, *Fbln1* KO mice display a significant reduction in mineralization followed by reduced bone volume and size in the calvarial and frontal bones, at least in part by impeding *Sp7* induction by BMP2 (Cooley et al., 2014). In zebrafish, *fbln1* expression was observed in posterior presomitic mesoderm, the tail tip and regions of somite formation. At later stages, it is expressed in fin mesenchymal cells (Feitosa et al., 2012) and in the myocardium (Patra et al., 2011), however its role in skeletal development of zebrafish is unknown. In that context, it is also noteworthy that human osteoarthritis, a condition due to degradation of cartilage in joints and increased subchondral bone

formation, is characterized by modifications in the content of cartilage and bone ECM proteins (Sanchez et al., 2018).

Here, to further increase our understanding of skeletal formation using the zebrafish as a model system, we first investigated the early zebrafish osteoblast specific transcriptome by isolating *sp7*-expressing cells using the *Tg(sp7:sp7-GFP)* reporter line described earlier (Sojan et al., 2022). Based on their *sp7* expression, we identified two distinct subpopulations of osteoblasts that differentially expressed two ECM protein genes, *col10a1a* and *fbln1* whose function in bone development was unknown in zebrafish. We generated mutant zebrafish lines for these two genes, and we show that the *col10a1a* and *fbln1* mutants present opposite effects on skeletal elements at early development stages and in adults. In conclusion, we show that ECM proteins, in addition to their structural role in the bone matrix, also substantially contribute to the development and mineralization of the bone skeleton.

## 2. Materials and Methods

*Fish and Embryo Maintenance*

Zebrafish (*Danio rerio*) were reared in a recirculating system from Techniplast (Buguggiate, Italy) at a maximal density of 7 fish/L. The water characteristics were as follows: pH = 7.4, conductivity = 50 mS/m, temperature = 28 °C. The light cycle was controlled (14 h light, 10 h dark). Fish were fed twice daily with dry food (ZM fish food®, Zebrafish Management Ltd, Winchester, UK) with size adapted to their age, and once daily with fresh nauplii from *Artemia salina* (ZM fish food®). Larvae aged less than 14 days were also fed twice daily with a live paramecia culture. Wild type zebrafish from the AB strain and mutant lines were used. The *Tg(sp7:sp7-GFP)* transgenic line has been generated in-house as described earlier (ulg071 Tg) (Sojan et al., 2022).

In general, two males and two females were used for breeding in the morning, eggs were collected and raised in E3 (5 mM Na Cl, 0.17 mM KCl, 0.33 mM $CaCl_2$, 0.33 mM MgSO4, 0.00001 % methylene blue).

*Dissociation of 4 dpf larvae to obtain osteoblasts and preparation for FACS sorting*

A *Tg(sp7:sp7-GFP)* (ulg071 Tg) heterozygous transgenic parent was outcrossed with a WT parent to obtain a clutch of transgenic and non-transgenic offspring. At 3 dpf, the transgenic, fluorescent larvae were separated from their non-transgenic siblings and raised separately in two different plates. At 4 dpf, around 100-150 larvae were euthanized by adding MS-222 (Ethyl 3-aminobenzoate methane sulfonate; Merck, Overijse) (0.048% w/v), and transferred to "gentle MACS™ C" tubes (Miltenyi Biotec, Leiden, Netherlands) in an excess of E3 medium (Westerfield, 2007). The supernatant was removed and replaced with 1–1.5 ml of de-yolk (Westerfield, 2007) buffer. The yolk was removed by vigorously pipetting up and down several times for 10 minutes and the supernatant discarded. The larvae were washed twice with $HBSS^-$ buffer (without $Ca^{+2}$ and $Mg^{+2}$ ions and phenol red free) and the supernatant was discarded. The larvae were resuspended in 1.5ml digestion buffer (1x HBSS-, 10 mM HEPES (0.5 %), 2 mM EDTA, TrypLe™ Select 1x (Thermo Fisher Scientific, Merelbeke, Belgium), Proteinase K 0.2 μg/μl (Thermo Fisher Scientific, Merelbeke, Belgium), Collagenase-2 0.2 mg/ml (Worthington Biolabs, Lakewood, NJ, USA) at 28°C and dissociation was

performed running the protocols m_brain_01 and m_brain_03 (according to the manufacturer's instructions in the Neural Tissue Dissociation Kit (T)) once on a gentleMACS™ Dissociator machine (Miltenyi Biotec, Leiden, Netherlands), followed by three runs of m_brain_03, 2 runs of protocol m_brain_02, five runs of m_brain_03, each run separated by continuous shaking in the water bath at 28 °C for 5 min. Then m_brain_01 protocol was run before adding 30 ul of Enzyme A as supplied by Miltenyi Biotec (Neural Tissue Dissociation Kit (T) 130-093-231) followed by 4 additional runs of the m_brain_03 protocol, separated by 5 min incubation at 28 °C with continuous shaking and the tube transferred on ice. The samples were centrifuged at 4 °C at 300 g for 10 min and the supernatant discarded as gently as possible to avoid cell resuspension. The pellet was very quickly resuspended in 1ml $HBSS^-$ buffer and filtered through mesh to eliminate cell clumps and aggregates. The filtered cells were collected in polypropylene tubes and viability dye 10% v/v propidium iodide (Fisher Scientific, Merelbeek, Belgium) was added to distinguish live cells from dead cells /cell debris while sorting. It is very important to ensure that the steps following centrifugation are carried out by placing the tubes on ice. The cells were then brought to the FACS Aria III sorter (BD Biosciences, Erembodegem, Belgium) and the green fluorescent cells were sorted into a 1.5 ml Eppendorf tube containing 500 µl of PBS buffer with RNAse inhibitor (Promega, Leiden, Netherlands) and 1% bovine serum albumin (BSA, Sigma-Aldrich/Merck, Overijse, Belgium). Note that a preliminary run was performed using the non-transgenic siblings to ensure that the GFP-positive cells were truly due to transgene expression, not to autofluorescence.

*mRNA sequencing*

Cells coming from cell sorting (about 30,000–50,000 cells) were immediately lysed in 0.5% Triton X-100 containing 2 U/µl RNAsin and stored at −80 °C. cDNAs were prepared from these lysed cells according to the SMART-Seq 2.0 protocol (Illumina, San Diego, CA, USA) for low input RNA sequencing, while libraries were prepared using the Nextera XT DNA library kit (Ma et al.). Only high-quality libraries were kept for sequencing (5 for the P1 and 3 for the P2 subpopulations). For the whole larvae mRNAs extracted from wt and fbln1 mutants, the cDNA libraries were generated from 100 to 500 ng of extracted total RNA using the Illumina Truseq mRNA stranded kit (Illumina, San Diego, CA, USA) according to the manufacturer's instructions. All cDNA libraries were sequenced on a NovaSeq sequencing system (Illumina, San Diego, CA, USA), in 1 ×100 bp (single end). Approximatively 20–25 M reads were sequenced per sample. The sequencing reads were processed through the Nf-core rnaseq pipeline 3.0 (Ewels et al., 2020) with default parameters and using the zebrafish reference genome (GRCz11) and the annotation set from Ensembl release 103 (www.ensembl.org; accessed 1 May 2020). Differential gene expression analysis was performed using the DESeq2 pipeline (Love et al., 2014). Pathway and biological function enrichment analysis was performed using the WEB-based "Gene SeT AnaLysis Toolkit" (http://www.webgestalt.org; accessed on 10 November 2022) based on the integrated GO (Gene Ontology Consortium, 2021), KEGG (Kanehisa et al., 2022), Panther, and WikiPathways databases (all accessed on 19 April 2023 via

http://www.webgestalt.org). Two additional databases were generated using data from zfin (zfin.org) and based on phenotypes associated to gene mutations ((Geno-Pheno) or on location of gene expression (Expression).

*Generation of mutant lines*

Mutant lines for *fbln1* (zfin Id: ulg075) and *col10a1a* (zfin Id: ulg076) were generated using the CRISPR/Cas9 method as previously described (Doudna and Charpentier, 2014; Hwang et al., 2013). The guide RNAs have been introduced into the Alt-R™ Cas9 system from Integrated DNA Technologies (IDT, Leuven, Belgium), the gRNA sequence used are, respectively: 5'-CCTGGTGGCCTTGACGGCTGCCC-3' for *col10a1a*, and 5'-CACCAGATAGTCACGCCCGT-3' for *fbln1*.

The Alt-R crRNA (gRNA for the gene of interest) and tracrRNA were resuspended in nuclease-free IDTE Buffer to a final concentration of 100 µM each. The two components were mixed according to the manufacturer's instructions, heated to 95 °C for 5 minutes and cooled to 22°C (gRNA). The 10 µg/µL Cas9 protein was diluted to 0.5 µg/µL using Cas9 Buffer consisting of 20 mM HEPES, 150 mM KCl with pH = 7.5 in a final volume of 10 µL. 3 µL of gRNA were mixed with 3 µL of the Cas9 solution, incubated at 37 °C for 10 minutes, cooled to 22°C and mixed with a 0.5 µL tracer dye (0.5 mg/mL, Rhodamine dextran (RD), Molecular Probes, Carlsbad, California USA) Microinjection of 2–3 nL per embryo was carried out on single cell stage (20-60 min post-fertilization) zebrafish embryos using an InjectMan micromanipulator (Eppendorf, Hamburg, Germany) assembled on a Leica M165 FC stereomicroscope.

DNA was isolated from larvae or finclips from adults/juveniles at various stages of development in 50 mM NaOH by heating at 95 °C for 20 minutes. The solution was cooled down on ice for 10 minutes, neutralized by adding Tris-HCl 1 M, pH = 8.0, 1/5$^{th}$ the volume of NaOH, spun down using a desktop centrifuge for 2 minutes to recover the supernatant, and stored at 4 °C. Genomic fragments covering the targeted region were obtained by PCR using the above primers. The primers for PCR genotyping were, respectively: forward 5'-CAGATTTGACTTCAGAGAATGGA-3', reverse 5'-AGAAACACAGCTTTTCCGAGAG-3' for *col10a1a* and forward 5'-GTTGGGTCAGATGTGCTGTG-3', reverse 5'-ATGAGTCTGACCGTGTGCTG-3' for *fbln1*. The mutants were identified using Heteroduplex Mobility shift Analysis (HMA) by polyacrylamide gel electrophoresis, selected DNAs were further processed for Sanger sequencing to identify the exact position and extent of the mutation.

*Genotyping and RNA extraction of WT and mutant larvae*

Homozygous mutants were obtained by crossing heterozygous parents carrying the desired mutation. Resulting larvae were first sacrificed, fixed in para-formaldehyde (PFA) 4 % or stained, then photographed and, finally DNA was extracted from individual larvae to genotype them as described above. Only homozygous WT or mutants were then assigned to their photograph for phenotype determination.

For the RNA-Seq experiment on mutants, 10 dpf larvae were stored in RNA later (Fisher Scientific, Merelbeek, Belgium). Individual fish were decapitated, the heads were individually stored in a 96 well plate,

while the body was used for DNA extraction and genotyping. Once the genotypes were known, the heads were recovered and pooled to constitute three independent batches of, respectively 21 WT and mutant individuals. The RNA was extracted using the RNA mini extraction kit (Qiagen, Hilden, Germany) according to the manufacturer's instructions. The RNA was treated with DNAseI (Qiagen, Hilden, Germany) to avoid DNA contamination. Quantity and quality of each extract was assessed by nanodrop spectrophotometer measurements. The pellets were further purified by lithium chloride precipitation, followed by 2 times pellet washing with 70% ethanol, resuspended in 51 µL of RNAse-free water and stored at −80 °C. The integrity of total RNA extracts was assessed using the BioAnalyzer (Agilent, Santa Clara, CA, USA). RIN (RNA integrity number) scores were > 9 for each sample.

*Alizarin red (AR) staining*

Larvae were sacrificed at 5 dpf and 10 dpf. The larvae were fixed in PFA 4% overnight at 4 °C and thereafter rinsed three times with Phosphate Buffered Saline/0.1 % Tween (PBST) for 10 minutes. Bleaching was performed by adding 6 ml of $H_2O_2$ 3% / KOH 0.5% during 30 minutes for 5 dpf and 45 minutes for 10 dpf respectively, followed by washing twice for 20 minutes with 1ml 25% glycerol / 0,1 KOH to remove bleaching solution. The larvae were stained with AR (Merck, Overijse, Belgium) at 0.05% in the dark for 30 minutes on low agitation. Rinsing and destaining was performed thrice at 50% glycerol / 0.1% KOH for 30 minutes. The solution was replaced with a fresh solution of 50% glycerol / 0.1% KOH and stored at 4°C. The larvae were placed in lateral or ventral view onto glycerol (100%) for imaging. Images of stained larvae (n = 60–100 larvae) in three or more independent experiments were obtained on a binocular (Olympus, cell B software).

*Alcian blue (AB) staining*

Larvae were sacrificed by exposure to MS-222 (Ethyl 3-aminobenzoate methane sulfonate; Merck, Overijse, Belgium)(0.048% w/v) at 5 dpf and 10 dpf. The larvae were fixed in PFA 4%, ON at 4 °C and thereafter rinsed three times with PSBT for 10 minutes. The larvae were stained with 1ml of alcian blue at 0.04% alcian blue (Sigma-Aldrich/Merck, Overijse, Belgium) / 10mM $MgCl_2$ / 80% EtOH pH 7.5 O/N, on low agitation. Thorough rinsing was performed at least 7 to 8 times with 80% EtOH / 10mM MgCl2 / water, on low agitation till excess of blue stain is washed and the washing solution appears clear. The larvae were washed with 50% EtOH pH 7,5 for 5min and then with 25% EtOH pH 7,5 for 5min. Bleaching was performed by adding 6 ml of $H_2O_2$ 3% / KOH 0.5% during 30 minutes for 5 dpf and 45 minutes for 10 dpf respectively. Then, washing was performed twice for 20 minutes with 1ml 25% glycerol / 0.1 KOH to remove bleaching solution. Rinsing and destaining was performed thrice at 50% glycerol / 0.1% KOH for 30 minutes. The solution was replaced with a fresh solution of 50% glycerol / 0.1% KOH and stored at 4 °C. The larvae were placed in lateral side or ventral side onto glycerol (100%) for imaging. Images of stained larvae (n = 60–100 larvae) in three or more independent experiments were obtained on a stereomicroscope (Olympus, cell B software), taking care to always use the same lighting and magnification conditions.

*Image analysis of larvae stained for cartilage or bone*

Image analysis was performed on the pictures of larvae stained with alcian blue for cartilage or alizarin red for bone. According to (Aceto et al., 2015a), cartilage (alcian blue) images were analyzed by measuring the distances from anterior to the posterior end of the ethmoid plate (head length-hl), between the two hyosymplectics (d-hyo), between the articulations joining the Meckel's cartilage to the palatoquadrate (d-art), and the angle formed by the two ceratohyals (a-cer); while bone (alizarin red) images were evaluated by estimating the degree of mineralization (absent, low, normal/intermediate, high) of the following elements (Aceto et al., 2016a): maxillary (m), dentary (d), parasphenoid (p), entopterygoid (en), branchiostegal rays 1 and 2 (br1/br2), opercle (o), ceratohyal (ch), hyomandibular (hm), vertebral bodies (vb)(see also **Fig. III-4A, C** for illustration).

*Micro-computed tomography scanning (μCT) and analysis*

Wt and their respective mutant siblings were grown in the same tank at identical zebrafish density to minimize variability. The zebrafish were sacrificed, their standard length documented, then fixed for 14-16 h at 4 °C in 4% (w/v) PFA and prepared for μCT analysis. The individual zebrafish were kept hydrated in a sponge covering and placed in a sample holder during μCT acquisitions (SKYSCAN 1272 scanner (Bruker Corporation, Kontick, Belgium). Whole body scans were acquired at 70 kV and 100 μA with a 0.50 mm aluminum filter and at an isotropic voxel size of 21 μm. For high-resolution scans and quantitative analysis of the first precaudal vertebrae, zebrafish were scanned at 70 kV and 100 μA with a 0.5 mm aluminum filter at an isotropic voxel size of 7 μm. For all samples, ring artifact and beam hardening correction was kept constant and no smoothing was applied during reconstruction (NRecon, Bruker). Reconstruction of the scans was performed using the NRecon software (Bruker Corporation) and resulted in a single dicom file for each voxel size. Images with 7 μm voxel size were manually segmented using PMOD (PMOD Technologies, Zurich, Switzerland) to extract precaudal vertebrae 6-8 and both vertebral thickness and vertebral length were determined.

Further analysis of the 21 μm images was performed using the FishCuT Software (Hur et al., 2017; Watson et al., 2020b). Briefly, FishCut is a matlab toolbox (Hur et al., 2017) designed to analyse microCT image of zebrafish and extract morphological and densitometric quantitative information of zebrafish for 25 vertebrae per individual in the case of fbln1$^{-/-}$ mutants whereas for col10a1a$^{-/-}$ mutants, only 23 vertebrae were analyzed due to the fusion of the caudal fin vertebrae. Since FishCut was initially developed on images obtained with a vivaCT40 (Scanco Medical, Switzerland), we first adapted the parameters (intercept and slope) that should be used in the TMD conversion formula (Hur et al., 2017). These parameters were estimated from the calibration scan performed on the same day of the data acquisition. The following combinatorial measures were considered and quantified for each vertebra: centrum surface area (Cent.SA), centrum thickness (Cent.Th), centrum tissue mineral density (Cent.TMD), centrum length (Cent.Le), haemal arch surface area (Haem.SA), haemal arch thickness (Haem.Th), haemal arch tissue mineral density (Haem.TMD), neural arch surface area (Neur.SA), neural arch thickness (Neur.Th), neural arch tissue

mineral density (Neur.TMD), vertebral surface area (Vert, SA), vertebral thickness (Vert.Th), vertebral tissue mineral density (Vert.TMD), and were measured. Vertebral measures (Vert) represent the total vertebral body, with all three elements (centrum, haemal arch, neural arch) combined.

*Statistical analysis*

Statistics were performed using GraphPad Prism9 software (v. 9.4.1). An unpaired t-test was used for comparing distances (d-hyo, hl, and d-art) and angle (a-cer) for cartilage elements in larvae, while for vertebral thickness and length in adults an ordinary one-way ANOVA was used. For comparing the degree of mineralization, we used a Chi-square test on contingency table between WT and mutants. Multivariate analysis (Multiple linear regression analysis) was used for statistical analysis of the FishCut output data. Comparison of left and right opercular areas were performed using Sidak's multiple comparisons test of mixed effect analysis. All the values are expressed as mean ± SEM and statistical significance was set at $p<0.05$.

**3. Results**

*Analysis of sp7-expressing cells from transgenic zebrafish larvae reveals the presence of two distinct osteoblast populations at 4 dpf.*

To analyze the transcriptome of living osteoblasts isolated from developing larvae, we employed the transgenic line *Tg(sp7:sp7-GFP)* (ulg071 Tg) that carries the GFP reporter cDNA inserted into the endogenous, osteoblast-specific *sp7*(osterix) gene (Sojan et al., 2022). Transgenic larvae were dissociated at 4 dpf and the cells were analyzed using Fluorescence Activated Cell Sorting (FACS). Interestingly, when looking at the fluorescence distribution of individual cells, we observed two clear subpopulations based on their GFP fluorescent intensities, referred to as P1 (weakly positive for GFP) and P2 (strongly positive for GFP), respectively (**Fig. III-1A**). Both populations were not observed in cells obtained from non-transgenic siblings of the larvae (not shown). Whole transcriptome RNA sequencing was performed to compare the transcriptomes of these two subpopulations (P1 and P2). In addition, we also compared each subpopulation's transcriptome to that of a 4 dpf whole larvae gene expression data set ("All") from a public database (https://www.ebi.ac.uk/ena/browser/view/PRJEB7244).

Analysis of the Differentially Expressed Genes (DEGs) ($p<0.001$, log(fold-change)>1.6) lists revealed, respectively 4308 DEGs in P1 and 4531 DEGs in P2 relative to the "All" population ("AllvsP1" and "AllvsP2"), but only 966 DEGs were observed between P1 and P2 subpopulations ("P1vsP2")(**Fig. III-1B** and **Table S1**). A Venn diagram analysis showed that a vast majority of genes (3648) were common to the "AllvsP1" and "AllvsP2" (**Fig. III-1C**), which encompassed also a majority of those differentially expressed in the subpopulations "P1vsP2". Principal Component Analysis, based on the 500 most variable genes, revealed that the two subpopulations P1 and P2 were very distinct from the general "All" cell population (PC1; 89% of the variance), however the P1 and P2 cells clearly clustered separately (PC2; 4% of the variance), indicating that they may be distinct subpopulations of

osteoblasts (**Fig. III-1D**). We then analyzed the different DEG lists for enrichment in various databases (GO terms, KEGG, Panther, Reactome, and Wikipathways) to identify biological functions, cellular components, or pathways that may be affected. GSEA analysis revealed that, relative to "All", in the P1 population ("AllvsP1") immune response and cardiovascular development were the top biological processes that were up-regulated, while in the P2 subpopulation ("AllvsP2"), ossification and biomineral tissue development were significantly induced (**Fig. III-1E** and **Table S2**). Also, "extracellular region part" and "collagen trimer" were identified as the major cellular components.

A

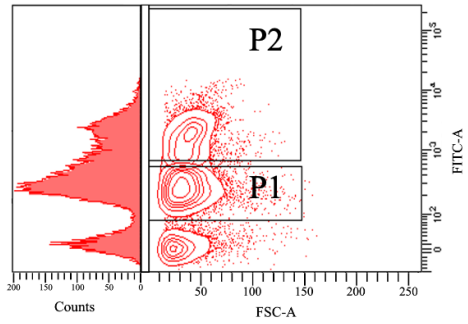


B

| | AllvsP1 | AllvsP2 | P1vsP2 |
|---|---|---|---|
| UP | 2196 | 2367 | 355 |
| DOWN | 2112 | 2164 | 611 |
| TOTAL | 4308 | 4531 | 966 |

C

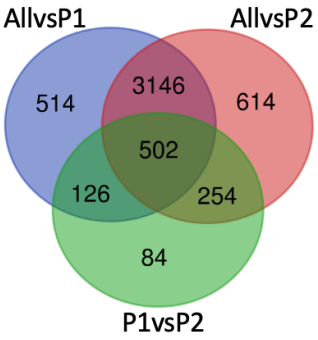


D

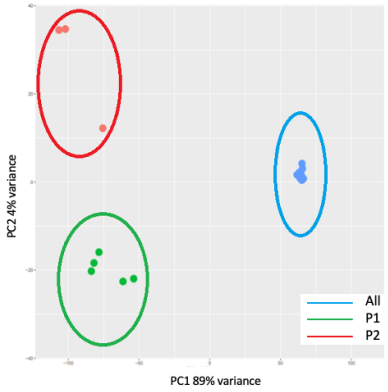


E

| Gene set | Database | geneSet | description | normalized Enrichment Score | FDR |
|---|---|---|---|---|---|
| AllvsP1 GSEA | GO-BP | GO:0006955 | immune response | 2.39 | 1.17E-02 |
| | | GO:0072358 | cardiovascular system devpt | 2.35 | 9.74E-03 |
| | | GO:0099504 | synaptic vesicle cycle | -2.36 | 1.08E-03 |
| | | GO:0006836 | neurotransmitter transport | -2.49 | 3.23E-04 |
| AllvsP2 GSEA | GO-BP | GO:0001503 | ossification | 2.37 | 1.51E-03 |
| | | GO:0072358 | cardiovascular system devpt | 2.37 | 1.26E-03 |
| | | GO:0031214 | biomineral tissue development | 2.20 | 5.65E-03 |
| | | GO:0099504 | synaptic vesicle cycle | -2.35 | 7.13E-04 |
| | | GO:0006836 | neurotransmitter transport | -2.53 | 3.56E-04 |
| AllvsP2 GSEA | GO-CC | GO:0044421 | extracellular region part | 2.35 | 1.25E-03 |
| | | GO:0005581 | collagen trimer | 1.93 | 3.31E-02 |
| P1vsP2 GSEA | GO-BP | GO:0031214 | biomineral tissue development | 2.28 | 7.31E-03 |
| | | GO:0001503 | ossification | 2.28 | 1.10E-02 |
| P1vsP2 GSEA | Wiki | WP1383 | Endochondral Ossification | 2.61 | 0.00E+00 |
| | | WP1367 | TGF beta Receptor Signaling | 2.19 | 2.81E-03 |
| | | WP211 | BMP signaling pathway | 1.52 | 2.93E-01 |
| | | WP215 | Noncanonical Wnt Pathway | 1.26 | 4.58E-01 |
| | | WP566 | Canonical wnt signaling | 1.11 | 5.59E-01 |
| | | WP1337 | MAPK Signaling Pathway | 1.00 | 5.54E-01 |

**Figure III-1. The osteoblasts at 4 dpf reveal two distinct populations based on the GFP fluorescence intensity and differential gene expression.** (A) FACS plot showing forward scattering (FSC-A) and GFP fluorescence in singlet, living cells

in gates P1 and P2. Cell distribution according to their GFP fluorescence is also shown to illustrate the two subpopulations P1 and P2. Gates were set to exclude the 100-fold larger population of non-fluorescent cells for illustration. (B) Number of DEGs that are up- or down-regulated in the different comparisons. (C) Venn diagram comparing the DEGs in "AllvsP1", "AllvsP2", and "P1vsP2". (D) PCA plot showing that the two cell subpopulations P1 and P2 are clearly different from each other, but very different from the whole larvae "All" population at 4 dpf. (E) Selected terms enriched in the DEG lists "AllvsP1", "AllvsP2", and "P1vsP2" as determined by GSEA analysis; columns represent the list concerned, the database used, the dataset concerned, its name, the normalized enrichment score, and the false discovery rate value (FDR). Positive enrichment scores indicate up-regulated terms (highlighted in red), negative ones refer to down-regulated terms (highlighted in green).

Finally, comparison of the P1 and P2 transcriptomes clearly identified "biomineral tissue development", "ossification", and "Endochondral ossification" as significantly up-regulated in P2, as well as the signaling pathways initiated by TGFbeta, BMP, Wnt, and MAPkinases. GSEA analysis using databases for known phenotypes upon mutation (Pheno-Geno in **Table S2**) or expression domains of specific genes in zebrafish (Expression in **Table S2**) revealed a near perfect enrichment in genes expressed in and affecting skeletal elements for genes up-regulated in the P2 subpopulation, relative to P1 and "All". Cardiovascular genes were also up-regulated in P2, while both subpopulations revealed down-regulation of genes involved and expressed in neural development.

Taken together, a picture emerges of a P1 population that is already engaged into skeletal differentiation, while the P2 population appears as resolutely committed to the osteoblast fate with many specific genes being strongly upregulated, such as *runx2b*, *col10a1a*, or *spp1*. Therefore, we will in the following analysis consider the P1 population as osteoblast-like cells clearly distinct from the general cells of the whole larva ("All"), and possibly a precursor to the more mature P2 osteoblast population. Different patterns emerged for individual genes when looking at their changes in expression in the different cell populations, as illustrated for selected genes displayed in a clustered heat map based on the change in the number of reads relative to the "All" population (**Fig. III-2A**). Genes unaffected or slightly upregulated in P1, but strongly upregulated in P2 would be known osteoblast markers such as *sp7* (and the transgene GFP, as expected from the FACS sorting method), but also *bmp2a*, *col10a1a*, *panx3*, and *spp1* (**Fig. III-2B**). Others were increased in P1, and remained high in P2 (*fbln1*, *col1a1*, *col2a2a*, *col2a2b*). The last group of genes show increased expression in P1 relative to "All", and a decrease in P2 (*lrp2a*, *omd*, *stcl1*). These observations indicate the involvement of a complex pattern of gene regulations comparing the general larvae cell population "All" to the P1 and P2 subpopulations.

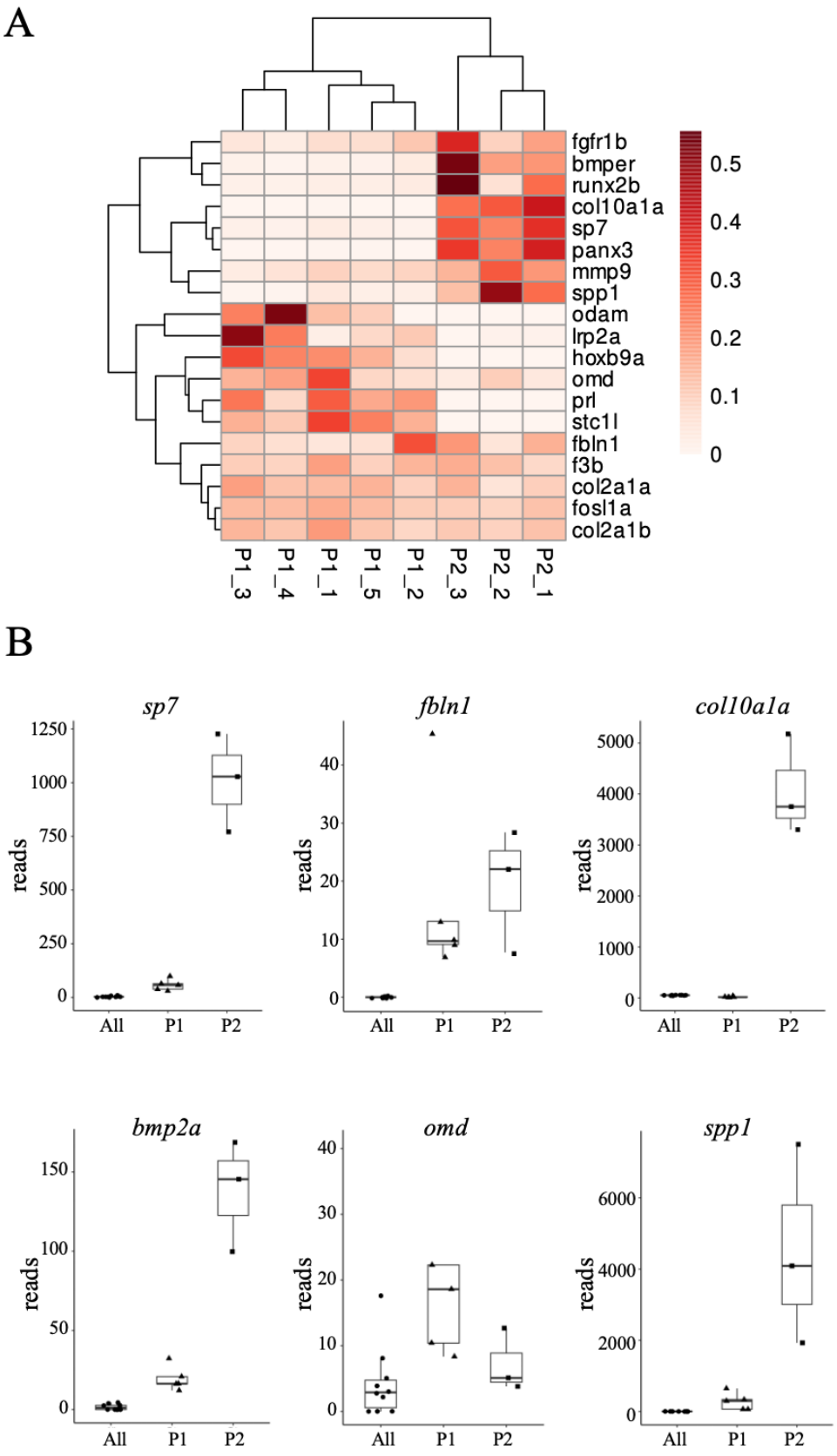


**Figure III-2. Specific genes present variable expression patterns when comparing the different cell populations.** (A) change in the number of reads relative to the "All" population of selected genes; For each gene, the color code indicates the number of reads relative to the total number of reads for this gene

in all the samples. (B) relative gene expression in the different cell populations. All samples are represented here: 10 for the "All" population, 5 for the P1 and 3 for the P2 subpopulations.

To gain further insight into the mechanisms involved in these differentiation processes, we decided to overlay the differential expression data between P1 relative to "All", and those between P1 and P2, to specific process networks. First, we collected the genes with annotations "Mineralization" or "Ossification" to construct a network of genes involved in the main function of osteoblasts (**Fig. III-3**)(Maynard and Downes). Genes upregulated in both P1 and P2 include the bone-related *sp7* and *vdra* transcription factor genes and the ECM protein genes (*spp1*, *bglapl*, *col1a1*, *mgp*). Genes for enzymes controlling extracellular phosphate concentration to ensure mineralization (Entpd5a, Alpl, Phospho1) were strongly induced in both population, as were those for some extracellular peptidases (Mmp9, Mmp14a and b) and some cell membrane proteins such as Panx3 and Tmem119a. Activation of the Hedgehog pathway is clearly indicated by the induction of the *ptch1* and *ptch2* genes, while the Bmp pathway appears to be activated mainly through Bmp3, Bmp1a, and Ltbp1. The Wnt pathway is mainly activated by Wnt5b in both P1 and P2, while the *wnt9a* gene is mainly induced in P2, and the *wls* and *lrp5* genes in P1. Thus, complex gene expression patterns emerge distinguishing the two osteoblast populations P1 and P2. As an example, the Hedgehog ligands display a complex pattern, with the *ihhb* gene induced in P2, the *ihha* gene expression reduced in P1 and induced in P2, while the *shha* and *dhh* genes were both down-regulated in P2 relative to P1.

We then looked more specifically at the BMP signaling network (**Fig. III-S1**). It appears very clearly that the genes for ligands Bmp2a, Bmp3 and Bmper were strongly upregulated in both P1 and P2, while *bmp4*, *bmp6*, *bmp7a* were more strongly induced in P1, or *bmp1a* and *bmp2b* only in P2. Other genes are only weakly affected (*bmp1b*) or follow a decrease-increase pattern (*bmp15*). Note that Bmp1 proteins are not *bona fide* BMP ligands but are rather involved in the collagen synthesis process through their peptidase activity. Considering BMP receptors, we observe that the *bmpr1aa*, *bmpr1ba*, *bmpr1bb*, and *acvrl1* genes are strongly induced mainly in P1, while *bmpr2a* and *acvr2ba* are induced both in P1 and P2. Genes *smad4a*, *smad4b*, *smad6b*, and *smad9*, coding for the Bmp signal transducing transcription factors, are up-regulated in both subpopulations. Down-regulated genes in P2, relative to P1, are the transcription factors of the Gata family, involved in hematopoiesis, cardiac and vascular development, as well as genes coding for extracellular inhibitors of BMP signaling, such as follistatins (*fsta*, *fstb*, and *fstl1a*). Other BMP antagonists are mainly upregulated in P1 and not changed in P2 (*grem1b*, *grem2a*), while *bambia* and *bambib* are strongly upregulated in both subpopulations, possibly reflecting their role in enabling Wnt signaling (Lin et al., 2008; Zhao et al., 2020).

Analysis of the WNT signaling pathway leads to similar observations (**Fig.III-S2**). The genes for Wnt1, Wnt5b, and Wnt10a are upregulated in both P1 and P2, while those for Wnt5a, Wnt11, Wnt11f2, Wnt7bb are strongly upregulated in P1 and those for Wnt3 and Wnt 6b are downregulated. Some of the WNT ligand genes are up-regulated in P1, and down-regulated in P2 (*wnt7aa*, *wnt7ab*, *wnt5a*, and *wnt4b*). In terms of receptors, the genes for Fzd1, Fzd2, Fzb8b, Lrp4, Lrp5, and Lrp6

are mainly upregulated, as well as the downstream mediators such as Axin2, disheveled proteins Dvl1a and Dvl1b as well as beta catenins Ctnnb1 and Ctnnb2 are upregulated. WNT pathway target transcription factors Jun and Tcf7 are strongly upregulated.

Taken together, a picture emerges where, compared to the general cell population "All", two distinct subpopulations of osteoblasts are present in 4 dpf zebrafish larvae based on their *sp7* (or the transgene GFP) expression. Both subpopulations present clear features of skeletal cell gene expression, with the P2 population more clearly identified as osteoblasts. However, the different components: transcription factors, ECM proteins, signaling ligands, receptors, and downstream effectors present a complex pattern of changes in expression in the two subpopulations, probably reflecting the requirement for precise coordination and regulation of the various players involved.

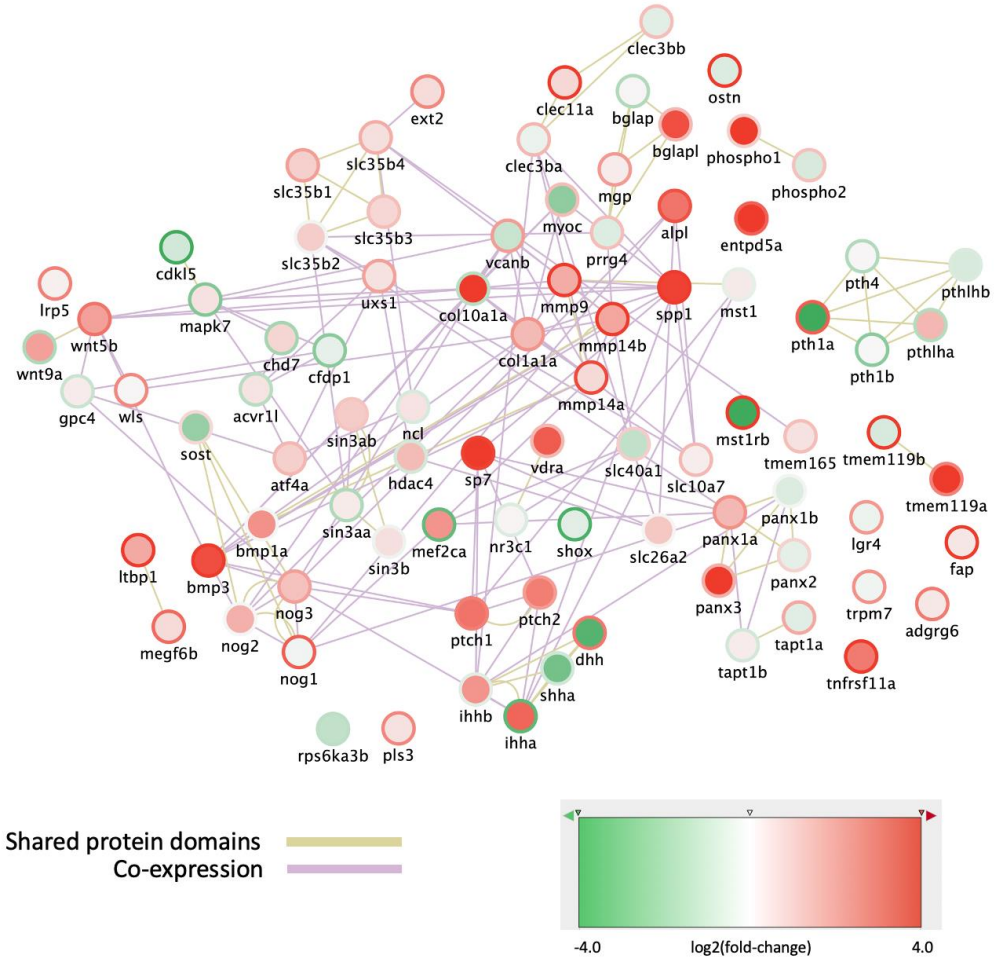


**Figure III-3**: **Expression changes in osteoblast subpopulations of genes involved in bone mineralization and ossification.** The nodes represent genes, outer ring color represents the log(fold-change) between "All" to the P1 subpopulation, while the fill color represents the log(fold-change) between P1 and P2 subpopulations. The network was generated in Cytoscape, using the GeneMANIA databases for zebrafish Shared protein domains and Co-expression.

The ECM protein gene *col10a1a* attracted our special attention at this stage. First, in contrast to its specific expression in hypertrophic chondrocytes as is generally accepted in mammals, it is also expressed in osteoblasts in zebrafish (Niu et al., 2017; Simões et al., 2006; van der Kraan and van den Berg, 2012). Moreover, our analysis of the osteoblast transcriptome at 4 dpf revealed *col10a1a* as one of the most highly upregulated genes in the P2 osteoblast population relative to P1 (**Table S1**, **Fig. III-2**), while it was slightly down-regulated in P1 relative to "All" (**Fig. III-3**, log(fold-change)= -1.34, p-value= $4.7\ 10^{-7}$). These considerations prompted us to investigate its function in zebrafish, which was unknown.

Another ECM protein whose function was unknown in zebrafish is Fibulin1, although its involvement in skeletal development was already shown in a mouse model (Cooley et al., 2014). The *fbln1* gene, different from *col10a1a*, displayed increased expression in the P1 subpopulation relative to "All", and a further increase in the P2 population (**Fig. III-2A**, **B**), thus following the expression pattern of *sp7*. We thus decided to also investigate the function of this gene in skeletal development.

*Analysis of col10a1a$^{-/-}$ zebrafish mutants.*

To elucidate the role of *col10a1a* in zebrafish skeletal development, we generated a mutant line (ulg076) disrupting the *col10a1a* coding region with a 34-nucleotide insertion and we compared the effects of this mutation in the developing larvae and in adults. No difference was observed in the standard length of WT compared to *col10a1a$^{-/-}$* siblings at 10 dpf, respectively (p value = 0.97). Staining of the larvae at 5 dpf with Alcian blue to elucidate the effects of the mutation on cranial cartilage (**Fig. III-4A**) revealed a significant reduction of the chondrocranium in the *col10a1a* mutants, as indicated by the smaller distance between the two hyosymplectics (d-hyo) and the head length (hl) in mutants compared to WT (**Fig. III-4B**). Alizarin Red staining at 10 dpf revealed an overall decreased mineralization in *col10a1a* mutants for elements of the cranial skeletal such as m, d, en, p and br1 in comparison to wt controls (**Figs. III-4C, D**). These observations are consistent with those made using another mutant carrying a 7-nucleotide deletion at the same location (not shown).

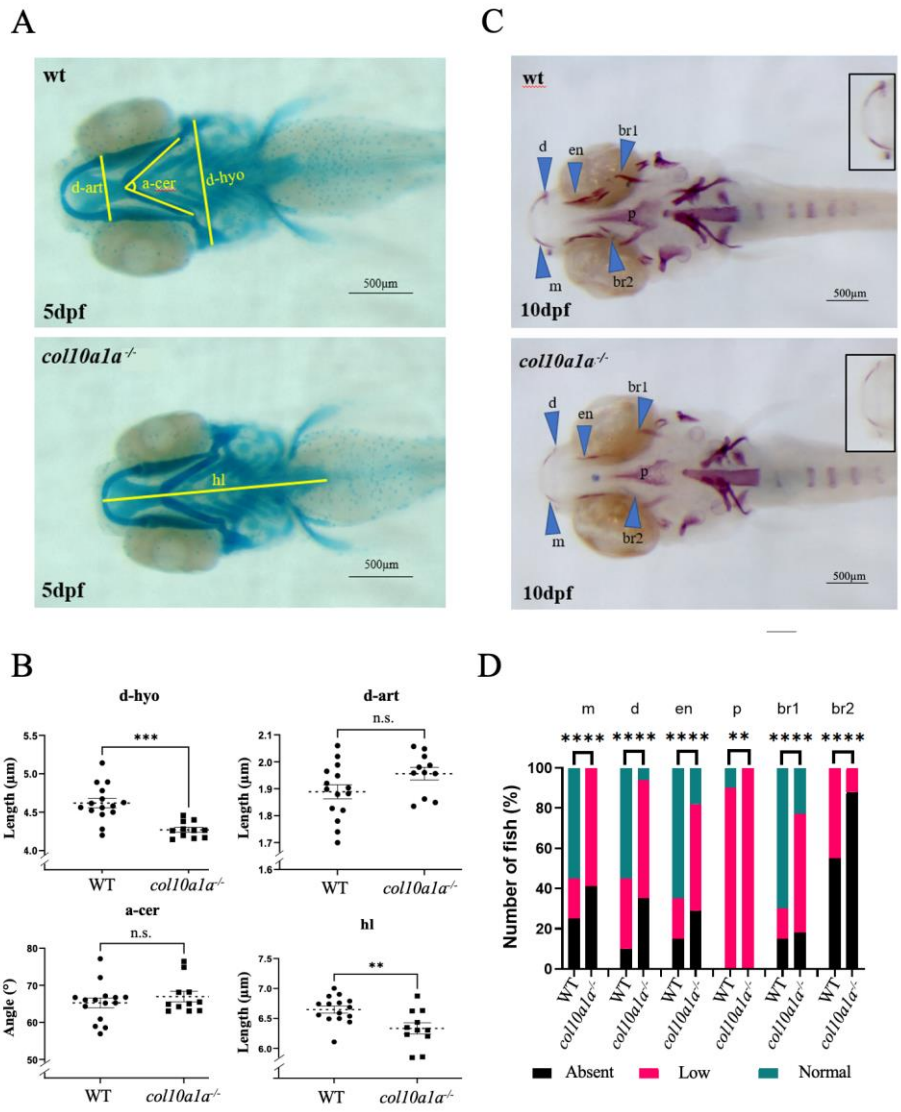


**Figure III-4. col10a1a$^{-/-}$mutants display a small chondrocranium at 5 dpf and decreased mineralization at 10 dpf compared to wt controls.** A) Ventral view of alcian blue stained WT and *col10a1a*$^{-/-}$ larvae at 5 dpf. The distances measured are indicated as described in Mat. and Meth. B) *col10a1a*$^{-/-}$ reveal reduced head size at 5 dpf compared to WT ($p<0.01$; WT n =12, *col10a1a*$^{-/-}$ n =15). Measures are: distances from anterior to the posterior end of the ethmoid plate (head length-hl), between the two hyosymplectics (d-hyo), between the articulations joining the Meckel's cartilage to the palatoquadrate (d-art), and the angle formed by the two ceratohyals (a-cer). C) Ventral view of alizarin red stained WT and *col10a1a*$^{-/-}$ larvae at 10 dpf. The blue arrowheads point to the skeletal elements: maxillary (m), dentary (d), parasphenoid (p), entopterygoid (en), branchiostegal rays 1 and 2 (br1/br2). Inserts show the maxillary and dentary. D) Fraction (%) of individuals presenting a high (green), reduced (red), or absent (Black et al.) level of bone mineralization in the different bone elements in WT and *col10a1a*$^{-/-}$ fish at 10 dpf. (WT n =20, *col10a1a*$^{-/-}$ n=17). significance: **$p<0.01$, ***$p<0.001$ and ****$p<0.0001$.

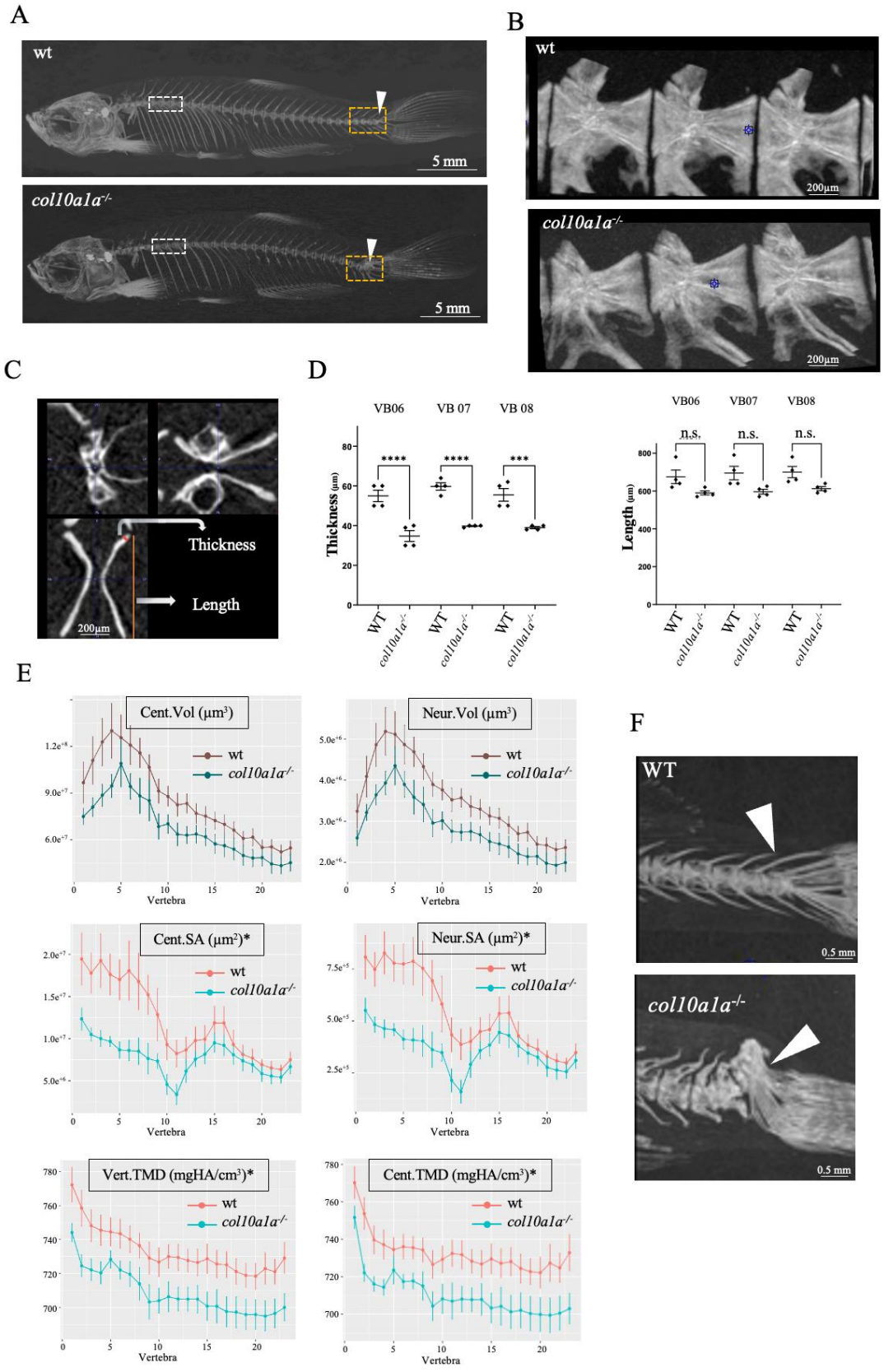


**Figure III-5. Adult *col10a1a*$^{-/-}$ zebrafish have decreased vertebral TMD and altered bone properties.** A) Representative µCT scans (MIPi = Maximum Intensity Projected image) of a year-old adult WT (top) and *col10a1a*$^{-/-}$ (bottom) reveal a decreased mineralization and fusion of the caudal fin vertebrae in the

mutant. B) Lateral view of pre-caudal vertebrae 6-8 (L to R) for WT and *col10a1a*$^{-/-}$ fish. C) Representative μCT scan of a vertebra in 3 planar views, showing the two morphometric measurements: vertebral thickness (μm) and vertebral length (μm). D) Comparison of morphometric measures on precaudal vertebrae 6-8 (n= 4 fish/group) in WT and *col10a1a*$^{-/-}$ fish. VTh and VL. E) Line plots generated using the FishCut software revealing significantly decreased TMDs in vertebra (Vert.TMD) and centra (Cent.TMD), as well as neural arch volumes and surface areas (Neur.Vol, Neur.SA) in *col10a1a*$^{-/-}$ relative to WT, while centra volume (Cent.Vol) and surface area (Cent.SA) were not significantly affected (*p<0.05), (n= 6 fish/group). F) *col10a1a*$^{-/-}$ mutants display fusion of the tail fin vertebra. significance: **p<0.01, ***p<0.001 and ****p<0.0001.

The mutant larvae and their WT siblings were grown throughout adulthood and the one-year-old fish were subjected to μCT analysis. No significant difference in the standard length was observed between WT and *col10a1a* mutants (n-6, p=0.259). No major deformities were detected in the head or vertebral column, however a projected image of a μCT scan revealed a decreased mineralization in *col10a1a*$^{-/-}$fish relative to WT (**Fig. III-5A**), and fusion of vertebral bodies at the tail fin was detected (**Fig. III-5A,F**). The μCT images were analyzed using two different approaches. First, three precaudal vertebral bodies (number 6-8) were selected, as shown in (**Fig. III-5B**) and morphometric measurements of vertebral thickness (at equivalent positions) and vertebral length were carried out as illustrated in the 3 different planar sectional view (**Fig. III-5C**). This analysis (n = 4 fish/group) revealed a significantly decreased vertebral length (p<0.05) and vertebral thickness in all three vertebrae in *col10a1a*$^{-/-}$ adult zebrafish compared to WT (**Fig. III-5D**). An additional analysis was performed by quantifying combinatorial measures over the entire vertebral column (**Fig. III-5E**).The TMD of the vertebrae and centra, as well as the haemal and neural arches (not shown) (n = 6 individuals/group and 23 vertebrae/individual) was significantly decreased in the *col10a1a*$^{-/-}$ mutants compared to WT controls (p<0.05) (**Fig. III-5E**), while surface area and volume were only affected in neural arches (Neur.SA)(Neur.Vol). A closer look at the μCT of the tail fin vertebrae revealed a complex vertebral fusion in 4 out of 6 *col10a1a*$^{-/-}$ animals (**Fig. III-5F**).

*Analysis of the fbln1*$^{-/-}$ *mutant line*

To elucidate the role of *fbln1* in skeletal development, we generated a mutant line presenting a 16-nucleotide deletion in the *fibulin1* coding region (ulg075) and performed phenotypic analysis by staining for cartilage using AB and for bone using AR staining at developmental stages 5 dpf and 10 dpf. No significant differences were observed in standard length for *fbln1*$^{-/-}$ mutants at 5 dpf (p value = 0.671) or 10 dpf (p value = 0.857) compared to WT. Looking at the 5 dpf chondrocranium (**Fig. III-6A**), we observed that the *fbln1* mutants exhibit significant reduction in the ceratohyal angle (a-cer) (p-value = 0.0154), while no significant effects were observed in the other measures (d-hyo, d-art, hl) (**Fig. III-6B**). Looking at the calcified bone matrix (**Fig. III-6C-F**), the level of mineralization for skeletal elements such as en, br1, p and vb was significantly increased in mutants at 5 dpf and 10 dpf (**Fig. III-6D, F**).

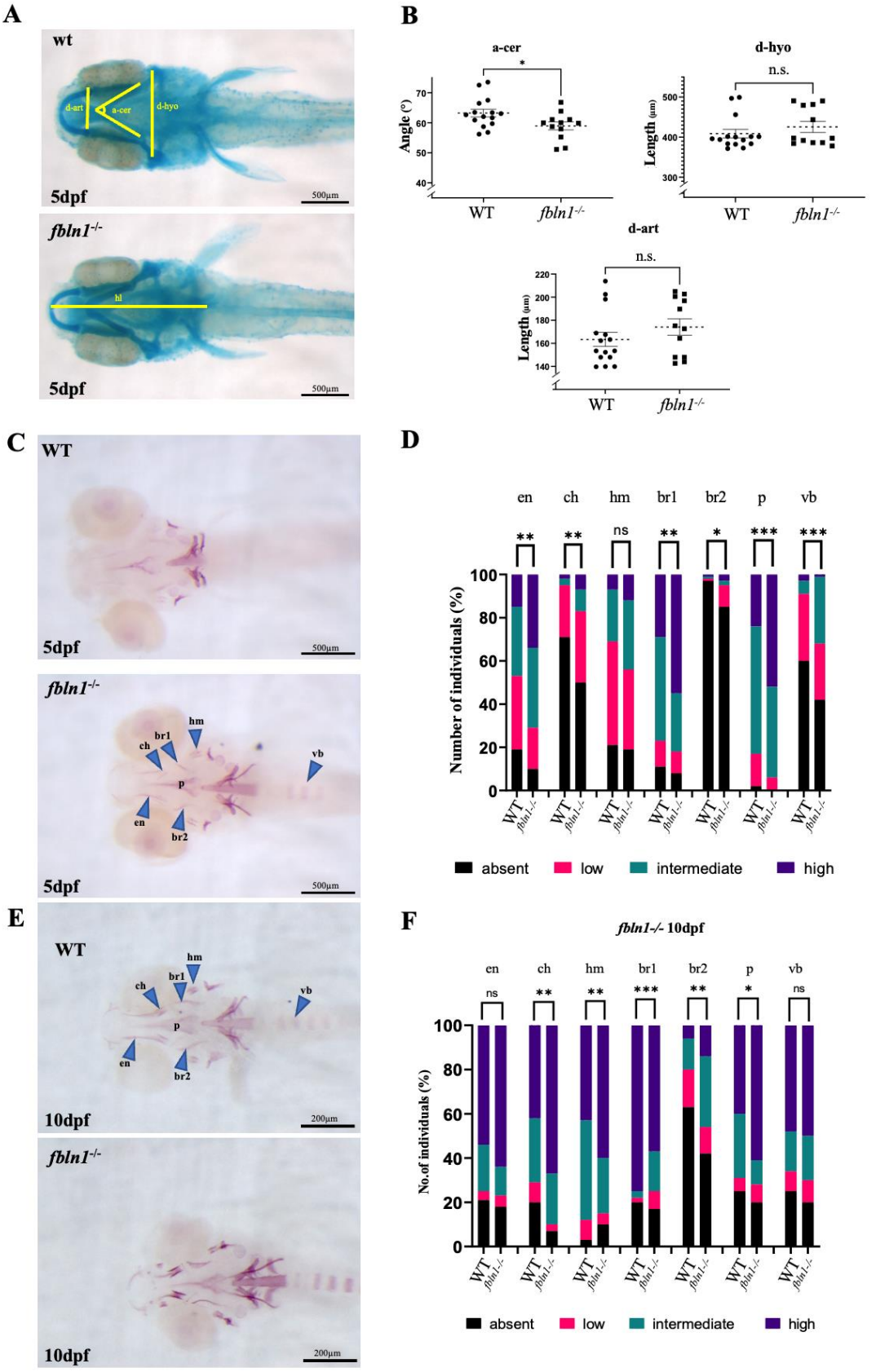


**Figure III-6. *fbln1*$^{-/-}$ mutants present increased mineralization at 5 dpf compared to WT.** A) Ventral view of alcian blue stained WT and *fbln1*$^{-/-}$ larvae at 5 dpf. The distances measured are indicated. B) *fbln1*$^{-/-}$ reveal reduced angle

between ceratohyals (a-cer) at 5 dpf compared to WT (WT n =15, fbln1-/- n =12). C) Ventral view of alizarin red stained WT and *fbln1*$^{-/-}$ larvae at 5 dpf. The blue arrowheads point to the skeletal elements: ceratohyal (ch), parasphenoid (p), entopterygoid (en), branchiostegal rays 1 and 2 (br1/br2), hyomandibular (hm), and vertebral body (vb). D) Fraction (%) of individuals presenting a high (dark blue), intermediate (green), low (red), or absent (Black et al.) level of bone mineralization in the different bone elements in WT and *fbln1*$^{-/-}$ fish at 5 dpf. (WT n =52, *fbln1*$^{-/-}$ n=68). E) Ventral view of alizarin red stained WT and *fbln1*$^{-/-}$ larvae at 10 dpf. F) Fraction (%) of individuals presenting a high (dark blue), intermediate (green), low (red), or absent (Black et al.) level of bone mineralization in the different bone elements in WT and *fbln1*$^{-/-}$ fish at 10 dpf. (WT n =35, *fbln1*$^{-/-}$ n=40).

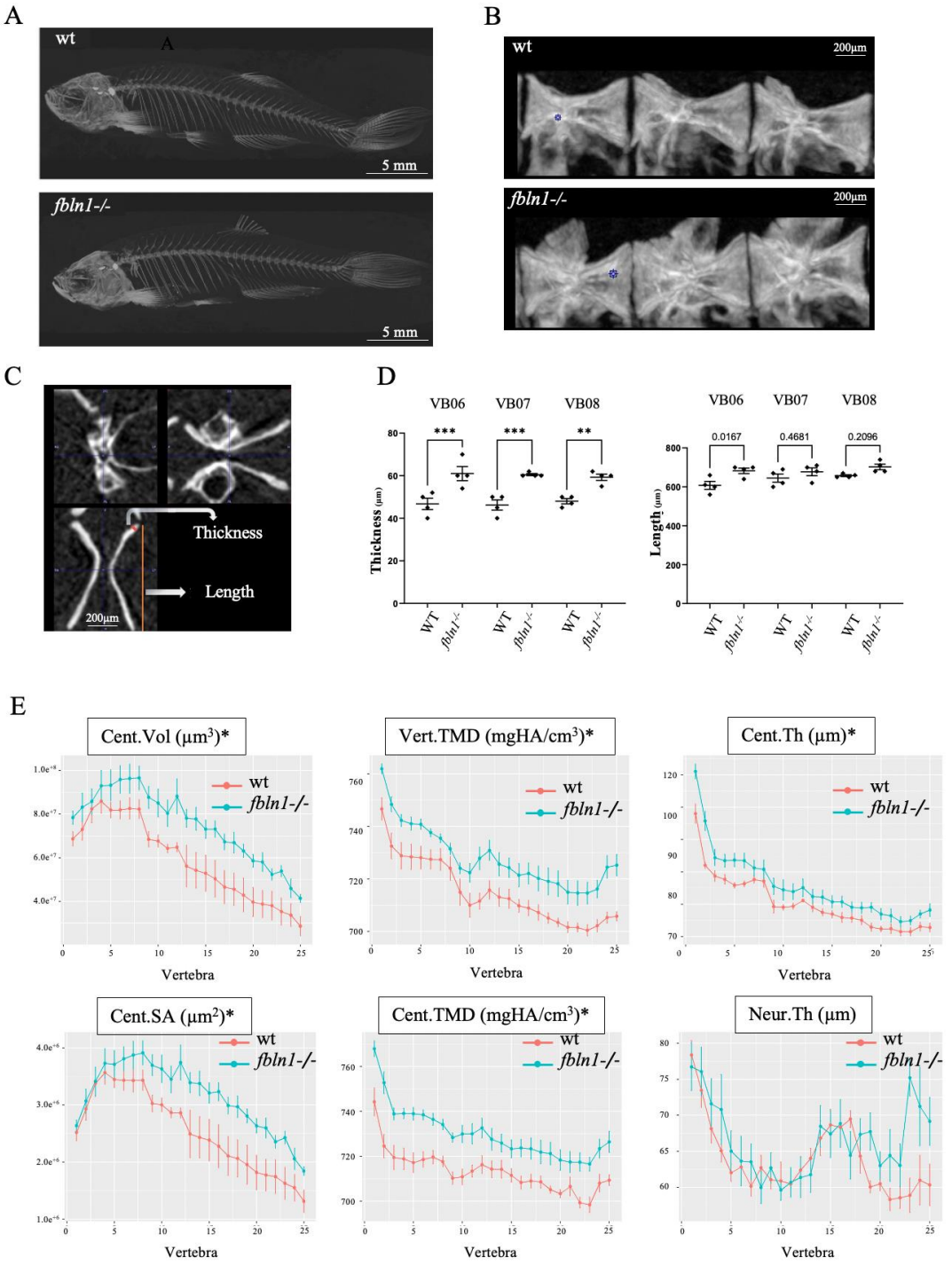


**Figure III-7. *fbln1*$^{-/-}$ adult zebrafish exhibit increased vertebral TMD and vertebral thickness.** A) µCT scans (MIPi = Maximum Intensity Projected image) of 1 year old adult WT and mutants. *fbln1*$^{-/-}$- show an increased mineralization. B) Lateral view of Vertebrae 6-8 (L to R) for WT and *fbln1*$^{-/-}$ respectively. C) Representative µCT scan of a vertebra in 3 planar views, showing two morphometric measurements: vertebral thickness (µm) and vertebral length (µm). D) Morphometric analysis of individual precaudal vertebral body numbers 6-8 (n= 4 fish/group) revealed a significantly increased thickness and length of the vertebral body in *fbln1*$^{-/-}$ compared to WT controls. E) Line plots generated using FishCuT software show significantly increased centra volume

(Cent.Vol) and surface area (Cent.SA) in *fbln1*$^{-/-}$ compared to WT controls (n= 7 fish/group). Similarly, both vertebral (Vert.TMD) and centra TMD (Cent.TMD) are significantly increased in *fbln1*$^{-/-}$. Significance: *p <0.05, ** p<0.01, and ***p<0.001.

No lethality or no major physical defect were observed in the on-growing *fbln1*$^{-/-}$ mutants, thus we let them grow alongside their WT siblings until one year of age to perform µ-CT analysis. High mineralization was easily visible in *fbln1* $^{-/-}$ zebrafish in a whole body projected image of the µ-CT scans compared to WT (**Fig. III-7A**). Using the pmod software, we segmented the precaudal vertebral centra of the precaudal vertebrae 6-8 (**Fig. III-7B**). Morphometric measurements, as illustrated in the 3 different planar sectional views (**Fig. III-8C**) revealed (n = 4 fish/group) a significantly increased vertebral length (p<0.01) and vertebral thickness (p<0.0001) in *fbln1*$^{-/-}$ adults relative to WT (**Fig. III-7D**). Using the FishCuT software to performed combinatorial measurements on all individual 25 vertebral bodies/fish (Hur et al., 2017), we observed a significantly increased volume (Cent.Vol), surface area, (Cent.SA), thickness (Cent.Th), and TMD (Cent.TMD) for the vertebral centra in *fbln1*$^{-/-}$ as compared to the WT controls (n=7 individuals /group, p<0.05) (**Fig. III-7E**). In addition, whole vertebra TMD (Vert.TMD) was increased, while overall neural arch thickness (Neur.Th) was not affected.

To complete our analyses of the *fbln1*$^{-/-}$ line, whole larvae mRNA was extracted from WT and homozygous mutant larvae at 10 dpf to compare their expression level by whole genome sequencing. 2511 DEGs (p-value<0.05, log(fold-change)>0.5) were observed (2214 up-regulated, 297 down regulated in the mutant) (**Fig. III-8A** & **B** and **Table S3**). Among the most strongly up-regulated genes were the *col10a1a*, *col1a1a*, *col11a1a*, and the *col2a1a* genes, but also many bone-related genes such as *entpd5*, *enpp1*, *sp7*, and *spp1* (**Fig. III-8A**). Among the small number of down-regulated genes, we spotted *runx2b* and *alpl*, both markers for osteoblast differentiation, that were minimally affected. The *fbln1* mRNA was decreased in the mutant, indicating that the mutation caused some degree of RNA degradation. Functional annotation using GSEA revealed that mainly one biological process was up-regulated: collagen biosynthesis, trimerization, and endochondral ossification (**Fig. III-8B**). Interestingly, all three signaling pathways for Bmp, Wnt and Fgf ligands were identified as slightly downregulated. We constructed a network around collagen biosynthesis which revealed the consistent up-regulation of all the collagen genes, but also some genes coding for integrins *(itgb1a*), matrilins, fibronectin, or for enzymes involved in collagen maturation (*plod1a*, *plod2*, *p3h1*, *p3h3*) (**Fig. III-8C**). Taken together, these results correlate with an increase of bone matrix deposition and mineralization, although some markers for osteoblast differentiation were not significantly affected.

A

| Gene name | Log(fold) | p-Value |
|---|---|---|
| col10a1a | 4.55 | 2.6E-115 |
| col1a1a | 4.32 | 1.4E-264 |
| col11a1a | 3.31 | 7.7E-86 |
| col2a1a | 3.02 | 5.5E-131 |
| col1a1b | 2.93 | 3.4E-141 |
| col2a1b | 2.2 | 9.1E-62 |
| entpd5a | 1.79 | 3.3E-06 |
| bmper | 1.17 | 1.2E-03 |
| sp7 | 0.87 | 4.8E-02 |
| enpp1 | 0.8 | 4.0E-03 |
| plod2 | 0.8 | 8.6E-03 |
| spp1 | 0.32 | 4.5E-01 |
| bmp2a | 0.21 | 7.4E-01 |
| runx2b | -0.04 | 9.4E-01 |
| alpl | -0.11 | 6.9E-01 |
| fbln1 | -0.49 | 2.5E-01 |

B

| GSEA | geneSet | description | normalized Enrichment Score | pValue | FDR |
|---|---|---|---|---|---|
| GO-CC | GO:0005581 | collagen trimer | 2.08 | 0.00E+00 | 0.00E+00 |
| | GO:0097458 | neuron part | -1.82 | 0.00E+00 | 6.42E-02 |
| GO-MF | GO:0005198 | structural molecule activity | 1.81 | 0.00E+00 | 1.72E-01 |
| | GO:0003707 | steroid hormone receptor activity | -2.22 | 0.00E+00 | 9.13E-03 |
| KEGG | dre00100 | Steroid biosynthesis | 2.15 | 0.00E+00 | 1.74E-03 |
| | dre04512 | ECM-receptor interaction | 1.87 | 0.00E+00 | 6.86E-02 |
| Reactome | R-DRE-8948216 | Collagen chain trimerization | 2.24 | 0.00E+00 | 0.00E+00 |
| | R-DRE-2022090 | Assembly of collagen fibrils and other multimeric structures | 2.19 | 0.00E+00 | 8.10E-04 |
| | R-DRE-1442490 | Collagen degradation | 2.14 | 0.00E+00 | 8.10E-04 |
| | R-DRE-1650814 | Collagen biosynthesis and modifying enzymes | 2.09 | 0.00E+00 | 1.78E-03 |
| | R-DRE-1474290 | Collagen formation | 2.01 | 1.02E-03 | 5.58E-03 |
| | R-DRE-3000178 | ECM proteoglycans | 2.00 | 0.00E+00 | 6.24E-03 |
| Wiki | WP4020 | PPAR Signaling Pathway | 1.70 | 8.31E-03 | 6.75E-02 |
| | WP1383 | Endochondral Ossification | 1.67 | 4.81E-03 | 7.00E-02 |
| | WP211 | BMP signaling pathway | -1.47 | 6.14E-02 | 1.35E-01 |
| | WP215 | Noncanonical Wnt Pathway | -1.53 | 4.44E-02 | 1.16E-01 |
| | WP152 | FGF signaling pathway | -1.57 | 5.00E-02 | 1.23E-01 |

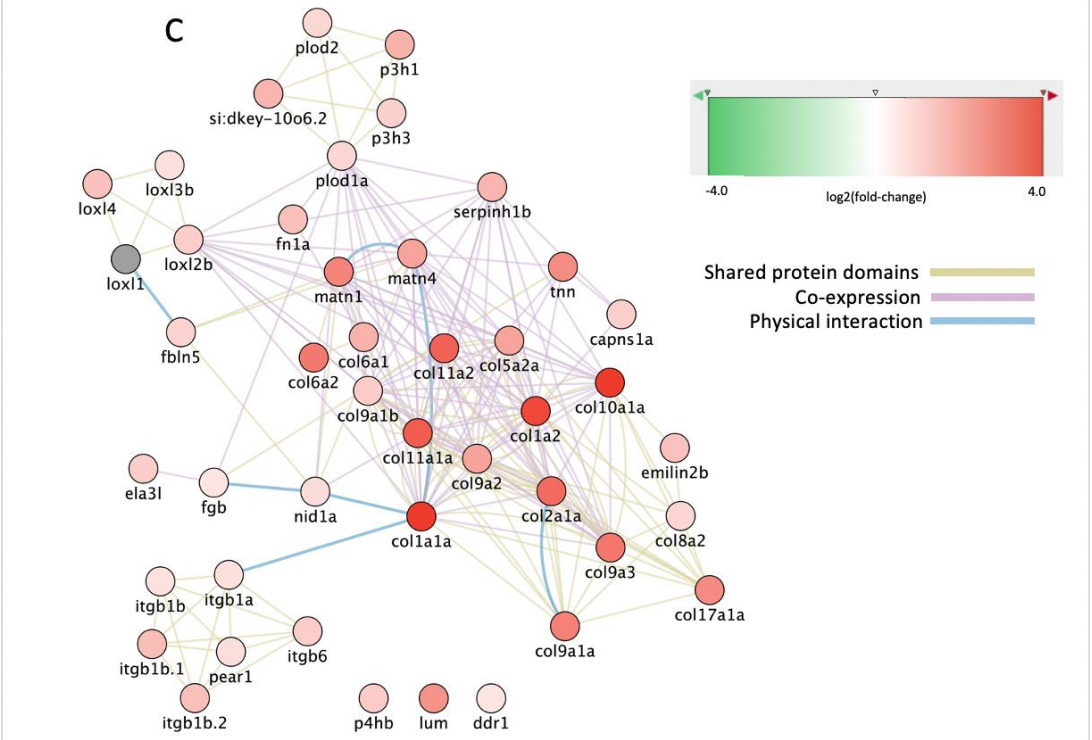


**Figure III-8. Changes of transcriptome in *fbln1*$^{-/-}$ mutants relative to WT at 10 dpf.** A) Log(fold-change) and p-values for some genes selected for their known role in osteogenesis. B) Selected functional annotations of the list of DEGs in *fbln1*$^{-/-}$ mutants. C) Network of DEGs centered around the genes involved in collagen biosynthesis. Red color refers to functions or genes that are upregulated, Green indicates genes or functions that are down-regulated in the mutants. In C), the edges are color-coded according to the nature of interaction between nodes (genes) as indicated.

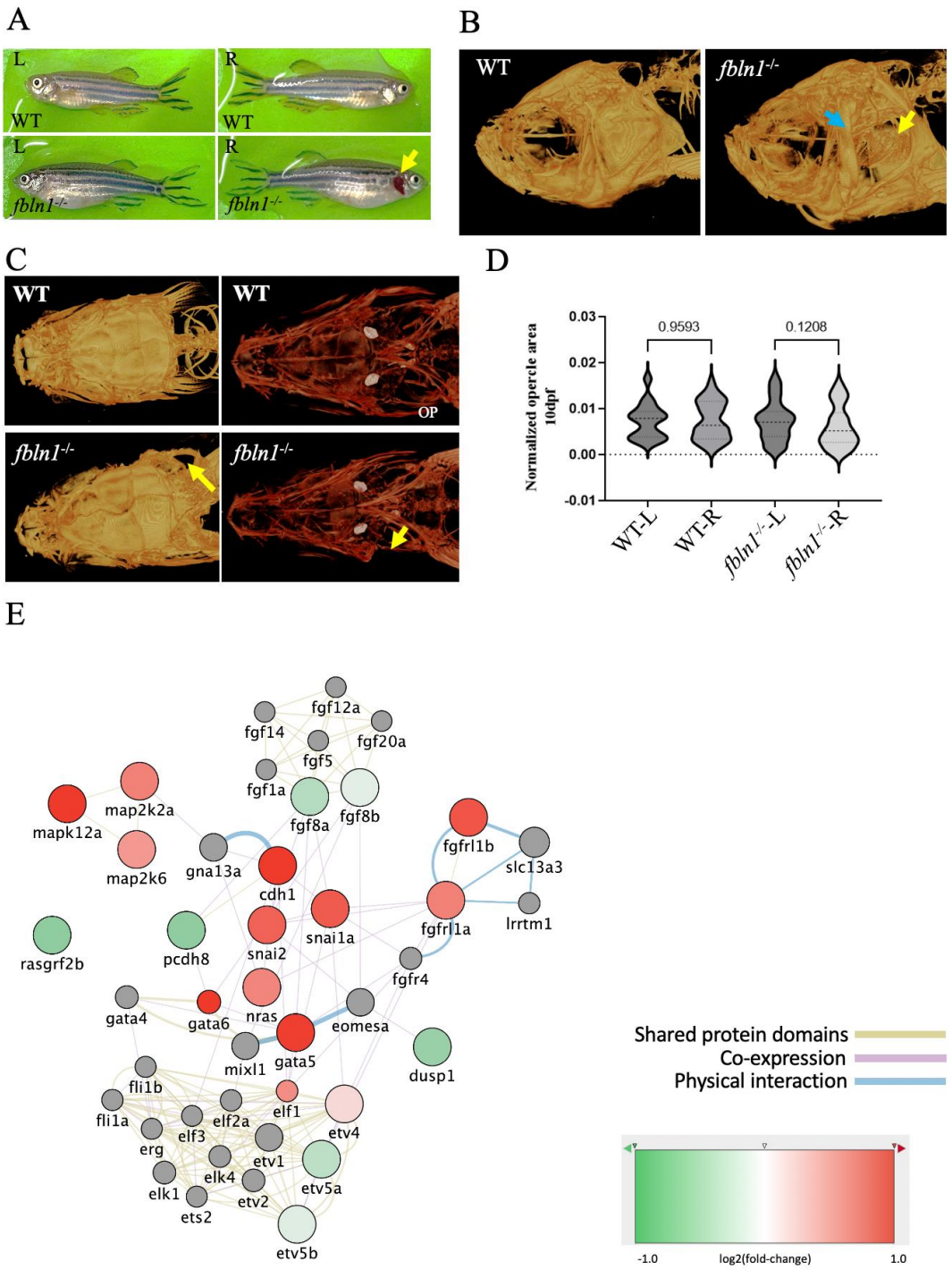


**Figure III-9. fbln1$^{-/-}$ mutant zebrafish show missing opercle on the right side.** A) Adult *fbln1*$^{-/-}$ fish bright field image showing the missing opercle (yellow arrow). B) 3D Reconstructed images from µCT scans of adult WT control and *fbln1*$^{-/-}$ fish head (yellow arrow: missing opercle, blue arrow: thickened subopercular bone). C)10 dpf Alizarin red stained zebrafish in ventral view (yellow arrow: missing opercle). D. Left (L) and Right (R) opercle area measured in ventral view on 10 dpf alizarin red stained WT control and *fbln1*$^{-/-}$zebrafish larvae show the trend of asymmetry between the L and R opercles in *fbln1*$^{-/-}$ mutant zebrafish (n= 34 WT, n= 37 *fbln1*$^{-/-}$ mutants). E) Differentially expressed genes in *fbln1*$^{-/-}$ mutants that are involved in Fgf and Mapk signaling.

*The fbln1*$^{-/-}$ *mutant lacks an opercle specifically on the right side.*

Another unexpected phenotype that we observed was that 75% of 3 months-old *fbln1*$^{-/-}$ mutants were missing an opercle on the right side (9 out of 12 individuals), compared to none in the WT controls. Simple observation of one year old adult homozygous *fbln1*$^{-/-}$ zebrafish clearly revealed this missing opercle, always on the right side compared to the contralateral left side or the WT (**Fig. III-9A**). The μ-CT scans of *fbln1*$^{-/-}$ adult zebrafish heads confirmed this observation; we can clearly observe the missing opercle (**Fig. III-9B**). In addition, closer examination of these μ-CT scans of *fbln1*$^{-/-}$ adults revealed a thickening of the cavity walls and of the subopercular bone at the site of the missing opercle (**Fig. III-9C**). The surprising asymmetry in opercle development in the adults prompted us to find out when it arises, and to measure the opercle area on alizarin red stained 10 dpf larvae, this time comparing the left (L) and right (R) opercle in mutants and WT (**Fig. III-9D**). The *fbln1*$^{-/-}$ mutants exhibited a trend (p=0.12) to a smaller opercle on the right side compared to the left one, which is not observed in wt siblings. This unique phenotype is reminiscent of the condition previously observed in *ace*$^{ti282a/fgf8}$ heterozygote zebrafish due to *fgf8* haploinsufficiency (Albertson and Yelick, 2007). These *fgf8*$^{ti282a/+}$ presented an asymmetric jaw and various size reductions of the opercle always on the right side, often displaying fusion of the opercle with the branchiostegal rays1 and 2. *fgf8* expression was observed in distinct regions of the opercle, jaws and in the cranial sutures (Albertson and Yelick, 2007). Thus, our results suggest a probable role of Fbln1 in modifying Fgf8 signaling specifically regulating opercle development. To further investigate this hypothesis, we analyzed the changes in gene expression in the *fbln1*$^{-/-}$ mutants specifically in the context of FGF signaling (**Fig. III-9E**). Interestingly, we observe a slight down-regulation of the *fgf8a* and *fgf8b* genes, along with induction of FGF receptor genes *fgfrl1a* and *fgfrl1b*, and several MAPkinase genes. Looking at known marker genes and specific targets for Fgf8 signaling (Roehl and Nüsslein-Volhard, 2001), we observe that *etv4* is slightly up-regulated (log(fold-change)= 0.16, p= 0.6), but *etv5a* and *etv5b* are down-regulated (respectively (log(fold-change)= -0.32, p= 0.016 and (log(fold-change)= -0.13, p= 0.44).

**4. Discussion**

Omics technologies have been used in the past to reveal the entire transcriptome of osteoblasts from human bone marrow progenitor cells (Qi et al., 2003), differentiating primary fibroblasts (Rakar et al., 2012), or primary mouse bone marrow stem cells (Bartelt et al., 2014; Kim et al., 2018; Rendenbach et al., 2014) by micro-array analysis. More recently, deep sequencing was applied to analyze the transcriptome of human osteoblasts from osteoarthritic patients (Grundberg et al., 2008) or from mouse tibias (Hsu et al., 2018). In all these studies, the cells were isolated from a specific location (often calvarial bone marrow) in adult individuals and kept in culture for some time before submitting them to a differentiating treatment. Some recent studies investigated primary osteoblasts directly after surgery, such as comparing primary human osteoblasts to osteoblastomas (Moriarity et al., 2015) or mouse primary calvarial osteoblasts (Wattanachanya et al., 2015). Interestingly, one such study revealed that cells isolated from rat skull or ulnar bones presented distinct transcriptomes (Rawlinson et al., 2009). Recently, the single cell transcriptome of two-months old zebrafish tail muscle tissue revealed

the presence of osteoblast-type cells (Nie et al., 2022). These studies confirmed the presence of crucial transcription factors, such as SOX9, RUNX2, and SP7 in differentiating osteoblasts, but they all relied on cells obtained from mature tissues in adults.

We decided to take advantage of the quite unique opportunity given by the zebrafish model to obtain, easily and without dissection, developmentally early osteoblasts from 4 dpf larvae. This was achieved by isolating fluorescent cells from transgenic larvae carrying the *GFP* reporter cDNA inserted into the endogenous *sp7* gene. Our assumption that this was the best way to drive GFP expression into developing osteoblasts is verified by the RNA-Seq analysis, as the highly fluorescent cells (subpopulation P2) preferentially express bone-related genes (such as *sp7* itself, but also *runx2b*, *spp1*, *entpd5a*, *alpl*, *col10a1a*), while the functional annotations specifically point to induction of ossification, ECM formation and mineralization. This identifies subpopulation P2 as mature osteoblasts. The presence of a larger, weakly fluorescent population (subpopulation P1) came as a surprise. These cells are distinct from the P2 cells, however many of the genes involved in bone development are also expressed, albeit at lower levels (*sp7*, *bmp2a*, *spp1*, *fbln1*) (**Fig. III-2** and **Table S1**). Other genes, such as *col1a1*, *col2a2a*, and *col2a2b* are equally expressed in P1 and P2, while still others are downregulated in P2 relative to P1 (*hoxb9a*, *omd*, *stc1l*). Thus, while it is tempting to speculate that population P1 would constitute a discrete osteoblast precursor population due to its very similar transcriptome to P2 (**Fig. III-1C, D**), it is at present unclear whether the P1 and P2 subpopulations can be placed in a continuous differentiation lineage or whether they represent two independent lines. One possibility would be that the P2 osteoblasts are related to intramembranous ossification, as at 4 dpf mainly this type of bone elements is mineralizing. The P1 population would correspond to the higher number of precursor cells. These precursor cells do not (or not yet) express late marker genes such as *spp1* or *col10a1a*. This is also consistent with previous reports showing *col10a1a* expression nearly exclusively in bones at 4 dpf (Kim et al., 2013c; Ling et al., 2017), while its expression in chondrocytes is observed at 6 dpf (Eames et al., 2012).

Further comparison of the P1 and P2 subpopulations revealed various patterns of gene expression (**Fig. III-3** and **Figs. S1** and **S2**), illustrating the complex regulatory events occurring in these cells. Two other genes caught our attention: the *stanniocalcin 1-like* (*stc1l*) gene and the *osteocrin* (*ostn*) gene, which both were strongly up-regulated in P1, but down-regulated in P2 (**Fig. III-2B** and **3**). These genes play a role in calcium homeostasis (Lin et al., 2017) and skeletal development (Chiba et al., 2017; Wang et al., 2021), respectively, and both are expressed specifically, but not exclusively in the corpuscles of Stannius. Whether this means that the P1 population contains this type of cells, which would express low amounts of *sp7*, or whether these genes are also expressed transiently in osteoblast precursor cells remains to be seen.

Further insight into the function of the two subpopulations may be gained from the phenotypes of the mutants that we analyzed. The *col10a1a* gene is interesting in this respect, as it is down-regulated in the P1, but dramatically up-regulated in the P2 subpopulation. Furthermore, its mammalian homolog is considered not to be expressed in osteoblasts. This expression pattern is consistent with the report that the Sp7

transcription factor directly regulates the *col10a1a* gene during zebrafish development (Niu et al., 2017), however it appears that only high *sp7* expression leads to high *col10a1a* expression. The otherECM protein gene that drew our attention is the *fibulin1 (fbln1)* gene, which is up-regulated in both P1 and P2 subpopulations. Analysis of the mutants we generated revealed opposing effects upon mutation of the *col10a1a* or the *fbln1* genes, with respectively a decreased or increased mineralization in both larval and adult stages. These phenotypes are consistent with a role for the *col10a1a* gene mainly in the P2 mature osteoblasts, while *fbln1* is already required in the P1 precursors, possibly by facilitating proliferation or recruitment to the osteogenic lineage. Such a role would be consistent with the observed increase in expression of mature osteoblast genes in the *fbln1*$^{-/-}$ animals, among which actually *col10a1a*.

The decreased mineralization we observed in the *col10a1a* mutants is coherent with the observations made in mice and humans. It is also consistent with the high expression of this gene in osteoblasts, which also extends to the axial skeleton at 6 dpf and later in the entire vertebral column (Renn et al., 2013; Tian et al., 2022). Interestingly, although *col10a1a* is a direct transcriptional target of the Sp7 transcription factor, we did not observe the dramatic defects in opercula, tail fin, and craniofacial development that were described in *sp7*$^{-/-}$ mutants (Niu et al., 2017), indicating that Col10a1a is only one of the factors regulated by Sp7 to be required for correct osteogenesis. We only observed a vertebral fusion at the tail end of the vertebral column in the *col10a1a* mutants.

In the *fbln1*$^{-/-}$ mutants, the increased mineralization is consistent with the observed *fbln1*$^{-/-}$ transcriptomic profile, showing a significant increase in several of the collagen family genes such as *col1a1a/1b*, *col2a1a/1b*, *col10a1a*, and *col11a1a*, as well as several genes for enzymes involved in collagen biosynthesis and maturation, such as *plod1a*, *plod2*, *p3h1* or *p3h3* (**Fig. III-8**). Interestingly, many of the genes up-regulated in *fbln1*$^{-/-}$ mutants at 10 dpf are also among those that are up-regulated in the P1 and P2 osteoblast subpopulations at 4 dpf, such as *col10a1a*, *entpd5a*, *enpp1*, and *spp1*. Some of these genes are also target genes for the transcription factor Sp7 (Albertson and Yelick, 2007), whose expression is significantly induced in the *fbln1*$^{-/-}$ mutant (**Fig. III-8A**). This is a sharp difference to the mouse *Fbln1* KO, where *Sp7* expression was clearly reduced (Cooley et al., 2014), possibly explaining the divergent effect of Fibulin1 depletion in zebrafish and mouse. Increased Sp7 expression may be one of the driving mechanisms for the increased bone matrix deposition and mineralization in *fbln1* mutants, even though some of the osteoblast differentiation marker genes like *runx2b* and *alpl* are downregulated.

In contrast to the findings in *Fbln1* KO mice, the survival rate of *fbln1*$^{-/-}$ zebrafish is normal until adulthood and without any malformations or defects that could impact its development and growth. A possible explanation for this discrepancy may be given by the fact that the *fbln1* gene belongs to a family of 8 ECM proteins (Mahajan et al., 2021), whose increased (possibly ectopic) expression may lead to the recently described phenomenon of "transcriptional adaptation" (Sztal and Stainier, 2020). In zebrafish, members of this family such as *fbln7 or fbln8* are expressed in skeletal structures (Russell et al., 2014), and *hmcn2* is co-expressed with *fbln1* in the fin mesenchymal cells and developing somites (Feitosa et al., 2012). Increased expression of FBLN2 was indeed

shown to rescue the function of FBLN1 in the placenta of KO mice (Singh et al., 2006) (Kostka et al., 2001). Our analysis of the *fbln1*$^{-/-}$ mutant transcriptome, compared to WT, did reveal a down-regulation of the *fbln1* gene, together with an up-regulation of *fbln2*, *fbln5*, *hmcn1*, *hmcn2* at 10 dpf. Thus, although the general function of these genes remains largely unknown in zebrafish, we cannot rule out the possibility that one of them may rescue the lethal phenotypes in our *fbln1*$^{-/-}$ mutant zebrafish, as described in mouse.

Other, more morphological effects probably result from perturbations of morphogenetic signaling pathways, as Fibulins are known to interact with signaling molecules such as BMPs, WNTs, or FGFs (Mahajan et al., 2021). The most striking such defect was obviously the missing opercle on the right side detected in 75% of *fbln1*$^{-/-}$ mutants (**Fig. III-8**) that was already detectable in 10 dpf mutant larvae (**Fig. III-8D**). Closer inspection revealed a thickening of the opercular cavity walls and of the subopercular bone at the location of the missing opercle (Fig.8B), suggesting that fusion of the developing opercle occurred in these animals as was described in haploinsufficient *fgf8*$^{ti282a/+}$ mutants (Albertson and Yelick, 2007). Transcriptome analysis of the mutant was consistent with a down-regulation of the FGF8 signaling pathway. The role of Fgf8 in zebrafish left-right asymmetry was previously shown (Albertson and Yelick, 2005), while the Fgf8 dosage was also shown in mouse to influence craniofacial shape and symmetry (Zbasnik et al., 2022). Furthermore, tight binding has been shown between mouse FBLN1 and FGF8, while downregulation of FBLN1 inhibits FGF8 expression (Fresco et al., 2016). Taken together, these observations suggest that *fbln1* mutation leads to downregulation of FGF8 signaling, resulting in absence of the opercle on the right side.

## 5. Conclusions

Taken together, we show that a population of *sp7*-expressing osteoblasts isolated from 4 dpf zebrafish larvae could be discriminated in two subpopulations, each one characterized by a specific expression pattern of bone-promoting genes. Pathway analysis revealed a complex pattern of signaling pathway components, transcription factors and ECM protein genes that characterize each of the subpopulations. Investigation of mutant zebrafish for two genes encoding ECM proteins revealed that both *col10a1a* and *fbln1* play important roles in maintain skeletal integrity, interestingly with opposite effects. Our results point to a central role for the transcription factor Sp7, activating expression of the *col10a1a* gene (among others) in regulating bone and vertebral column mineralization, while the *fbln1* mutant provides a hint that Fgf8 signaling controls the growth and morphogenesis of specific elements. Analyzing the detailed, and probably various effects of the mutations on different regions of the zebrafish skeleton (head, skull, vertebrae, fins) will require more work in the future.

**Supplementary Materials:** The following supporting information can be downloaded at: www.mdpi.com/xxx/s1, **Figure III-S1**: **Gene expression changes in genes involved in BMP signaling.** The nodes represent genes, outer ring color represents the log(fold-change) between "AllvsP1", while the fill color represents the log(fold-change) between "P1vsP2" populations. The network was generated in Cytoscape, using the GeneMANIA databases for zebrafish Shared protein domains, Co-expression, and Physical interaction.; **Figure III-S2**: **Gene**

**expression changes in genes involved in Wnt signaling.** The nodes represent genes, outer ring color represents the log(fold-change) between "AllvsP1", while the fill color represents the log(fold-change) between "P1vsP2" populations. The network was generated in Cytoscape, using the GeneMANIA databases for zebrafish Shared protein domains, Co-expression, Physical interaction, and Genetic interaction.; **Table S1**: **List of genes differentially expressed genes when comparing, respectively population P1 to population P2 (P1vsP2), whole larvae to population P1 (AllvsP1), or whole larvae to population P2 (AllvsP2).** Only significantly regulated ($p<0.001$, log(fold-change)>1.6) genes are listed, raw data and complete gene list are available at https://www.ncbi.nlm.nih.gov/geo/query/acc.cgi?acc=GSE237934. On each page, the columns give ENSEMBL gene name, the zebrafish gene name, the log(fold-change), p-value, and adjusted p-value.; **Table S2**: **Gene ontology analysis of differentially expressed genes when comparing, respectively population P1 to population P2 (P1vsP2), whole larvae to population P1 (AllvsP1), or whole larvae to population P2 (AllvsP2).** On each page, the table first lists the GSEA (Gen Set Enrichment Analysis) analysis using the databases GO, KEGG, Panther, Reactome, and Wikipathways on "Webgestalt", followed by home-made zebrafish mutant gene-phenotype (Pheno-Geno) and gene expression in zebrafish databases. The table further shows a separate over-representation analysis (ORA) of up (UP)- or down (DOWN)-regulated genes carried out using the same databases. Columns "gene set" and "description" give the names of the corresponding term, "NormalizedEnrichment" or "EnrichmentRatio" indicates the enrichment factor in the term, pValue and FDR (False Discovery Rate) indicate the statistical significance of the enrichment, while "size" and "overlap" indicates the number of genes respectively in the term and the dataset, and finally "gene names" holds the list of the overlapping genes in the dataset. Highlighted in red are selected terms/processes that are up-regulated, in green those that are down-regulated.; **Table S3**: **List of genes differentially expressed between WT and *fbln1*$^{-/-}$ mutants.** Only significantly regulated (p-value<0.05, log(fold-change)>0.5) genes are listed, raw data and complete gene list are available at https://www.ncbi.nlm.nih.gov/geo/query/acc.cgi?&acc=GSE238059. The columns give ENSEMBL gene name, the zebrafish gene name, the log(fold-change), and adjusted p-value. The second page focuses on selected genes involved in collagen synthesis, Fgf signaling, and on members of the fibulin family.

**Author Contributions:** Conceptualization, Ratish Raman, Jérémie Zappia, Jörg Renn and Marc Muller; Data curation, Ratish Raman and Marc Muller; Formal analysis, Ratish Raman, Renaud Nivelle, Arnaud Lavergne, Priyanka Kumari, Mohammed Ali, Corine Collet, Martine Cohen-Solal and Marc Muller; Funding acquisition, Martine Cohen-Solal, Yves Henrotin and Marc Muller; Investigation, Ratish Raman and Mishal Anthony; Methodology, Ratish Raman, Jérémie Zappia, Gustavo Guerrero Limon, Caroline Caetano da Silva, Jörg Renn and Marc Muller; Project administration, Marc Muller; Resources, Christian Degueldre, Agnes Ostertag and Alain Plenevaux; Software, Renaud Nivelle, Arnaud Lavergne, Christian Degueldre, Mohammed Ali, Agnes Ostertag and Marc Muller; Supervision, Agnes Ostertag, Corine Collet, Yves Henrotin and Marc Muller; Validation, Marc Muller; Visualization, Ratish Raman, Arnaud Lavergne and Agnes Ostertag; Writing – original draft, Ratish Raman, Mohammed Ali and Marc Muller; Writing – review & editing, Ratish Raman, Jérémie Zappia, Martine Cohen-Solal, Yves Henrotin, Jörg Renn and Marc Muller. All authors have read and agreed to the published version of the manuscript.".

**Funding:** This work was supported by the EU MSCA-ITN project BioMedAqu (GA 766347) that has received funding from the European Union's Horizon 2020 research and innovation programme under the Marie Skłodowska-Curie grant agreement No 766347. Further, R.R. received the Jean Henrotin Prize 2021 from

the Fondation Arthrose. R.R and C.C.dS. were MSCA PhD fellows. M.M. is a "Maître de Recherche au F.N.R.S.".

**Institutional Review Board Statement:** This study adheres to the code of ethics for scientific research in Belgium, which is compliant with European Directive 2010/63/EU. Animals were obtained from the GIGA zebrafish facility (approval number LA1610002), experiments were approved by the "Commission d'Ethique Animale Université de Liège" under the file numbers 16-1801 (20/12/2021), 16-1961 (07/11/2017) and 19-2135 (12/07/2019). Concerning biosecurity and biotechnology, European Directive 2009/41/EC was applied under the approval number SBB 219 2010/0333.

**Data Availability Statement:** The raw sequencing data are available at the Gene expression Omnibus (GEO) repository, respectively at https://www.ncbi.nlm.nih.gov/geo/query/acc.cgi?acc=GSE237934 for the osteoblast sequencing and at https://www.ncbi.nlm.nih.gov/geo/query/acc.cgi?&acc=GSE238059 for the *fbln1*$^{-/-}$ mutant.

**Acknowledgments:** We wish to thank the GIGA-R zebrafish facility for providing zebrafish adults and fertilized eggs, the GIGA imaging facility for help in FACS sorting and microscopyas well as the GIGA-R genomics/sequencing facility for providing sequencing instrumentation and manpower.

**Conflicts of Interest:** The authors declare no conflict of interest. The funders had no role in the design of the study; in the collection, analyses, or interpretation of data; in the writing of the manuscript; or in the decision to publish the results.

## References

1. Long, F. Building strong bones: molecular regulation of the osteoblast lineage. *Nature Reviews Molecular Cell Biology* **2012**, *13*, 27-38, doi:10.1038/nrm3254.
2. Komori, T. Roles of Runx2 in Skeletal Development. *Adv Exp Med Biol* **2017**, *962*, 83-93, doi:10.1007/978-981-10-3233-2_6.
3. Nakashima, K.; Zhou, X.; Kunkel, G.; Zhang, Z.; Deng, J.M.; Behringer, R.R.; de Crombrugghe, B. The novel zinc finger-containing transcription factor osterix is required for osteoblast differentiation and bone formation. *Cell* **2002**, *108*, 17-29.
4. DeLaurier, A.; Eames, B.F.; Blanco-Sanchez, B.; Peng, G.; He, X.; Swartz, M.E.; Ullmann, B.; Westerfield, M.; Kimmel, C.B. Zebrafish sp7:EGFP: a transgenic for studying otic vesicle formation, skeletogenesis, and bone regeneration. *Genesis* **2010**, *48*, 505-511, doi:10.1002/dvg.20639.
5. Lin, X.; Patil, S.; Gao, Y.G.; Qian, A. The Bone Extracellular Matrix in Bone Formation and Regeneration. *Frontiers in pharmacology* **2020**, *11*, 757, doi:10.3389/fphar.2020.00757.
6. Apschner, A.; Schulte-Merker, S.; Witten, P.E. Not all bones are created equal - using zebrafish and other teleost species in osteogenesis research. *Methods Cell Biol* **2011**, *105*, 239-255, doi:10.1016/B978-0-12-381320-6.00010-2.
7. Hammond, C.L.; Moro, E. Using transgenic reporters to visualize bone and cartilage signaling during development in vivo. *Front Endocrinol (Lausanne)* **2012**, *3*, 91, doi:10.3389/fendo.2012.00091.
8. Le Pabic, P.; Dranow, D.B.; Hoyle, D.J.; Schilling, T.F. Zebrafish endochondral growth zones as they relate to human bone size, shape and disease. *Frontiers in Endocrinology* **2022**, *13*.
9. Staal, Y.C.M.; Meijer, J.; van der Kris, R.J.C.; de Bruijn, A.C.; Boersma, A.Y.; Gremmer, E.R.; Zwart, E.P.; Beekhof, P.K.; Slob, W.; van der Ven, L.T.M. Head skeleton malformations in zebrafish (Danio rerio) to assess adverse effects of mixtures of compounds. *Archives of toxicology* **2018**, *92*, 3549-3564, doi:10.1007/s00204-018-2320-y.
10. Schilling, T.F.; Kimmel, C.B. Segment and cell type lineage restrictions during pharyngeal arch development in the zebrafish embryo. *Development* **1994**, *120*, 483-494.
11. Paudel, S.; Gjorcheska, S.; Bump, P.; Barske, L. Patterning of cartilaginous condensations in the developing facial skeleton. *Dev Biol* **2022**, doi:10.1016/j.ydbio.2022.03.010.
12. Tonelli, F.; Bek, J.W.; Besio, R.; De Clercq, A.; Leoni, L.; Salmon, P.; Coucke, P.J.; Willaert, A.; Forlino, A. Zebrafish: A Resourceful Vertebrate Model to Investigate Skeletal Disorders. *Front Endocrinol (Lausanne)* **2020**, *11*, 489, doi:10.3389/fendo.2020.00489.

13. Verreijdt, L.; Vandervennet, E.; Sire, J.Y.; Huysseune, A. Developmental differences between cranial bones in the zebrafish (Danio rerio): some preliminary light and TEM observations. *Connect Tissue Res* **2002**, *43*, 109-112.
14. Caetano da Silva, C.; Ostertag, A.; Raman, R.; Muller, M.; Cohen-Solal, M.; Collet, C. wnt11f2 Zebrafish, an Animal Model for Development and New Insights in Bone Formation. *Zebrafish* **2023**, *20*, 1-9, doi:10.1089/zeb.2022.0042.
15. Dietrich, K.; Fiedler, I.A.; Kurzyukova, A.; Lopez-Delgado, A.C.; McGowan, L.M.; Geurtzen, K.; Hammond, C.L.; Busse, B.; Knopf, F. Skeletal Biology and Disease Modeling in Zebrafish. *J Bone Miner Res* **2021**, *36*, 436-458, doi:10.1002/jbmr.4256.
16. Li, N.; Felber, K.; Elks, P.; Croucher, P.; Roehl, H.H. Tracking gene expression during zebrafish osteoblast differentiation. *Dev Dyn* **2009**, *238*, 459-466, doi:10.1002/dvdy.21838.
17. Nie, C.H.; Zhang, N.A.; Chen, Y.L.; Chen, Z.X.; Wang, G.Y.; Li, Q.; Gao, Z.X. A comparative genomic database of skeletogenesis genes: from fish to mammals. *Comparative biochemistry and physiology. Part D, Genomics & proteomics* **2021**, *38*, 100796, doi:10.1016/j.cbd.2021.100796.
18. Niu, P.; Zhong, Z.; Wang, M.; Huang, G.; Xu, S.; Hou, Y.; Yan, Y.; Wang, H. Zinc finger transcription factor Sp7/Osterix acts on bone formation and regulates col10a1a expression in zebrafish. *Sci Bull (Beijing)* **2017**, *62*, 174-184, doi:10.1016/j.scib.2017.01.009.
19. Fisher, S.; Jagadeeswaran, P.; Halpern, M.E. Radiographic analysis of zebrafish skeletal defects. *Dev Biol* **2003**, *264*, 64-76.
20. Cotti, S.; Huysseune, A.; Larionova, D.; Koppe, W.; Forlino, A.; Witten, P.E. Compression Fractures and Partial Phenotype Rescue With a Low Phosphorus Diet in the Chihuahua Zebrafish Osteogenesis Imperfecta Model. *Front Endocrinol (Lausanne)* **2022**, *13*, 851879, doi:10.3389/fendo.2022.851879.
21. Bergen, D.J.M.; Kague, E.; Hammond, C.L. Zebrafish as an Emerging Model for Osteoporosis: A Primary Testing Platform for Screening New Osteo-Active Compounds. *Front. Endocrinol* **2019**, *10*, Article 6; doi.org/10.3389/fendo.2019.00006, doi:doi.org/10.3389/fendo.2019.00006.
22. Gray, R.S.; Wilm, T.P.; Smith, J.; Bagnat, M.; Dale, R.M.; Topczewski, J.; Johnson, S.L.; Solnica-Krezel, L. Loss of col8a1a function during zebrafish embryogenesis results in congenital vertebral malformations. *Developmental Biology* **2014**, *386*, 72-85, doi:https://doi.org/10.1016/j.ydbio.2013.11.028.
23. Kim, Y.-I.; Lee, S.; Jung, S.-H.; Kim, H.-T.; Choi, J.-H.; Lee, M.-S.; You, K.-H.; Yeo, S.-Y.; Yoo, K.-W.; Kwak, S.; et al. Establishment of a bone-specific col10a1:GFP transgenic zebrafish. *Molecules and cells* **2013**, *36*, 145-150, doi:10.1007/s10059-013-0117-7.
24. Renn, J.; Buttner, A.; To, T.T.; Chan, S.J.; Winkler, C. A col10a1:nlGFP transgenic line displays putative osteoblast precursors at the medaka notochordal sheath prior to mineralization. *Dev Biol* **2013**, *381*, 134-143, doi:10.1016/j.ydbio.2013.05.030.
25. Simões, B.; Conceição, N.; Viegas, C.S.B.; Pinto, J.P.; Gavaia, P.J.; Hurst, L.D.; Kelsh, R.N.; Cancela, M.L. Identification of a Promoter Element within the Zebrafish colXα1 Gene Responsive to Runx2 Isoforms Osf2/Cbfa1 and til-1 but not to pebp2αA2. *Calcified Tissue International* **2006**, *79*, 230-244, doi:10.1007/s00223-006-0111-6.
26. Gudmann, N.S.; Karsdal, M.A. Chapter 10 - Type X Collagen. *In: Biochemistry of Collagens, Laminins and Elastin: Structure, Function and Biomarkers. Eds MA Karsdal, Academic Press* **2016**, 73-76, doi:https://doi.org/10.1016/B978-0-12-809847-9.00010-6.
27. He, Y.; Siebuhr, A.S.; Brandt-Hansen, N.U.; Wang, J.; Su, D.; Zheng, Q.; Simonsen, O.; Petersen, K.K.; Arendt-Nielsen, L.; Eskehave, T.; et al. Type X collagen levels are elevated in serum from human osteoarthritis patients and associated with biomarkers of cartilage degradation and inflammation. *BMC Musculoskelet Disord* **2014**, *15*, 309, doi:10.1186/1471-2474-15-309.
28. Bateman, J.F.; Wilson, R.; Freddi, S.; Lamandé, S.R.; Savarirayan, R. Mutations of COL10A1 in Schmid metaphyseal chondrodysplasia. *Human mutation* **2005**, *25*, 525-534.
29. van der Kraan, P.M.; van den Berg, W.B. Chondrocyte hypertrophy and osteoarthritis: role in initiation and progression of cartilage degeneration? *Osteoarthritis Cartilage* **2012**, *20*, 223-232, doi:10.1016/j.joca.2011.12.003.
30. Kwan, K.M.; Pang, M.K.; Zhou, S.; Cowan, S.K.; Kong, R.Y.; Pfordte, T.; Olsen, B.R.; Sillence, D.O.; Tam, P.P.; Cheah, K.S. Abnormal compartmentalization of cartilage matrix components in mice lacking collagen X: implications for function. *The Journal of cell biology* **1997**, *136*, 459-471.
31. Jacenko, O.; LuValle, P.A.; Olsen, B.R. Spondylometaphyseal dysplasia in mice carrying a dominant negative mutation in a matrix protein specific for cartilage-to-bone transition. *Nature* **1993**, *365*, 56-61, doi:10.1038/365056a0.
32. Rutkovskiy, A.; Stenslokken, K.O.; Vaage, I.J. Osteoblast Differentiation at a Glance. *Med Sci Monit Basic Res* **2016**, *22*, 95-106, doi:10.12659/msmbr.901142.

33. Venkatesh, B.; Lee, A.P.; Ravi, V.; Maurya, A.K.; Lian, M.M.; Swann, J.B.; Ohta, Y.; Flajnik, M.F.; Sutoh, Y.; Kasahara, M.; et al. Elephant shark genome provides unique insights into gnathostome evolution. *Nature* **2014**, *505*, 174-179, doi:10.1038/nature12826.
34. Ling, I.T.; Rochard, L.; Liao, E.C. Distinct requirements of wls, wnt9a, wnt5b and gpc4 in regulating chondrocyte maturation and timing of endochondral ossification. *Dev Biol* **2017**, *421*, 219-232, doi:10.1016/j.ydbio.2016.11.016.
35. Mahajan, D.; Kancharla, S.; Kolli, P.; Sharma, A.K.; Singh, S.; Kumar, S.; Mohanty, A.K.; Jena, M.K. Role of Fibulins in Embryonic Stage Development and Their Involvement in Various Diseases. *Biomolecules* **2021**, *11*, doi:10.3390/biom11050685.
36. Kobayashi, N.; Kostka, G.; Garbe, J.H.; Keene, D.R.; Bächinger, H.P.; Hanisch, F.G.; Markova, D.; Tsuda, T.; Timpl, R.; Chu, M.L.; et al. A comparative analysis of the fibulin protein family. Biochemical characterization, binding interactions, and tissue localization. *J Biol Chem* **2007**, *282*, 11805-11816, doi:10.1074/jbc.M611029200.
37. Cooley, M.A.; Harikrishnan, K.; Oppel, J.A.; Miler, S.F.; Barth, J.L.; Haycraft, C.J.; Reddy, S.V.; Scott Argraves, W. Fibulin-1 is required for bone formation and Bmp-2-mediated induction of Osterix. *Bone* **2014**, *69*, 30-38, doi:10.1016/j.bone.2014.07.038.
38. Singh, U.; Sun, T.; Larsson, T.; Elliott, R.W.; Kostka, G.; Fundele, R.H. Expression and functional analysis of fibulin-1 (Fbln1) during normal and abnormal placental development of the mouse. *Placenta* **2006**, *27*, 1014-1021, doi:10.1016/j.placenta.2005.10.009.
39. Cooley, M.A.; Kern, C.B.; Fresco, V.M.; Wessels, A.; Thompson, R.P.; McQuinn, T.C.; Twal, W.O.; Mjaatvedt, C.H.; Drake, C.J.; Argraves, W.S. Fibulin-1 is required for morphogenesis of neural crest-derived structures. *Dev Biol* **2008**, *319*, 336-345, doi:10.1016/j.ydbio.2008.04.029.
40. Feitosa, N.M.; Zhang, J.; Carney, T.J.; Metzger, M.; Korzh, V.; Bloch, W.; Hammerschmidt, M. Hemicentin 2 and Fibulin 1 are required for epidermal-dermal junction formation and fin mesenchymal cell migration during zebrafish development. *Dev Biol* **2012**, *369*, 235-248, doi:10.1016/j.ydbio.2012.06.023.
41. Patra, C.; Diehl, F.; Ferrazzi, F.; van Amerongen, M.J.; Novoyatleva, T.; Schaefer, L.; Mühlfeld, C.; Jungblut, B.; Engel, F.B. Nephronectin regulates atrioventricular canal differentiation via Bmp4-Has2 signaling in zebrafish. *Development* **2011**, *138*, 4499-4509, doi:10.1242/dev.067454.
42. Sanchez, C.; Mazzucchelli, G.; Lambert, C.; Comblain, F.; DePauw, E.; Henrotin, Y. Comparison of secretome from osteoblasts derived from sclerotic versus non-sclerotic subchondral bone in OA: A pilot study. *PLoS One* **2018**, *13*, e0194591, doi:10.1371/journal.pone.0194591.
43. Sojan, J.M.; Raman, R.; Muller, M.; Carnevali, O.; Renn, J. Probiotics Enhance Bone Growth and Rescue BMP Inhibition: New Transgenic Zebrafish Lines to Study Bone Health. *International journal of molecular sciences* **2022**, *23*, doi:10.3390/ijms23094748.
44. Westerfield, M. THE ZEBRAFISH BOOK, 5th Edition; A guide for the laboratory use of zebrafish (Danio rerio), Eugene, University of Oregon Press. **2007**.
45. Ma, X.; Wang, Y.W.; Zhang, M.Q.; Gazdar, A.F. DNA methylation data analysis and its application to cancer research. *Epigenomics* **2013**, *5*, 301-316, doi:10.2217/epi.13.26.
46. Ewels, P.A.; Peltzer, A.; Fillinger, S.; Patel, H.; Alneberg, J.; Wilm, A.; Garcia, M.U.; Di Tommaso, P.; Nahnsen, S. The nf-core framework for community-curated bioinformatics pipelines. *Nat Biotechnol* **2020**, *38*, 276-278, doi:10.1038/s41587-020-0439-x.
47. Love, M.I.; Huber, W.; Anders, S. Moderated estimation of fold change and dispersion for RNA-seq data with DESeq2. *Genome Biol* **2014**, *15*, 550, doi:10.1186/s13059-014-0550-8.
48. Gene Ontology Consortium. The Gene Ontology resource: enriching a GOld mine. *Nucleic Acids Res* **2021**, *49*, D325-D334, doi:10.1093/nar/gkaa1113.
49. Kanehisa, M.; Sato, Y.; Kawashima, M. KEGG mapping tools for uncovering hidden features in biological data. *Protein Sci* **2022**, *31*, 47-53, doi:10.1002/pro.4172.
50. Doudna, J.A.; Charpentier, E. Genome editing. The new frontier of genome engineering with CRISPR-Cas9. *Science* **2014**, *346*, 1258096, doi:10.1126/science.1258096.
51. Hwang, W.Y.; Fu, Y.; Reyon, D.; Maeder, M.L.; Tsai, S.Q.; Sander, J.D.; Peterson, R.T.; Yeh, J.R.; Joung, J.K. Efficient genome editing in zebrafish using a CRISPR-Cas system. *Nat Biotechnol* **2013**, *31*, 227-229, doi:10.1038/nbt.2501.
52. Aceto, J.; Nourizadeh-Lillabadi, R.; Maree, R.; Dardenne, N.; Jeanray, N.; Wehenkel, L.; Alestrom, P.; van Loon, J.J.; Muller, M. Zebrafish bone and general physiology are differently affected by hormones or changes in gravity. *PLoS One* **2015**, *10*, e0126928, doi:10.1371/journal.pone.0126928.
53. Aceto, J.; Nourizadeh-Lillabadi, R.; Bradamante, S.; Maier, J.; Alestrom, P.; Van Loon, J.; Muller, M. Effects of microgravity simulation on zebrafish transcriptomes and bone physiology; exposure starting at 5 days post-fertilization. *npj Microgravity* **2016**, *2*, 16010, doi:doi:10.1038/npjmgrav.2016.10.

54. Hur, M.; Gistelinck, C.A.; Huber, P.; Lee, J.; Thompson, M.H.; Monstad-Rios, A.T.; Watson, C.J.; McMenamin, S.K.; Willaert, A.; Parichy, D.M.; et al. MicroCT-based phenomics in the zebrafish skeleton reveals virtues of deep phenotyping in a distributed organ system. *eLife* **2017**, *6*, doi:10.7554/eLife.26014.
55. Watson, C.J.; Monstad-Rios, A.T.; Bhimani, R.M.; Gistelinck, C.; Willaert, A.; Coucke, P.; Hsu, Y.H.; Kwon, R.Y. Phenomics-Based Quantification of CRISPR-Induced Mosaicism in Zebrafish. *Cell Syst* **2020**, *10*, 275-286 e275, doi:10.1016/j.cels.2020.02.007.
56. Maynard, R.L.; Downes, N. Chapter 3 - Introduction to the Skeleton : Bone, Cartilage and Joints. *In: Anatomy and Histology of the Laboratory Rat in Toxicology and Biomedical Research; Ed. P. Gonzalez, Academic Press, Elsevier, London, UK* **2019**, 11-22, doi:10.1016/B978-0-12-811837-5.00003-4.
57. Lin, Z.; Gao, C.; Ning, Y.; He, X.; Wu, W.; Chen, Y.G. The pseudoreceptor BMP and activin membrane-bound inhibitor positively modulates Wnt/beta-catenin signaling. *J Biol Chem* **2008**, *283*, 33053-33058, doi:10.1074/jbc.M804039200.
58. Zhao, H.J.; Chang, H.M.; Klausen, C.; Zhu, H.; Li, Y.; Leung, P.C.K. Bone morphogenetic protein 2 induces the activation of WNT/β-catenin signaling and human trophoblast invasion through up-regulating BAMBI. *Cell Signal* **2020**, *67*, 109489, doi:10.1016/j.cellsig.2019.109489.
59. Albertson, R.C.; Yelick, P.C. Fgf8 haploinsufficiency results in distinct craniofacial defects in adult zebrafish. *Dev Biol* **2007**, *306*, 505-515, doi:10.1016/j.ydbio.2007.03.025.
60. Roehl, H.; Nüsslein-Volhard, C. Zebrafish pea3 and erm are general targets of FGF8 signaling. *Curr Biol* **2001**, *11*, 503-507, doi:10.1016/s0960-9822(01)00143-9.
61. Qi, H.; Aguiar, D.J.; Williams, S.M.; La Pean, A.; Pan, W.; Verfaillie, C.M. Identification of genes responsible for osteoblast differentiation from human mesodermal progenitor cells. *Proc Natl Acad Sci U S A* **2003**, *100*, 3305-3310, doi:10.1073/pnas.0532693100.
62. Rakar, J.; Lonnqvist, S.; Sommar, P.; Junker, J.; Kratz, G. Interpreted gene expression of human dermal fibroblasts after adipo-, chondro- and osteogenic phenotype shifts. *Differentiation* **2012**, *84*, 305-313, doi:10.1016/j.diff.2012.08.003.
63. Bartelt, A.; Beil, F.T.; Muller, B.; Koehne, T.; Yorgan, T.A.; Heine, M.; Yilmaz, T.; Ruther, W.; Heeren, J.; Schinke, T.; et al. Hepatic lipase is expressed by osteoblasts and modulates bone remodeling in obesity. *Bone* **2014**, *62*, 90-98, doi:10.1016/j.bone.2014.01.001.
64. Rendenbach, C.; Yorgan, T.A.; Heckt, T.; Otto, B.; Baldauf, C.; Jeschke, A.; Streichert, T.; David, J.P.; Amling, M.; Schinke, T. Effects of extracellular phosphate on gene expression in murine osteoblasts. *Calcif Tissue Int* **2014**, *94*, 474-483, doi:10.1007/s00223-013-9831-6.
65. Kim, M.; Yu, Y.; Moon, J.H.; Koh, I.; Lee, J.H. Differential Expression Profiling of Long Noncoding RNA and mRNA during Osteoblast Differentiation in Mouse. *Int J Genomics* **2018**, *2018*, 7691794, doi:10.1155/2018/7691794.
66. Grundberg, E.; Brandstrom, H.; Lam, K.C.; Gurd, S.; Ge, B.; Harmsen, E.; Kindmark, A.; Ljunggren, O.; Mallmin, H.; Nilsson, O.; et al. Systematic assessment of the human osteoblast transcriptome in resting and induced primary cells. *Physiol Genomics* **2008**, *33*, 301-311, doi:10.1152/physiolgenomics.00028.2008.
67. Hsu, W.B.; Hsu, W.H.; Hung, J.S.; Shen, W.J.; Hsu, R.W. Transcriptome analysis of osteoblasts in an ovariectomized mouse model in response to physical exercise. *Bone Joint Res* **2018**, *7*, 601-608, doi:10.1302/2046-3758.711.Bjr-2018-0075.R2.
68. Moriarity, B.S.; Otto, G.M.; Rahrmann, E.P.; Rathe, S.K.; Wolf, N.K.; Weg, M.T.; Manlove, L.A.; LaRue, R.S.; Temiz, N.A.; Molyneux, S.D.; et al. A Sleeping Beauty forward genetic screen identifies new genes and pathways driving osteosarcoma development and metastasis. *Nat Genet* **2015**, *47*, 615-624, doi:10.1038/ng.3293.
69. Wattanachanya, L.; Wang, L.; Millard, S.M.; Lu, W.-D.; O'Carroll, D.; Hsiao, E.C.; Conklin, B.R.; Nissenson, R.A. Assessing the osteoblast transcriptome in a model of enhanced bone formation due to constitutive Gs–G protein signaling in osteoblasts. *Experimental Cell Research* **2015**, *333*, 289-302, doi:https://doi.org/10.1016/j.yexcr.2015.02.009.
70. Rawlinson, S.C.; McKay, I.J.; Ghuman, M.; Wellmann, C.; Ryan, P.; Prajaneh, S.; Zaman, G.; Hughes, F.J.; Kingsmill, V.J. Adult rat bones maintain distinct regionalized expression of markers associated with their development. *PLoS One* **2009**, *4*, e8358, doi:10.1371/journal.pone.0008358.
71. Nie, C.-H.; Wan, S.-M.; Chen, Y.-L.; Huysseune, A.; Wu, Y.-M.; Zhou, J.-J.; Hilsdorf, A.W.S.; Wang, W.-M.; Witten, P.E.; Lin, Q.; et al. Single-cell transcriptomes and runx2b−/− mutants reveal the genetic signatures of intermuscular bone formation in zebrafish. *National Science Review* **2022**, *9*, doi:10.1093/nsr/nwac152.
72. Kim, Y.I.; Lee, S.; Jung, S.H.; Kim, H.T.; Choi, J.H.; Lee, M.S.; You, K.H.; Yeo, S.Y.; Yoo, K.W.; Kwak, S.; et al. Establishment of a bone-specific col10a1:GFP transgenic zebrafish. *Molecules and cells* **2013**, *36*, 145-150, doi:10.1007/s10059-013-0117-7.
73. Eames, B.F.; Amores, A.; Yan, Y.L.; Postlethwait, J.H. Evolution of the osteoblast: skeletogenesis in gar and zebrafish. *BMC Evol Biol* **2012**, *12*, 27, doi:10.1186/1471-2148-12-27.

74. Lin, C.-H.; Hu, H.-J.; Hwang, P.-P. Molecular Physiology of the Hypocalcemic Action of Fibroblast Growth Factor 23 in Zebrafish (Danio rerio). *Endocrinology* **2017**, *158*, 1347-1358, doi:10.1210/en.2016-1883.
75. Chiba, A.; Watanabe-Takano, H.; Terai, K.; Fukui, H.; Miyazaki, T.; Uemura, M.; Hashimoto, H.; Hibi, M.; Fukuhara, S.; Mochizuki, N. Osteocrin, a peptide secreted from the heart and other tissues, contributes to cranial osteogenesis and chondrogenesis in zebrafish. *Development* **2017**, *144*, 334-344, doi:10.1242/dev.143354.
76. Wang, J.S.; Kamath, T.; Mazur, C.M.; Mirzamohammadi, F.; Rotter, D.; Hojo, H.; Castro, C.D.; Tokavanich, N.; Patel, R.; Govea, N.; et al. Control of osteocyte dendrite formation by Sp7 and its target gene osteocrin. *Nat Commun* **2021**, *12*, 6271, doi:10.1038/s41467-021-26571-7.
77. Tian, Y.; Wang, W.; Lautrup, S.; Zhao, H.; Li, X.; Law, P.W.N.; Dinh, N.D.; Fang, E.F.; Cheung, H.H.; Chan, W.Y. WRN promotes bone development and growth by unwinding SHOX-G-quadruplexes via its helicase activity in Werner Syndrome. *Nat Commun* **2022**, *13*, 5456, doi:10.1038/s41467-022-33012-6.
78. Sztal, T.E.; Stainier, D.Y.R. Transcriptional adaptation: a mechanism underlying genetic robustness. *Development* **2020**, *147*, doi:10.1242/dev.186452.
79. Russell, M.W.; Raeker, M.O.; Geisler, S.B.; Thomas, P.E.; Simmons, T.A.; Bernat, J.A.; Thorsson, T.; Innis, J.W. Functional analysis of candidate genes in 2q13 deletion syndrome implicates FBLN7 and TMEM87B deficiency in congenital heart defects and FBLN7 in craniofacial malformations. *Hum Mol Genet* **2014**, *23*, 4272-4284, doi:10.1093/hmg/ddu144.
80. Kostka, G.; Giltay, R.; Bloch, W.; Addicks, K.; Timpl, R.; Fassler, R.; Chu, M.L. Perinatal lethality and endothelial cell abnormalities in several vessel compartments of fibulin-1-deficient mice. *Mol Cell Biol* **2001**, *21*, 7025-7034, doi:10.1128/MCB.21.20.7025-7034.2001.
81. Albertson, R.C.; Yelick, P.C. Roles for fgf8 signaling in left-right patterning of the visceral organs and craniofacial skeleton. *Dev Biol* **2005**, *283*, 310-321, doi:10.1016/j.ydbio.2005.04.025.
82. Zbasnik, N.; Dolan, K.; Buczkowski, S.A.; Green, R.M.; Hallgrímsson, B.; Marcucio, R.S.; Moon, A.M.; Fish, J.L. Fgf8 dosage regulates jaw shape and symmetry through pharyngeal-cardiac tissue relationships. *Dev Dyn* **2022**, *251*, 1711-1727, doi:10.1002/dvdy.501.
83. Fresco, V.M.; Kern, C.B.; Mohammadi, M.; Twal, W.O. Fibulin-1 Binds to Fibroblast Growth Factor 8 with High Affinity: EFFECTS ON EMBRYO SURVIVAL. *J Biol Chem* **2016**, *291*, 18730-18739, doi:10.1074/jbc.M115.702761.

## 2. Function of Efemp1 in zebrafish skeletal development:

Preliminary Notice: This section presents the main results covering objective **2**.

Our collaborator from mSKIL Lab at CHU, Université de Liège have detected EFEMP1 (Fib3) protein in the serum and urine of human osteoarthritic (OA) patients. A mutation in *EFEMP1* gene has been reported to cause macular degeneration in humans. In mice, lack of *Efemp1* results in early aging, herniation, and skeletal deformities, as illustrated in the graphical summary. This work provides insights into the expression and function of *efemp1* in zebrafish skeletal development.

The results are summarized in a manuscript entitled "A zebrafish mutant in the extracellular matrix protein gene *efemp1* as a model for spinal osteoarthritis."

Animals (Basel). 2023 Dec 24;14(1):74.doi: 10.3390/ani14010074

The supporting information can be downloaded
at: https://www.mdpi.com/article/10.3390/ani14010074/s1

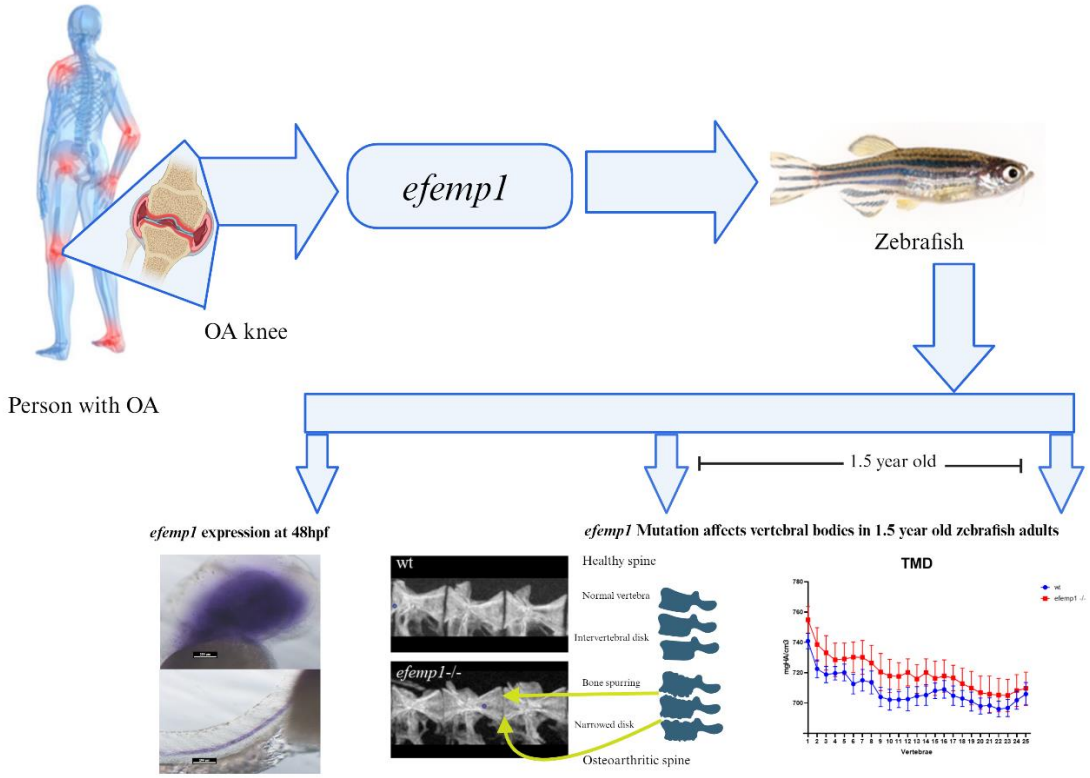

*Article*

# A Zebrafish Mutant in the Extracellular Matrix Protein Gene *efemp1* as a Model for Spinal Osteoarthritis

**Ratish Raman [1], Mohamed Ali Bahri [2], Christian Degueldre [2], Caroline Caetano da Silva [3], Christelle Sanchez [4], Agnes Ostertag [3], Corinne Collet [3,5], Martine Cohen-Solal [3], Alain Plenevaux [2], Yves Henrotin [4] and Marc Muller [1,*]**

[1] Laboratory for Organogenesis and Regeneration (LOR), GIGA Institute, University of Liège,
4000 Liège, Belgium; ratish.raman@uliege.be
[2] GIGA CRC In Vivo Imaging, University of Liege, Sart Tilman, 4000 Liège, Belgium; m.bahri@uliege.be (M.A.B.); christian.degueldre@uliege.be (C.D.); alain.plenevaux@uliege.be (A.P.)
[3] Hospital Lariboisière, Reference Centre for Rare Bone Diseases, INSERM U1132, Université de Paris-Cité, F-75010 Paris, France; cakaetano@hotmail.com (C.C.d.S.); agnes.ostertag@inserm.fr (A.O.); corinne.collet@aphp.fr (C.C.); martine.cohen-solal@inserm.fr (M.C.-S.)
[4] MusculoSKeletal Innovative Research Lab, Center for Interdisciplinary Research on Medicines,
University of Liège, 4000 Liège, Belgium; christelle.sanchez@uliege.be (C.S.); yhenrotin@uliege.be (Y.H.)
[5] UF de Génétique Moléculaire, Hôpital Robert Debré, APHP, F-75019 Paris, France
* Correspondence: m.muller@uliege.be; Tel.: +32-473993074

**Citation:** Raman, R.; Bahri, M.A.; Degueldre, C.; da Silva, C.C.; Sanchez, C.; Ostertag, A.; Collet, C.; Cohen-Solal, M.; Plenevaux, A.; Henrotin, Y.; et al. A Zebrafish Mutant in the Extracellular Matrix Protein Gene *efemp1* as a Model for Spinal Osteoarthritis. *Animals* **2024**, *14*, x. https://doi.org/10.3390/xxxxx

Academic Editors: Patricia Diogo and Paulo Jorge Gavaia

Received: 26 October 2023
Revised: 17 December 2023
Accepted: 21 December 2023
Published: date



**Simple Summary:** Osteoarthritis is a debilitating and painful joint disease affecting mainly aging animals and people. Previous results indicated that Efemp1, a protein present in the extracellular matrix that surrounds each cell, is increased in the blood, urine, and bone of osteoarthritic patients. We used the zebrafish as a model system to investigate the role of the Efemp1 protein in skeletal development and homeostasis. We showed that the *efemp1* gene is expressed in the brain, the pharyngeal cartilage, and the developing notochord which will later form the vertebral column. We generated a mutant in this gene, devoid of a functional Efemp1 protein, to show that this mutant presents transient deformities in its head cartilage at early stages. More importantly, adult mutants expressed a phenotype characterized by a smaller distance between vertebrae and ruffled edges (bone spurs) at the vertebral ends. This defect is reminiscent of that observed in spinal osteoarthritis; we therefore propose the *efemp1*−/− mutant line as the first zebrafish model to study this condition.

**Abstract:** Osteoarthritis is a degenerative articular disease affecting mainly aging animals and people. The extracellular matrix protein Efemp1 was previously shown to have higher turn-over and increased secretion in the blood serum, urine, and subchondral bone of knee joints in osteoarthritic patients. Here, we use the zebrafish as a model system to investigate the function of Efemp1 in vertebrate skeletal development and homeostasis. Using in situ hybridization, we show that the *efemp1* gene is expressed in the brain, the pharyngeal arches, and in the chordoblasts surrounding the notochord at 48 hours post-fertilization.

We generated an *efemp1* mutant line, using the CRISPR/Cas9 method, that produces a severely truncated Efemp1 protein. These mutant larvae presented a medially narrower chondrocranium at 5 days, which normalized later at day 10. At age 1.5 years, μCT analysis revealed an increased tissue mineral density and thickness of the vertebral bodies, as well as a decreased distance between individual vertebrae and ruffled borders of the vertebral centra. This novel defect, which has, to our knowledge, never been described before, suggests that the *efemp1* mutant represents the first zebrafish model for spinal osteoarthritis.

**Keywords:** zebrafish; skeletal development; ECM; *efemp1*; notochord; vertebra; osteoarthritis

## 1. Introduction

Vertebrate skeletal development depends on transcription factors and signaling pathways controlling the differentiation and maturation of crucial cell types such as chondrocytes and osteoblasts (Kobayashi and Kronenberg, 2005). These cells secrete the specific cartilage and bone extracellular matrix (ECM), respectively (Alcorta-Sevillano et al., 2020; Kozhemyakina et al., 2015; Lin et al., 2020). It is this ECM, made up of an organic and an inorganic component, that confers the mechanical and structural functions to the skeleton. The major collagens are obviously crucial for the structural integrity of the skeleton, as illustrated by mutations in their genes (Ricard-Blum, 2011). Other collagenous and non-collagenous proteins play additional roles in structuring and fine-tuning the functions of the skeletal ECM. Furthermore, increasing evidence shows that ECM proteins also play a role in controlling and shaping skeletal development (Alcorta-Sevillano et al., 2020; Lin et al., 2020). ECM proteins such as osteocalcin (Gavaia et al., 2006), osteopontin (Kwon et al., 2019; Thurner et al., 2010), osteonectin (Sparc), and bone sialoprotein (Malaval et al.) shape the skeleton by binding calcium during mineralization but also by interacting with BMP, Wnt, or integrin signaling pathways.

Fibulins are highly conserved glycoproteins that can associate with numerous components of the extracellular matrix, such as the basement membrane and elastic microfibers (Mahajan et al., 2021). Two subgroups of fibulins can be distinguished by the length and structure of their modules. The first subgroup is made up of lengthy fibulins (Fibulin-1, -2, -6 and -8) that have a propensity to form dimers. The second subgroup is comprised of short fibulins (Fibulin-3, -4, -5, and -7), all of which are monomeric forms. All fibulins have the same fundamental structure, composed of three domains, where the N-terminal domain I varies most amongst different members of the fibulin family. Domain-II, located centrally, is characterized by a varying number of EGF-like modules that contain calcium-binding sequences (cbEGF). Finally, the unique C-terminal domain-III consists of 120–140 amino acids and is also known as the fibulin-type module (Timpl et al., 2003). The short fibulins have an additional cbEGF-like module in domain-I, while the long fibulins contain three anaphylatoxin modules (Chu and Tsuda, 2004). Though fibulins are close in terms of their structure and, to some extent, location, they have varied functions and binding partners (Timpl et al., 2003). They play an important part in tissue remodeling during embryonic development, in

maintaining the structural integrity of basement membranes and elastic fibers, and in other cellular activities (Giltay et al., 1999; Miosge et al., 1996; Papke and Yanagisawa, 2014). Some fibulins have been linked to tissue organogenesis, vasculogenesis, fibrogenesis, and cancer because of their participation in the production and stabilization of the ECM (Kobayashi et al., 2007).

Fibulin-3, now renamed as EGF-containing fibulin extracellular matrix protein 1 (EFEMP1) (Ehlermann et al., 2003), is highly expressed all over the body. It is most prevalent in tissues that are rich in elastic fibers and in ocular structures (Zhang and Marmorstein, 2010). In humans, mutations in the *EFEMP1* gene cause Malattia Leventinese/Doyne honeycomb retinal dystrophy (ML/DHRD), a form of early onset macular degeneration (Marmorstein, 2004). They have also been linked in genome-wide association studies to a variety of complex phenotypes, including developmental anthropometric factors and defects in connective tissue function (Livingstone et al., 2020) or inguinal hernia (Jorgenson et al., 2015). In addition, alterations in EFEMP1 expression have been linked in humans to a variety of cancers (Livingstone et al., 2020). In mice, EFEMP1 is expressed in the heart, lungs, placenta, skeletal muscle (Giltay et al., 1999), and in the condensing mesenchyme that gives rise to bone and cartilage, suggesting its role in skeleton development (Ehlermann et al., 2003). An *Efemp1*−/− KO mouse displayed reduced fertility, premature aging, decreased body mass, lordokyphosis, as well as generalized fat, muscle and organ atrophy (McLaughlin et al., 2007). Hernias, including inguinal hernias were also observed, possibly resulting from a marked reduction of elastic fibers that was observed in the fascia, a thin connective tissue surrounding and protecting structures throughout the body. Interestingly, no macular degeneration was observed in these mice, while expression of a mutated version (R345W) of EFEMP1 did cause deposits in the retinal pigment epithelium (Fu et al., 2007; Marmorstein et al., 2007). Overexpression of EFEMP1 in mouse inhibits angiogenesis and chondrocyte differentiation by affecting the creation of cartilage nodes, as well as the production of proteoglycans (Wakabayashi et al., 2010). EFEMP1 is also known to interact with the matrix-bound matrix metalloproteinases (MMPs) inhibitor, the basement membrane protein known as extracellular matrix protein 1 (ECM1) and tissue inhibitor of metalloproteinase-3 (TIMP-3) (Klenotic et al., 2004b).

Osteoarthritis (OA) is a condition of increasing interest in aging populations that is characterized by joint pain, loss of articular cartilage, and sclerosis of the subchondral bone (Aspden and Saunders, 2019). Recently, higher levels of EFEMP1 fragments (Fib3-1, Fib3-2, and Fib3-3) have been detected in the serum and urine of OA patients, thus representing potential biomarkers for screening OA (Henrotin, 2022; Henrotin et al., 2012; Runhaar et al., 2016). In addition, secretome data revealed that sclerotic osteoblasts collected from OA subchondral bone secrete significantly higher amounts of the 3 EFEMP1 fragments than healthy tissue (Sanchez et al., 2018). Furthermore, it was shown that EFEMP1 was highly expressed in sections of articular cartilage in knee joints from OA patients (Hasegawa et al., 2017).

Here, we decided to investigate in more detail the function of EFEMP1 in vertebrate skeletal development, using the zebrafish (*Danio rerio*) as a model system. The zebrafish has recently become an excellent

model system for studying teleost and mammalian skeletal development and homeostasis. Indeed, the major signaling pathways are conserved among vertebrates and many genes were shown to play similar roles in this species (Lleras-Forero et al., 2020; Witten et al., 2017). Here, we investigate for the first time the early expression pattern of the *efemp1* gene in zebrafish embryos, and we characterize the effect on skeletal development of a mutation in this gene, both in larval stages and adults.

## 2. Materials and Methods

### *2.1. Fish and Embryo Maintenance*

Zebrafish (*Danio rerio*) were reared in a recirculating system from Techniplast (Buguggiate, Italy) at a maximal density of 7 fish/L. The water characteristics were as follows: pH = 7.4, conductivity = 50 mS/m, and temperature = 28 °C. The light cycle was controlled (14 h light, 10 h dark). Fish were fed twice daily with dry powder (ZM fish food®, Zebrafish Management Ltd., Winchester, UK) with size adapted to their age, and once daily with fresh nauplii from *Artemia salina* (ZM fish food®). Larvae aged less than 14 days were also fed twice daily with a live paramecia culture. Wild type from the AB strain and mutant lines were used. The day before breeding, two males and two females were placed in breeding tanks out of the recirculating system, with an internal divider to prevent unwanted mating. On the day of breeding, fish were placed in fresh aquarium water and the divider was removed to allow mating. Eggs were raised in E3 (5 mM Na Cl, 0.17 mM KCl, 0.33 mM $CaCl_2$, 0.33 mM $MgSO_4$, 0.00001% methylene blue).

### *2.2. In Situ Hybridization*

In situ labelling was performed as previously described (Close et al., 2002). The probe was made for *efemp1* using nested PCR (first PCR: primers F: 5′-AGTACGGGTGTGTGAACAGC-3′: R: 5′-CACACTGCCTACTAGTGTTTCAGG-3′; nested: primer R: 5′-GCGAATTGTAATACGACTCACTATAGGGGCAACAGACAGAACGCAGAAG-3′) (655 bp covering part of the 3′-untranslated region) and the antisense probe RNA was synthesized via in vitro transcription using the DIG SP6/T7 Transcription kit Roche (Merck, Overijse, Belgium). In situ hybridization was performed as previously described (Quiroz et al., 2012); the larvae were photographed under a stereomicroscope (Leica, Wetzlar, Germany) or a dissecting microscope (Olympus, Antwerp, Belgium)

### *2.3. Generation of Mutant Lines*

The mutant line for *efemp1* was created using CRISPR/Cas9 as previously described (Doudna and Charpentier, 2014; Hwang et al., 2013). The target site for the CRISPR guide RNA was AAGTGTATAAACCACTACGG, located in coding exon 3 of the *efemp1* gene. The generated deletion (line *efemp1*$^{ulg074}$) induces a frameshift in the coding sequence at amino acid 62 and a STOP codon at position 77.

For genotyping, DNA was isolated from fin clips from adults or larvae at various stages of development in 50 mM NaOH via heating in a 95 °C water bath for 20 min. The mix was cooled down on ice for 10 min and the DNA extraction was stopped by adding Tris-HCl pH = 8.0, 1/5th the volume of NaOH, and spun down using a desktop centrifuge for 2 min. The extracted DNA was stored at 4 °C, or directly used for PCR.

Primers for genotyping were F: 5′-CGAGTGTGTCCTCGTGTCTG-3′; R: 5′-CGTGGCAGTAGTTGTGTTGG-3′.

*2.4. RNA Extraction and Sequencing*

The RNA was extracted from dissected adult caudal complex using the RNA mini extraction kit (Qiagen, Hilden, Germany) according to the manufacturer's instructions. The RNA was treated with DNAseI (Qiagen, Hilden, Germany) to avoid DNA contamination. The quantity and quality of each extract was assessed via nanodrop spectrophotometer measurements, then the RNAs were stored at −80 °C. The integrity of total RNA extracts was assessed using the BioAnalyzer (Agilent, Santa Clara, CA, USA). RIN (RNA integrity number) scores were >9 for each sample.

The cDNA libraries were generated from 100 to 500 ng of extracted total RNA using the "Stranded Total RNA Prep" kit (Illumina, San Diego, CA, USA) according to the manufacturer's instructions. All cDNA libraries were sequenced on a NextSequ550 sequencing system (Illumina, San Diego, CA, USA), in 2 × 76 bp (paired end). Approximatively 20–25 M reads were sequenced per sample. The sequencing reads were processed through the Nf-core rnaseq pipeline 3.0 (Ewels et al., 2020) with default parameters and using the zebrafish reference genome (GRCz11) and the annotation set from Ensembl release 103 (www.ensembl.org; accessed 1 May 2020). Differential gene expression analysis was performed using the DESeq2 pipeline (Love et al., 2014).

*2.5. Alcian Blue (AB) Staining*

AB staining is one of the most widely applied techniques for staining ECM glycosaminoglycans to observe cartilage structures. Larvae were sacrificed by exposure to MS-222 (Ethyl 3-aminobenzoate methane sulfonate; Merck, Overijse, Belgium) (0.048% *w*/*v*) at 5 dpf or 10 dpf. The larvae were fixed in para-formaldehyde (PFA) 4% for 14–16 h at 4 °C and thereafter rinsed three times with Phosphate Buffered Saline/Triton 0.1% for 10 min. The larvae were stained in 1 mL of alcian blue 8Gx (Sigma Aldrich, Hoeilaart, Belgium) at 0.04% alcian blue/10 mM $MgCl_2$/80% EtOH pH 7.5 O/N, on low agitation. Thorough rinsing was performed at least 7 to 8 times with 80% EtOH/10 mM $MgCl_2$, on low agitation till the excess of blue stain was washed and the washing solution appeared clear. The larvae were washed with 50% EtOH pH 7.5 for 5 min and then with 25% EtOH pH 7.5 for 5 min. Bleaching was performed by adding 6 mL of $H_2O_2$ 3%/KOH 0.5% for 30 min for 5dpf and 45 min for 10 dpf larvae, respectively. Then, washing was performed twice for 20 min with 1 mL 25% glycerol/0.1% KOH to remove the bleaching solution. Rinsing and destaining was performed thrice at 50% glycerol/0.1% KOH for 30 min. The solution was replaced with a fresh solution of 50% glycerol/0.1% KOH and stored at 4 °C. The larvae were placed in lateral or ventral view onto glycerol (100%) for imaging. Images of stained larvae ($n$ = 20–30 larvae) in three or more independent experiments were obtained on a dissecting microscope (Olympus, cell B software).

*2.6. Alizarin Red (AR) Staining*

Larvae were sacrificed at 5 dpf and fixed in PFA 4% for 14–16 h at 4 °C and thereafter rinsed three times with Phosphate Buffered Saline/0.1% Tween (PBST) for 10 min. Bleaching was performed by adding 6 mL of $H_2O_2$ 3%/KOH 0.5% for 30 min for 5 dpf, followed by

washing twice for 20 min with 1 mL 25% glycerol/0.1% KOH to remove the bleaching solution. The larvae were stained with AR (Merck, Overijse, Belgium) at 0.05% in the dark for 30 min on low agitation. Rinsing and de-staining was performed thrice at 50% glycerol/0.1% KOH for 30 min. The solution was replaced with a fresh solution of 50% glycerol/0.1% KOH and stored at 4 °C. The larvae were placed in lateral or ventral view onto glycerol (100%) for imaging. Images of stained larvae in two independent experiments were obtained on a binocular (Olympus, cell B software).

*2.7. Image Analysis of Larvae Stained for Cartilage or Bone*

Image analysis was performed on the pictures of larvae stained with alcian blue for cartilage or alizarin red for bone. According to Aceto et al., 2015 (Aceto et al., 2015a), cartilage (alcian blue) images were analyzed by measuring the distances from anterior to ethmoid plate, anterior to posterior (head length-hl), articulation left to articulation right (d-art), ceratohyal ext. left to ceratohyal ext. right (d-cer), ethmoid plate to posterior, hyosymplectic left to hyosymplectic right (d-hyo), and the angle formed by the two ceratohyals (a-cer). Bone (alizarin red) images were evaluated by estimating the degree of mineralization (absent, low, normal/intermediate, high) of the following elements (Aceto et al., 2016a): maxillary (m), dentary (d), parasphenoid (p), entopterygoid (en), branchiostegal ray-1 (br1), opercle (o), ceratohyal (ch), and hyomandibular (hm) (see also Figure III-S1 for illustration).

*2.8. Micro-Computed Tomography Scanning (μCT)*

WT and *efemp1−/−* zebrafish siblings were grown in the same tank at identical density to minimize variability before being analyzed with μCT. For quantitative evaluation, 6 wt and 6 *efemp1−/−* at 1 year old were selected to document the standard length and thereafter analyzed. The zebrafish were sacrificed and fixed overnight at 4 °C in 4% (*w*/*v*) PFA. Individual zebrafish were kept hydrated in a sponge covering and placed in a sample holder during μCT acquisitions (SKYSCAN 1272 scanner, Bruker Corporation, Kontick, Belgium).

Whole body scans were acquired at 70 kV and 100 μA with a 0.50 mm aluminum filter and at an isotropic voxel size of 21 μm. For high-resolution scans and quantitative analysis of the first precaudal vertebrae, zebrafish were scanned at 70 kV and 100 μA with a 0.5 mm aluminum filter at an isotropic voxel size of 7 μm. For all samples, ring artifact and beam hardening correction was kept constant, and no smoothing was applied during reconstruction (NRecon, Bruker). Reconstruction of the scans was performed using the NRecon version 2.0 software (Bruker Corporation) and resulted in a single dicom file for each voxel size 21 and 7 μm. Images with 7 μm voxel size were manually segmented using PMOD version 4.0 (PMOD Technologies, Zurich, Switzerland) to extract precaudal vertebrae and both vertebral thickness and vertebral length. GraphPad Prism9 was used to perform ordinary one-way ANOVA test for comparing wt controls versus mutants.

Further analysis of the 21 μm images was performed using the FishCuT version 1.2 Software (Hur et al., 2017; Watson et al., 2020b). Briefly, FishCuT is a matlab toolbox designed to analyze microCT images of zebrafish and extract morphological and densitometric quantitative information of zebrafish (Hur et al., 2017). Since FishCuT

was initially developed on images obtained with a vivaCT40 (Scanco Medical, Brüttisellen, Switzerland), we first adapted the parameters (intercept and slope) that should be used in the TMD conversion formula (https://doi.org/10.7554/eLife.26014, accessed on 07/02/2022). These parameters were estimated from the calibration scan performed on the same day of the data acquisition. FishCuT output data were then subjected to statistical analysis (multiple linear regression analysis with post hoc d'Agostino–Pearson normality testing) in GraphPad Prism9 software (9.4.1).

The following combinatorial measures were considered and quantified for each vertebra: centrum surface area (Cent.SA), centrum thickness (Cent.Th), centrum tissue mineral density (Cent.TMD), centrum length (Cent.Le), haemal arch surface area (Haem.SA), haemal arch thickness (Haem.Th), haemal arch tissue mineral density (Haem.TMD), neural arch surface area (Neur.SA), neural arch thickness (Neur.Th), neural arch tissue mineral density (Neur.TMD), vertebral surface area (Vert.SA), vertebral thickness (Vert.Th), and vertebral tissue mineral density (Vert.TMD). Vertebral measures (Vert) represent the total vertebral body, with all three elements (centrum, haemal arch, and neural arch) combined. Multivariate analysis was performed for statistical significance.

## 3. Results

### *3.1. efemp1 Expression in Zebrafish*

To gain insight into the expression domain of the *efemp1* gene during early zebrafish development, we performed whole mount in situ hybridization experiments on 48 hours post-fertilization (hpf) zebrafish embryos (**Fig. III-10**). *efemp1* was expressed in the brain (br), in the pharyngeal region (pa), and in the notochord (nt) along the entire length of the trunk (**Fig. III-10A,B**). Closer inspection of the expression in the notochord revealed that it was seen in the chordoblasts (cb) (**Fig. III-10C,D**), responsible for secretion of the notochordal sheet (nts) (Grotmol et al., 2005; Pogoda et al., 2018a). No labelling was observed in 24, 96, or 120 hpf larvae.

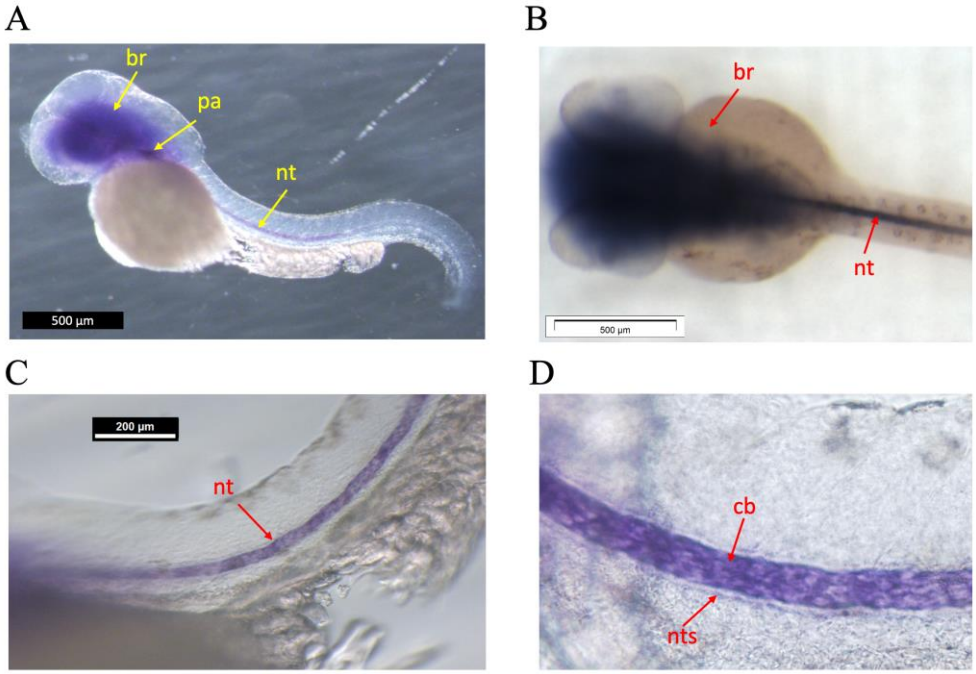


**Figure III-10.** Whole mount in situ hybridization on 48 hpf zebrafish embryos. (**A**) Lateral view, anterior to the left. Expression is seen in the brain (br), the pharyngeal area (pa), and in the notochord (nt) (**B**) Dorsal view, anterior to the left. Dissection microscope picture. Expression is seen in brain and notochord. (**C**,**D**) Lateral views, anterior to the left. Enlarged view of expression in the notochord, specifically (**D**) in the chordoblasts (cb) immediately adjacent to the notochordal sheath (nts). Other, non-related probes served as negative control.

*3.2. Characterization of Early Skeletal Development in a Mutant in the efemp1 Gene*

To gain insight into the function of the *efemp1* gene during development, we generated a mutant (*efemp1*$^{ulg074}$) carrying a 5-nucleotide deletion (delin −7+2) at position 184 relative to the ATG, leading to disruption of the coding sequence at amino acid 62 and a STOP codon at position 77. Heterozygous parents carrying this mutation were crossed and their offspring larvae were stained for cartilage with alcian blue at 5 and 10 days post-fertilization (dpf).

Each larva was photographed, and its DNA was subsequently extracted for individual genotyping. Morphometric measurements were performed (Aceto et al., 2015a) and assigned to, respectively, wt and homozygous *efemp1*−/− mutants. Measurements on 5 dpf larvae revealed a significant ($p$ = 0.032 and 0.047, respectively) decrease in the distance between the Meckel's-palatoquadrate articulations (d-ar) and between the posterior end of the ceratohyals (d-cer), while the angle between ceratohyals (a-cer) ($p$ = 0.19) and the head length (hl) ($p$ = 0.76) were not affected. Thus, it appears that the chondrocranium was narrower in the *efemp1*-/- mutants at 5dpf (**Figure III-11A,C**). The head width seemed to be restored with age, as in 10dpf larvae the d-ar and d-cer were not significantly different anymore (**Figure III-11B,D**).

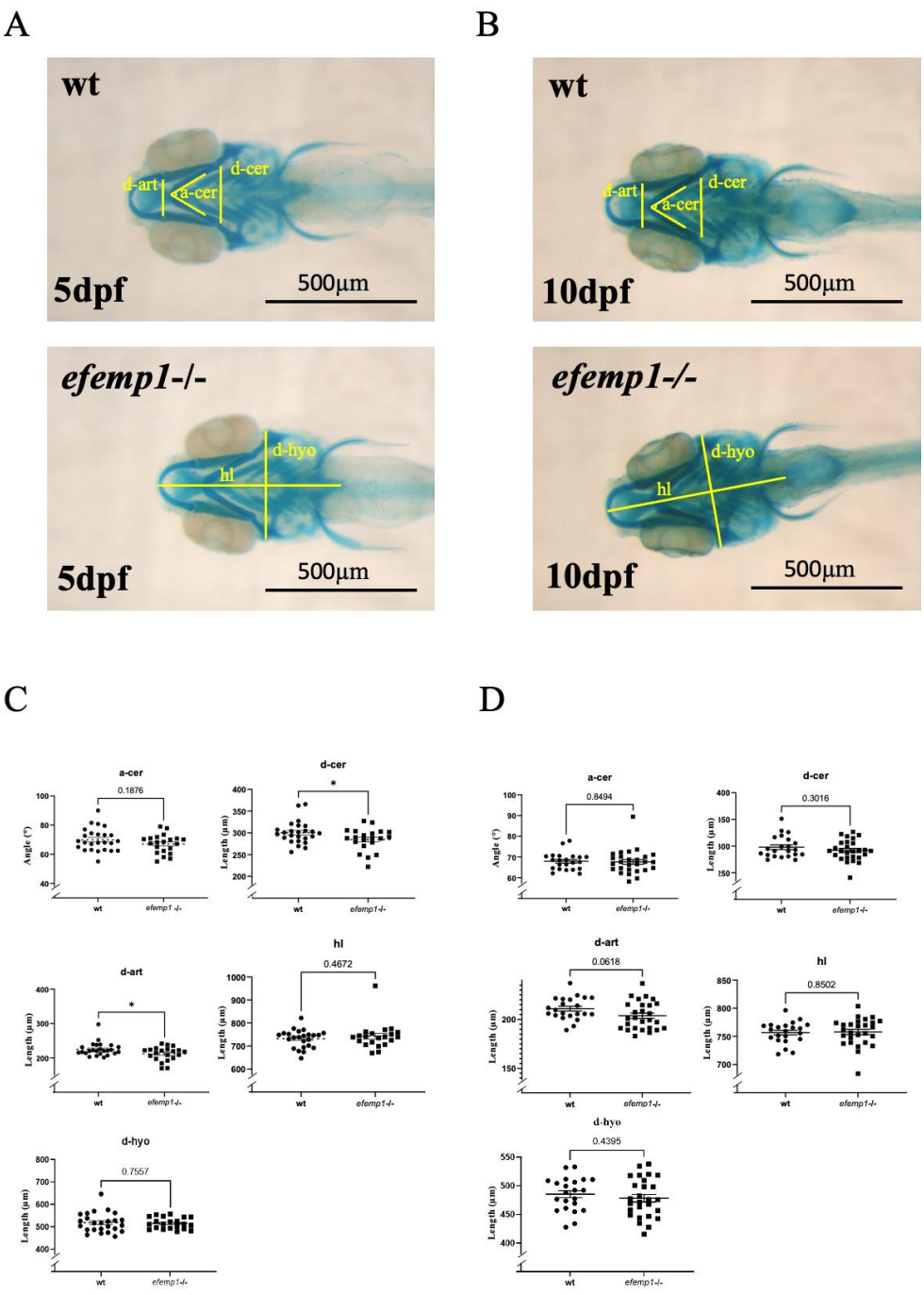


**Figure III-11.** Cartilage staining with alcian blue of 5 dpf (**A**,**C**) and 10 dpf (**B**,**D**) wt and *efemp1*−/− mutant larvae. The different measures are illustrated in (**A**,**B**): d-ar: distance between the Meckel's-palatoquadrate articulations; d-cer: distance between the posterior ends of the ceratohyals; a-cer: angle between the ceratohyals; hl: head length and d-hyo: head width. (**C**) *efemp1*−/− reveal a reduced distance between the articulation (d-ar) and narrower distance between the ceratohyal elements (d-cer) at 5 dpf compared to wt (wt $n$ = 24, *efemp1*−/− $n$ =21). (**D**) No difference in the cartilage elements in *efemp1*−/− at 10dpf compared to wt (wt $n$ = 22, *efemp1*−/− $n$ = 27). The graphs show the individual data points, the mean value ± SEM; significance: * $p < 0.05$ (unpaired student's $t$-test).

We also performed staining of the mineralized bones with alizarin red on 5 dpf larvae; no significant difference was observed on bone mineralization between wt and mutant larvae (**Figure III-S1**).

*3.3. The Skeleton in Adult efemp1−/− Mutants*

No impact was observed on the survival or growth of the *efemp1*−/− mutants relative to their wt siblings. Therefore, we grew them to 1.5 years in order to analyze their adult skeleton with μCT analysis (Fiedler et al., 2018). No difference was apparent in the projected images of the μCT scans (**Fig. III-12A**). We then selected the precaudal vertebrae 6–8 (**Fig. III-12B**) for further morphometric analysis. In particular, we measured the vertebral length and the vertebral thickness (**Fig. III-12C**). No difference was observed in the vertebral length; however, the vertebral thickness was increased in the *efemp1*−/− mutants relative to wt in all three vertebrae, although never reaching significance ($p < 0.05$, $n = 6$) (**Fig. III-12D**). We further analyzed the vertebral column over its entire length by quantifying combinatorial measures for each vertebra. This analysis revealed that the tissue mineral density (TMD) was significantly increased ($p = 0.04$) in all vertebrae and in vertebral centra ($p = 0.04$) of *efemp1*−/− mutants compared to wt siblings, while all other bone properties were unaffected (**Fig. III-12E**).

Upon closer inspection of the images of the precaudal vertebrae 6–8, we observed a decrease in the intervertebral distance between individual vertebrae (**Fig. III-13A**). This distance was significantly reduced for both the vb06-vb07 (0.0051) and vb07-vb08 ($p$= 0.021, respectively) (**Fig. III-13B**). In addition, we also observed that the anterior and posterior ends of each vertebral body, facing the neighboring one, appeared to be ruffled in the mutants, compared to the smooth surface observed in the wt (**Fig. III-13A**).

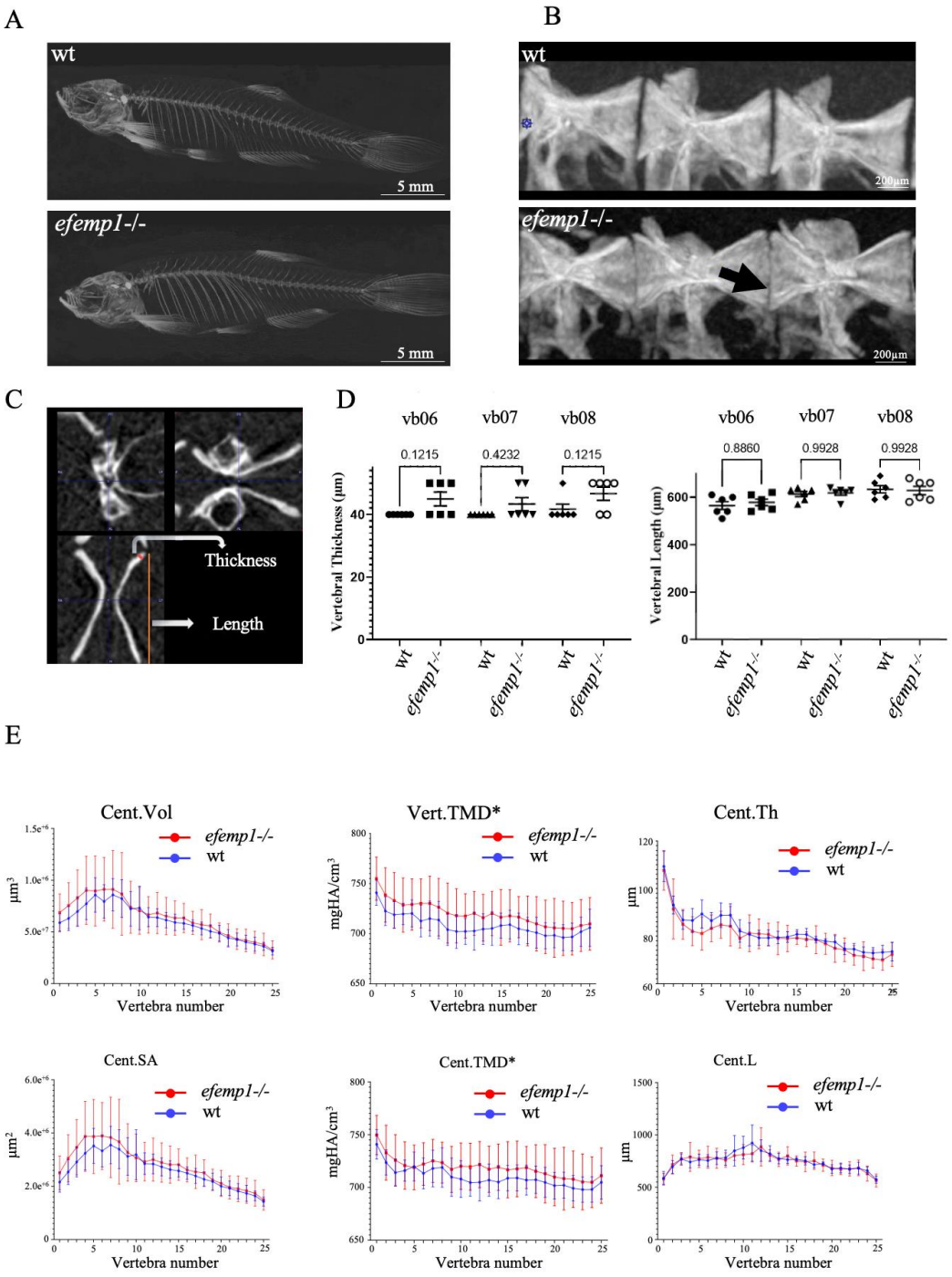


**Figure III-12.** Increased TMD in *efemp1*−/− mutants. (**A**) Representative µCT scans (MIPi = Maximum Intensity Projected image) of a 1.5-year-old wt (top) and *efemp1*−/− (bottom) adult. (**B**) Lateral view of pre-caudal vertebrae 6–8 (L to R) for the two groups; wt and *efemp1*−/−. The black arrow points to the decreased intervertebral distance and ruffled border. (**C**) Representative µCT scan of a vertebra in three planar views, showing the two morphometric measurements: vertebral thickness (µm) and vertebral length (µm). (**D**) Morphometric analysis comparing vertebral thickness and vertebral length of individual precaudal vertebral body numbers 6–8 ($n$ = 6 fish/group) in *efemp1*−/− compared to wt. The values are expressed as mean ± SEM (standard error on mean), statistical significance as determined with ordinary one-way ANOVA test. (**E**) Line plots generated using the GraphPad Prism9 Software (v.9.4.1) of the data points

obtained from the FishCuT Software revealing significantly increased TMDs in the entire vertebrae (Vert.TMD) and in the vertebral centra (Cent.TMD) of *efemp1−/−* adults relative to wt ($p < 0.0001$), with no significant differences observed in other combinatorial measures, ($n = 6$ fish/group and total no. of vertebrae analyzed = 25/individual). The values are expressed as mean ± SEM, significance: * $p < 0.05$, as determined via multiple linear regression analysis.

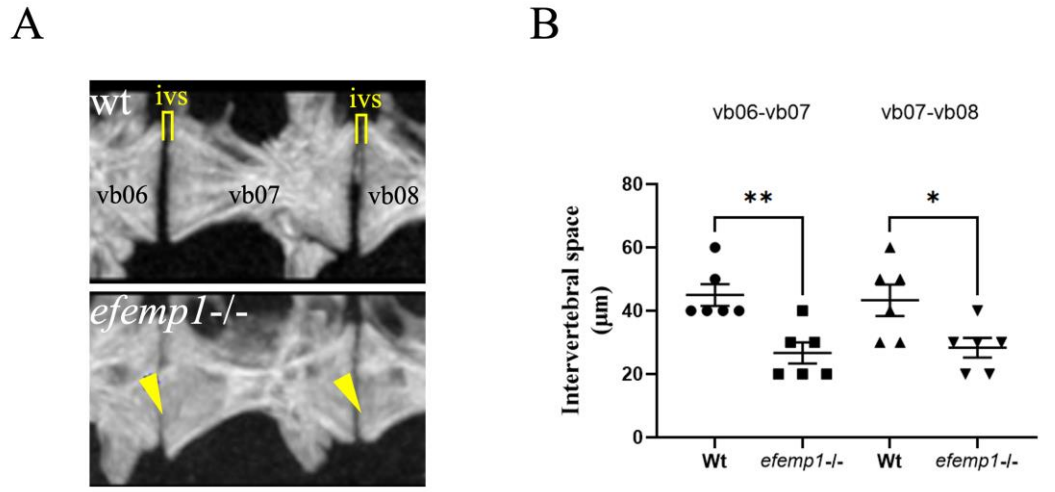


**Figure III-13.** Reduced intervertebral disk space and bone spurs observed in the spine of *efemp1−/−* adult zebrafish. (**A**) Closeup view of pre-caudal vertebrae 6–8 (L to R) for wt and *efemp1−/−*, clearly showing reduced intervertebral disk space and bone spurs, indicated by yellow bar and arrowheads, respectively. (**B**) Intervertebral disk space calculated between vb06-vb07 and vb07-vb08 ($n = 6$ fish/group), revealing significant reduction of the intervertebral disk space in the *efemp1−/−* zebrafish adults. The values are expressed as mean ± SEM, significance: * $p < 0.05$, ** $p < 0.01$, as determined by ordinary one-way ANOVA test.

## 4. Discussion

The ECM is a complex network made up of a variety of multidomain proteins that interact with each other in a specific manner to produce a composite stable structure (Yue, 2014). These structures contribute to the mechanical properties of tissues and play a crucial role in controlling the most fundamental characteristics of cells, such as proliferation, adhesion, migration, polarity, differentiation, and apoptosis (de Vega et al., 2009; Lu et al., 2011; Mecham, 2012). In that context, it is very important to understand and study the role of ECM proteins in skeletal development and homeostasis.

Among the non-collagenous ECM proteins, EFEMP1/FIBULIN3 has been shown in humans and mice to be expressed in a wide range of tissues, including cartilage and bone (Ehlermann et al., 2003), and to be involved in numerous connective tissue diseases. Very little is known about Efemp1 in zebrafish and especially its role in skeletal development. Our study provides a first characterization of the *efemp1* gene in zebrafish development. In situ hybridization revealed *efemp1* expression in the head, pharyngeal region and in the notochord in 48hpf zebrafish embryos (**Fig. III-10**). Using the CRISPR/Cas9 gene editing method, we generated a mutant carrying a deletion of five nucleotides in the *efemp1* coding region, introducing a premature STOP codon and thus coding for a protein devoid of its major functional domains. Although

we were not able to confirm the absence of Efemp1 protein in the mutants for lack of available antibodies, we did thoroughly genotype each individual larva and adult to identify the bona fide homozygous mutants before analysis. In addition, we showed via RNA-Seq that in adult mutant fish, the *efemp1* RNA was slightly decreased (log(fold-change) = −0.44, *p*-value = 0.27), indicating some extent of degradation of the mutant RNA. The described phenotypes were always shared by all the mutants, and not present in wt individuals for *efemp1*, excluding the involvement of an inadvertent off-target gene. We therefore believe that this mutation is actually causing the phenotype.

Our first morphometric characterizations of the *efemp1*−/− line during early stages revealed some effects in the head cartilage, with significant decreases in the distance between the lower jaw articulations (d-art) and some decrease in the ceratohyal angle (a-cer) at 5 dpf (**Fig. III-11**). These findings indicate a narrowing of the medial chondrocranium at 5 dpf, which, however, disappears at 10dpf, possibly due to some compensatory mechanism in the developing larvae. Bone structures were also not affected at these early stages.

In contrast, the 1.5-year-old *efemp1*−/− zebrafish display an increased TMD of the vertebral centra and the entire vertebrae, along with a slightly increased thickness in vertebral centrae 6–8. The most striking effect was, however, the significantly decreased distance between the vertebral bodies in all mutants. This reduced intervertebral disk space was concomitant of the appearance of ruffled edges, or bone spurs, at the extreme ends of the vertebral bodies (**Fig. III-13**). This phenotype is reminiscent of the osteoarthritic OA-like phenotype of the spine as described in humans (Gellhorn et al., 2013; Laplante and DePalma, 2012; Sarzi-Puttini et al., 2005). OA in synovial joints is characterized by articular cartilage degeneration, synovial inflammation, and changes in the periarticular and subchondral bone (Yuan et al., 2014). There are many different locations within the body where an individual could possibly develop OA, including the leg, the synovial knee, ankle, wrist, elbow, shoulder, or hip joint (Wallace et al., 2017), but also the facet joints of the vertebra in the spine (Goode et al., 2019; Laplante and DePalma, 2012; Sarzi-Puttini et al., 2005). The degeneration of the cartilage surface causes the formation of vertebral osteophytes, or bone spurs, followed by inflammation of the facet joints, ultimately causing narrowing of the intervertebral disc space (Gellhorn et al., 2013).

OA studies in the zebrafish have been previously proposed (Brunt et al., 2017; Brunt et al., 2015; Dietrich et al., 2021a; Lawrence et al., 2018b; Mitchell et al., 2013); however, they focused on the study of the jaw joint (the articulation between the palatoquadrate and the Meckel's), while spinal deformities resembling osteoarthritis have been previously described in aging zebrafish (Hayes et al., 2013). Taken together, these observations indicate that the *efemp1*−/− mutant described here represents the first zebrafish model for spinal osteoarthritis. Recently, it was shown that both age-related and experimentally induced osteoarthritis in the knee joints was more severe in *Efemp1*−/− mice (Hasegawa et al., 2017), further supporting our proposal that the *efemp1*−/− zebrafish constitute a valid model for studying the pathogenesis and putative treatments of vertebral osteoarthritis.

Although we found that the early skeletal development was largely unaffected in the *efemp1*−/− mutant, our results indicate that the mutation

affects the health of the vertebral column at later stages. In this context, the early expression of *efemp1* in the zebrafish notochord is interesting, as closer inspection revealed that the expression takes place in the chordoblasts, surrounding the notochord and responsible for secreting the notochordal sheath (Bagnat and Gray, 2020). This structure is known to encase the notochord and comprises of three layers: a thin inner layer of elastin, a thick layer containing lamellar collagen type II, and an outside layer also made of elastin, the *elastica externa*. The chordoblasts are found at the level of the collagen type II fibers, while osteoblasts and collagen type I are located on the outside layer (Pogoda et al., 2018b). Later, in teleost species like zebrafish, the formation of vertebral centra (chordacentra) takes place in the absence of cartilage via the mineralization of the notochordal sheath (Bensimon-Brito et al., 2012). This mineralization is initiated by chordoblasts, which are derived from the notochord and not from sclerotome-derived osteoblasts (Lleras Forero et al., 2018). It is tempting to speculate that the *efemp1* expression in early chordoblasts would be able to affect the health of the vertebral column in adults. However, at this time, it is unclear how the *efemp1* mutation affects the structure of elastic fibers in the notochordal sheath, or precisely how it leads to an increased vertebral thickness, vertebral TMD, and the phenotype of spinal OA in older individuals. Further investigations into histological changes at various stages, as well as changes in signaling pathways, will be required to better understand the onset of spinal OA in this model.

## 5. Conclusions

Taken together, our results show that a mutation of the *efemp1* gene in zebrafish causes transient deformities in chondrocranium at 5dpf, which, however, disappear at later stages. Interestingly, μCT analysis of 1.5-year-old mutants revealed that the distance between individual vertebrae was reduced in the mutants, along with the presence of a ruffled border, indicative of bone spurs. This defect very much resembles that observed in human spinal osteoarthritis, making this mutant the first zebrafish model for this condition. Zebrafish may indeed be the better animal model for spinal osteoarthritis in fish and bipedal land animals, as the loading direction on the vertebral column is axial in fish (Fiaz et al., 2012a), similar to humans and in contrast to other, quadruped rodent models. It is, at present, unclear how far the increased TMD that was also observed in the adult mutants plays a role in the onset of the spinal OA condition. Similarly, the role of *efemp1* expression in the early chordoblasts, possibly via strengthening the elastic properties of the vertebral sheath, will need to be investigated in future research.

**Supplementary Materials:** The following supporting information can be downloaded at: www.mdpi.com/xxx/s1, **Figure III-S1**. No significant effect on bone mineralization in efemp1−/− mutants at 5 dpf compared to WT. A) Ventral view of alizarin red stained WT and efemp1−/− larvae at 5 dpf. The blue arrowheads point to the skeletal elements: branchiostegal ray1 (br1), ceratohyal (ch), dentary (d), entopterygoid (en), hyomandibular (hm), maxillary (m), opercle (op) and parasphenoid (*p*). B) Fraction (%) of individuals presenting a high (maroon), normal/intermediate (red), reduced/ low (light red), or absent (white) level of bone mineralization in the different bone elements in WT and *efemp1*−/− fish at 5dpf. (WT $n = 24$, *efemp1*−/− $n = 15$).

**Author Contributions:** Conceptualization, C.S. and M.M.; Data curation, R.R., M.A.B., A.O. and M.M.; Formal analysis, M.A.B.; Funding acquisition, M.C.-S., Y.H. and M.M.; Investigation, R.R.; Methodology, R.R., C.C.d.S., A.O., A.P. and M.M.; Project administration, M.M.; Resources, M.M.; Software, C.D. and A.O.; Supervision, M.A.B., C.C., M.C.-S. and M.M.; Validation, C.D., A.O., C.C., M.C.-S. and Y.H.; Visualization, M.A.B., C.D. and C.C.d.S.; Writing—original draft, R.R. and M.M.; Writing—review and editing, R.R., M.A.B. and M.M. All authors have read and agreed to the published version of the manuscript.

**Funding:** This work was supported by the EU MSCA-ITN project BioMedAqu (GA 766347) that has received funding from the European Union's Horizon 2020 research and innovation programme under the Marie Skłodowska-Curie grant agreement No 766347. Further, R.R. received the Jean Henrotin Prize 2021 from the Arthrose Foundation. R.R. and C.C.d.S. were MSCA PhD fellows. M.M. is a "Maître de Recherche au F.N.R.S.".

**Institutional Review Board Statement:** This study adheres to the code of ethics for scientific research in Belgium, which is compliant with European Directive 2010/63/EU. Animals were obtained from the GIGA zebrafish facility (approval number LA1610002), experiments were approved by the ethical committee under the file numbers 16-1801, 16-1961 and 19-2135. Concerning biosecurity and biotechnology, European Directive 2009/41/EC was applied under the approval number SBB 219 2010/0333.

**Data Availability Statement:** All photographs used for the generation of this manuscript will be made publicly available (https://hdl.handle.net/2268/310280, accessed 23/12/2023).

**Acknowledgments:** We wish to thank the GIGA-R zebrafish facility for providing zebrafish adults and fertilized eggs, as well as the GIGA-R genomics/sequencing facility for providing sequencing instrumentation and manpower.

**Conflicts of Interest:** The authors declare no conflicts of interest. The funders had no role in the design of the study; in the collection, analyses, or interpretation of data; in the writing of the manuscript; or in the decision to publish the results.

## References

1. Kobayashi, T.; Kronenberg, H. Minireview: Transcriptional regulation in development of bone. *Endocrinology* **2005**, *146*, 1012–1017. https://doi.org/10.1210/en.2004-1343.
2. Kozhemyakina, E.; Lassar, A.B.; Zelzer, E. A pathway to bone: Signaling molecules and transcription factors involved in chondrocyte development and maturation. *Development* **2015**, *142*, 817–831. https://doi.org/10.1242/dev.105536.
3. Lin, X.; Patil, S.; Gao, Y.G.; Qian, A. The Bone Extracellular Matrix in Bone Formation and Regeneration. *Front. Pharmacol.* **2020**, *11*, 757. https://doi.org/10.3389/fphar.2020.00757.
4. Alcorta-Sevillano, N.; Macías, I.; Infante, A.; Rodríguez, C.I. Deciphering the Relevance of Bone ECM Signaling. *Cells* **2020**, *9*, 2630. https://doi.org/10.3390/cells9122630.
5. Ricard-Blum, S. The collagen family. *Cold Spring Harb. Perspect. Biol.* **2011**, *3*, a004978. https://doi.org/10.1101/cshperspect.a004978.
6. Gavaia, P.J.; Simes, D.C.; Ortiz-Delgado, J.B.; Viegas, C.S.; Pinto, J.P.; Kelsh, R.N.; Sarasquete, M.C.; Cancela, M.L. Osteocalcin and matrix Gla protein in zebrafish (*Danio rerio*) and Senegal sole (*Solea senegalensis*): Comparative gene and protein expression during larval development through adulthood. *Gene Expr. Patterns* **2006**, *6*, 637–652. https://doi.org/10.1016/j.modgep.2005.11.010.
7. Thurner, P.J.; Chen, C.G.; Ionova-Martin, S.; Sun, L.; Harman, A.; Porter, A.; Ager, J.W.; Ritchie, R.O.; Alliston, T. Osteopontin deficiency increases bone fragility but preserves bone mass. *Bone* **2010**, *46*, 1564–1573. https://doi.org/10.1016/j.bone.2010.02.014.
8. Kwon, R.Y.; Watson, C.J.; Karasik, D. Using zebrafish to study skeletal genomics. *Bone* **2019**, *126*, 37–50. https://doi.org/10.1016/j.bone.2019.02.009.

9. Malaval, L.; Wade-Guéye, N.M.; Boudiffa, M.; Fei, J.; Zirngibl, R.; Chen, F.; Laroche, N.; Roux, J.P.; Burt-Pichat, B.; Duboeuf, F.; et al. Bone sialoprotein plays a functional role in bone formation and osteoclastogenesis. *J. Exp. Med.* **2008**, *205*, 1145–1153. https://doi.org/10.1084/jem.20071294.
10. Mahajan, D.; Kancharla, S.; Kolli, P.; Sharma, A.K.; Singh, S.; Kumar, S.; Mohanty, A.K.; Jena, M.K. Role of Fibulins in Embryonic Stage Development and Their Involvement in Various Diseases. *Biomolecules* **2021**, *11*, 685. https://doi.org/10.3390/biom11050685.
11. Timpl, R.; Sasaki, T.; Kostka, G.; Chu, M.L. Fibulins: A versatile family of extracellular matrix proteins. *Nat. Rev. Mol. Cell Biol.* **2003**, *4*, 479–489. https://doi.org/10.1038/nrm1130.
12. Chu, M.L.; Tsuda, T. Fibulins in development and heritable disease. *Birth Defects Res. C Embryo Today* **2004**, *72*, 25–36. https://doi.org/10.1002/bdrc.20003.
13. Miosge, N.; Götz, W.; Sasaki, T.; Chu, M.L.; Timpl, R.; Herken, R. The extracellular matrix proteins fibulin-1 and fibulin-2 in the early human embryo. *Histochem. J.* **1996**, *28*, 109–116. https://doi.org/10.1007/bf02331415.
14. Giltay, R.; Timpl, R.; Kostka, G. Sequence, recombinant expression and tissue localization of two novel extracellular matrix proteins, fibulin-3 and fibulin-4. *Matrix Biol.* **1999**, *18*, 469–480. https://doi.org/10.1016/s0945-053x(99)00038-4.
15. Papke, C.L.; Yanagisawa, H. Fibulin-4 and fibulin-5 in elastogenesis and beyond: Insights from mouse and human studies. *Matrix Biol.* **2014**, *37*, 142–149. https://doi.org/10.1016/j.matbio.2014.02.004.
16. Kobayashi, N.; Kostka, G.; Garbe, J.H.; Keene, D.R.; Bächinger, H.P.; Hanisch, F.G.; Markova, D.; Tsuda, T.; Timpl, R.; Chu, M.L.; et al. A comparative analysis of the fibulin protein family. Biochemical characterization, binding interactions, and tissue localization. *J. Biol. Chem.* **2007**, *282*, 11805–11816. https://doi.org/10.1074/jbc.M611029200.
17. Ehlermann, J.; Weber, S.; Pfisterer, P.; Schorle, H. Cloning, expression and characterization of the murine Efemp1, a gene mutated in Doyne-Honeycomb retinal dystrophy. *Gene Expr. Patterns* **2003**, *3*, 441–447.
18. Zhang, Y.; Marmorstein, L.Y. Focus on molecules: Fibulin-3 (EFEMP1). *Exp. Eye Res.* **2010**, *90*, 374–375. https://doi.org/10.1016/j.exer.2009.09.018.
19. Marmorstein, L. Association of EFEMP1 with malattia leventinese and age-related macular degeneration: A mini-review. *Ophthalmic Genet.* **2004**, *25*, 219–226. https://doi.org/10.1080/13816810490498305.
20. Livingstone, I.; Uversky, V.N.; Furniss, D.; Wiberg, A. The Pathophysiological Significance of Fibulin-3. *Biomolecules* **2020**, *10*, 1294. https://doi.org/10.3390/biom10091294.
21. Jorgenson, E.; Makki, N.; Shen, L.; Chen, D.C.; Tian, C.; Eckalbar, W.L.; Hinds, D.; Ahituv, N.; Avins, A. A genome-wide association study identifies four novel susceptibility loci underlying inguinal hernia. *Nat. Commun.* **2015**, *6*, 10130. https://doi.org/10.1038/ncomms10130.
22. McLaughlin, P.J.; Bakall, B.; Choi, J.; Liu, Z.; Sasaki, T.; Davis, E.C.; Marmorstein, A.D.; Marmorstein, L.Y. Lack of fibulin-3 causes early aging and herniation, but not macular degeneration in mice. *Hum. Mol. Genet.* **2007**, *16*, 3059–3070. https://doi.org/10.1093/hmg/ddm264.
23. Fu, L.; Garland, D.; Yang, Z.; Shukla, D.; Rajendran, A.; Pearson, E.; Stone, E.M.; Zhang, K.; Pierce, E.A. The R345W mutation in EFEMP1 is pathogenic and causes AMD-like deposits in mice. *Hum. Mol. Genet.* **2007**, *16*, 2411–2422. https://doi.org/10.1093/hmg/ddm198.
24. Marmorstein, L.Y.; McLaughlin, P.J.; Peachey, N.S.; Sasaki, T.; Marmorstein, A.D. Formation and progression of sub-retinal pigment epithelium deposits in Efemp1 mutation knock-in mice: A model for the early pathogenic course of macular degeneration. *Hum. Mol. Genet.* **2007**, *16*, 2423–2432. https://doi.org/10.1093/hmg/ddm199.
25. Wakabayashi, T.; Matsumine, A.; Nakazora, S.; Hasegawa, M.; Iino, T.; Ota, H.; Sonoda, H.; Sudo, A.; Uchida, A. Fibulin-3 negatively regulates chondrocyte differentiation. *Biochem. Biophys. Res. Commun.* **2010**, *391*, 1116–1121. https://doi.org/10.1016/j.bbrc.2009.12.034.
26. Klenotic, P.A.; Munier, F.L.; Marmorstein, L.Y.; Anand-Apte, B. Tissue Inhibitor of Metalloproteinases-3 (TIMP-3) Is a Binding Partner of Epithelial Growth Factor-containing Fibulin-like Extracellular Matrix Protein 1 (EFEMP1): Implications for macular degenerations. *J. Biol. Chem.* **2004**, *279*, 30469–30473. https://doi.org/10.1074/jbc.M403026200.
27. Aspden, R.M.; Saunders, F.R. Osteoarthritis as an organ disease: From the cradle to the grave. *Eur. Cells Mater.* **2019**, *37*, 74–87. https://doi.org/10.22203/eCM.v037a06.
28. Henrotin, Y.; Gharbi, M.; Mazzucchelli, G.; Dubuc, J.E.; De Pauw, E.; Deberg, M. Fibulin 3 peptides Fib3-1 and Fib3-2 are potential biomarkers of osteoarthritis. *Arthritis Rheum.* **2012**, *64*, 2260–2267. https://doi.org/10.1002/art.34392.
29. Runhaar, J.; Sanchez, C.; Taralla, S.; Henrotin, Y.; Bierma-Zeinstra, S.M.A. Fibulin-3 fragments are prognostic biomarkers of osteoarthritis incidence in overweight and obese women. *Osteoarthr. Cartil.* **2016**, *24*, 672–678. https://doi.org/10.1016/j.joca.2015.10.013.
30. Henrotin, Y. Osteoarthritis in year 2021: Biochemical markers. *Osteoarthr. Cartil.* **2022**, *30*, 237–248. https://doi.org/10.1016/j.joca.2021.11.001.

31. Sanchez, C.; Mazzucchelli, G.; Lambert, C.; Comblain, F.; DePauw, E.; Henrotin, Y. Comparison of secretome from osteoblasts derived from sclerotic versus non-sclerotic subchondral bone in OA: A pilot study. *PLoS ONE* **2018**, *13*, e0194591. https://doi.org/10.1371/journal.pone.0194591.
32. Hasegawa, A.; Yonezawa, T.; Taniguchi, N.; Otabe, K.; Akasaki, Y.; Matsukawa, T.; Saito, M.; Neo, M.; Marmorstein, L.Y.; Lotz, M.K. Role of Fibulin 3 in Aging-Related Joint Changes and Osteoarthritis Pathogenesis in Human and Mouse Knee Cartilage. *Arthritis Rheumatol.* **2017**, *69*, 576–585. https://doi.org/10.1002/art.39963.
33. Witten, P.E.; Harris, M.P.; Huysseune, A.; Winkler, C. Small teleost fish provide new insights into human skeletal diseases. *Methods Cell Biol.* **2017**, *138*, 321–346. https://doi.org/10.1016/bs.mcb.2016.09.001.
34. Lleras-Forero, L.; Winkler, C.; Schulte-Merker, S. Zebrafish and medaka as models for biomedical research of bone diseases. *Dev. Biol.* **2020**, *457*, 191–205. https://doi.org/10.1016/j.ydbio.2019.07.009.
35. Close, R.; Toro, S.; Martial, J.A.; Muller, M. Expression of the zinc finger Egr1 gene during zebrafish embryonic development. *Mech. Dev.* **2002**, *118*, 269–272.
36. Quiroz, Y.; Lopez, M.; Mavropoulos, A.; Motte, P.; Martial, J.A.; Hammerschmidt, M.; Muller, M. The HMG-Box Transcription Factor Sox4b Is Required for Pituitary Expression of gata2a and Specification of Thyrotrope and Gonadotrope Cells in Zebrafish. *Mol. Endocrinol.* **2012**, *26*, 1014–1027. https://doi.org/10.1210/me.2011-1319.
37. Doudna, J.A.; Charpentier, E. Genome editing. The new frontier of genome engineering with CRISPR-Cas9. *Science* **2014**, *346*, 1258096. https://doi.org/10.1126/science.1258096.
38. Hwang, W.Y.; Fu, Y.; Reyon, D.; Maeder, M.L.; Tsai, S.Q.; Sander, J.D.; Peterson, R.T.; Yeh, J.R.; Joung, J.K. Efficient genome editing in zebrafish using a CRISPR-Cas system. *Nat. Biotechnol.* **2013**, *31*, 227–229. https://doi.org/10.1038/nbt.2501.
39. Ewels, P.A.; Peltzer, A.; Fillinger, S.; Patel, H.; Alneberg, J.; Wilm, A.; Garcia, M.U.; Di Tommaso, P.; Nahnsen, S. The nf-core framework for community-curated bioinformatics pipelines. *Nat. Biotechnol.* **2020**, *38*, 276–278. https://doi.org/10.1038/s41587-020-0439-x.
40. Love, M.I.; Huber, W.; Anders, S. Moderated estimation of fold change and dispersion for RNA-seq data with DESeq2. *Genome Biol.* **2014**, *15*, 550. https://doi.org/10.1186/s13059-014-0550-8.
41. Aceto, J.; Nourizadeh-Lillabadi, R.; Maree, R.; Dardenne, N.; Jeanray, N.; Wehenkel, L.; Alestrom, P.; van Loon, J.J.; Muller, M. Zebrafish bone and general physiology are differently affected by hormones or changes in gravity. *PLoS ONE* **2015**, *10*, e0126928. https://doi.org/10.1371/journal.pone.0126928.
42. Aceto, J.; Nourizadeh-Lillabadi, R.; Bradamante, S.; Maier, J.; Alestrom, P.; Van Loon, J.; Muller, M. Effects of microgravity simulation on zebrafish transcriptomes and bone physiology; exposure starting at 5 days post-fertilization. *NPJ Microgravity* **2016**, *2*, 16010, https://doi.org/10.1038/npjmgrav.2016.10.
43. Hur, M.; Gistelinck, C.A.; Huber, P.; Lee, J.; Thompson, M.H.; Monstad-Rios, A.T.; Watson, C.J.; McMenamin, S.K.; Willaert, A.; Parichy, D.M.; et al. MicroCT-based phenomics in the zebrafish skeleton reveals virtues of deep phenotyping in a distributed organ system. *eLife* **2017**, *6*, e26014. https://doi.org/10.7554/eLife.26014.
44. Watson, C.J.; Monstad-Rios, A.T.; Bhimani, R.M.; Gistelinck, C.; Willaert, A.; Coucke, P.; Hsu, Y.H.; Kwon, R.Y. Phenomics-Based Quantification of CRISPR-Induced Mosaicism in Zebrafish. *Cell Syst.* **2020**, *10*, 275–286.e275. https://doi.org/10.1016/j.cels.2020.02.007.
45. Pogoda, H.M.; Riedl-Quinkertz, I.; Lohr, H.; Waxman, J.S.; Dale, R.M.; Topczewski, J.; Schulte-Merker, S.; Hammerschmidt, M. Direct activation of chordoblasts by retinoic acid is required for segmented centra mineralization during zebrafish spine development. *Development* **2018**, *145*, dev159418. https://doi.org/10.1242/dev.159418.
46. Grotmol, S.; Nordvik, K.; Kryvi, H.; Totland, G.K. A segmental pattern of alkaline phosphatase activity within the notochord coincides with the initial formation of the vertebral bodies. *J. Anat.* **2005**, *206*, 427–436. https://doi.org/10.1111/j.1469-7580.2005.00408.x.
47. Fiedler, I.A.K.; Schmidt, F.N.; Wölfel, E.M.; Plumeyer, C.; Milovanovic, P.; Gioia, R.; Tonelli, F.; Bale, H.A.; Jähn, K.; Besio, R.; et al. Severely Impaired Bone Material Quality in Chihuahua Zebrafish Resembles Classical Dominant Human Osteogenesis Imperfecta. *J. Bone Miner. Res.* **2018**, *33*, 1489–1499. https://doi.org/10.1002/jbmr.3445.
48. Yue, B. Biology of the extracellular matrix: An overview. *J. Glaucoma* **2014**, *23*, S20–S23. https://doi.org/10.1097/IJG.0000000000000108.
49. De Vega, S.; Iwamoto, T.; Yamada, Y. Fibulins: Multiple roles in matrix structures and tissue functions. *Cell. Mol. Life Sci.* **2009**, *66*, 1890–1902. https://doi.org/10.1007/s00018-009-8632-6.
50. Mecham, R.P. Overview of Extracellular Matrix. In *Current Protocols in Cell Biology*; Chapter 10; John Wiley and Sons: Hoboken, NJ, USA, 2012. https://doi.org/10.1002/0471143030.cb1001s57.
51. Lu, P.; Takai, K.; Weaver, V.M.; Werb, Z. Extracellular matrix degradation and remodeling in development and disease. *Cold Spring Harb. Perspect. Biol.* **2011**, *3*, a005058. https://doi.org/10.1101/cshperspect.a005058.

52. Gellhorn, A.C.; Katz, J.N.; Suri, P. Osteoarthritis of the spine: The facet joints. *Nat. Rev. Rheumatol.* **2013**, *9*, 216–224. https://doi.org/10.1038/nrrheum.2012.199.
53. Laplante, B.L.; DePalma, M.J. Spine osteoarthritis. *PMR* **2012**, *4*, S28–S36. https://doi.org/10.1016/j.pmrj.2012.03.005.
54. Sarzi-Puttini, P.; Atzeni, F.; Fumagalli, M.; Capsoni, F.; Carrabba, M. Osteoarthritis of the spine. *Semin. Arthritis Rheum.* **2005**, *34*, 38–43.
55. Yuan, X.L.; Meng, H.Y.; Wang, Y.C.; Peng, J.; Guo, Q.Y.; Wang, A.Y.; Lu, S.B. Bone-cartilage interface crosstalk in osteoarthritis: Potential pathways and future therapeutic strategies. *Osteoarthr. Cartil.* **2014**, *22*, 1077–1089. https://doi.org/10.1016/j.joca.2014.05.023.
56. Wallace, I.J.; Worthington, S.; Felson, D.T.; Jurmain, R.D.; Wren, K.T.; Maijanen, H.; Woods, R.J.; Lieberman, D.E. Knee osteoarthritis has doubled in prevalence since the mid-20th century. *Proc. Natl. Acad. Sci. USA* **2017**, *114*, 9332–9336. https://doi.org/10.1073/pnas.1703856114.
57. Goode, A.P.; Cleveland, R.J.; Schwartz, T.A.; Nelson, A.E.; Kraus, V.B.; Hillstrom, H.J.; Hannan, M.T.; Flowers, P.; Renner, J.B.; Jordan, J.M.; et al. Relationship of joint hypermobility with low Back pain and lumbar spine osteoarthritis. *BMC Musculoskelet. Disord.* **2019**, *20*, 158. https://doi.org/10.1186/s12891-019-2523-2.
58. Brunt, L.H.; Norton, J.L.; Bright, J.A.; Rayfield, E.J.; Hammond, C.L. Finite element modelling predicts changes in joint shape and cell behaviour due to loss of muscle strain in jaw development. *J. Biomech.* **2015**, *48*, 3112–3122. https://doi.org/10.1016/j.jbiomech.2015.07.017.
59. Brunt, L.H.; Begg, K.; Kague, E.; Cross, S.; Hammond, C.L. Wnt signalling controls the response to mechanical loading during zebrafish joint development. *Development* **2017**, *144*, 2798–2809. https://doi.org/10.1242/dev.153528.
60. Dietrich, K.; Fiedler, I.A.; Kurzyukova, A.; Lopez-Delgado, A.C.; McGowan, L.M.; Geurtzen, K.; Hammond, C.L.; Busse, B.; Knopf, F. Skeletal Biology and Disease Modeling in Zebrafish. *J. Bone Miner. Res.* **2021**, *36*, 436–458. https://doi.org/10.1002/jbmr.4256.
61. Lawrence, E.A.; Kague, E.; Aggleton, J.A.; Harniman, R.L.; Roddy, K.A.; Hammond, C.L. The mechanical impact of col11a2 loss on joints; col11a2 mutant zebrafish show changes to joint development and function, which leads to early-onset osteoarthritis. *Philos. Trans. R Soc. Lond B Biol. Sci.* **2018**, *373*, 20170335. https://doi.org/10.1098/rstb.2017.0335.
62. Mitchell, R.E.; Huitema, L.F.; Skinner, R.E.; Brunt, L.H.; Severn, C.; Schulte-Merker, S.; Hammond, C.L. New tools for studying osteoarthritis genetics in zebrafish. *Osteoarthr. Cartil.* **2013**, *21*, 269–278. https://doi.org/10.1016/j.joca.2012.11.004.
63. Hayes, A.J.; Reynolds, S.; Nowell, M.A.; Meakin, L.B.; Habicher, J.; Ledin, J.; Bashford, A.; Caterson, B.; Hammond, C.L. Spinal deformity in aged zebrafish is accompanied by degenerative changes to their vertebrae that resemble osteoarthritis. *PLoS ONE* **2013**, *8*, e75787. https://doi.org/10.1371/journal.pone.0075787.
64. Bagnat, M.; Gray, R.S. Development of a straight vertebrate body axis. *Development* **2020**, *147*, dev175794. https://doi.org/10.1242/dev.175794.
65. Bensimon-Brito, A.; Cardeira, J.; Cancela, M.L.; Huysseune, A.; Witten, P.E. Distinct patterns of notochord mineralization in zebrafish coincide with the localization of Osteocalcin isoform 1 during early vertebral centra formation. *BMC Dev. Biol.* **2012**, *12*, 28. https://doi.org/10.1186/1471-213X-12-28.
66. Lleras Forero, L.; Narayanan, R.; Huitema, L.F.; VanBergen, M.; Apschner, A.; Peterson-Maduro, J.; Logister, I.; Valentin, G.; Morelli, L.G.; Oates, A.C.; et al. Segmentation of the zebrafish axial skeleton relies on notochord sheath cells and not on the segmentation clock. *eLife* **2018**, *7*, e33843. https://doi.org/10.7554/eLife.33843.
67. Pogoda, H.M.; Riedl-Quinkertz, I.; Hammerschmidt, M. Direct BMP signaling to chordoblasts is required for the initiation of segmented notochord sheath mineralization in zebrafish vertebral column development. *Front. Endocrinol.* **2023**, *14*, 1107339. https://doi.org/10.3389/fendo.2023.1107339.
68. Fiaz, A.W.; Leon-Kloosterziel, K.M.; Gort, G.; Schulte-Merker, S.; van Leeuwen, J.L.; Kranenbarg, S. Swim-training changes the spatio-temporal dynamics of skeletogenesis in zebrafish larvae (*Danio rerio*). *PLoS ONE* **2012**, *7*, e34072. https://doi.org/10.1371/journal.pone.0034072.

# 3. Effect of probiotics on skeletal development and health in the zebrafish model.

Preliminary Notice: This section presents the main result covering objective **3**.

Probiotics are microbes that bestow health benefits upon the host when administered in adequate proportions. Recent studies have demonstrated that dietary supplements and probiotics play an important role in regulating bone health through gut microbiotia modulation in the gastrointestinal tract. Previous study from our lab has reported that inhibition of BMP signaling between 48 hpf and 72 hpf led to reduction of bone mineralization, whereas osteoblast function and bone formation was less affected. Based on the literature, the aim of the present study was to investigate the potential effects of the administration of probiotics on the bone matrix development after BMP treatment using fluorescent reporter lines. We present two new lines; Tg(Col10a1a:Col10a1a:GFP) where the fusion protein is secreted outside the cell and labels the bone matrix and Tg(Sp7:Sp7:GFP) where the fusion protein is secreted in the cell and labels the osteoblasts. We show that upon BMP inhibitor treatment the bone matrix is significantly reduced that is restored by the probiotic's exposure. A graphical illustration is presented below to provide an overview of the study.

The results are summarized in a manuscript entitled "Probiotics Enhance Bone Growth and Rescue BMP Inhibition: New Transgenic Zebrafish Lines to Study Bone Health."

Int J Mol Sci. 2022 Apr 26;23(9):4748.doi: 10.3390/ijms23094748

The supporting information can be downloaded at: https://www.mdpi.com/article/10.3390/ijms23094748/s1

Please note: The transgenic lines were generated by Jörg Renn.

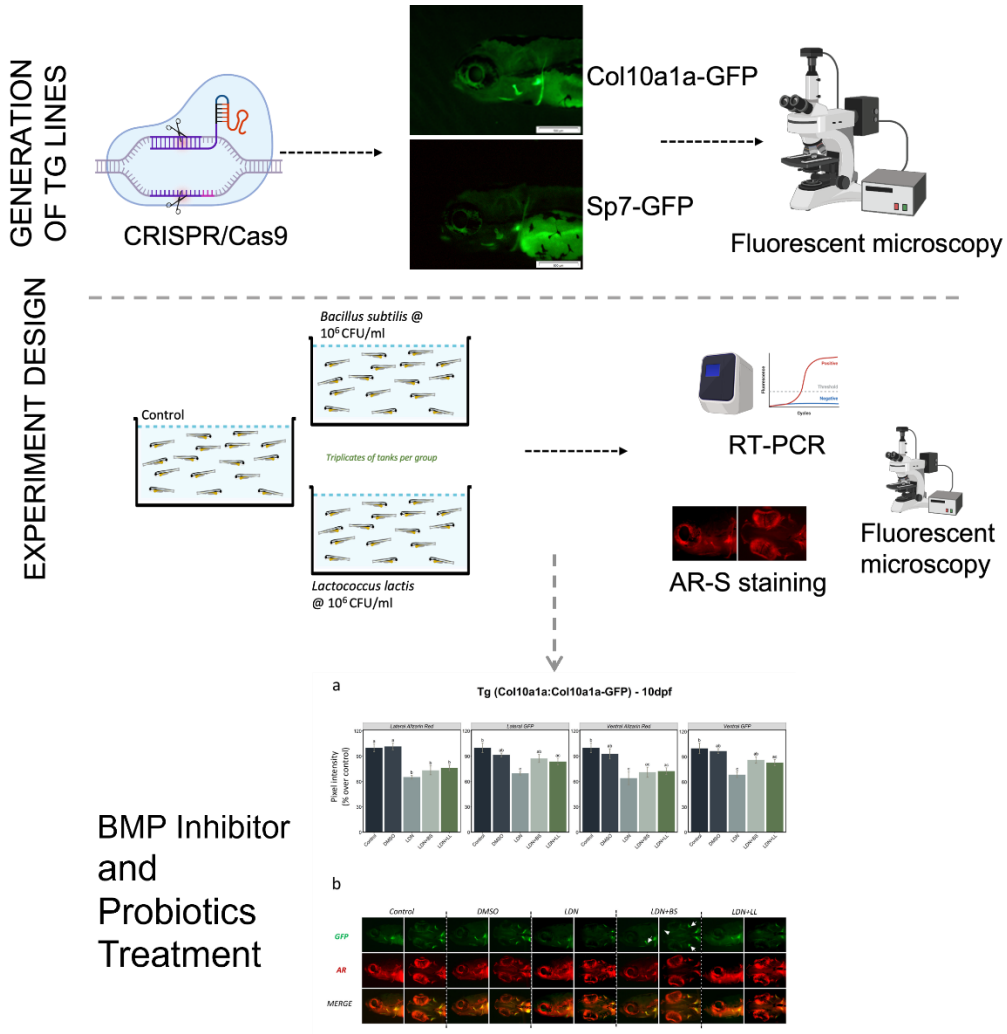
GENERATION OF TG LINES
CRISPR/Cas9
Col10a1a-GFP
Sp7-GFP
Fluorescent microscopy
EXPERIMENT DESIGN
Bacillus subtilis @ 10⁶ CFU/ml
Control
Triplicates of tanks per group
Lactococcus lactis @ 10⁶ CFU/ml
RT-PCR
AR-S staining
Fluorescent microscopy
BMP Inhibitor and Probiotics Treatment
a
Tg (Col10a1a:Col10a1a-GFP) - 10dpf
Pixel intensity (% over control)
b
Control
DMSO
LDN
LDN+RS
LDN+LL
GFP
AR
MERGE

*Article*

# Probiotics Enhance Bone Growth and Rescue BMP Inhibition: New Transgenic Zebrafish Lines to Study Bone Health

**Jerry Maria Sojan [1,†], Ratish Raman [2,†], Marc Muller [2,*], Oliana Carnevali [1] and Jörg Renn [2]**

[1] Department of Life and Environmental Sciences, Università Politecnica delle Marche, via Brecce Bianche, 60131 Ancona, Italy; j.m.sojan@pm.univpm.it (J.M.S.); o.carnevali@staff.univpm.it (O.C.)
[2] Laboratoire d'Organogenèse et Régénération, GIGA-I3, B34, Université de Liège, 4000 Liège, Belgium; ratish.raman@uliege.be (R.R.); joergrenn@yahoo.de (J.R.)
* Correspondence: m.muller@uliege.be; Tel.: +32-4-366-4437
† J.M.S and R.R. should be considered equivalent first authors.

**Citation:** Sojan, J.M.; Raman, R.; Muller, M.; Carnevali, O.; Renn, J. **Probiotics** Enhance Bone Growth **and** Rescue **BMP** Inhibition**:** New Transgenic Zebrafish Lines **to** Study Bone Health. *Int. J. Mol. Sci.* **2022**, *23*, x. https://doi.org/10.3390/xxxxx

Academic Editor(s):

Received: date
Accepted: date
Published: date



**Abstract:** Zebrafish larvae, especially gene-specific mutants and transgenic lines, are increasingly used to study vertebrate skeletal development and human pathologies such as osteoporosis, osteopetrosis and osteoarthritis. Probiotics have been recognized in recent years as a prophylactic treatment for various bone health issues in humans. Here, we present two new zebrafish transgenic lines containing the coding sequences for fluorescent proteins inserted into the endogenous genes for *sp7* and *col10a1a* with larvae displaying fluorescence in developing osteoblasts and the bone extracellular matrix (mineralized or non-mineralized), respectively. Furthermore, we use these transgenic lines to show that exposure to two different probiotics, *Bacillus subtilis* and *Lactococcus lactis*, leads to an increase in osteoblast formation and bone matrix growth and mineralization. Gene expression analysis revealed the effect of the probiotics, particularly *Bacillus subtilis*, in modulating several skeletal development genes, such as *runx2*, *sp7*, *spp1* and *col10a1a*, further supporting their ability to improve bone health. *Bacillus subtilis* was the more potent probiotic able to significantly reverse the inhibition of bone matrix formation when larvae were exposed to a BMP inhibitor (LDN212854).

**Keywords:** *Danio rerio*; zebrafish; transgenic lines; bone matrix; probiotics; mineralization; BMP inhibitors; bone growth

## 1. Introduction

Probiotics are beneficial microbes that contribute health benefits to the host when provided in suitable quantities [1]. Bone growth and health are proven to be affected by probiotics since they rely on the gut mainly for the absorption of minerals and vitamins [2]. The novel term "osteomicrobiology" was coined for microbiota and bone health research [3]. There are many reports on the positive effects of various probiotic bacteria strains on bone health in various animal models and human studies [4–8]. Lactobacillus strains and Bifidobacterium were proven to prevent ovariectomized (OVX)-mediated bone loss in mice and rat models [9–12]. *Bacillus subtilis* supplementation was able to reduce bone loss due to periodontitis in rats [13]. In humans, there are multiple reports on the prevention of bone loss by various probiotics in post-

menopausal women [14,15]. In zebrafish, Maradonna and others showed an increase in calcification after probiotic administration [16]. There are various possible modes of action for probiotics on bones. Osteoimmunology is a field of study that explores the close association between immune and skeletal systems and has found inflammatory conditions are associated with osteoporosis [17]. Some Lactobacillus strains have been shown to increase vitamin D receptor (VDR) expression by human and mouse epithelial cells [18]. Probiotics, through a possible interaction with oestrogens, inhibit bone loss linked to steroid deficiency, as was previously demonstrated in studies with mice [19]. The gut microbiome and its interaction with dietary calcium was also previously shown as another way to affect bone health, since calcium is essential for the maintenance of bone health by decreasing bone resorption [20]. Some beneficial strains are also an important source of vitamin K2, which acts as a cofactor in carboxylation of the matrix protein BGLAP (osteocalcin), thereby supporting bone mineralization [21–23].

The zebrafish (*Danio rerio*) has been increasingly used as a model species for skeletal development, since the basic regulatory networks and metabolic pathways are largely conserved between fish and mammals. A number of mutants have been described in zebrafish that mimic human pathologies such as osteoporosis, osteopetrosis, osteoarthritis [24], thus illustrating how homologous genes play similar roles in both species. In addition, zebrafish larvae can advantageously replace cell culture to test pro- or anti-osteogenic properties of specific compounds because they can reproduce the complex regulatory interactions taking place between different tissues. Although developing larvae may be fixed at different stages to undergo specific staining for various tissues and features (cartilage, bone matrix, etc), the optical clarity of zebrafish embryos and larvae allow for continuous observation of live animals. To that purpose, several transgenic lines are available that express a fluorescent protein (GFP, mCherry, citrine) under the control of a synthetic or natural transcription regulatory region [25,26]. Specific transgenic lines have revealed in vivo activation of canonical BMP, Hedgehog, or Wnt pathways [27–31] during bone development. Others have used cell-specific promoter regions or recombinant bacterial artificial chromosomes (BACs) to target the expression of the reporter protein to chondrocytes, early or late osteoblasts, or osteoclasts [32].

Even with all the reported therapeutic effects of probiotics or gut microbiota on bones, there is still a lack of a clear understanding on how they are able to influence bone homeostasis [33]. Here, we present two newly generated transgenic zebrafish lines that were obtained by inserting a reporter protein coding sequence directly into the coding region of two endogenous genes. These new transgenic lines express the GFP protein under transcriptional control of the endogenous regulatory regions for (i) the osteoblast marker *sp7* (Sp7 transcription factor) gene and (ii) its downstream target gene *col10a1a* encoding the osteoblast- and hypertrophic chondrocyte-specific collagen type X alpha 1a chain. We describe the expression pattern of each reporter gene and apply them to testing the efficacy of osteogenic strains of probiotics. We analysed the modulatory effects of two probiotics, *Bacillus subtilis* and *Lactococcus lactis*, on osteoblast differentiation and early skeletal growth in zebrafish using these two lines. Furthermore, we tested the ability of each

probiotic to counteract the deleterious effect of BMP inhibitor treatment on the bone matrix. The results presented here emphasize yet again that zebrafish, particularly transgenic lines, are an ideal model for live studies on skeletogenesis, including the impact of probiotics.

## 2. Results

### *2.1. Generation and Characterization of New Transgenic Lines*

#### 2.1.1. *Tg(col10a1a:col10a1a-GFP)* line

We generated the *Tg(col10a1a:col10a1a-GFP)* transgenic line where the expression of a fusion protein between Col10a1a and GFP is driven by the endogenous zebrafish *col10a1a* promoter (**Fig. III-14a, b**). To characterize this line, we crossed it with the *Tg(Ola.Sp7:mCherry)* line that expresses the red fluorescent mCherry protein in osteoblast cells [34]. We found GFP expression localized very specifically in the same regions as osteoblasts expressing the mCherry protein. This includes the early appearance of the cleithrum, opercle and pharyngeal tooth bud at 3 days post-fertilization (dpf), the parasphenoid and branchiostegal rays at 4 dpf, as well as maxillary, dentary, and entopterygoids at 5-6 dpf (**Fig. III-14c**), consistent with previous *in situ* hybridization studies [35]. Alizarin red (AR) live fluorescent staining of *Tg(col10a1a:col10a1a-GFP)* larvae (**Fig. III-14d**) confirmed the presence of GFP in mineralized bone matrix.

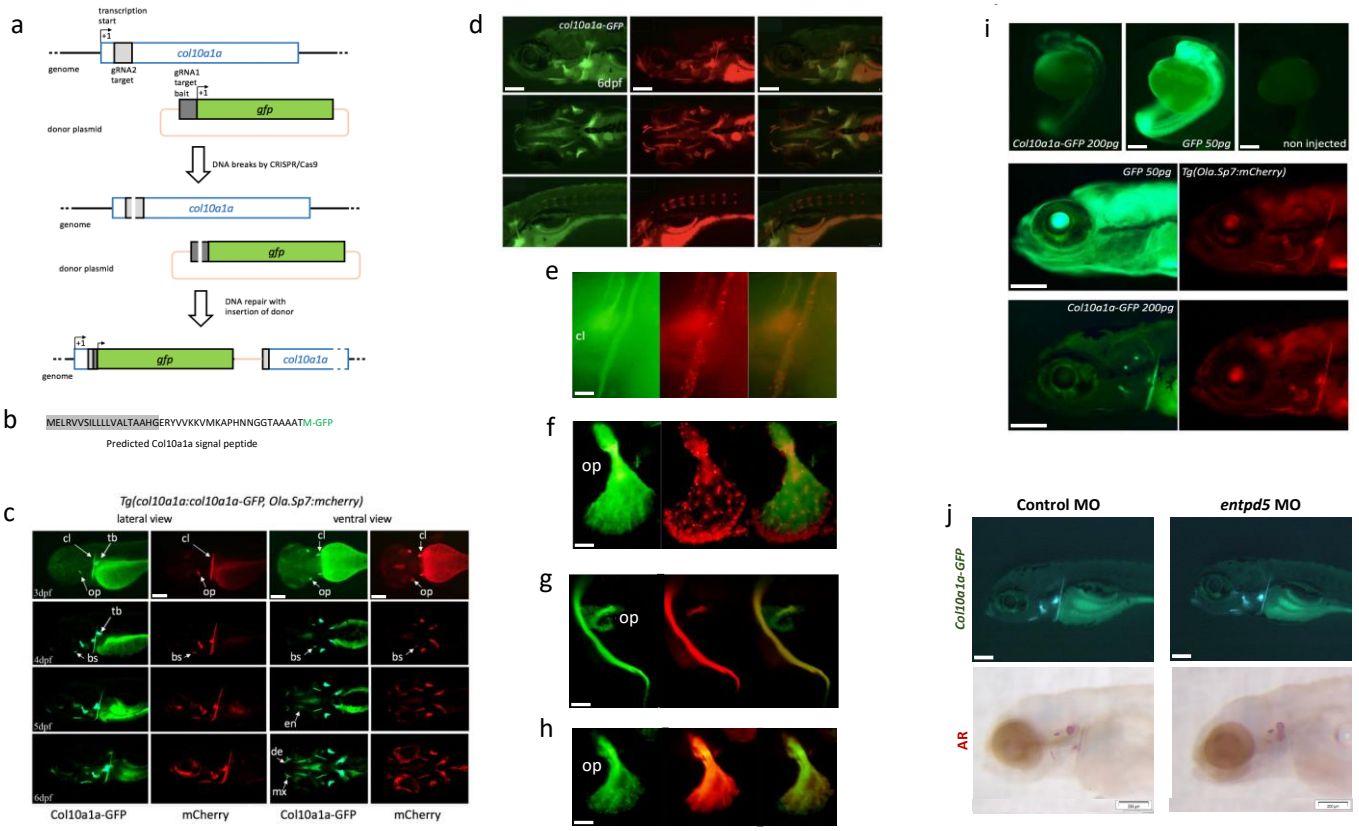


**Figure III-14.** Characterisation of the *Tg(col10a1a:col10a1a-GFP)* transgenic line. (**a**) Schematic representation of the endogenous *col10a1a* gene (top line), the plasmids used for microinjection along with the two gRNAs (bait and *col10a1a*, respectively gRNA1 and gRNA2), the resulting cuts in the genomic DNA and plasmids, and the expected reporter construct in the transgenic genome. (**b**) N-

terminal end of the fusion protein produced by the *Tg(col10a1a:col10a1-GFP)* transgenic line, with the predicted signal peptide in grey and the original GFP translational start site (M) in green. (**c**) Timeline of expression of GFP (green fluorescence) and mCherry (red fluorescence) in double-transgenic larvae *Tg(col10a1a:col10a1a-GFP*; *Ola.Sp7:mCherry)*. Lateral and ventral views at different developmental stages as indicated, anterior to the left. White arrows point to specific elements: (bs) branchiostegal ray, (cl) cleithrum, (de) dentary, (en) entopterygoid, (mx) maxillary, (op) opercle and (tb) tooth bud. (**d**) Expression of Col10a1a-GFP protein (green) in 6 dpf *Tg(col10a1a:col10a1a-GFP)* larvae live-stained with AR to visualize mineralized bone. (**e**–**h**) Close inspection of Col10a1a-GFP localization (green) compared to mCherry expression by osteoblasts in (**e**) the cleithrum (cl) or the opercle (**f**) of 9 dpf *Tg(col10a1a:col10a1a-GFP*; *Ola.Sp7:mCherry*) zebrafish larvae. (**g, h**) Expression of GFP protein (green) in *Tg(col10a1a:col10a1a-GFP*) 6 dpf larvae live-stained with AR to visualize bone matrix. Close inspection of the cleithrum (**g**) and the opercle (**h**). (**i**) Zebrafish *Tg(Ola.Sp7:mCherry)* larvae after microinjection of mRNA coding for GFP or for the fusion protein Col10a1a-GFP. Top: embryos at 1 dpf, showing weak fluorescence of Col10a1a-GFP, extremely strong fluorescence of GFP, and no fluorescence in controls. Bottom: the same larvae at 5 dpf, still showing strong GFP expression in the entire body and weak, but specific fluorescence of Col10a1a-GFP located in bone elements (cleithrum and opercle) as confirmed by the red fluorescence of osteoblast-specific mCherry. (**j**) Morpholino injection into *Tg(col10a1a:col10a1a-GFP*) larvae. The Col10a1a-GFP protein labels cranial bone elements at 4 dpf in both control and *entpd5* MO injected larvae (top), but AR staining is absent in *entpd5* morphants (bottom). The scale bars, given in the left bottom corner of the images, represent 200 μm, except for e-h, where they indicate 20 μm.

The Col10a1a-GFP protein produced by the *Tg(col10a1a:col10a1a-GFP)* line contained the original Col10a1a N-terminal signal peptide that would lead to its secretion into the extracellular space, which suggested that it would be secreted from the producing cells and bound by the nearby extracellular bone matrix to generate the observed labelling pattern. To investigate this hypothesis in detail, we turned back to the *Tg(col10a1a:col10a1a-GFP*; *Ola.Sp7:mCherry*) double transgenic line and dissected individual bone elements for analysis. Looking at the developing cleithrum (cl) (**Fig. III-14e**), we observed that most of the Col10a1a-GFP protein was associated with the extracellular bone matrix. This conclusion was even more apparent when looking at the developing opercle (**Fig. III-14f**). Here, the Col10a1a-GFP was mainly present in the proximal part that contained less cells, whereas the majority of mCherry-expressing osteoblasts were found at the distal growth fringe of the opercle. In only some cases, fluorescence could be observed inside cells. This predominant bone matrix staining was further confirmed by comparing the Col10a1a-GFP pattern in *Tg(col10a1a:col10a1a-GFP)* transgenic larvae with AR staining performed on the same animal (**Fig. III-14g, h**).

In the next step, we wondered whether the fact that the transgene was expressed in osteoblasts would favour its preferential binding to the nearby bone matrix. Therefore, we engineered a synthetic mRNA coding for the Col10a1a-GFP fusion protein that we directly injected into fertilized eggs so that it would be translated in every cell within the embryo. Microinjection of a control mRNA coding for GFP lead to an intense, widely distributed green fluorescence at 5 dpf (**Fig. III-14i**). In contrast, microinjection of the col10a1a-GFP mRNA resulted in weak fluorescence specifically restricted to the cleithrum and the opercle (**Fig. III-14i**, right), further supporting the notion that this fusion protein specifically binds to the bone matrix. Finally, to test the binding of Col10a1a-GFP to unmineralized bone matrix, we took advantage of the finding that the *entpd5* gene is required for bone mineralization [36]. We designed morpholino antisense oligonucleotides against *entpd5* mRNA and injected them into fertilized eggs derived from a heterozygous *Tg(col10a1a:col10a1a-GFP)* parent. As expected, about half of the larvae (44/85) revealed Col10a1a-GFP fluorescence in control-injected larvae, while 50/109 displayed similar fluorescence in *entpd5* morphants (**Fig. III-14j**, top), indicating that *entpd5* knockdown did not affect bone staining. In contrast, AR staining for mineralized bone was completely absent or very weak in all morphants when compared to the control-injected larvae (**Fig. III-14j**, bottom).

### 2.1.2. *Tg(sp7:sp7-GFP)* line

Using the same CRISPR/Cas9 method, we generated another transgenic line by targeting the insertion of GFP reporter cDNA into the endogenous *sp7* coding region, resulting in a line expressing a fusion protein between Sp7 and GFP (**Fig. III-15a**). This new line, *Tg(sp7:sp7-GFP)*, was analysed for green fluorescence in parallel with red fluorescence in the *Tg(Ola.Sp7:mCherry)* line. Comparison of the two lines (**Fig. III-15b**) revealed that the expression of both transgenes largely overlapped, starting at 3 dpf in the cleithrum and opercle and extending to the maxillary, dentary, branchiostegal rays and entopterygoids at later stages. However, some differences in the

expression pattern were also apparent, mainly earlier expression in the pharyngeal tooth bud at 3 dpf and stronger expression in the entopterygoid at 6 dpf in the *Tg(sp7:sp7-GFP)* line. Both lines displayed weakened expression at 10 dpf and beyond (not shown).

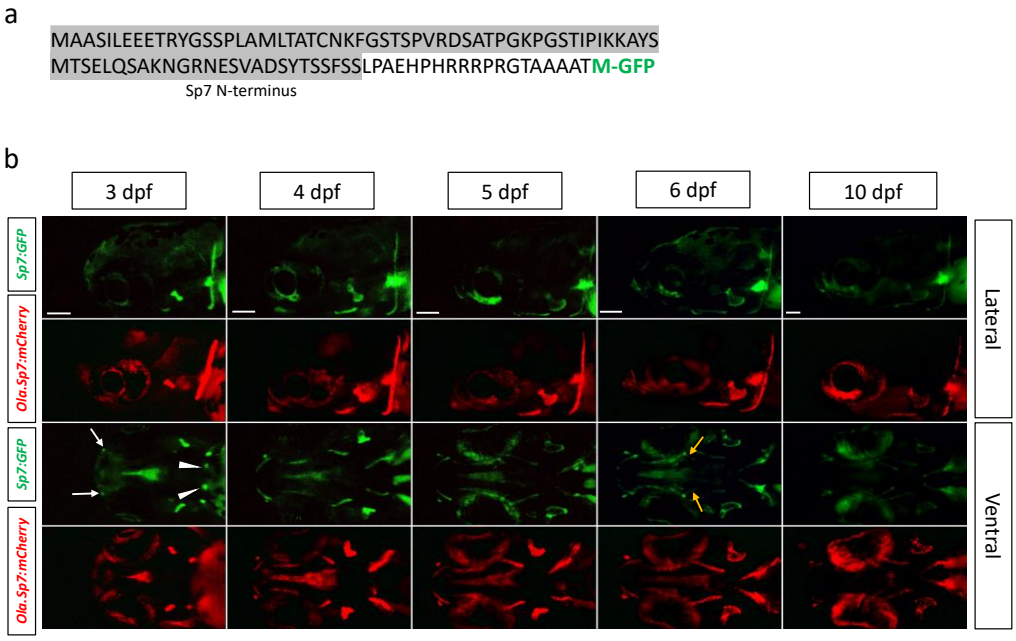


**Figure III-15.** GFP expression in the *Tg(sp7:sp7-GFP)* transgenic line. (**a**) N-terminal end of the fusion protein produced by the *Tg(sp7:sp7-GFP)* transgenic line, with the predicted signal peptide in grey and the original GFP translational start site (M) in green. (**b**) Transgene expression in the *Tg(sp7:sp7-GFP)* and the previously described *Tg(Ola.Sp7:mCherry)* lines tracked in the head region (top: lateral view and bottom: ventral view) from 3 dpf to 10 dpf. Earlier transgene expression occurs in the maxillary (white arrows) and pharyngeal tooth buds (white arrowheads) at 3 dpf and in the entopterygoid (yellow arrows) at 6 dpf of the *Tg(sp7:sp7-GFP)* line. The scale bars, given in the left bottom corner of the images in the top row, correspond to 100 µm.

### *2.2. Effect of Probiotics*

#### 2.2.1. Effect of Probiotics on Bone Formation

In a preliminary experiment, we used WT zebrafish larvae to test the effect of probiotics on specific mRNA levels. Total RNA was extracted from 7 dpf larvae grown in control (E3 + water) or E3 supplemented with *Bacillus subtilis* (BS) or *Lactococcus lactis* (LL) probiotics. Using RT-PCR, we observed that all bone-related gene mRNA levels were significantly increased upon exposure to the probiotics. Interestingly, expression of the specific marker genes *sp7*, *col10a1a*, *spp1* and *runx2b* were more extensively induced by BS, but *bglap* mRNA levels were not significantly affected. In contrast, induction of *cyp26b1*, coding for an enzyme degrading retinoic acid, was significantly higher with LL (**Fig. III-16**).

To facilitate and complement this observation, we decided to test the effects of the two different probiotics on bone development by direct live observation of developing bone elements using three transgenic lines. Two lines were based on the osteoblast-specific *sp7* promoter, one

from medaka, *Tg(Ola.Sp7:mCherry)* [34], and the other from the endogenous zebrafish *sp7* gene, *Tg(sp7:sp7-GFP)* presented above. The third line was the *Tg(col10a1a:col10a1a-GFP)* line presented above, based on the endogenous *col10a1a* promoter, which preferentially reveals unmineralized or mineralized bone matrix.

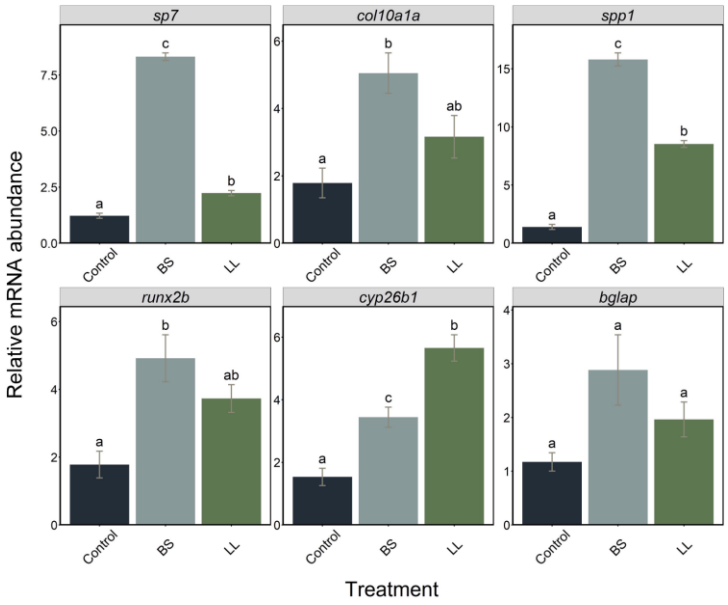


**Figure III-16.** Relative expression levels of *sp7*, *col10a1a*, *spp1*, *runx2b*, *cyp26b1* and *bglap* genes in larvae (n = 7) treated with two probiotics, BS and LL, sampled at 7 dpf. Data are presented as mean ± S.D. One-way ANOVA and Tukey's multiple comparison tests are used. Different letters denote statistically significant differences ($p < 0.05$) between the experimental groups.

Control and probiotic enrichment conditions were applied to individuals of each of the three transgenic lines. For the two transgenic lines based on the *sp7* promoter, *Tg(Ola.Sp7:mcherry)* and *Tg(sp7:sp7-GFP)*, we determined the integrated pixel intensity in the head areas (lateral and ventral view) at 7 dpf (**Fig. III-17a, b**). We observed a significant increase in fluorescence upon exposure to both BS and LL probiotics in the head and opercle areas in lateral views, but areas in ventral views achieved significance only in the *Tg(Ola.Sp7:mCherry)* line. In all cases, the increase was consistently more intense with BS than LL. Representative images of larvae from the corresponding conditions illustrate the measured trends (**Fig. III-17c**). Using the *Tg(col10a1a:col10a1a-GFP)* line, we decided to extend the observations to a later stage, and 10 dpf was selected since most cranial bone elements are detectable. In addition, we performed live AR staining before observation in order to further illustrate predominant staining of the bone matrix in this line. The pixel intensities were significantly higher than the control in all areas for both probiotics (**Fig. III-17d**). Furthermore, BS caused a significantly higher GFP pixel intensity compared to LL in the ventral view. Simultaneous staining with AR confirmed that mineralization in the BS-treated larvae had the highest integrated pixel intensity in the total head—(lateral and ventral). Representative images of larvae from the corresponding conditions illustrate the measured trends (**Fig. III-17e**), while merged images

confirm the near-perfect overlap of GFP and AR fluorescence for both signal positive areas as well as pixel intensity.

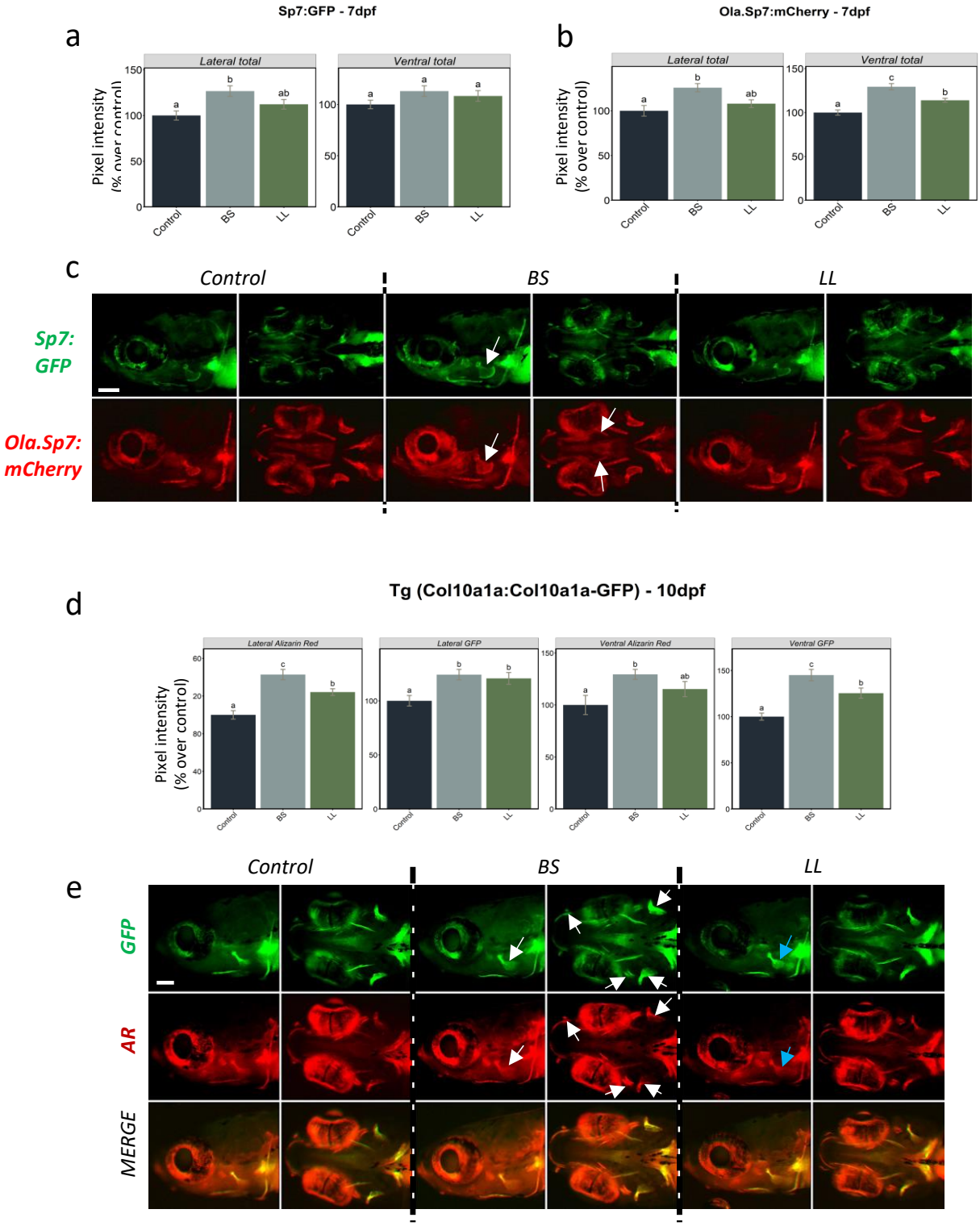


**Figure III-17.** Integrated pixel intensity values for various areas measured in 7 dpf zebrafish from (**a**) *Tg(sp7:sp7-GFP)* and (**b**) *Tg(Ola.Sp7:mCherry)* larvae in controls and upon two different probiotic treatments. (**c**) Signal expression images (lateral and ventral views) of the head area of *Tg(sp7:sp7-GFP)* and *Tg(Ola.Sp7:mCherry)* larvae under the different conditions. (**d**) Integrated pixel intensity values for various areas measured in 10 dpf *Tg(col10a1a:col10a1a-GFP)*

zebrafish larvae from the different treatment groups and stained with AR. (**e**) GFP, AR fluorescence and merged images of the head area (lateral and ventral views) of *Tg(col10a1a:col10a1a-GFP)* larvae from the different treatment groups. Increased GFP and AR fluorescence in various bony structures are denoted by white and blue arrows, respectively, in BS- and LL-treated fish. One-way ANOVA and Tukey's multiple comparison tests are used, and statistical significance was set at $p < 0.05$. Different letters denote statistically significant differences between experimental groups. The scale bars, given in the left bottom corner of the first image in the top row, correspond to 100 μm.

### 2.2.2. BMP Inhibitor Exposure Followed by Probiotic Treatment

BMP signalling is known to be required for osteoblast differentiation and for bone mineralization [37,38]. The most eminent marker gene widely used for investigating osteoblast differentiation in mammals and teleost species is the *sp7* gene [39–41]. We treated *Tg(Ola.Sp7:mCherry)* transgenic larvae with the BMP inhibitor LDN212854 from 2 dpf until 4 dpf at two different concentrations (10 μM and 20 μM) to test its effect on the osteoblast population. We observed a weak but significant increase in mCherry expression in the 20 μM concentration group when compared to the control (DMSO) group at 5 dpf (**Fig. III-18**), suggesting that, at this concentration, osteoblast proliferation and/or differentiation is affected by BMP inhibition.

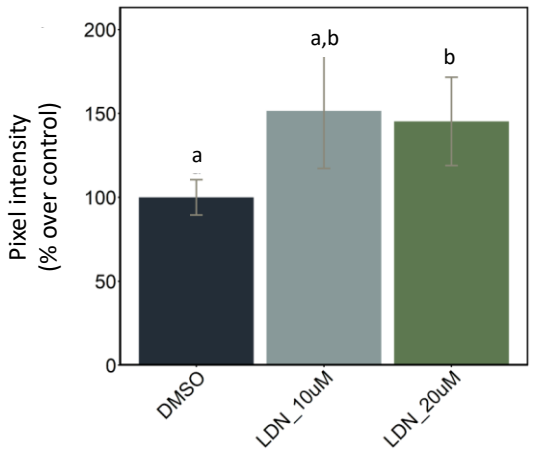


**Figure III-18.** Effects of LDN212854 on *sp7* expression. Integrated pixel intensity values (mCherry red fluorescence) for 5 dpf *Tg(Ola.Sp7:mCherry)* larvae measured in ventral view treated with 10 μM and 20 μM LDN212854 from 2 dpf to 4 dpf. Different letters denote statistically significant differences between experimental groups (one-way ANOVA, $p < 0.05$, followed by Tukey's post hoc test).

Furthermore, we used the *Tg(col10a1a:col10a1a-GFP)* line to observe the effects of the BMP inhibitor LDN212854 at 20 μM on bone matrix formation and mineralization, and to investigate the potential protective properties of the probiotics. LDN212854 was administered from 2 dpf to 4 dpf, followed by probiotic supplementation (BS or LL) from 5 dpf to 10 dpf. DMSO was used as a second control since the inhibitor was dissolved in DMSO. Sampling was performed at 10 dpf, and additional staining with AR was used to visualise mineralized structures in the larvae. Compared to both control and DMSO, we observed a dramatic decrease in the integrated pixel intensity values in all analysed areas in

the presence of LDN, both for Col10a1a-GFP and live AR staining. Compared to BMP inhibition alone, additional treatment with probiotics resulted in significantly increased *Col10a1a-GFP* fluorescence in both lateral and ventral observation, but the increase in live AR staining never reached significance. These observations suggest that probiotics, particularly BS, can revert the deleterious effect of BMP inhibition on bone matrix formation, while AR staining indicated that the effect was not evident for mineralization (**Fig. III-19a, b**).

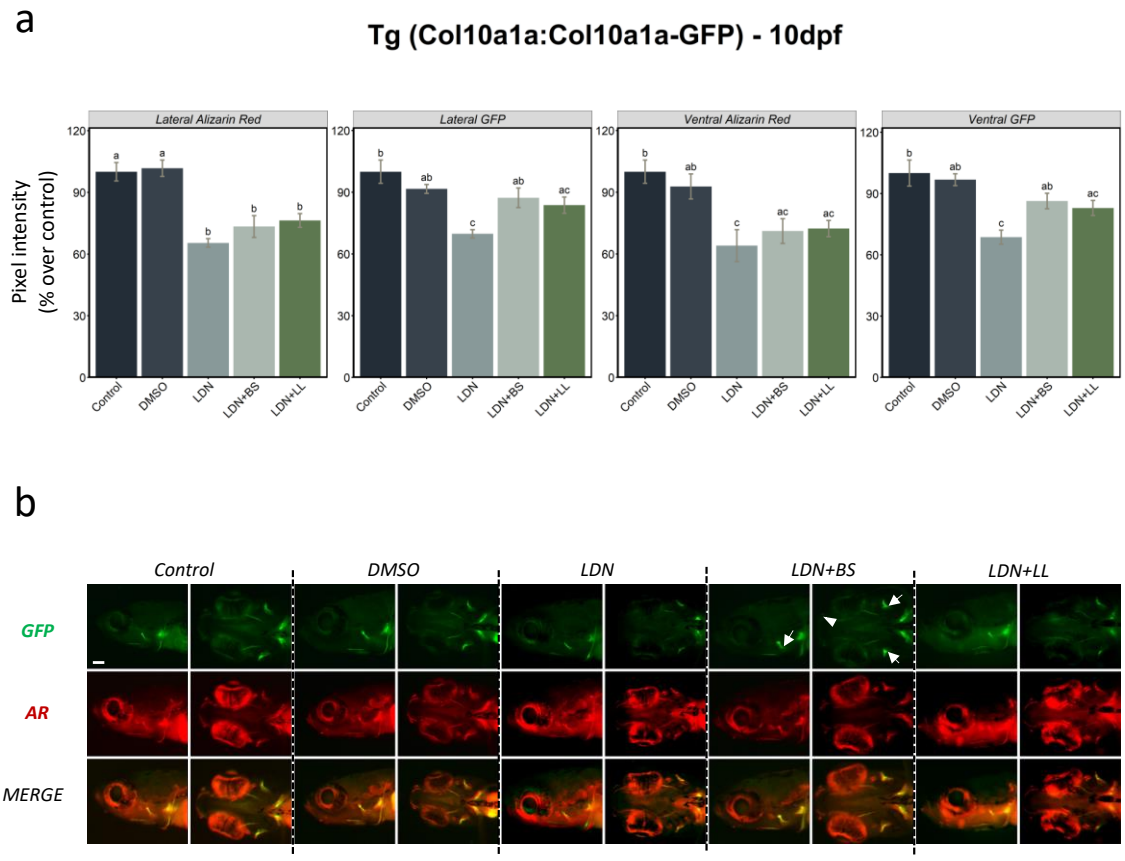


**Figure III-19.** BMP inhibitor exposure followed by two probiotics treatments in *Tg(col10a1a:col10a1a-GFP*) larvae. (**a**) Integrated pixel intensity values for various areas measured in 10 dpf zebrafish *Tg(col10a1a:col10a1a-GFP)* larvae divided into various groups—control, DMSO, LDN, LDN+BS and LDN+LL—and stained with AR. DMSO was used as additional control since it was employed as the solvent for LDN. One-way ANOVA and Tukey's multiple comparison tests were used, and statistical significance was set at $p < 0.05$. Different letters denote statistically significant differences among the experimental groups. (**b**) GFP, AR staining and merged images of the head area (lateral and ventral views) of *Tg(col10a1a:col10a1a-GFP)* larvae of the different treated groups. White arrows denote GFP in various bony structures and the white arrowhead indicates the presence of a signal in additional structures (that was absent in other groups) in BS-treated fish after LDN exposure (LDN+BS).

## 3. Discussion

Transgenic zebrafish reporter lines with specific expression of fluorescent proteins for following the development of specific organs, tissues, and cells in living larvae are now widely used in developmental biology. Here we present two new transgenic lines, namely, *Tg(sp7:sp7-GFP)* and *Tg(col10a1a:col10a1a-GFP),* which we obtained by inserting the GFP coding sequence into the endogenous *sp7* or *col10a1a* gene coding sequence with CRISPR/Cas9 technology. We used these lines to visualize formation of the zebrafish skeleton and to evaluate the effects of two types of probiotics on this process, first in the absence and then in the presence of a BMP inhibitor.

Several transgenic zebrafish lines expressing fluorescent reporter genes under the control of the sp7 promoter have been described in recent years. However, there are important differences between these lines and the *Tg(sp7:sp7-GFP)* line presented here: (i) previously described lines, such as the *Tg(Ola.Sp7:mCherry)* [34,42] or *Tg(Ola.Sp7:mCherry-NTR)* [43] use the heterologous promoter from medaka (*Oryzias latipes*, Ola) to drive expression of the transgene [44]; (ii) these lines were obtained by insertion of an artificial construct at one or more random, unknown locations in the genome. In contrast, the *Tg(sp7:sp7-GFP)* carries the reporter gene in place of the endogenous *sp7* gene, it is under the control of the endogenous regulatory regions, and thus, should reproduce more correctly the *sp7* expression pattern. Indeed, consistent with the pattern observed here in the transgenic line, *in situ* hybridization has revealed *sp7* expression in the tooth buds at 4 dpf [45], and in the maxillary [46,47] and the entopterygoid at 3 dpf [39]. In comparison, the higher mCherry expression observed in earlier studies could be due to the random location of the transgene. Despite these differences in the exact timing of expression patterns, these two lines display fluorescence in many overlapping regions, such as the opercle, cleithrum or branchiostegal rays [46,47].

Col10a1a is a secreted protein, and in our *Tg(col10a1a:col10a1a-GFP)* zebrafish, GFP insertion preserves the N-terminal signal peptide of Col10a1a (see **Fig. III-14a, b**). Thus, these transgenic fish encode a fusion protein that is secreted by cells. Although we observed some fluorescent cells in this line, it appears that the main fluorescent structure is the extracellular bone matrix. The Col10a1a-GFP fusion protein strongly binds to the extracellular bone matrix after secretion, as shown by an overlapping pattern with AR staining, irrespective of where it was expressed, since microinjection of *col10a1a-GFP* mRNA led to expression in essentially all embryonic cells and resulted in the same specific fluorescent staining of bone elements. We further showed with knockdown of the *entpd5* gene [36] that bone mineralization was not required for fluorescent labelling of the bone matrix (**Fig. III-14j**). Therefore, we consider the *Tg(col10a1a:col10a1a-GFP)* line as the first reporter line that reveals the extracellular bone matrix, mineralized or not. As such, it represents an important tool for analysing the sequential events of osteoblast differentiation, bone matrix deposition and its mineralization in live larvae when combined with transgenic lines such as the *Tg(sp7:sp7-GFP)* and AR staining.

A preliminary test for the effects of probiotics revealed that the transcription of several marker genes for bone development were significantly upregulated upon probiotic treatment at 7 dpf.

Interestingly, expression of the pro-osteogenic genes *sp7*, *col10a1a*, *spp1* and *runx2b* was significantly higher after BS treatment, but *cyp26b1* expression was significantly higher after LL treatment. The *cyp26b1* gene codes for a protein with retinoic acid 4 hydroxylase activity, whose mutation leads to severe defects in head cartilage formation [48], increased ossification of the vertebral column [42,49] with complex effects on skeletal formation, depending on timing and location [50]. It is therefore difficult to predict how this differential response to the different probiotics will affect skeletal development. None of the probiotics affected *bglap* expression by mature osteoblasts compared to a more predominant effect on *spp1* expressing immature osteoblasts; this could be due to the degree of osteoblast differentiation at the particular stage studied here [51]. Since *runx2b* expression has to be downregulated for immature osteoblasts to differentiate into mature osteoblasts and formation of mature bone [52], the stage of osteoblast differentiation observed here appears to be more transitional, from immature to mature, with high upregulation of *spp1* and *sp7* and no downregulation of *runx2b* by both probiotic treatments that was more significant for BS. All this preliminary evidence from the expression pattern of genes related to skeletal development directed us to further explore the possibility of using reporter lines to confirm the results.

Transgenic reporter lines offer the opportunity to follow the formation of specific tissues in living embryos and larvae over time and in specific locations. The two new lines presented here both drive their transgene expression from endogenous regulatory regions and reveal either the location of osteoblasts (*Tg(sp7:sp7-GFP)* line) or of the bone matrix (*Tg(col10a1a:col10a1a-GFP)* line). When we tested probiotics exposure with these transgenic lines, BS was found to significantly induce *sp7*-driven expression in osteoblasts at 7 dpf and Col10a1a-GFP labelling of the bone matrix at 10 dpf. These results observed for the bony structures of the head are clearly in agreement with the mRNA results. Additional AR staining of the *Tg(col10a1a:col10a1a-GFP)* line revealed that probiotics induced a significant increase in mineralized bone matrix as well. The positive influence of BS on bone matrix formation and mineralization was significant when the bony structures were analysed from both lateral and ventral views of the head, whereas the weaker effect of LL produced non-significant effects in both views. This indicates that the different bacteria have varying abilities for modulating the process of bone formation, and in our study, *B. subtilis* was more efficient at positively influencing osteogenesis than *L. lactis*. In addition, we showed that treatment with the BMP inhibitor LDN212854 dramatically decreased bone matrix labelling by Col10a1a-GFP and bone mineralization as assessed by AR. In contrast, BMP inhibitor treatment of the *Tg(Ola.Sp7:mCherry)* line had little or no effect on osteoblast-specific expression (**Fig. III-18**), in line with previous observations showing that the BMP inhibitors dorsomorphin and K02288 decreased bone mineralization without affecting osteoblast numbers [38]. Although BMP signalling is required for a vast number of events in early embryogenesis, treatment from 2 dpf does not affect the general morphology, as illustrated by the lack of an effect on cranial cartilage formation as previously observed [38]. Studies in mice, using various conditional gene knock outs or transgenic expression of BMP inhibitors, have also indicated that BMPs may play dual roles, facilitating osteoblast

differentiation by inducing Runx2 and Sp7 expression, and independently, osteoblast function by stimulating bone matrix production [53]. The finding that probiotic treatment induced both osteoblast regulators (*runx2b* and *sp7*) and bone matrix protein genes (*spp1* and *col10a1a*) hints at a possible mechanism for rescuing the negative effect of BMP inhibition on bone. Interestingly, we observed that BS was able to partially revert this effect on bone matrix deposition but could not rescue bone mineralization. These results suggest a decoupling of bone matrix deposition from bone mineralization that may be differentially affected by probiotics (or BMP signalling), possibly related to the absence of induction of the late marker *bglap* by probiotics.

Osteoblast or bone matrix reporter transgenic lines combined with staining techniques like AR are useful for following osteoblast differentiation, bone matrix deposition and bone mineralization simultaneously. Future studies may take further advantage of these transgenic lines by focusing on continuous monitoring of transgene expression during development and in adults or on specific bone structures. In this respect, studies in zebrafish can also provide important insights into skeletal development for mammals and humans; indeed, many examples of zebrafish genes playing similar roles to their human homologs have been described [24,25]. It is important, however, to note that a whole genome duplication occurred in teleosts, leaving many duplicated genes in fish genomes relative to mammals that may have functionally diverged. This situation requires either mutagenesis of both orthologs in zebrafish or, at least, a thorough analysis of their spatio-temporal expression pattern. In our study, the new transgenic lines *Tg(sp7:sp7-GFP*) and *Tg(col10a1a:col10a1a-GFP*) clearly evidenced the pro-osteogenic effects of two probiotics strains that were in agreement with the gene expression results. Thus, we can conclude that the probiotics are clearly pro-osteogenic, both alone and in the presence of a BMP inhibitor, with a clear advantage for BS (*Bacillus subtilis*). These findings open a new outlook for the use of probiotics as a prophylactic treatment for improving bone growth and health, which is currently a very under-explored area of research.

## 4. Materials and Methods

### *4.1. Generation of Transgenic Lines Using the CRISPR/Cas9 Method*

To generate fluorescent reporter lines where the expression of the fluorescent protein GFP would be driven by endogenous bone-specific promoters, we engineered a plasmid containing the coding sequence for GFP and a specific sequence (Mbait) for which we also engineered a corresponding gRNA (gRNA1, see **Fig. III-14a**) [54]. By co-injecting the bait gRNA1, specific col10a1a or sp7 gRNA, plasmid, and *Cas9* nuclease into fertilized eggs as previously described [54], we generated double-stranded breaks within the endogenous gene and we linearized the plasmid with GFP cDNA. Injected individuals were then screened for fluorescence in bone structures, indicating that the GFP cDNA was inserted in frame and in the correct orientation within the endogenous target gene (**Fig. III-14a**). Positive individuals were grown, tested for germ line transmission into the F1 generation, and the exact sequence at the insertion point was determined. In each case, insertion of the GFP coding sequence resulted in a sequence coding for a fusion protein containing the N-terminus of the target gene and GFP expressed under

the control of the *col10a1a* or the *sp7* regulatory regions (**Fig. 14a, b** and **15a**).

Sequence of guide RNAs:

- Mbait: gRNA1: GGCTGCTGCGGTTCCAGAGG
- *col10a1a*: gRNA2: GGAGTAAGGCTGGTACTGCG
- *sp7*: gRNA3: GGCTCATTCAGCTCAAGCGG

Sequence of primers for insertion site sequencing:

- GFP-rev: GGTCTTGTAGTTGCCGTCGT
- *col10a1a*-for: TTGTCAAGAAGGTGATGAAGG
- *sp7*-for: AAAAGGCCTACAGCATGACTTC

*4.2. Morpholino Injection*

One to two cell-stage embryos were injected as previously described [55] with 3 ng of antisense morpholino oligonucleotides (MO, Gene Tools Inc., Philomath, OR, USA) complementary to the translational start site of the *entpd5* gene. Morpholinos were diluted in Danieau buffer and tetramethylrhodamine dextran (Invitrogen, Merelbeke, Belgium) was added at 0.5% to verify proper injection of the embryos by fluorescence stereomicroscopy. Standard control morpholino (MOcon) was injected at the same concentration. Although no increase of cell death was observed in the morphants, parallel co-injection experiments with 4.5 ng of a morpholino directed against p53 [56] were performed to ensure inhibition of MO-induced non-specific cell death [57]. The effects of morpholino injection were tested on at least 100 individuals performed in at least three independent experiments.

Sequence of the morpholino oligonucleotides:

- MO*entpd5*: AATTTAGTCTTACCTTTTCAGGC
- MOcon: random sequence
- MOp53: GACCTCCTCTCCACTAAACTACGAT

*4.3. RNA Extraction and Quantification*

Total RNA was extracted from larvae (n = 8) using RNAeasy Microkit (Qiagen, Hilden, Germany) and eluted in 20 uL of molecular grade nuclease free water. Final RNA concentrations were determined using a nanophotometer (Implen, Munich, Germany). Total RNA was treated with DNase according to the manufacturer's instructions (Sigma-Aldrich, St. Louis, MO, USA). One milligram of total RNA was used for cDNA synthesis using iScript cDNA Synthesis Kit (Bio-Rad, Hercules, CA, USA) and stored at −20 °C until further use as described previously [58].

*4.4. Real Time PCR (RT-PCR)*

RT-PCR reactions were performed with the SYBR green method in a CFX thermal cycler (Bio-Rad, Italy) in triplicate as described previously [59]. Primers were used at a final concentration of 10 pmol/mL. The thermal profile for all reactions commenced with 3 min at 95 °C, followed by 45 cycles of 20 s at 95 °C, then 20 s at 60 °C and 20 s at 72 °C. Dissociation curve analysis revealed a single peak in all cases. Ribosomal protein L13a (*rpl13a*) and ribosomal protein, large, P0 (*rplp0*) were used as the housekeeping genes to standardize the results by eliminating

variation in mRNA and cDNA quantity and quality. No amplification product was observed in negative controls and primer-dimer formation was never seen. Data was analysed using iQ5 Optical System version 2.1 (Bio-Rad) including Genex Macro iQ5 Conversion and Genex Macro iQ5 files. Modification of gene expression between the experimental groups is reported as relative mRNA abundance (arbitrary units). All primer sequences used in the study are listed in Table 1.

**Table 1.** List of primers used for RT-PCR.

| Gene Acronym | NCBI Gene Accession No | Forward | Reverse |
|---|---|---|---|
| ***col10a1a*** | ***NM_001083827.1*** | ***CCCATCCACATCACATCAAA*** | ***GCGTGCATTTCTCAGAACAA*** |
| ***runx2b*** | ***NM_212862.2*** | ***GTGGCCACTTACCACAGAGC*** | ***TCGGAGAGTCATCCAGCTT*** |
| ***spp1*** | ***NM_001002308.1*** | ***GAGCCTACACAGACCACGCCA ACAG*** | ***GGTAGCCCAAACTGTCTCCCCG*** |
| ***cyp26b1*** | ***NM_212666.1*** | ***GCTGTCAACCAGAACATTCCC*** | ***GGTTCTGATTGGAGTCGAGGC*** |
| ***sp7*** | ***NM_212863.2*** | ***AACCCAAGCCCGTCCCGACA*** | ***CCGTACACCTTCCCGCAGCC*** |
| ***bglap*** | ***NM_001083857.3*** | ***GCCTGATGACTGTGTGTCTGAG CG*** | ***AGTTCCAGCCCTCTTCTGTCTC AT*** |
| ***rpl13a*** | ***NM_212784.1*** | ***TCTGGAGGACTGTAAGAGGTAT GC*** | ***AGACGCACAATCTTGAGAGCAG*** |
| ***rplp0*** | ***NM_131580.2*** | ***CTGAACATCTCGCCCTTCTC*** | ***TAGCCGATCTGCAGACACAC*** |

*4.5. Zebrafish Transgenic Lines Maintenance*

Broodstock from the transgenic lines used in our experiments, *Tg(col10a1a:col10a1a-GFP*), *Tg(sp7:sp7-GFP)* and *Tg(Ola.Sp7:mCherry)*, were maintained at the zebrafish facilities, GIGA-R, University of Liège, Belgium in a recirculating water system (Tecniplast, Buguggiate, VA, Italy). To collect fertilised eggs in the morning, brooders were maintained at a 1:2 male to female ratio the day before and set for overnight breeding in tanks with slopes. Collected eggs were maintained in small tanks until hatching at 3 dpf. Using a fluorescent stereomicroscope (Olympus SZX10), larvae expressing the reporter proteins were screened and randomly distributed into 6 well plates at a density of 15 larvae per well with 10 mL of E3 medium per well until 7 dpf and then in small tanks with 15 larvae per 45 mL of E3 medium until 10 dpf. Seventy percent of the medium was exchanged daily. Commercial feed and live feed (paramecia) were administered from 5 dpf to 10 dpf along with the treatments.

*4.6. Exposure to LDN212854 and Probiotics*

Two probiotics, *Bacillus subtilis* (BS) and *Lactococcus lactis* (LL), were obtained from Fermedics (Machelen, Belgium) as lyophilized powder at a commercially formulated concentration of $10^{11}$ CFU/g. After preliminary tests, larvae were exposed at a concentration of $10^{6}$ CFU/mL administered in water from 5 dpf to 10 dpf. The type 1 BMP receptor inhibitor LDN212854 (Cat. No. 6151; Bio-Techne Ltd. TOCRIS, Bristol, United Kingdom) was dissolved in DMSO and used at concentrations of 10 μM and 20 μM, starting at 2 dpf until 4 dpf. Combined treatments

were performed by exposing the larvae to LDN212854 from 2 dpf until 5 dpf, followed by probiotic treatment until 10 dpf. Each experiment was performed in triplicate.

*4.7. Alizarin red (AR) Staining*

AR staining is one of the most common techniques for observing the extent of bone mineralization [60]. Larvae were sacrificed by exposure to MS-222 (ethyl 3-aminobenzoate methane sulfonate; Merck, Overijse, Belgium) and stained with 0.01% AR-S (Merck, Overijse, Belgium) for 15 min. They were then placed lateral side down onto glycerol (100%) for imaging.

*4.8. Image Acquisition and Analysis*

Imaging was performed with a Leica fluorescence stereomicroscope (Leica, Wetzlar, Germany) equipped with either a red fluorescence filter (λex = 546/10 nm, ET-DSR) for *Tg(Ola.Sp7:mCherry*) and AR-stained fish or a green fluorescence filter (λex = 470/40 nm) for *Tg(sp7:sp7-GFP)* and *Tg(col10a1a: col10a1a-GFP).* All images were acquired with a DFC7000T colour camera (Leica, Wetzlar, Germany) according to the following parameters: 24-bit coloured image, exposure time 2s (green filter EGFP) or 1s (red filter ET-DSR), gamma 1.00, image format 1920 × 1440 pixels, binning 1 × 1. Images were acquired using constant parameters and analysed using ImageJ version 2.1.0/1.53c software after splitting the colour channels of the RGB images. The green or red channel 8-bit images were adjusted uniformly for optimum contrast and brightness for improved visibility of the structures. The integrated pixel intensity was measured inside the total bone areas (in lateral and ventral view) of each fish and the integrated pixel intensity from the eye was subtracted. The values were further corrected for the head area (pixel intensity/head area) to eliminate possible inter-specimen size variability due to non-homogenous growth. The corrected values were plotted relative to the control arbitrarily set to 100%. A representative image showing how the pixel intensity was measured in both lateral and ventral head views is presented (Supplementary **Fig. III-S1**).

*4.9. Statistical Analysis*

Data from all groups were normally distributed, as assessed by a Shapiro–Wilk's test ($p > 0.05$), and the variances were homogenous, as assessed by Levene's test for equality of variances ($p > 0.05$). The differences between the control and the treatments were tested with a one-way analysis of variance (ANOVA) followed by Tukey's post hoc test ($p < 0.05$) for all image analysis data and gene expression differences between groups. All the tests were performed using R version 4.0.2 and plots were generated using ggplot2 within R [61]. In our graphs, we use an alphabetic code to indicate statistically significant differences between groups in multiple comparison tests as a simple way to present all pair-wise comparisons. Every group is compared to every other group, and the groups that share the same letters are not statistically different. For instance, three treatments that are all significantly different from one another would be labelled a,b, and c; if two of the treatments differed from each other, but neither differed significantly from the third, they would be labelled a, b, and ab. The significance level was set

at a constant $p < 0.05$ in all cases, but the focus was on all possible pair-wise comparisons.

## 5. Conclusions

We present two transgenic zebrafish lines based on insertion of a fluorescent protein coding cDNA into the coding regions of two bone-specific genes, *sp7* and *col10a1a*, which allow osteoblast formation and bone matrix growth, respectively, to be monitored in living animals. Using these two transgenic lines, the bone protection properties of two probiotics, *B.subtilis* and *L.lactis*, were revealed in addition to the specific ability of *B.subtilis* to counter the action of a BMP inhibitor. Our study therefore confirms the relevance of probiotics in promoting bone growth and bone health maintenance.

**Supplementary Materials:** The following supporting information can be downloaded at: www.mdpi.com/xxx/s1.

**Author Contributions:** Formal analysis—J.M.S., R.R., M.M., O.C. and J.R.; conceptualization—J.M.S., R.R., M.M., O.C. and J.R.; validation—J.M.S., R.R., M.M., O.C. and J.R.; methodology—J.M.S., R.R., M.M., O.C. and J.R.; writing—original draft preparation—J.M.S., R.R., M.M., O.C. and J.R.; writing—review and editing—J.M.S., R.R., M.M., O.C. and J.R. All authors have read and agreed to the published version of the manuscript.

**Funding:** This work was supported by the European Space Agency (Fish-μGenomics), the Belgian Space Agency Prodex (FISHSIM), and the EU MSCA-ITN project BioMedAqu (GA 766347) that has received funding from the European Union's Horizon 2020 research and innovation programme under the Marie Skłodowska-Curie grant agreement No 766347. J.M.S. and R.R were MSCA PhD fellows. M.M. is a 'Maître de Recherche au F.N.R.S.'

**Institutional Review Board Statement:** This study adheres to the code of ethics for scientific research in Belgium, which is compliant with European Directive 2010/63/EU. Animals were obtained from the GIGA zebrafish facility (approval number LA1610002), experiments were approved by the ethical committee under the file numbers 16-1801, 16-1961 and 19-2135. Concerning biosecurity and biotechnology, European Directive 2009/41/EC was applied under the approval number SBB 219 2010/0333.

Data Availability Statement: The complete set of images used in this study will be made available in an institutional repository (https://hdl.handle.net/2268/289903; accessed 25 April 2022).

**Acknowledgments:** We wish to thank the GIGA-R zebrafish facility for providing zebrafish adults and fertilized eggs. We thank K.D. Poss (Duke University Medical Center, U.S.A.).

**Conflicts of Interest:** The authors declare no conflict of interest.

## References

1. Hill, C.; Guarner, F.; Reid, G.; Gibson, G.R.; Merenstein, D.J.; Pot, B.; Morelli, L.; Canani, R.B.; Flint, H.J.; Salminen, S.; et al. The International Scientific Association for Probiotics and Prebiotics Consensus Statement on the Scope and Appropriate Use of the Term Probiotic. *Nat. Rev. Gastroenterol. Hepatol.* **2014**, *11*, 506–514. https://doi.org/10.1038/nrgastro.2014.66.
2. McCabe, L.; Britton, R.A.; Parameswaran, N. Prebiotic and Probiotic Regulation of Bone Health: Role of the Intestine and Its Microbiome. *Curr. Osteoporos. Rep.* **2015**, *13*, 363–371. https://doi.org/10.1007/s11914-015-0292-x.
3. Ohlsson, C.; Sjögren, K. Osteomicrobiology: A New Cross-Disciplinary Research Field. *Calcif. Tissue Int.* **2018**, *102*, 426–432. https://doi.org/10.1007/s00223-017-0336-6.
4. Rizzoli, R.; Biver, E. Are Probiotics the New Calcium and Vitamin D for Bone Health? *Curr. Osteoporos. Rep.* **2020**, *18*, 273–284. https://doi.org/10.1007/s11914-020-00591-6.

5. Cosme-Silva, L.; Dal-Fabbro, R.; Cintra, L.T.A.; Ervolino, E.; Plazza, F.; Mogami Bomfim, S.; Duarte, P.C.T.; Junior, V.E.D.S.; Gomes-Filho, J.E. Reduced Bone Resorption and Inflammation in Apical Periodontitis Evoked by Dietary Supplementation with Probiotics in Rats. *Int. Endod. J.* **2020**, *53*, 1084–1092. https://doi.org/10.1111/iej.13311.
6. Gholami, A.; Dabbaghmanesh, M.H.; Ghasemi, Y.; Talezadeh, P.; Koohpeyma, F.; Montazeri-Najafabady, N. Probiotics Ameliorate Pioglitazone-Associated Bone Loss in Diabetic Rats. *Diabetol. Metab. Syndr.* **2020**, *12*, 78. https://doi.org/10.1186/s13098-020-00587-3.
7. Huidrom, S.; Beg, M.A.; Masood, T. Post-Menopausal Osteoporosis and Probiotics. *Curr. Drug Targets* **2021**, *22*, 816–822. https://doi.org/10.2174/1389450121666201027124947.
8. Jia, L.; Tu, Y.; Jia, X.; Du, Q.; Zheng, X.; Yuan, Q.; Zheng, L.; Zhou, X.; Xu, X. Probiotics Ameliorate Alveolar Bone Loss by Regulating Gut Microbiota. *Cell Prolif.* **2021**, *54*, e13075. https://doi.org/10.1111/cpr.13075.
9. Britton, R.A.; Irwin, R.; Quach, D.; Schaefer, L.; Zhang, J.; Lee, T.; Parameswaran, N.; McCabe, L.R.; Probiotic, L. Reuteri Treatment Prevents Bone Loss in a Menopausal Ovariectomized Mouse Model. *J. Cell. Physiol.* **2014**, *229*, 1822–1830. https://doi.org/10.1002/jcp.24636.
10. Chiang, S.-S.; Pan, T.-M. Antiosteoporotic Effects of Lactobacillus-Fermented Soy Skim Milk on Bone Mineral Density and the Microstructure of Femoral Bone in Ovariectomized Mice. *J. Agric. Food Chem.* **2011**, *59*, 7734–7742. https://doi.org/10.1021/jf2013716.
11. Ohlsson, C.; Engdahl, C.; Fåk, F.; Andersson, A.; Windahl, S.H.; Farman, H.H.; Movérare-Skrtic, S.; Islander, U.; Sjögren, K. Probiotics Protect Mice from Ovariectomy-Induced Cortical Bone Loss. *PLoS ONE* **2014**, *9*, e92368. https://doi.org/10.1371/journal.pone.0092368.
12. Parvaneh, K.; Ebrahimi, M.; Sabran, M.R.; Karimi, G.; Hwei, A.N.M.; Abdul-Majeed, S.; Ahmad, Z.; Ibrahim, Z.; Jamaluddin, R. Probiotics (Bifidobacterium Longum) Increase Bone Mass Density and Upregulate Sparc and Bmp-2 Genes in Rats with Bone Loss Resulting from Ovariectomy. *BioMed. Res. Int.* **2015**, *2015*, e897639. https://doi.org/10.1155/2015/897639.
13. Foureaux, R. de C.; Messora, M.R.; de Oliveira, L.F.F.; Napimoga, M.H.; Pereira, A.N.J.; Ferreira, M.S.; Pereira, L.J. Effects of Probiotic Therapy on Metabolic and Inflammatory Parameters of Rats with Ligature-Induced Periodontitis Associated with Restraint Stress. *J. Periodontol.* **2014**, *85*, 975–983. https://doi.org/10.1902/jop.2013.130356.
14. Nilsson, A.G.; Sundh, D.; Bäckhed, F.; Lorentzon, M. Lactobacillus Reuteri Reduces Bone Loss in Older Women with Low Bone Mineral Density: A Randomized, Placebo-Controlled, Double-Blind, Clinical Trial. *J. Intern. Med.* **2018**, *284*, 307–317. https://doi.org/10.1111/joim.12805.
15. Takimoto, T.; Hatanaka, M.; Hoshino, T.; Takara, T.; Tanaka, K.; Shimizu, A.; Morita, H.; Nakamura, T. Effect of *Bacillus Subtilis* C-3102 on Bone Mineral Density in Healthy Postmenopausal Japanese Women: A Randomized, Placebo-Controlled, Double-Blind Clinical Trial. *Biosci. Microbiota Food Health* **2018**, *37*, 87–96. https://doi.org/10.12938/bmfh.18-006.
16. Maradonna, F.; Gioacchini, G.; Falcinelli, S.; Bertotto, D.; Radaelli, G.; Olivotto, I.; Carnevali, O. Probiotic Supplementation Promotes Calcification in Danio Rerio Larvae: A Molecular Study. *PLoS ONE* **2013**, *8*, e83155. https://doi.org/10.1371/journal.pone.0083155.
17. Terashima, A.; Takayanagi, H. Overview of Osteoimmunology. *Calcif. Tissue Int.* **2018**, *102*, 503–511. https://doi.org/10.1007/s00223-018-0417-1.
18. Wu, S.; Yoon, S.; Zhang, Y.-G.; Lu, R.; Xia, Y.; Wan, J.; Petrof, E.O.; Claud, E.C.; Chen, D.; Sun, J. Vitamin D Receptor Pathway Is Required for Probiotic Protection in Colitis. *Am. J. Physiol. Gastrointest. Liver Physiol.* **2015**, *309*, G341–G349. https://doi.org/10.1152/ajpgi.00105.2015.
19. Li, J.-Y.; Chassaing, B.; Tyagi, A.M.; Vaccaro, C.; Luo, T.; Adams, J.; Darby, T.M.; Weitzmann, M.N.; Mulle, J.G.; Gewirtz, A.T.; et al. Sex Steroid Deficiency–Associated Bone Loss Is Microbiota Dependent and Prevented by Probiotics. *J. Clin. Investig.* **2016**, *126*, 2049–2063. https://doi.org/10.1172/JCI86062.
20. Chaplin, A.; Parra, P.; Laraichi, S.; Serra, F.; Palou, A. Calcium Supplementation Modulates Gut Microbiota in a Prebiotic Manner in Dietary Obese Mice. *Mol. Nutr. Food Res.* **2016**, *60*, 468–480. https://doi.org/10.1002/mnfr.201500480.
21. Atkins, G.J.; Welldon, K.J.; Wijenayaka, A.R.; Bonewald, L.F.; Findlay, D.M. Vitamin K Promotes Mineralization, Osteoblast-to-Osteocyte Transition, and an Anticatabolic Phenotype by γ-Carboxylation-Dependent and -Independent Mechanisms. *Am. J. Physiol. Cell Physiol.* **2009**, *297*, C1358–C1367. https://doi.org/10.1152/ajpcell.00216.2009.
22. Booth, S.L. Roles for Vitamin K Beyond Coagulation. *Annu. Rev. Nutr.* **2009**, *29*, 89–110. https://doi.org/10.1146/annurev-nutr-080508-141217.
23. Castaneda, M.; Strong, J.M.; Alabi, D.A.; Hernandez, C.J. The Gut Microbiome and Bone Strength. *Curr. Osteoporos. Rep.* **2020**, *18*, 677–683. https://doi.org/10.1007/s11914-020-00627-x.
24. Lleras-Forero, L.; Winkler, C.; Schulte-Merker, S. Zebrafish and Medaka as Models for Biomedical Research of Bone Diseases. *Dev. Biol.* **2020**, *457*, 191–205. https://doi.org/10.1016/j.ydbio.2019.07.009.
25. Bergen, D.J.M.; Kague, E.; Hammond, C.L. Zebrafish as an Emerging Model for Osteoporosis: A Primary Testing Platform for Screening New Osteo-Active Compounds. *Front. Endocrinol.* **2019**, *10*, 6. https://doi.org/10.3389/fendo.2019.00006.
26. Sun, X.; Zhang, R.; Chen, H.; Du, X.; Chen, S.; Huang, J.; Liu, M.; Xu, M.; Luo, F.; Jin, M.; et al. Fgfr3 Mutation Disrupts Chondrogenesis and Bone Ossification in Zebrafish Model Mimicking CATSHL Syndrome Partially via Enhanced Wnt/β-Catenin Signaling. *Theranostics* **2020**, *10*, 7111–7130. https://doi.org/10.7150/thno.45286.
27. Jacobs, C.T.; Huang, P. Notch Signalling Maintains Hedgehog Responsiveness via a Gli-Dependent Mechanism during Spinal Cord Patterning in Zebrafish. *eLife* **2019**, *8*, e49252. https://doi.org/10.7554/eLife.49252.
28. Alhazmi, N.; Carroll, S.H.; Kawasaki, K.; Woronowicz, K.C.; Hallett, S.A.; Macias Trevino, C.; Li, E.B.; Baron, R.; Gori, F.; Yelick, P.C.; et al. Synergistic Roles of Wnt Modulators R-Spondin2 and R-Spondin3 in Craniofacial Morphogenesis and Dental Development. *Sci. Rep.* **2021**, *11*, 5871. https://doi.org/10.1038/s41598-021-85415-y.
29. Lovely, C.B.; Swartz, M.E.; McCarthy, N.; Norrie, J.L.; Eberhart, J.K. Bmp Signaling Mediates Endoderm Pouch Morphogenesis by Regulating Fgf Signaling in Zebrafish. *Development* **2016**, *143*, 2000–2011. https://doi.org/10.1242/dev.129379.

30. Schiavone, M.; Rampazzo, E.; Casari, A.; Battilana, G.; Persano, L.; Moro, E.; Liu, S.; Leach, S.D.; Tiso, N.; Argenton, F. Zebrafish Reporter Lines Reveal in Vivo Signaling Pathway Activities Involved in Pancreatic Cancer. *Dis. Model Mech.* **2014**, *7*, 883–894. https://doi.org/10.1242/dmm.014969.
31. Westphal, M.; Panza, P.; Kastenhuber, E.; Wehrle, J.; Driever, W. Wnt/β-Catenin Signaling Promotes Neurogenesis in the Diencephalospinal Dopaminergic System of Embryonic Zebrafish. *Sci. Rep.* **2022**, *12*, 1030. https://doi.org/10.1038/s41598-022-04833-8.
32. Ando, K.; Shibata, E.; Hans, S.; Brand, M.; Kawakami, A. Osteoblast Production by Reserved Progenitor Cells in Zebrafish Bone Regeneration and Maintenance. *Dev. Cell* **2017**, *43*, 643-650.e3. https://doi.org/10.1016/j.devcel.2017.10.015.
33. Cooney, O.D.; Nagareddy, P.R.; Murphy, A.J.; Lee, M.K.S. Healthy Gut, Healthy Bones: Targeting the Gut Microbiome to Promote Bone Health. *Front. Endocrinol.* **2021**, *11*, 1159. https://doi.org/10.3389/fendo.2020.620466.
34. Renn, J.; Pruvot, B.; Muller, M. Detection of Nitric Oxide by Diaminofluorescein Visualizes the Skeleton in Living Zebrafish. *J. Appl. Ichthyol.* **2014**, *30*, 701–706. https://doi.org/10.1111/jai.12514.
35. Debiais-Thibaud, M.; Simion, P.; Ventéo, S.; Muñoz, D.; Marcellini, S.; Mazan, S.; Haitina, T. Skeletal Mineralization in Association with Type X Collagen Expression Is an Ancestral Feature for Jawed Vertebrates. *Mol. Biol. Evol.* **2019**, *36*, 2265–2276. https://doi.org/10.1093/molbev/msz145.
36. Huitema, L.F.A.; Apschner, A.; Logister, I.; Spoorendonk, K.M.; Bussmann, J.; Hammond, C.L.; Schulte-Merker, S. Entpd5 Is Essential for Skeletal Mineralization and Regulates Phosphate Homeostasis in Zebrafish. *Proc. Natl. Acad. Sci. USA* **2012**, *109*, 21372–21377. https://doi.org/10.1073/pnas.1214231110.
37. Zinck, N.W.; Jeradi, S.; Franz-Odendaal, T.A. Elucidating the Early Signaling Cues Involved in Zebrafish Chondrogenesis and Cartilage Morphology. *J. Exp. Zool. B Mol. Dev. Evol.* **2021**, *336*, 18–31. https://doi.org/10.1002/jez.b.23012.
38. Windhausen, T.; Squifflet, S.; Renn, J.; Muller, M. BMP Signaling Regulates Bone Morphogenesis in Zebrafish through Promoting Osteoblast Function as Assessed by Their Nitric Oxide Production. *Molecules* **2015**, *20*, 7586–7601. https://doi.org/10.3390/molecules20057586.
39. Li, N.; Felber, K.; Elks, P.; Croucher, P.; Roehl, H.H. Tracking Gene Expression during Zebrafish Osteoblast Differentiation. *Dev. Dyn.* **2009**, *238*, 459–466. https://doi.org/10.1002/dvdy.21838.
40. Azetsu, Y.; Inohaya, K.; Takano, Y.; Kinoshita, M.; Tasaki, M.; Kudo, A. The Sp7 Gene Is Required for Maturation of Osteoblast-Lineage Cells in Medaka (Oryzias Latipes) Vertebral Column Development. *Dev. Biol.* **2017**, *431*, 252–262. https://doi.org/10.1016/j.ydbio.2017.09.010.
41. Hammond, C.L.; Moro, E. Using Transgenic Reporters to Visualize Bone and Cartilage Signaling during Development in Vivo. *Front. Endocrinol.* **2012**, *3*, 91. https://doi.org/10.3389/fendo.2012.00091.
42. Spoorendonk, K.M.; Peterson-Maduro, J.; Renn, J.; Trowe, T.; Kranenbarg, S.; Winkler, C.; Schulte-Merker, S. Retinoic Acid and Cyp26b1 Are Critical Regulators of Osteogenesis in the Axial Skeleton. *Development* **2008**, *135*, 3765–3774. https://doi.org/10.1242/dev.024034.
43. Singh, S.P.; Holdway, J.E.; Poss, K.D. Regeneration of Amputated Zebrafish Fin Rays from de Novo Osteoblasts. *Dev. Cell* **2012**, *22*, 879–886. https://doi.org/10.1016/j.devcel.2012.03.006.
44. Renn, J.; Winkler, C. Osterix-MCherry Transgenic Medaka for in Vivo Imaging of Bone Formation. *Dev. Dyn.* **2009**, *238*, 241–248. https://doi.org/10.1002/dvdy.21836.
45. Wiweger, M.I.; Zhao, Z.; Merkesteyn, R.J.P. van; Roehl, H.H.; Hogendoorn, P.C.W. HSPG-Deficient Zebrafish Uncovers Dental Aspect of Multiple Osteochondromas. *PLoS ONE* **2012**, *7*, e29734. https://doi.org/10.1371/journal.pone.0029734.
46. Clément, A.; Wiweger, M.; Hardt, S. von der; Rusch, M.A.; Selleck, S.B.; Chien, C.-B.; Roehl, H.H. Regulation of Zebrafish Skeletogenesis by Ext2/Dackel and Papst1/Pinscher. *PLOS Genet.* **2008**, *4*, e1000136. https://doi.org/10.1371/journal.pgen.1000136.
47. Yan, Y.-L.; Bhattacharya, P.; He, X.J.; Ponugoti, B.; Marquardt, B.; Layman, J.; Grunloh, M.; Postlethwait, J.H.; Rubin, D.A. Duplicated Zebrafish Co-Orthologs of Parathyroid Hormone-Related Peptide (PTHrP, Pthlh) Play Different Roles in Craniofacial Skeletogenesis. *J. Endocrinol.* **2012**, *214*, 421–435. https://doi.org/10.1530/JOE-12-0110.
48. Reijntjes, S.; Rodaway, A.; Maden, M. The Retinoic Acid Metabolising Gene, CYP26B1, Patterns the Cartilaginous Cranial Neural Crest in Zebrafish. *Int. J. Dev. Biol.* **2003**, *51*, 351–360. https://doi.org/10.1387/ijdb.062258sr.
49. Laue, K.; Jänicke, M.; Plaster, N.; Sonntag, C.; Hammerschmidt, M. Restriction of Retinoic Acid Activity by Cyp26b1 Is Required for Proper Timing and Patterning of Osteogenesis during Zebrafish Development. *Development* **2008**, *135*, 3775–3787. https://doi.org/10.1242/dev.021238.
50. Laue, K.; Pogoda, H.-M.; Daniel, P.B.; van Haeringen, A.; Alanay, Y.; von Ameln, S.; Rachwalski, M.; Morgan, T.; Gray, M.J.; Breuning, M.H.; et al. Craniosynostosis and Multiple Skeletal Anomalies in Humans and Zebrafish Result from a Defect in the Localized Degradation of Retinoic Acid. *Am. J. Hum. Genet.* **2011**, *89*, 595–606. https://doi.org/10.1016/j.ajhg.2011.09.015.
51. Maruyama, Z.; Yoshida, C.A.; Furuichi, T.; Amizuka, N.; Ito, M.; Fukuyama, R.; Miyazaki, T.; Kitaura, H.; Nakamura, K.; Fujita, T.; et al. Runx2 Determines Bone Maturity and Turnover Rate in Postnatal Bone Development and Is Involved in Bone Loss in Estrogen Deficiency. *Dev. Dyn.* **2007**, *236*, 1876–1890. https://doi.org/10.1002/dvdy.21187.
52. Komori, T. Regulation of Bone Development and Extracellular Matrix Protein Genes by RUNX2. *Cell Tissue Res.* **2009**, *339*, 189. https://doi.org/10.1007/s00441-009-0832-8.
53. Lowery, J.W.; Rosen, V. The BMP Pathway and Its Inhibitors in the Skeleton. *Physiol. Rev.* **2018**, *98*, 2431–2452. https://doi.org/10.1152/physrev.00028.2017.
54. Kimura, Y.; Hisano, Y.; Kawahara, A.; Higashijima, S. Efficient Generation of Knock-in Transgenic Zebrafish Carrying Reporter/Driver Genes by CRISPR/Cas9-Mediated Genome Engineering. *Sci. Rep.* **2014**, *4*, 6545. https://doi.org/10.1038/srep06545.

55. Dalcq, J.; Pasque, V.; Ghaye, A.; Larbuisson, A.; Motte, P.; Martial, J.A.; Muller, M. RUNX3, EGR1 and SOX9B Form a Regulatory Cascade Required to Modulate BMP-Signaling during Cranial Cartilage Development in Zebrafish. *PLoS ONE* **2012**, *7*, e50140. https://doi.org/10.1371/journal.pone.0050140.
56. Larbuisson, A.; Dalcq, J.; Martial, J.A.; Muller, M. Fgf Receptors Fgfr1a and Fgfr2 Control the Function of Pharyngeal Endoderm in Late Cranial Cartilage Development. *Differentiation* **2013**, *86*, 192–206. https://doi.org/10.1016/j.diff.2013.07.006.
57. Robu, M.E.; Larson, J.D.; Nasevicius, A.; Beiraghi, S.; Brenner, C.; Farber, S.A.; Ekker, S.C. P53 Activation by Knockdown Technologies. *PLoS Genet.* **2007**, *3*, e78. https://doi.org/10.1371/journal.pgen.0030078.
58. Maradonna, F.; Nozzi, V.; Dalla Valle, L.; Traversi, I.; Gioacchini, G.; Benato, F.; Colletti, E.; Gallo, P.; Di Marco Pisciottano, I.; Mita, D.G.; et al. A Developmental Hepatotoxicity Study of Dietary Bisphenol A in Sparus Aurata Juveniles. *Comp. Biochem. Physiol. Part C: Toxicol. Pharmacol.* **2014**, *166*, 1–13. https://doi.org/10.1016/j.cbpc.2014.06.004.
59. Carnevali, O.; Notarstefano, V.; Olivotto, I.; Graziano, M.; Gallo, P.; Di Marco Pisciottano, I.; Vaccari, L.; Mandich, A.; Giorgini, E.; Maradonna, F. Dietary Administration of EDC Mixtures: A Focus on Fish Lipid Metabolism. *Aquat. Toxicol.* **2017**, *185*, 95–104. https://doi.org/10.1016/j.aquatox.2017.02.007.
60. Bensimon-Brito, A.; Cardeira, J.; Dionísio, G.; Huysseune, A.; Cancela, M.L.; Witten, P.E. Revisiting in Vivo Staining with Alizarin Red S—A Valuable Approach to Analyse Zebrafish Skeletal Mineralization during Development and Regeneration. *BMC Dev. Biol.* **2016**, *16*, 2. https://doi.org/10.1186/s12861-016-0102-4.
61. R Core Team *R. A Language and Environment for Statistical Computing;* R Foundation for Statistical Computing: Vienna, Austria, 2020; https://www.yumpu.com/s/Fxit5xIdza5bKZeV.

# IV. DISCUSSION & CONCLUSIONS

Our studies investigating the zebrafish osteoblast transcriptome at 4dpf revealed that there are two clearly separate subpopulations of osteoblasts present based on their GFP intensity, which exhibit a distinct differential gene expression pattern related to osteoblast differentiation and bone formation. Pathway analysis brought to light an intricate arrangement of signaling pathway components, TFs, and ECM protein genes that are specific to each of the subpopulations.

The subsequent phenotypic characterizations conducted to elucidate the role of two ECM protein coding genes, *col10a1a* and *fbln1*, revealed that both are essential for preserving the skeletal integrity, interestingly displaying opposite effects on skeletal development. Our results clearly show that the *col10a1a* gene is required for bone and vertebral column mineralization, while the *fbln1* gene appears to play an inhibitory in pre-osteoblast on their further proliferation or differentiation. Furthermore, the absence of an operculum in adult *fbln1* mutant zebrafish suggests that Fgf8 might be playing a role in controlling the growth and morphogenesis of certain skeletal elements.

Preliminary characterization of the *efemp1* mutant zebrafish adults reveals impaired bone properties such as increased vertebral TMD and thickness, as well as a decrease in the intervertebral space and ruffled edges reminiscent of spinal OA in humans.

Thus, we were able to highlight the importance of ECM protein coding genes in skeletal development of zebrafish.

Furthermore, we showed that probiotics are able to increase mineralized bone formation, and that *Bacillus subtilis* significantly reverted the detrimental effect of BMP inhibition on the bone matrix formation, primarily by affecting deposition of the unmineralized bone matrix.

These results contribute to a better understanding of skeletal formation in general, and in zebrafish in particular. However, as is often the case for scientific investigations, they also leave us with unanswered and new questions that will need to be addressed in the future. Some of these will be discussed in the following sections.

## 1. Various osteoblast populations in developing zebrafish.

The presence of subpopulations in our osteoblast transcriptome data clearly indicates that there are more than one population of osteoblast involved in the formation of skeletal elements in zebrafish at 4dpf, but many of the specifics in this regard are still open to investigation. The transcription factor Sp7 is a well-known marker of osteoblasts, it initiates differentiation into functional osteoblasts, regulates many of the osteoblast-specific genes, and is conserved across species (DeLaurier et al., 2010b; Nakashima et al., 2002; Renn and Winkler, 2014). Using a fluorescent reporter line, we surprisingly found that two subpopulations of *sp7* expressing osteoblasts are present in zebrafish larvae at 4dpf. We were clearly able to distinguish and separate the two subpopulations based on the differential gene expression pattern; we identified the "*sp7* high" (GFP high) sub-population P2 as "mature osteoblast" and the "*sp7* low" (GFP low) sub-population P1 as precursor cells, "osteoblast-like cells" or "skeletal like cells", as shown in (**Fig.IV-1**).

Furthermore, transcriptomic analysis revealed a complex pattern of expression in osteoblasts of genes involved in the BMP and WNT signaling pathways, with BMP components gradually increasing from P1 to P2, while the WNT ligands and receptors display a more diverse pattern.

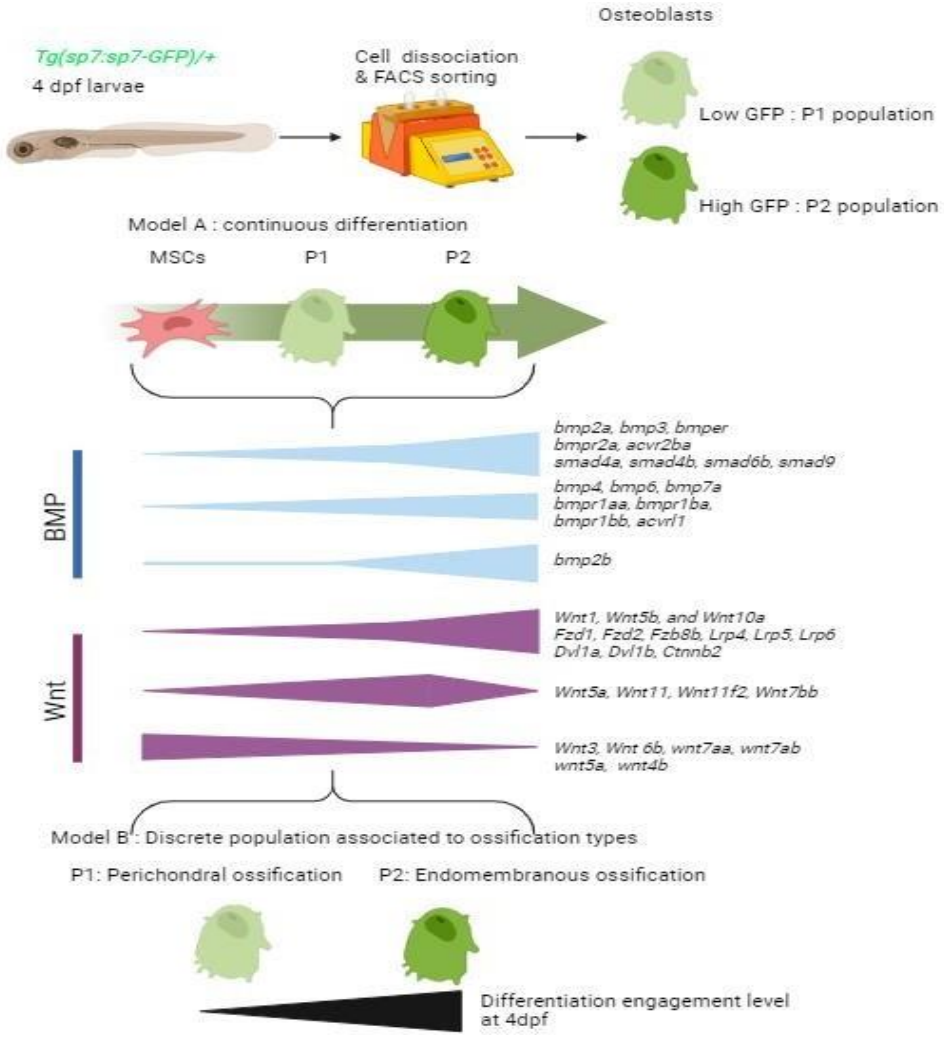


**Figure IV-1. Illustration showing the isolation of two subpopulations of osteoblasts from zebrafish at 4dpf and their respective transcriptomic profiles.**

The P2 subpopulation has to be considered as functional osteoblasts, since the majority of osteoblast markers (*sp7, runx2b, col10a1a*) and bone-related genes (*spp1, bmp2a, panx3*) are expressed, and their functional annotations also point to bone formation and osteoblast function. Previous work analyzing the spatio-temporal expression pattern of several bone-related genes using *in situ* hybridization had proposed to classify osteoblasts into early (no *sp7* expression), intermediate (expressing *sp7*), and mature osteoblasts expressing *col1a2, osn*, but not *sp7* (Li et al., 2009). It is important to note in this context that the P2 sub-population actually corresponds to the *sp7* high expressing osteoblasts, which could thus be regarded as "intermediate stage" osteoblasts, while the "mature osteoblasts" according to this classification would not be present in our analysis. Other analyzed genes support this

conclusion. In addition to the genes mentioned previously, we have also observed the chondrocyte marker gene *sox9a* to be upregulated in the two subpopulations of osteoblasts, whereas *sox9b* was not detected. We also found the expression of pannexin 3 (*panx3)* to be significantly upregulated in the P2 subpopulation of osteoblasts, together with high expression of *sp7* and *col10a1a*. It was previously shown in mouse that pannexin 3, an endoplasmic reticulum $Ca^{+2}$ channel, is a regulator of bone formation, since newborn *Panx3* KO mice harbor skeletal deformities and decreased terminal differentiation of hypertrophic chondrocytes and osteoblasts (Ishikawa and Yamada, 2017). Moreover, phosphorylation of Panx3 is essential to control its gating to promote osteogenesis (Ishikawa et al., 2019). In zebrafish, it has been reported that the expression of *panx3* overlaps with the expression of *col10a1a* in zebrafish at 2, 3 and 4 dpf in the developing cranial skeletal elements, whereas osteoblast differentiation and mineralization, as well as the expression of *col10a1a* were delayed in *panx3* morphants (Oh et al., 2015). Whether the two subpopulations can be placed in a continuous series of osteoblast differentiation lineage, or discrete populations associated to different ossification types, as shown above (**Fig.IV-1**) requires further investigation, however the P2 subpopulation clearly seems to fit into the osteoblast differentiation scheme as functional osteoblasts.

The P1 subpopulation is somewhat difficult to define. The fact that these cells express a series of osteoblast markers, but not all, and weakly express *sp7* obviously identify them as osteoblast precursors, also according to the previous classification (Li et al 2009). However, we also observed some upregulated genes that suggested that this population may be more heterogenous, while keeping in mind that *sp7* expression is slightly increased in these cells. We previously mentioned the stanniocalcin 1-like (*stc1l*) and osteocrin (*ostn*) genes, expressed specifically, but not exclusively in corpuscles of Stannius. Similarly, it is interesting to find markers associated to osteoclasts, such as *ctsk*, *acp5a* and *tnfrsf1b* (Sharif et al., 2014) to be significantly upregulated in this subpopulation. Expression of these genes was indeed observed in developing bone of early-stage larvae by *in situ* hybridization, however the nature of these cells was not investigated. Further studies, also involving single cell sequencing of the transcriptome of *sp7*-expressing cells, will in the future help to identify these cells.

Taken together, our findings raise a significant number of questions on zebrafish bone formation and the osteoblast population. For example, how many osteoblast populations do exist in a developing larvae, at various stages of development, what maintains the balance between recruiting osteoblast precursors and forming other cell types to avoid depleting the embryonic mesenchymal stem cell population, which lineage markers of skeletal differentiation are expressed simultaneously or at different time points in individual cells, and how does the orchestration of morphogenesis and differentiation look like during bone development. Although *sp7* is conserved across all species from humans to non-mammalian vertebrates such as zebrafish and medaka, some differences exist. *Sp7* KO mouse die before birth (Nakashima et al., 2002), however conditionally inactivating the mouse *Sp7* gene postnatally causes functional defects in osteoblasts and reduction in bone formation, indicating that the gene is required for maintaining osteoblast function and bone homeostasis (Baek et al., 2010). This phenomenon is also observed in medaka, where inactivation of *sp7* blocks osteoblast differentiation and leads to dramatic intra-membranous and perichondral ossification defects, including larval lethality in homozygous mutants (Yu et al., 2017). On

the contrary, *sp7*$^{-/-}$ zebrafish do not completely recapitulate the defects as reported in mouse mutants. The mutants are still viable, with normally patterned skeleton, with only minor defects in bone growth and mineralization, followed by skeletal deformities in the cranium and axial skeleton at later stages (Kague et al., 2016). It is possible that genetic compensation, where another related gene replaces the function of Sp7 in the *sp7*$^{-/-}$ mutants. Candidates are Sp1, Sp3 or other Sp factors that can bind to the same promoters as reported in osteoblastic cells (Goto et al., 2006). These findings raise the question of what is essentially required for bone formation in zebrafish and this phenomenon requires further investigation.

Nevertheless, *sp7* may still be considered as a marker gene for osteoblasts, as also confirmed by our transcriptomic results. As explained above, these data suggest that the P1 population represents osteoblast precursors, while P2 represents functional osteoblasts. However, alternative explanations can be envisaged. It has been reported that based on differential sensitivity to hedgehog signaling there are at least three populations of osteoblasts in developing zebrafish (Hammond and Schulte-Merker, 2009). Osteoblasts forming dermal bones were unaffected by HH signaling, while those forming endochondral bones required HH signaling to different degrees. Thus, although the highly HH-responsive cells (termed osteo-chondrocytes by the authors) only appear as *sp7*-expressing cells at 6 dpf, we cannot rule out at present that the two subpopulations P1 and P2 at 4 dpf may represent osteoblasts forming dermal and endochondral bones, respectively. In any case, there is a high probability that at least two subpopulations of osteoblasts are present in a developing zebrafish at any given stage. By nature, our results are specific to *sp7*-expressing cells, we already mentioned that late stage, mature osteoblasts (Li et al., 2009) do not express *sp7* anymore; therefore, it would be exciting to investigate the transcriptomic profile of cells expressing other known marker genes for osteoblasts such as *runx2b*, *col10a1a*, *bglap*, or *spp1*.

## 2. Inactivation of genes coding for extracellular matrix proteins.

We decided to study the function of ECM proteins in zebrafish skeletal development by generating mutants using the CRISPR/Cas9 technology. We focused on three genes based on their different expression pattern in the P1 and P2 subpopulations (*col10a1a*, *fbln1*) and on the reported involvement of their human homologs in osteoarthritis (*col10a1a*, *efemp1*). Note that *fbln1* and *efemp1*(*fbln3*) belong to the same family of ECM proteins. Taken together, our results clearly show that these ECM proteins play a role in skeletal development and bone formation. As a general observation, it appears that mutation of these genes mainly affects the skeleton at later stages, as revealed by µCT scanning in the vertebrae, deformities in the caudal vertebrae (*col10a1a*), or a missing opercle (*fbln1*). Such a result may have been expected, as these proteins are expressed by osteoblasts, after the early morphogenesis events have already defined the location of the different bone elements. It is obvious that depletion of a major regulator gene, such as *runx2a* or *sox9a*, or a major ECM component like Col1, should have more drastic consequences on bone development.

Nevertheless, we do observe some effects on early development assessed in the head skeleton, which we assume to result from interference with morphogenic signaling pathways,

such as the BMP, WNT, or FGF pathways. Indeed, all three proteins are known to interact with the receptors and ligands of these signaling pathways (Amano et al., 2014; Camaj et al., 2009; Cooley et al., 2014; Fresco et al., 2016; Zhang et al., 2022). Mutation of *col10a1a* in early zebrafish development clearly results in marked reduction in the distance between the hyosymplectics and head length at 5dpf and decreased mineralization for all elements of the cranial skeleton at 10dpf. Absence of *fbln1* in early developmental stages of zebrafish causes a marked decrease in the ceratohyal angle at 5dpf and increased mineralization for all elements in the cranial skeleton at 5 and 10 dpf, respectively. The mutants lacking *efemp1* display reduced distance between the articulations between Meckel's cartilage and the palatoquadrate and between the posterior ends of the ceratohyals at 5 dpf. All three genes belong to huge gene families, thus one cannot rule out the possibility of transcriptional adaptation by members of the same family or genes that are similar in expression pattern (Sztal and Stainier, 2020). Thus, this phenomenon requires further investigation in all our mutants.(Cooley et al., 2014; Debeer et al., 2002). It would be fascinating to investigate how these mutations affect early osteogenesis by examining osteoblast formation and bone development in the mutants by *in situ* hybridization using osteoblast differentiation markers such as *runx2a/b*, *col10a1a* and *sp7* (Avaron et al., 2006; Eames et al., 2012; Flores et al., 2006; Flores et al., 2004; Niu et al., 2017; Pinto et al., 2005), but also genes coding for components of the signaling pathways. Examining cartilage formation at various stages of development in zebrafish *col10a1a* mutant line could provide insights into impairment of chondrocyte stacking, since it has been shown that cell polarity is crucial for proper alignment of chondrocytes in zebrafish (Le Pabic et al., 2014).

The effects observed at later stages, even in adults, draw our attention to another aspect of skeletal biology, bone homeostasis. Indeed, with the exception of the missing opercle in *fbln1*$^{-/-}$ or the deformed caudal vertebrae in col10a1a, higher or lower bone densities in the vertebrae may well result from a differential response to mechanical stress in the mutants. It was shown that changes in mechanical conditions, such as gravitational load (Aceto et al., 2016b; Aceto et al., 2015b) or forced swimming (Fiaz et al., 2012b; Suniaga et al., 2018) may affect various parts of the skeleton. Future studies of the ECM protein mutants may thus include their response to mechanical challenges.

## 3. Col10a1a

It was already known that, in contrast to mammals, the zebrafish *col10a1a* gene is expressed in osteoblasts during early development. In 4-5 dpf larvae, its expression is actually predominantly in the forming bones (dentary, maxillary, ethmoid plate, opercle and cleithrum) (Eames et al., 2012), interestingly including dermal bones that form without a cartilage matrix. This pattern is consistent with the dramatic increase in *col10a1a* expression in the P2 subpopulation of functional (intermediate) osteoblasts. We therefore wanted to investigate the function of Col10a1a in zebrafish by generating a mutant. We observed, besides fusion of the caudal vertebrae, a distinct phenotype of decreased mineralization in the adult *col10a1a* zebrafish mutant. In humans, mutations in the *COL10A1* gene cause abnormal chondrocyte hypertrophy leading to multiple skeletal dysplasias (Ikegawa et al., 1998; Jacenko et al., 1993; McIntosh et al., 1994; Olsen, 1995). The gene is also dysregulated in

osteoarthritis (Drissi et al., 2005; Eerola et al., 1998; Girkontaite et al., 1996; von der Mark et al., 1995; Zheng et al., 2005). A specific *COL10A1* nutation in humans results in a rare autosomal dominant skeletal disorder called Schmid metaphyseal chondrodysplasia (SCMID), characterized by short stature, cox vara and an irregular growth indicating defective endochondral bone formation (Bateman et al., 2005; McIntosh et al., 1994; Richmond et al., 1993; Warman et al., 1993; Wu et al., 2021). *Col10a1* null mice display compressed growth plate comparable to SMCID in humans (Kwan et al., 1997; McIntosh et al., 1995). While our findings support the observations made in mice and human *COL10A1* mutants regarding decreased bone mineralization, we did not observe the dramatic anomalies in craniofacial development (in elements such as opercle, ceratohyal, dentary) that we had anticipated; we only observed a vertebral fusion in the caudal region. This may reflect the shift in zebrafish to a more predominant role for Col10a1 in osteoblast function compared to its absence in early cartilage elements.

Due to a teleost-specific whole genome duplication (TGD), the zebrafish has two paralogous genes coding for Col10a1, *col10a1a* and *col10a1b* (Taylor et al., 2003). Besides osteoblasts, zebrafish *col10a1a* is found to be highly expressed in mature chondrocytes of cartilage structures such as the ceratohyals and in the cells of the perichondrium (Eames et al., 2012). *col10a1a* is also expressed in the developing pharyngeal teeth at 4, 5 and 6 dpf, whereas *col10a1b* is only detected in the teeth at 4 and 6dpf. Additionally, the expressions of both *col10a1a* and *1b* were detected in the developing mesenchyme of older teeth with deposited matrix, while *col10a1b* was found in the epithelium of less developed teeth without deposited matrix (Debiais-Thibaud et al., 2019). This clearly implies that apart from being expressed in the osteoblasts and playing an important role in osteoblast differentiation, these genes may also play a role in the developing teeth. Hence, whether the mutation of *col10a1a* has an impact on the developing pharyngeal teeth should be investigated by looking at various stages of development in early and late (adult) stages in the *col10a1a* mutant. How far the two paralogs share the same function is not completely understood.

Much remains to be understood about the role of *col10a1a* in skeletal development of zebrafish. We hope our preliminary findings can provide the required impetus to further advance the research findings about this gene in more detail. It will be worthwhile to explore the effects of the mutation at the transcriptomic and histological levels.

## 4. Fbln1

The surprise phenotype of missing opercle on the right side at 3 months in 75% of the zebrafish *fbln1* mutants and the increased expression of *fbln1* in the two osteoblast subpopulations of at 4dpf makes it a compelling candidate for further study.

In zebrafish, *fbln1* and *hmcn2* are co-expressed in the fin mesenchymal cells and in developing somites, while *hmcn1* is expressed in the apical-most epidermal cells of the median fin folds (Feitosa et al., 2012; Liedtke et al., 2019). Our transcriptomic analysis on *fbln1*$^{-/-}$ mutants at 10 dpf also reveal the expression of *hmcn1* and *hmcn2* and of other genes belonging to the fibulin family such as *fbln2* and *fbln5* being upregulated, raising the

possibility that some compensation may arise for the mutation of *fbln1*. However, the transcriptomic data at 10dpf is consistent with the increased mineralization observed in that many bone marker genes, such as *sp7* and *col10a1a*, are upregulated along with the genes of the collagen family and those coding for enzymes involved in collagen biosynthesis and maturation. Furthermore, functional annotations of differentially expressed genes (DEGs) in *fbln1*$^{-/-}$ larvae revealed endochondral ossification and collagen synthesis as the major biological processes to be significantly upregulated. Furthermore, the transcriptomic data reveals significant upregulation of both *bmp2a* and *sp7* genes in *fbln1*$^{-/-}$ larvae. Indeed, BMPs (BMP-2, 4, 7) have been shown to be involved in osteoblast differentiation and bone formation (Bitgood and McMahon, 1995; Chen et al., 2004a; Chen et al., 2004b; Issack and DiCesare, 2003; Maridas et al., 2019), in particular BMP-2 upregulates *Sp7* expression (Matsubara et al., 2008; Nakashima et al., 2002; Ulsamer et al., 2008; Yagi et al., 2003). Interestingly, *bmp2a* and *sp7* are also significantly upregulated in both the P1 and P2 osteoblast subpopulations at 4 dpf, along with *fbln1*. This indicates that *fbln1* is involved in osteoblast differentiation.

Interestingly, the functional annotations of the transcriptomic analysis of 10dpf *fbln1* mutant zebrafish suggests that all the three signaling pathways; BMP, WNT, and FGF were identified as downregulated. To get a clear understanding of how Fbln1 interacts with and influences these signaling pathways, a comprehensive expression profile of *fbln1* along with genes that encode the ligands and targets from all these pathways should be conducted in the future.

Our findings in the *fbln1-/-* zebrafish mutant is in sharp contrast to those previously reported in the *Fbln1* KO mice, which reported decreased mineralization and reduced expression of Sp7 (Cooley et al., 2014). Thus, depletion of Fibulin1 has contrasting impact on zebrafish and mouse skeletal mineralization status, requiring additional scrutiny. First, it is interesting to note that the decreased mineralization and bone density was reported in the skull and calvarial bones of the neonate KO mice, whereas we have looked at the early developmental stages (5 and 10 dpf) in the cranial bone elements and at adult (1.5 years old) bone parameters in the vertebral column in *fbln1-/-* zebrafish. Second, although small organisms such as zebrafish and mice are widely used for building scientific knowledge and studying tissue and organ development and disease pathogenesis, there are differences that one must consider (Lleras-Forero et al., 2020). Both mice and zebrafish are different on many levels, such as one is quadrupedal and terrestrial while the other one is an aquatic organism. Mammalian bones have bone marrow, while teleosts such as zebrafish are devoid of bone marrow. Osteoblasts and osteoclasts are found in both mice and zebrafish, but the striking difference is that mammalian skeleton contains osteocytes, while early zebrafish skeleton, scales and fin rays are devoid of osteocytes, instead they are only found in adult zebrafish bone (Witten et al., 2017). Another notable distinction is that in mice, vertebral bodies develop through an intermediary stage of cartilaginous matrix before they undergo ossification, whereas in zebrafish, vertebral bodies form directly through mineralization of the notochord without the presence of a cartilage template (Arratia et al., 2001; Bensimon-Brito et al., 2012; Lleras Forero et al., 2018; Wopat et al., 2018). Furthermore, the bone mineral composition is conserved in both zebrafish, mice, and humans, with calcium, phosphate, and magnesium as the primary mineral components of mineralized skeletal structures. The difference is in terms of origin and absorption of minerals. For example, zebrafish acquire

calcium from water via their gills and skin through osmosis, but ingest phosphate through diet, whereas mice and humans ingest all minerals through dietary intake. Compared to terrestrial mammals, the ossification pathway in zebrafish is similar as they share calcium homeostasis hormones and functions, although their target organs and mineral sources are different (Lleras-Forero et al., 2020). In addition, the phosphate (promotes mineralization) and pyrophosphate (inhibitor) balance is essential for ossification (Michigami and Ozono, 2019). Taken together, all the above aspects could provide an explanation for the divergent effect due to depletion of Fibulin 1 in zebrafish and mice. Differential secondary effects, due to different genetic compensation or differential influence of neighboring tissues, would also need to be considered.

Concerning the missing opercle on the right side in adults, we show that at 10 dpf, *fbln1*$^{-/-}$ larvae are trending towards a smaller right opercle in comparison to the left one, thus indicating the beginning of opercle asymmetry. The transcriptomic profile in the *fbln1*$^{-/-}$ head at 10dpf revealed downregulation of *fgf8a*, *fgf8b*, *etv5a*, *etv5b*, but slight induction of *etv4*, and upregulation of FGF receptors *fgfrl1a* and *fgfrl1b*. Our preliminary observation thus indicates that Fbln1 interacts with Fgf8 and its receptors, thus promoting Fgf8 signaling. Thus, the absence of intact Fbln1 would lead to decreased signaling, reflected in the decreased expression of the *etv4* and *etv5b* genes, that have been reported as specific targets of the Fgf8 signaling pathway (Roehl and Nüsslein-Volhard, 2001). Additional evidence suggests that Fgf8 plays a crucial role in left-right asymmetry in zebrafish (Albertson and Yelick, 2005), while in mice Fgf8 dosage has been reported to affect craniofacial shape and symmetry (Zbasnik et al., 2022). Taken together, all the findings suggest that mutation of *fbln1* affects the Fgf8 signaling pathway required for normal late opercle development. It would be enlightening to investigate the effects of the *fbln1* mutation in the craniofacial area by looking at additional larval and juvenile development stages as well as in the adult skull and other elements in more detail.

## 5. Efemp1

The unexpected but striking spinal osteoarthritis like phenotype showing reduced intervertebral space (ivs) in the adult *efemp1*$^{-/-}$ mutant zebrafish that we observed makes this mutant an attractive candidate for conducting further studies. Interestingly, a previous study has shown that intervertebral disc phenotypes are a common feature occurring in aged zebrafish (Kague et al., 2021). The authors reported a strong correlation between abnormal (low or high) BMD and inter-vertebral disc degeneration, suggesting that the observed increased BMD in the adult *efemp1*$^{-/-}$ mutants would explain the alteration in the vertebral bodies.

We investigated the role of Efemp1 in zebrafish skeletal development due to the increased expression of its human homolog in articular cartilage from osteoarthritic patients (Hasegawa et al., 2017; Sanchez et al., 2018). Very little information was available about its expression in zebrafish, or its function in cartilage and bone development. First, we determined *efemp1* expression at 48hpf (2dpf) in brain, the pharyngeal arches, and in the chordoblasts surrounding the notochord. Segmentation of the notochordal sheath serves as a

blueprint for the patterning of vertebrae in the zebrafish spine (Wopat et al., 2018). It would be interesting to investigate how Efemp1 is involved in the process of spine development, by inspecting its expression at more advanced stages, the exact location of this expression, but also interactions of the Efemp1 protein with ligands or signaling molecules. First, studying the spatio-temporal expression pattern of *efemp1* will help reveal its expression within specific tissues at specific times during zebrafish development; generation of a transgenic *efemp1:GFP* reporter line along with two-, multi-photon, or light sheet microscopy would allow us to image tissues and organs expressing *efemp1* at a cellular/sub-cellular level, a comparative transcriptomic analysis of wildtype and mutant spine refined by spatial transcriptomics or single cell RNA sequencing (ScRNA seq.) on cells expressing *efemp1* might reveal further detailed information about transcription factors, signaling molecules, or pathways that regulate *efemp1*. A very recent preprint publication (Gomez et al. in "bioarchives" https://doi.org/10.1101/2024.02.16.580611) has reported characterization of two new zebrafish *efemp1* mutant alleles. The authors observed the standard length to be significantly increased compared to WT in both heterozygous and homozygous nonsense mutants, recapitulating in zebrafish the tall stature condition observed in patients afflicted with the autosomal dominant condition of Marfan Syndrome, a type of heritable disorder of connective tissues (HDCT) (Bizzari et al., 2020; Driver et al., 2020). Patients with Marfan-like clinical condition display joint laxity, craniofacial malformations, hyposcoliosis, inguinal hernia hyperextensible skin and tall stature (Forghani et al., 2024). However, no spinal osteoarthritis was observed in these mutants. This discrepancy presumably results from the different types of mutation that were induced. The insertion in our mutant *efemp1*$^{ulg074/ulg074}$ results in truncation of the encoded Efemp1 protein at amino acid 62, while the "Gomez" mutants *efemp1*$^{w1014/w1014}$ and *efemp1*$^{w1016/w1016}$ truncate the protein at amino acids 147 and 146. The latter results in a protein lacking the C-terminal Fibulin domain but leaving intact most of the N-terminal EGF-like domains that are involved in protein-protein interactions. The dominant nature of these variants, which would still be able to interact with their partners, but non-productively due to the absence of the Fibulin domain, thus contrast with the complete loss of function in the ulg074 variant that truncates the protein within the most N-terminal EGF-like domain. Future studies may reveal the exact function of the Efemp1 EGF-like domains.

It has been reported that in mouse, *Efemp1* is expressed in condensing mesenchyme, which contributes to the formation of bone and cartilage, as well as in developing axial and cranial bone structures (Kobayashi et al., 2007) and in the perichondrium at E15 mouse embryos (Ehlermann et al., 2003). Furthermore, it was shown that Efemp1 is a negative regulator of chondrocyte differentiation that inhibits cartilage nodule formation, proteoglycan production and ECM gene expression, while it also affects the expression of *Sox5, Sox6* by selectively maintaining *Sox9* expression (Wakabayashi et al., 2010). These transcription factors belong to the Sox family and are known to be required for early chondrogenesis (Akiyama, 2008; Goldring et al., 2006; Huang et al., 2001; Ikeda et al., 2005). Furthermore, *Efemp1* is known to be expressed in the superficial zone of articular cartilage (AC) in human and mouse knee joints that dwindle with age (Hasegawa et al., 2017). However, we did not observe any dramatic effects in the developing cartilage or early elements in the *efemp1*$^{ulg074/ulg074}$ mutant zebrafish. It would be fascinating to search for phenotypes in the jaw joint between the Meckel's and palatoquadrate cartilage, as this joint in zebrafish closely

resembles the synovial knee joint in humans and mice (Askary et al., 2016; Smeeton et al., 2017). Based on previous histological findings, a recent study reported that many characteristics of mammalian synovial joints, such as articular cartilage, a joint cavity, and synovium, are present in the jaw and fin joints of various fish species, including zebrafish, stickleback, and spotted gar (Haines, 1942).

It would have been interesting to couple the above techniques with Synchrotron X-ray Tomographic Microscopy (SRXTM) to visualize the mineralized and non-mineralized portions of a single vertebral body. In addition, nanoindentation would allow to analyze the mechanical properties such as Young's elasticity modulus (E), thickness, and hardness (H) of the vertebrae from control and mutant zebrafish and perform histological analysis. Synchrotron based CT microscopy is slowly getting popular for its wide range of high-resolution image analysis on small specimens in the field of skeletal research, but it has restrictions in terms of not being readily accessible to researchers due to limited availability of synchrotron sources and also being cost inefficient (Akhter MP and RR, 2021). The future shall provide greater opportunities for applying these state-of-the-art techniques in providing clearer and deeper understanding the skeletal development and the development of skeletal anomalies.

## 6. Dietary supplements for improving skeletal health.

Probiotics are microbes that, administered in adequate amounts, have garnered attention for their beneficial potential to enhance general health, potentially acting as a pivotal bridge between the gut microbiome and the skeletal system (Lyu et al., 2023). In this context, our investigation focused on the effects of two specific probiotics, *Bacillus subtilis* and *Lactococcus lactis*, selected for their roles in nutrient absorption enhancement, immune system modulation, and direct actions on bone cells (Jiang et al., 2021). Recent studies have clear clearly shown that supplementation of probiotics maintains healthy gut microbiota composition that promote bone formation and growth, offer protection against bone loss and act as regulator of bone mineral density (Behera et al., 2021; Lawenius et al., 2022; Sjögren et al., 2012; Uchida et al., 2018; Yan et al., 2016). Furthermore, it has been reported that alterations to gut microbiota leads to impaired mechanical bone properties such as reduced femur bone length and tibial metaphysis cortical TMD (Guss et al., 2017), suggesting the importance of having probiotic supplementation in the diet to ensure healthy bone.

Our study utilized novel transgenic zebrafish lines *Tg(sp7:sp7-GFP)* and *Tg(col10a1a:col10a1a-GFP)* designed to visualize osteoblasts and bone matrix development, allowing for the real-time observation of the probiotics effects on skeletal development. These novel lines were engineered to express fluorescent proteins under the control of promoters specific to osteoblasts and bone matrix proteins, such as *sp7* and *col10a1*a, marking a significant advancement in our ability to study bone health in vivo. The administration of *Bacillus subtilis* and *Lactococcus lactis* to these zebrafish models yielded remarkable findings. Notably, both probiotics significantly enhanced osteoblast activity and bone matrix development, as evidenced by increased fluorescence in transgenic lines indicating heightened activity of bone-forming cells and an enriched bone matrix. The molecular analysis conducted

on WT zebrafish after being exposed to these two probiotics revealed that they modulate key genes involved in skeletal development. The enhancements observed in osteoblast activity and bone matrix development underline the probiotic's potential as modulators of bone health and offers hope into understanding the interplay between the microbiome and bone physiology in the future. These results indicate a potential for developing targeted probiotic therapies aimed at improving bone health, highlighting the significant therapeutic potential of leveraging the microbiome in bone disease prevention and treatment. The comparative analysis of *Bacillus subtilis* and *Lactococcus lactis* in promoting bone health from our work presents a nuanced understanding of how different probiotics can distinctly influence bone physiology (Schepper et al., 2017). A striking finding was *Bacillus subtilis's* unique ability to mitigate the detrimental effects of BMP inhibitors on bone matrix formation. This suggests that *Bacillus subtilis* may interact with bone formation pathways in a manner that overrides BMP inhibition, whether it happens by upregulating alternative pathways or enhancing the bioavailability of essential nutrients for bone health will require further investigations.

Leveraging genetic and molecular insights from zebrafish models to develop targeted probiotic therapies represents a frontier in bone health research. Zebrafish models have elucidated the roles of specific genes and the potential of probiotics in modulating bone formation and health. Moreover, it would be captivating to understand how *Bacillus subtilis* counters BMP inhibitor effects at a molecular level as it could guide the formulation and usage of a specific probiotic strain or mix of strains that enhances bone matrix formation in humans.

Future research must delve deeper into the interactions between probiotics, genetic factors, and environmental influences on bone health. This includes understanding the molecular mechanisms by which probiotics influence bone health at the genetic level and how environmental factors such as diet and lifestyle interact with probiotics to affect bone health outcomes. Multi-omics approaches, including genomics, proteomics, and metabolomics, combined with advanced computational models, could unravel these complex interactions, paving the way for holistic approaches to understand bone health maintenance and disease (Graw et al., 2021). Thus, zebrafish models, together with the study of probiotics, hold substantial promise offering a unique window to conduct further explorations in this regard. The potential of probiotics as natural, non-invasive modulators of bone health is particularly exciting, and it is the need of the hour with the fast-aging population showing susceptibility to skeletal diseases like osteoporosis and osteoarthritis. In conclusion, the exploration of ECM protein coding genes *col10a1a*, *fbln1* and *efemp1*, their function in skeletal development, the study of zebrafish osteoblast specific transcriptome with the identification two subpopulations of osteoblasts and the beneficial effects of probiotics on bone health, through the lens of transgenic zebrafish reporter lines, marks a significant stride forward in skeletal research. It lays the groundwork for future studies aimed at translating these findings into mammalian models and ultimately into clinical applications, with the potential to revolutionize the prevention and treatment of bone diseases.

# V. BIBLIOGRAPHY

2015. OMIM Entry - * 602183 - NK3 HOMEOBOX 2; NKX3-2. Online Mendelian Inheritance In Man.
Abramyan, J., 2019. Hedgehog Signaling and Embryonic Craniofacial Disorders. J Dev Biol 7.
Aceto, J., Nourizadeh-Lillabadi, R., Bradamante, S., Maier, J., Alestrom, P., Van Loon, J., Muller, M., 2016a. Effects of microgravity simulation on zebrafish transcriptomes and bone physiology; exposure starting at 5 days post-fertilization. npj Microgravity 2, 16010.
Aceto, J., Nourizadeh-Lillabadi, R., Bradamante, S., Maier, J.A., Alestrom, P., van Loon, J.J., Muller, M., 2016b. Effects of microgravity simulation on zebrafish transcriptomes and bone physiology-exposure starting at 5 days post fertilization. NPJ Microgravity 2, 16010.
Aceto, J., Nourizadeh-Lillabadi, R., Maree, R., Dardenne, N., Jeanray, N., Wehenkel, L., Alestrom, P., van Loon, J.J., Muller, M., 2015a. Zebrafish bone and general physiology are differently affected by hormones or changes in gravity. PLoS One 10, e0126928.
Aceto, J., Nourizadeh-Lillabadi, R., Marée, R., Dardenne, N., Jeanray, N., Wehenkel, L., Aleström, P., van Loon, J.J.W.A., Muller, M., 2015b. Zebrafish Bone and General Physiology Are Differently Affected by Hormones or Changes in Gravity. PloS one 10, e0126928-e0126928.
Ackermann, G.E., Paw, B.H., 2003. Zebrafish: a genetic model for vertebrate organogenesis and human disorders. Front Biosci 8, d1227-1253.
Aghajanian, P., Mohan, S., 2018. The art of building bone: emerging role of chondrocyte-to-osteoblast transdifferentiation in endochondral ossification. Bone Res 6, 19.
Akhter MP, RR, R., 2021. High resolution imaging in bone tissue research-review. Bone 143.
Akiyama, H., 2008. Control of chondrogenesis by the transcription factor Sox9. Mod Rheumatol 18, 213-219.
Akkiraju, H., Nohe, A., 2015. Role of Chondrocytes in Cartilage Formation, Progression of Osteoarthritis and Cartilage Regeneration. J Dev Biol 3, 177-192.
Akter, F., Ibanez, J., 2016. Tissue Engineering Made Easy, Bone and cartilage tissue engineering Elsevier Inc, New York, pp. pp. 77-98.
Alberts, B., Johnson, A., Lewis, J., Raff, M., Roberts, K., Walter, P., 2002. Molecular Biology of the Cell, 4th edition ed. Garland Science, New York.
Albertson, R.C., Yelick, P.C., 2005. Roles for fgf8 signaling in left-right patterning of the visceral organs and craniofacial skeleton. Dev Biol 283, 310-321.
Albertson, R.C., Yelick, P.C., 2007. Fgf8 haploinsufficiency results in distinct craniofacial defects in adult zebrafish. Dev Biol 306, 505-515.
Albig, A.R., Neil, J.R., Schiemann, W.P., 2006. Fibulins 3 and 5 antagonize tumor angiogenesis in vivo. Cancer Res 66, 2621-2629.
Alcorta-Sevillano, N., Macías, I., Infante, A., Rodríguez, C.I., 2020. Deciphering the Relevance of Bone ECM Signaling. Cells 9.
Amano, K., Densmore, M., Nishimura, R., Lanske, B., 2014. Indian hedgehog signaling regulates transcription and expression of collagen type X via Runx2/Smads interactions. J Biol Chem 289, 24898-24910.
Apschner, A., Schulte-Merker, S., Witten, P.E., 2011. Not all bones are created equal - using zebrafish and other teleost species in osteogenesis research. Methods Cell Biol 105, 239-255.
Argraves, W.S., Dickerson, K., Burgess, W.H., Ruoslahti, E., 1989. Fibulin, a novel protein that interacts with the fibronectin receptor beta subunit cytoplasmic domain. Cell 58, 623-629.
Argraves, W.S., Greene, L.M., Cooley, M.A., Gallagher, W.M., 2003. Fibulins: physiological and disease perspectives. EMBO Rep 4, 1127-1131.
Arratia, G., Schultze, H.P., Casciotta, J., 2001. Vertebral column and associated elements in dipnoans and comparison with other fishes: development and homology. J Morphol 250, 101-172.

Asanbaeva, A., Masuda, K., Thonar, E.J., Klisch, S.M., Sah, R.L., 2007. Mechanisms of cartilage growth: modulation of balance between proteoglycan and collagen in vitro using chondroitinase ABC. Arthritis Rheum 56, 188-198.
Askary, A., Mork, L., Paul, S., He, X., Izuhara, A.K., Gopalakrishnan, S., Ichida, J.K., McMahon, A.P., Dabizljevic, S., Dale, R., Mariani, F.V., Crump, J.G., 2015. Iroquois Proteins Promote Skeletal Joint Formation by Maintaining Chondrocytes in an Immature State. Dev Cell 35, 358-365.
Askary, A., Smeeton, J., Paul, S., Schindler, S., Braasch, I., Ellis, N.A., Postlethwait, J., Miller, C.T., Crump, J.G., 2016. Ancient origin of lubricated joints in bony vertebrates. Elife 5.
Aspden, R.M., Saunders, F.R., 2019. Osteoarthritis as an organ disease: from the cradle to the grave. European cells & materials 37, 74-87.
Avaron, F., Hoffman, L., Guay, D., Akimenko, M.A., 2006. Characterization of two new zebrafish members of the hedgehog family: atypical expression of a zebrafish indian hedgehog gene in skeletal elements of both endochondral and dermal origins. Dev Dyn 235, 478-489.
Bae, W.J., Auh, Q.S., Lim, H.C., Kim, G.T., Kim, H.S., Kim, E.C., 2016. Sonic Hedgehog Promotes Cementoblastic Differentiation via Activating the BMP Pathways. Calcif Tissue Int 99, 396-407.
Baek, W.Y., de Crombrugghe, B., Kim, J.E., 2010. Postnatally induced inactivation of Osterix in osteoblasts results in the reduction of bone formation and maintenance. Bone 46, 920-928.
Bagnat, M., Gray, R.S., 2020. Development of a straight vertebrate body axis. Development 147.
Bai, L., Chang, H.M., Cheng, J.C., Chu, G., Leung, P.C.K., Yang, G., 2017. ALK2/ALK3-BMPR2/ACVR2A Mediate BMP2-Induced Downregulation of Pentraxin 3 Expression in Human Granulosa-Lutein Cells. Endocrinology 158, 3501-3511.
Balioğlu, M.B., Kargın, D., Albayrak, A., Atıcı, Y., 2018. The Treatment of Cleidocranial Dysostosis (Scheuthauer-Marie-Sainton Syndrome), a Rare Form of Skeletal Dysplasia, Accompanied by Spinal Deformities: A Review of the Literature and Two Case Reports. Case Rep Orthop 2018, 4635761.
Bartelt, A., Beil, F.T., Muller, B., Koehne, T., Yorgan, T.A., Heine, M., Yilmaz, T., Ruther, W., Heeren, J., Schinke, T., Niemeier, A., 2014. Hepatic lipase is expressed by osteoblasts and modulates bone remodeling in obesity. Bone 62, 90-98.
Bassett, D.I., Bryson-Richardson, R.J., Daggett, D.F., Gautier, P., Keenan, D.G., Currie, P.D., 2003. Dystrophin is required for the formation of stable muscle attachments in the zebrafish embryo. Development 130, 5851-5860.
Bassett, J.H., Williams, G.R., 2016. Role of Thyroid Hormones in Skeletal Development and Bone Maintenance. Endocr Rev 37, 135-187.
Bateman, J.F., Wilson, R., Freddi, S., Lamandé, S.R., Savarirayan, R., 2005. Mutations of COL10A1 in Schmid metaphyseal chondrodysplasia. Human mutation 25, 525-534.
Bay-Jensen, A.C., Liu, Q., Byrjalsen, I., Li, Y., Wang, J., Pedersen, C., Leeming, D.J., Dam, E.B., Zheng, Q., Qvist, P., Karsdal, M.A., 2011. Enzyme-linked immunosorbent assay (ELISAs) for metalloproteinase derived type II collagen neoepitope, CIIM--increased serum CIIM in subjects with severe radiographic osteoarthritis. Clin Biochem 44, 423-429.
Behera, J., Ison, J., Voor, M.J., Tyagi, N., 2021. Probiotics Stimulate Bone Formation in Obese Mice via Histone Methylations. Theranostics 11, 8605-8623.
Bennett, C.N., Ouyang, H., Ma, Y.L., Zeng, Q., Gerin, I., Sousa, K.M., Lane, T.F., Krishnan, V., Hankenson, K.D., MacDougald, O.A., 2007. Wnt10b increases postnatal bone formation by enhancing osteoblast differentiation. J Bone Miner Res 22, 1924-1932.

Bensimon-Brito, A., Cardeira, J., Cancela, M.L., Huysseune, A., Witten, P.E., 2012. Distinct patterns of notochord mineralization in zebrafish coincide with the localization of Osteocalcin isoform 1 during early vertebral centra formation. BMC Dev Biol 12, 28.
Bergen, D.J.M., Kague, E., Hammond, C.L., 2019. Zebrafish as an Emerging Model for Osteoporosis: A Primary Testing Platform for Screening New Osteo-Active Compounds. Front. Endocrinol 10, Article 6; doi.org/10.3389/fendo.2019.00006.
Bielajew, B.J., Hu, J.C., Athanasiou, K.A., 2020. Collagen: quantification, biomechanics, and role of minor subtypes in cartilage. Nat Rev Mater 5, 730-747.
Bird, N.C., Mabee, P.M., 2003. Developmental morphology of the axial skeleton of the zebrafish, Danio rerio (Ostariophysi: Cyprinidae). Dev Dyn 228, 337-357.
Birk, D.E., Fitch, J.M., Babiarz, J.P., Linsenmayer, T.F., 1988. Collagen type I and type V are present in the same fibril in the avian corneal stroma. J Cell Biol 106, 999-1008.
Birk, D.E., Trelstad, R.L., 1986. Extracellular compartments in tendon morphogenesis: collagen fibril, bundle, and macroaggregate formation. J Cell Biol 103, 231-240.
Bitgood, M.J., McMahon, A.P., 1995. Hedgehog and Bmp genes are coexpressed at many diverse sites of cell-cell interaction in the mouse embryo. Dev Biol 172, 126-138.
Bizzari, S., El-Bazzal, L., Nair, P., Younan, A., Stora, S., Mehawej, C., El-Hayek, S., Delague, V., Mégarbané, A., 2020. Recessive marfanoid syndrome with herniation associated with a homozygous mutation in Fibulin-3. Eur J Med Genet 63, 103869.
Black, D.M., Greenspan, S.L., Ensrud, K.E., Palermo, L., McGowan, J.A., Lang, T.F., Garnero, P., Bouxsein, M.L., Bilezikian, J.P., Rosen, C.J., Investigators, P.S., 2003. The effects of parathyroid hormone and alendronate alone or in combination in postmenopausal osteoporosis. N Engl J Med 349, 1207-1215.
Boerckel, J.D., Mason, D.E., McDermott, A.M., Alsberg, E., 2014. Microcomputed tomography: approaches and applications in bioengineering. Stem Cell Res Ther 5, 144.
Boergermann, J.H., Kopf, J., Yu, P.B., Knaus, P., 2010. Dorsomorphin and LDN-193189 inhibit BMP-mediated Smad, p38 and Akt signalling in C2C12 cells. Int J Biochem Cell Biol 42, 1802-1807.
Bonnans, C., Chou, J., Werb, Z., 2014. Remodelling the extracellular matrix in development and disease. Nat Rev Mol Cell Biol 15, 786-801.
Bosse, K., Betz, R.C., Lee, Y.A., Wienker, T.F., Reis, A., Kleen, H., Propping, P., Cichon, S., Nöthen, M.M., 2000. Localization of a gene for syndactyly type 1 to chromosome 2q34-q36. Am J Hum Genet 67, 492-497.
Boyan, B.D., Doroudi, M., Scott , K., Schwartz, Z., 2018. Chapter 24 - Cartilage in Vitamin D (Fourth Edition) , . Biochemistry, Physiology and Diagnostics Volume 1: Biochemistry, Physiology and Diagnostics, 405-417.
Breeland, G., Sinkler, M., Menezes, R., 2022. Embryology, Bone Ossification. StatPearls Publishing.
Britto, J.A., Evans, R.D., Hayward, R.D., Jones, B.M., 2001. From genotype to phenotype: the differential expression of FGF, FGFR, and TGFbeta genes characterizes human cranioskeletal development and reflects clinical presentation in FGFR syndromes. Plast Reconstr Surg 108, 2026-2039; discussion 2040-2026.
Brown, A.M., Fisher, S., Iovine, M.K., 2009. Osteoblast maturation occurs in overlapping proximal-distal compartments during fin regeneration in zebrafish. Dev Dyn 238, 2922-2928.
Bruderer, M., Richards, R.G., Alini, M., Stoddart, M.J., 2014. Role and regulation of RUNX2 in osteogenesis. Eur Cell Mater 28, 269-286.
Brunt, L.H., Begg, K., Kague, E., Cross, S., Hammond, C.L., 2017. Wnt signalling controls the response to mechanical loading during zebrafish joint development. Development 144, 2798-2809.

Brunt, L.H., Norton, J.L., Bright, J.A., Rayfield, E.J., Hammond, C.L., 2015. Finite element modelling predicts changes in joint shape and cell behaviour due to loss of muscle strain in jaw development. Journal of biomechanics 48, 3112-3122.
Buckwalter, J.A., Anderson, D.D., Brown, T.D., Tochigi, Y., Martin, J.A., 2013. The Roles of Mechanical Stresses in the Pathogenesis of Osteoarthritis: Implications for Treatment of Joint Injuries. Cartilage 4, 286-294.
Bush, J.O., Jiang, R., 2012. Palatogenesis: morphogenetic and molecular mechanisms of secondary palate development. Development 139, 231-243.
Busse, B., Galloway, J.L., Gray, R.S., Harris, M.P., Kwon, R.Y., 2020. Zebrafish: An Emerging Model for Orthopedic Research. J Orthop Res 38, 925-936.
Caetano da Silva, C., Ostertag, A., Raman, R., Muller, M., Cohen-Solal, M., Collet, C., 2023. wnt11f2 Zebrafish, an Animal Model for Development and New Insights in Bone Formation. Zebrafish 20, 1-9.
Caetano da Silva, C., Ricquebourg, M., Orcel, P., Fabre, S., Funck-Brentano, T., Cohen-Solal, M., Collet, C., 2021. More severe phenotype of early-onset osteoporosis associated with recessive form of LRP5 and combination with DKK1 or WNT3A. Mol Genet Genomic Med 9, e1681.
Camaj, P., Seeliger, H., Ischenko, I., Krebs, S., Blum, H., De Toni, E.N., Faktorova, D., Jauch, K.W., Bruns, C.J., 2009. EFEMP1 binds the EGF receptor and activates MAPK and Akt pathways in pancreatic carcinoma cells. Biol Chem 390, 1293-1302.
Carballo, G.B., Honorato, J.R., de Lopes, G.P.F., Spohr, T.C.L.S., 2018. A highlight on Sonic hedgehog pathway. Cell Commun Signal 16, 11.
Carroll, S.H., Macias Trevino, C., Li, E.B., Kawasaki, K., Myers, N., Hallett, S.A., Alhazmi, N., Cotney, J., Carstens, R.P., Liao, E.C., 2020. An Irf6- Esrp1/2 regulatory axis controls midface morphogenesis in vertebrates. Development 147.
Cashman, K., Ginty, F., 2003. Bone. Bone, pp. 1106-1112.
Chagin, A.S., Chu, T.L., 2023. The Origin and Fate of Chondrocytes: Cell Plasticity in Physiological Setting. Curr Osteoporos Rep 21, 815-824.
Chawla, S., Mainardi, A., Majumder, N., Dönges, L., Kumar, B., Occhetta, P., Martin, I., Egloff, C., Ghosh, S., Bandyopadhyay, A., Barbero, A., 2022. Chondrocyte Hypertrophy in Osteoarthritis: Mechanistic Studies and Models for the Identification of New Therapeutic Strategies. Cells 11.
Chen, D., Zhao, M., Harris, S.E., Mi, Z., 2004a. Signal transduction and biological functions of bone morphogenetic proteins. Front Biosci 9, 349-358.
Chen, D., Zhao, M., Mundy, G.R., 2004b. Bone morphogenetic proteins. Growth Factors 22, 233-241.
Chen, G., Deng, C., Li, Y.P., 2012. TGF-β and BMP signaling in osteoblast differentiation and bone formation. Int J Biol Sci 8, 272-288.
Chen, H., Tan, X.N., Hu, S., Liu, R.Q., Peng, L.H., Li, Y.M., Wu, P., 2021. Molecular Mechanisms of Chondrocyte Proliferation and Differentiation. Front Cell Dev Biol 9, 664168.
Chen, J.R., Lai, Y.H., Tsai, J.J., Hsiao, C.D., 2017. Live Fluorescent Staining Platform for Drug-Screening and Mechanism-Analysis in Zebrafish for Bone Mineralization. Molecules 22.
Chen, J.W., Galloway, J.L., 2014. The development of zebrafish tendon and ligament progenitors. Development 141, 2035-2045.
Chen, X., Wang, Z., Duan, N., Zhu, G., Schwarz, E.M., Xie, C., 2018. Osteoblast-osteoclast interactions. Connect Tissue Res 59, 99-107.
Chen, Z., Song, Z., Yang, J., Huang, J., Jiang, H., 2019. positively regulates. J Biosci 44.

Chiang, C., Litingtung, Y., Lee, E., Young, K.E., Corden, J.L., Westphal, H., Beachy, P.A., 1996. Cyclopia and defective axial patterning in mice lacking Sonic hedgehog gene function. Nature 383, 407-413.
Chiba, A., Watanabe-Takano, H., Terai, K., Fukui, H., Miyazaki, T., Uemura, M., Hashimoto, H., Hibi, M., Fukuhara, S., Mochizuki, N., 2017. Osteocrin, a peptide secreted from the heart and other tissues, contributes to cranial osteogenesis and chondrogenesis in zebrafish. Development 144, 334-344.
Choi, K.Y., Kim, H.J., Lee, M.H., Kwon, T.G., Nah, H.D., Furuichi, T., Komori, T., Nam, S.H., Kim, Y.J., Ryoo, H.M., 2005. Runx2 regulates FGF2-induced Bmp2 expression during cranial bone development. Dev Dyn 233, 115-121.
Christakos, S., Dhawan, P., Porta, A., Mady, J.M., Seth, T., 2011. Vitamin D and intestinal calcium absorption. Mol Cell Endocrinol 347, 25-29.
Chu, M.L., Tsuda, T., 2004. Fibulins in development and heritable disease. Birth Defects Res C Embryo Today 72, 25-36.
Ciurea, A.V., Toader, C., 2009. Genetics of craniosynostosis: review of the literature. J Med Life 2, 5-17.
Clarke, B., 2008. Normal bone anatomy and physiology. Clin J Am Soc Nephrol 3 Suppl 3, S131-139.
Close, R., Toro, S., Martial, J.A., Muller, M., 2002. Expression of the zinc finger Egr1 gene during zebrafish embryonic development. Mech Dev 118, 269-272.
Cole, A.G., Hall, B.K., 2004. Cartilage is a metazoan tissue; integrating data from nonvertebrate sources. Acta Zoologica 85, 69-80.
Cooley, M.A., Harikrishnan, K., Oppel, J.A., Miler, S.F., Barth, J.L., Haycraft, C.J., Reddy, S.V., Scott Argraves, W., 2014. Fibulin-1 is required for bone formation and Bmp-2-mediated induction of Osterix. Bone 69, 30-38.
Cooley, M.A., Kern, C.B., Fresco, V.M., Wessels, A., Thompson, R.P., McQuinn, T.C., Twal, W.O., Mjaatvedt, C.H., Drake, C.J., Argraves, W.S., 2008. Fibulin-1 is required for morphogenesis of neural crest-derived structures. Dev Biol 319, 336-345.
Cooper, G.M., 2000. Cells As Experimental Models, The Cell: A Molecular Approach., 2nd ed. Sinauer Associates.
Costa, J.M., Sartori, M.M.P., Nascimento, N.F.D., Kadri, S.M., Ribolla, P.E.M., Pinhal, D., Pezzato, L.E., 2018. Inadequate Dietary Phosphorus Levels Cause Skeletal Anomalies and Alter Osteocalcin Gene Expression in Zebrafish. Int J Mol Sci 19.
Cotti, S., Huysseune, A., Koppe, W., Rücklin, M., Marone, F., Wölfel, E.M., Fiedler, I.A.K., Busse, B., Forlino, A., Witten, P.E., 2020. More Bone with Less Minerals? The Effects of Dietary Phosphorus on the Post-Cranial Skeleton in Zebrafish. Int J Mol Sci 21.
Cotti, S., Huysseune, A., Larionova, D., Koppe, W., Forlino, A., Witten, P.E., 2022. Compression Fractures and Partial Phenotype Rescue With a Low Phosphorus Diet in the Chihuahua Zebrafish Osteogenesis Imperfecta Model. Front Endocrinol (Lausanne) 13, 851879.
Cubbage, C.C., Mabee, P.M., 1996. Development of the cranium and paired fins in the zebrafish Danio rerio (Ostariophysi, Cyprinidae). J Morphol 229, 121-160.
Cui, Y., Niziolek, P.J., MacDonald, B.T., Zylstra, C.R., Alenina, N., Robinson, D.R., Zhong, Z., Matthes, S., Jacobsen, C.M., Conlon, R.A., Brommage, R., Liu, Q., Mseeh, F., Powell, D.R., Yang, Q.M., Zambrowicz, B., Gerrits, H., Gossen, J.A., He, X., Bader, M., Williams, B.O., Warman, M.L., Robling, A.G., 2011. Lrp5 functions in bone to regulate bone mass. Nat Med 17, 684-691.
Culbert, A.L., Chakkalakal, S.A., Theosmy, E.G., Brennan, T.A., Kaplan, F.S., Shore, E.M., 2014. Alk2 regulates early chondrogenic fate in fibrodysplasia ossificans progressiva heterotopic endochondral ossification. Stem Cells 32, 1289-1300.

Dailey, L., Ambrosetti, D., Mansukhani, A., Basilico, C., 2005. Mechanisms underlying differential responses to FGF signaling. Cytokine Growth Factor Rev 16, 233-247.
Dalcq, J., Pasque, V., Ghaye, A., Larbuisson, A., Motte, P., Martial, J.A., Muller, M., 2012. RUNX3, EGR1 and SOX9B form a regulatory cascade required to modulate BMP-signaling during cranial cartilage development in zebrafish. PLoS One 7, e50140.
Dale, R.M., Topczewski, J., 2011. Identification of an evolutionarily conserved regulatory element of the zebrafish col2a1a gene. Dev Biol 357, 518-531.
Dallas, S.L., Prideaux, M., Bonewald, L.F., 2013. The osteocyte: an endocrine cell ... and more. Endocr Rev 34, 658-690.
Day, T.F., Guo, X., Garrett-Beal, L., Yang, Y., 2005. Wnt/beta-catenin signaling in mesenchymal progenitors controls osteoblast and chondrocyte differentiation during vertebrate skeletogenesis. Dev Cell 8, 739-750.
de Baat, P., Heijboer, M.P., de Baat, C., 2005. [Development, physiology, and cell activity of bone]. Ned Tijdschr Tandheelkd 112, 258-263.
de Vega, S., Iwamoto, T., Yamada, Y., 2009. Fibulins: multiple roles in matrix structures and tissue functions. Cell Mol Life Sci 66, 1890-1902.
Debeer, P., Schoenmakers, E.F., Twal, W.O., Argraves, W.S., De Smet, L., Fryns, J.P., Van De Ven, W.J., 2002. The fibulin-1 gene (FBLN1) is disrupted in a t(12;22) associated with a complex type of synpolydactyly. J Med Genet 39, 98-104.
Debiais-Thibaud, M., Simion, P., Ventéo, S., Muñoz, D., Marcellini, S., Mazan, S., Haitina, T., 2019. Skeletal Mineralization in Association with Type X Collagen Expression Is an Ancestral Feature for Jawed Vertebrates. Mol Biol Evol 36, 2265-2276.
Degnin, C.R., Laederich, M.B., Horton, W.A., 2010. FGFs in endochondral skeletal development. J Cell Biochem 110, 1046-1057.
DeLaurier, A., Eames, B.F., Blanco-Sanchez, B., Peng, G., He, X., Swartz, M.E., Ullmann, B., Westerfield, M., Kimmel, C.B., 2010a. Zebrafish sp7:EGFP: a transgenic for studying otic vesicle formation, skeletogenesis, and bone regeneration. Genesis 48, 505-511.
DeLaurier, A., Eames, B.F., Blanco-Sánchez, B., Peng, G., He, X., Swartz, M.E., Ullmann, B., Westerfield, M., Kimmel, C.B., 2010b. Zebrafish sp7:EGFP: a transgenic for studying otic vesicle formation, skeletogenesis, and bone regeneration. Genesis 48, 505-511.
Dennis, S.C., Berkland, C.J., Bonewald, L.F., Detamore, M.S., 2015. Endochondral ossification for enhancing bone regeneration: converging native extracellular matrix biomaterials and developmental engineering in vivo. Tissue Eng Part B Rev 21, 247-266.
Depew, M.J., Lufkin, T., Rubenstein, J.L., 2002. Specification of jaw subdivisions by Dlx genes. Science 298, 381-385.
Derynck, R., Zhang, Y.E., 2003. Smad-dependent and Smad-independent pathways in TGF-beta family signalling. Nature 425, 577-584.
Deshmukh, S.N., Dive, A.M., Moharil, R., Munde, P., 2016. Enigmatic insight into collagen. J Oral Maxillofac Pathol 20, 276-283.
Detsch, R., Boccaccini, A.R., 2015. The role of osteoclasts in bone tissue engineering. J Tissue Eng Regen Med 9, 1133-1149.
Dietrich, K., Fiedler, I.A., Kurzyukova, A., Lopez-Delgado, A.C., McGowan, L.M., Geurtzen, K., Hammond, C.L., Busse, B., Knopf, F., 2021a. Skeletal Biology and Disease Modeling in Zebrafish. J Bone Miner Res 36, 436-458.
Dietrich, K., Fiedler, I.A., Kurzyukova, A., López-Delgado, A.C., McGowan, L.M., Geurtzen, K., Hammond, C.L., Busse, B., Knopf, F., 2021b. Skeletal Biology and Disease Modeling in Zebrafish. J Bone Miner Res 36, 436-458.
Dooley, K., Zon, L.I., 2000. Zebrafish: a model system for the study of human disease. Curr Opin Genet Dev 10, 252-256.

Doudna, J.A., Charpentier, E., 2014. Genome editing. The new frontier of genome engineering with CRISPR-Cas9. Science 346, 1258096.
Doyle, A.J., Doyle, J.J., Bessling, S.L., Maragh, S., Lindsay, M.E., Schepers, D., Gillis, E., Mortier, G., Homfray, T., Sauls, K., Norris, R.A., Huso, N.D., Leahy, D., Mohr, D.W., Caulfield, M.J., Scott, A.F., Destrée, A., Hennekam, R.C., Arn, P.H., Curry, C.J., Van Laer, L., McCallion, A.S., Loeys, B.L., Dietz, H.C., 2012. Mutations in the TGF-β repressor SKI cause Shprintzen-Goldberg syndrome with aortic aneurysm. Nat Genet 44, 1249-1254.
Drissi, H., Zuscik, M., Rosier, R., O'Keefe, R., 2005. Transcriptional regulation of chondrocyte maturation: potential involvement of transcription factors in OA pathogenesis. Mol Aspects Med 26, 169-179.
Driver, S.G.W., Jackson, M.R., Richter, K., Tomlinson, P., Brockway, B., Halliday, B.J., Markie, D.M., Robertson, S.P., Wade, E.M., 2020. Biallelic variants in EFEMP1 in a man with a pronounced connective tissue phenotype. Eur J Hum Genet 28, 445-452.
Drábiková, L., Fjelldal, P.G., Clercq, A.D., Yousaf, M.N., Morken, T., McGurk, C., Witten, P.E., 2021. Vertebral column adaptations in juvenile Atlantic salmon Salmo salar, L. as a response to dietary phosphorus. Aquaculture 541, 736776.
Du, S.J., Frenkel, V., Kindschi, G., Zohar, Y., 2001. Visualizing normal and defective bone development in zebrafish embryos using the fluorescent chromophore calcein. Dev Biol 238, 239-246.
Dy, P., Wang, W., Bhattaram, P., Wang, Q., Wang, L., Ballock, R.T., Lefebvre, V., 2012. Sox9 directs hypertrophic maturation and blocks osteoblast differentiation of growth plate chondrocytes. Dev Cell 22, 597-609.
Eames, B.F., Amores, A., Yan, Y.L., Postlethwait, J.H., 2012. Evolution of the osteoblast: skeletogenesis in gar and zebrafish. BMC Evol Biol 12, 27.
Eames, B.F., DeLaurier, A., Ullmann, B., Huycke, T.R., Nichols, J.T., Dowd, J., McFadden, M., Sasaki, M.M., Kimmel, C.B., 2013. FishFace: interactive atlas of zebrafish craniofacial development at cellular resolution. BMC Developmental Biology 13, 23.
Eberhart, J.K., He, X., Swartz, M.E., Yan, Y.L., Song, H., Boling, T.C., Kunerth, A.K., Walker, M.B., Kimmel, C.B., Postlethwait, J.H., 2008. MicroRNA Mirn140 modulates Pdgf signaling during palatogenesis. Nat Genet 40, 290-298.
Eerola, I., Salminen, H., Lammi, P., Lammi, M., von der Mark, K., Vuorio, E., Säämänen, A.M., 1998. Type X collagen, a natural component of mouse articular cartilage: association with growth, aging, and osteoarthritis. Arthritis Rheum 41, 1287-1295.
Ehlermann, J., Weber, S., Pfisterer, P., Schorle, H., 2003. Cloning, expression and characterization of the murine Efemp1, a gene mutated in Doyne-Honeycomb retinal dystrophy. Gene Expr Patterns 3, 441-447.
Engvall, E., Hessle, H., Klier, G., 1986. Molecular assembly, secretion, and matrix deposition of type VI collagen. J Cell Biol 102, 703-710.
Ewels, P.A., Peltzer, A., Fillinger, S., Patel, H., Alneberg, J., Wilm, A., Garcia, M.U., Di Tommaso, P., Nahnsen, S., 2020. The nf-core framework for community-curated bioinformatics pipelines. Nat Biotechnol 38, 276-278.
Exposito, J.Y., Valcourt, U., Cluzel, C., Lethias, C., 2010. The fibrillar collagen family. Int J Mol Sci 11, 407-426.
Eyre, D.R., Weis, M.A., 2013. Bone collagen: new clues to its mineralization mechanism from recessive osteogenesis imperfecta. Calcif Tissue Int 93, 338-347.
Fan, C.M., Porter, J.A., Chiang, C., Chang, D.T., Beachy, P.A., Tessier-Lavigne, M., 1995. Long-range sclerotome induction by sonic hedgehog: direct role of the amino-terminal cleavage product and modulation by the cyclic AMP signaling pathway. Cell 81, 457-465.

Feitosa, N.M., Zhang, J., Carney, T.J., Metzger, M., Korzh, V., Bloch, W., Hammerschmidt, M., 2012. Hemicentin 2 and Fibulin 1 are required for epidermal-dermal junction formation and fin mesenchymal cell migration during zebrafish development. Dev Biol 369, 235-248.
Felson, D.T., Gale, D.R., Elon Gale, M., Niu, J., Hunter, D.J., Goggins, J., Lavalley, M.P., 2005. Osteophytes and progression of knee osteoarthritis. Rheumatology (Oxford) 44, 100-104.
Feng, X.H., Derynck, R., 2005. Specificity and versatility in tgf-beta signaling through Smads. Annu Rev Cell Dev Biol 21, 659-693.
Fiaz, A.W., Leon-Kloosterziel, K.M., Gort, G., Schulte-Merker, S., van Leeuwen, J.L., Kranenbarg, S., 2012a. Swim-training changes the spatio-temporal dynamics of skeletogenesis in zebrafish larvae (Danio rerio). PLoS One 7, e34072.
Fiaz, A.W., Léon-Kloosterziel, K.M., Gort, G., Schulte-Merker, S., van Leeuwen, J.L., Kranenbarg, S., 2012b. Swim-training changes the spatio-temporal dynamics of skeletogenesis in zebrafish larvae (Danio rerio). PLoS One 7, e34072.
Fiedler, I.A.K., Schmidt, F.N., Wölfel, E.M., Plumeyer, C., Milovanovic, P., Gioia, R., Tonelli, F., Bale, H.A., Jähn, K., Besio, R., Forlino, A., Busse, B., 2018. Severely Impaired Bone Material Quality in Chihuahua Zebrafish Resembles Classical Dominant Human Osteogenesis Imperfecta. J Bone Miner Res 33, 1489-1499.
Fisher, S., Jagadeeswaran, P., Halpern, M.E., 2003. Radiographic analysis of zebrafish skeletal defects. Dev Biol 264, 64-76.
Fleischmajer, R., MacDonald, E.D., Perlish, J.S., Burgeson, R.E., Fisher, L.W., 1990. Dermal collagen fibrils are hybrids of type I and type III collagen molecules. J Struct Biol 105, 162-169.
Fleming, A., Keynes, R., Tannahill, D., 2004. A central role for the notochord in vertebral patterning. Development 131, 873-880.
Florencio-Silva, R., Sasso, G.R., Sasso-Cerri, E., Simões, M.J., Cerri, P.S., 2015. Biology of Bone Tissue: Structure, Function, and Factors That Influence Bone Cells. Biomed Res Int 2015, 421746.
Flores, M.V., Lam, E.Y., Crosier, P., Crosier, K., 2006. A hierarchy of Runx transcription factors modulate the onset of chondrogenesis in craniofacial endochondral bones in zebrafish. Dev Dyn 235, 3166-3176.
Flores, M.V., Tsang, V.W., Hu, W., Kalev-Zylinska, M., Postlethwait, J., Crosier, P., Crosier, K., Fisher, S., 2004. Duplicate zebrafish runx2 orthologues are expressed in developing skeletal elements. Gene Expr Patterns 4, 573-581.
Florisson, J.M., Verkerk, A.J., Huigh, D., Hoogeboom, A.J., Swagemakers, S., Kremer, A., Heijsman, D., Lequin, M.H., Mathijssen, I.M., van der Spek, P.J., 2013. Boston type craniosynostosis: report of a second mutation in MSX2. Am J Med Genet A 161A, 2626-2633.
Flowers, P.P.E., Cleveland, R.J., Schwartz, T.A., Nelson, A.E., Kraus, V.B., Hillstrom, H.J., Goode, A.P., Hannan, M.T., Renner, J.B., Jordan, J.M., Golightly, Y.M., 2018. Association between general joint hypermobility and knee, hip, and lumbar spine osteoarthritis by race: a cross-sectional study. Arthritis Res Ther 20, 76.
Fontanil, T., Mohamedi, Y., Cobo, T., Cal, S., Obaya, Á., 2019. Novel Associations Within the Tumor Microenvironment: Fibulins Meet ADAMTSs. Front Oncol 9, 796.
Forghani, I., Lang, S.H., Rodier, M.J., Bivona, S.A., Morales, A.A., Zuchner, S., Bademci, G., Tekin, M., Network, U.D., 2024. EFEMP1 haploinsufficiency causes a Marfan-like hereditary connective tissue disorder. Am J Med Genet A, e63556.
Fortier, L.A., Barker, J.U., Strauss, E.J., McCarrel, T.M., Cole, B.J., 2011. The role of growth factors in cartilage repair. Clin Orthop Relat Res 469, 2706-2715.

Frantz, C., Stewart, K.M., Weaver, V.M., 2010. The extracellular matrix at a glance. J Cell Sci 123, 4195-4200.
Franz-Odendaal, T.A., Hall, B.K., Witten, P.E., 2006. Buried alive: how osteoblasts become osteocytes. Dev Dyn 235, 176-190.
Fratzl, P., Weinkamer, R., 2007. Nature's hierarchical materials. Progress in Materials Science 52, 1263-1334.
Freitas, R., Zhang, G., Cohn, M.J., 2006. Evidence that mechanisms of fin development evolved in the midline of early vertebrates. Nature 442, 1033-1037.
Fresco, V.M., Kern, C.B., Mohammadi, M., Twal, W.O., 2016. Fibulin-1 Binds to Fibroblast Growth Factor 8 with High Affinity: EFFECTS ON EMBRYO SURVIVAL. J Biol Chem 291, 18730-18739.
Fu, L., Garland, D., Yang, Z., Shukla, D., Rajendran, A., Pearson, E., Stone, E.M., Zhang, K., Pierce, E.A., 2007. The R345W mutation in EFEMP1 is pathogenic and causes AMD-like deposits in mice. Hum Mol Genet 16, 2411-2422.
Furumatsu, T., Ozaki, T., Asahara, H., 2009. Smad3 activates the Sox9-dependent transcription on chromatin. Int J Biochem Cell Biol 41, 1198-1204.
Galbusera, F., Bassani, T., 2019. The Spine: A Strong, Stable, and Flexible Structure with Biomimetics Potential. Biomimetics (Basel) 4.
Gavaia, P.J., Sarasquete, C., Cancela, M.L., 2000. Detection of mineralized structures in early stages of development of marine Teleostei using a modified alcian blue-alizarin red double staining technique for bone and cartilage. Biotech Histochem 75, 79-84.
Gavaia, P.J., Simes, D.C., Ortiz-Delgado, J.B., Viegas, C.S., Pinto, J.P., Kelsh, R.N., Sarasquete, M.C., Cancela, M.L., 2006. Osteocalcin and matrix Gla protein in zebrafish (Danio rerio) and Senegal sole (Solea senegalensis): comparative gene and protein expression during larval development through adulthood. Gene Expr Patterns 6, 637-652.
Gellhorn, A.C., Katz, J.N., Suri, P., 2013. Osteoarthritis of the spine: the facet joints. Nat Rev Rheumatol 9, 216-224.
Gelse, K., Pöschl, E., Aigner, T., 2003. Collagens--structure, function, and biosynthesis. Adv Drug Deliv Rev 55, 1531-1546.
Gene Ontology Consortium, 2021. The Gene Ontology resource: enriching a GOld mine. Nucleic Acids Res 49, D325-D334.
Gentili, C., Cancedda, R., 2009. Cartilage and bone extracellular matrix. Curr Pharm Des 15, 1334-1348.
Gibert, Y., Gajewski, A., Meyer, A., Begemann, G., 2006. Induction and prepatterning of the zebrafish pectoral fin bud requires axial retinoic acid signaling. Development 133, 2649-2659.
Giltay, R., Timpl, R., Kostka, G., 1999. Sequence, recombinant expression and tissue localization of two novel extracellular matrix proteins, fibulin-3 and fibulin-4. Matrix Biol 18, 469-480.
Girkontaite, I., Frischholz, S., Lammi, P., Wagner, K., Swoboda, B., Aigner, T., Von der Mark, K., 1996. Immunolocalization of type X collagen in normal fetal and adult osteoarthritic cartilage with monoclonal antibodies. Matrix Biol 15, 231-238.
Gistelinck, C., Gioia, R., Gagliardi, A., Tonelli, F., Marchese, L., Bianchi, L., Landi, C., Bini, L., Huysseune, A., Witten, P.E., Staes, A., Gevaert, K., De Rocker, N., Menten, B., Malfait, F., Leikin, S., Carra, S., Tenni, R., Rossi, A., De Paepe, A., Coucke, P., Willaert, A., Forlino, A., 2016. Zebrafish Collagen Type I: Molecular and Biochemical Characterization of the Major Structural Protein in Bone and Skin. Sci Rep 6, 21540.
Goldring, M.B., 2012a. Chondrogenesis, chondrocyte differentiation, and articular cartilage metabolism in health and osteoarthritis. Ther Adv Musculoskelet Dis 4, 269-285.
Goldring, M.B., Goldring, S.R., 2010. Articular cartilage and subchondral bone in the pathogenesis of osteoarthritis. Ann N Y Acad Sci 1192, 230-237.

Goldring, M.B., Otero, M., Tsuchimochi, K., Ijiri, K., Li, Y., 2008. Defining the roles of inflammatory and anabolic cytokines in cartilage metabolism. Ann Rheum Dis 67 Suppl 3, iii75-82.
Goldring, M.B., Tsuchimochi, K., Ijiri, K., 2006. The control of chondrogenesis. J Cell Biochem 97, 33-44.
Goldring, S.R., 2009. Role of bone in osteoarthritis pathogenesis. Med Clin North Am 93, 25-35, xv.
Goldring, S.R., 2012b. Alterations in periarticular bone and cross talk between subchondral bone and articular cartilage in osteoarthritis. Ther Adv Musculoskelet Dis 4, 249-258.
Gong, Y., Krakow, D., Marcelino, J., Wilkin, D., Chitayat, D., Babul-Hirji, R., Hudgins, L., Cremers, C.W., Cremers, F.P., Brunner, H.G., Reinker, K., Rimoin, D.L., Cohn, D.H., Goodman, F.R., Reardon, W., Patton, M., Francomano, C.A., Warman, M.L., 1999. Heterozygous mutations in the gene encoding noggin affect human joint morphogenesis. Nat Genet 21, 302-304.
Gong, Y., Slee, R.B., Fukai, N., Rawadi, G., Roman-Roman, S., Reginato, A.M., Wang, H., Cundy, T., Glorieux, F.H., Lev, D., Zacharin, M., Oexle, K., Marcelino, J., Suwairi, W., Heeger, S., Sabatakos, G., Apte, S., Adkins, W.N., Allgrove, J., Arslan-Kirchner, M., Batch, J.A., Beighton, P., Black, G.C., Boles, R.G., Boon, L.M., Borrone, C., Brunner, H.G., Carle, G.F., Dallapiccola, B., De Paepe, A., Floege, B., Halfhide, M.L., Hall, B., Hennekam, R.C., Hirose, T., Jans, A., Jüppner, H., Kim, C.A., Keppler-Noreuil, K., Kohlschuetter, A., LaCombe, D., Lambert, M., Lemyre, E., Letteboer, T., Peltonen, L., Ramesar, R.S., Romanengo, M., Somer, H., Steichen-Gersdorf, E., Steinmann, B., Sullivan, B., Superti-Furga, A., Swoboda, W., van den Boogaard, M.J., Van Hul, W., Vikkula, M., Votruba, M., Zabel, B., Garcia, T., Baron, R., Olsen, B.R., Warman, M.L., Group, O.-P.S.C., 2001. LDL receptor-related protein 5 (LRP5) affects bone accrual and eye development. Cell 107, 513-523.
Gonzalez, A.M., Hill, D.J., Logan, A., Maher, P.A., Baird, A., 1996. Distribution of fibroblast growth factor (FGF)-2 and FGF receptor-1 messenger RNA expression and protein presence in the mid-trimester human fetus. Pediatr Res 39, 375-385.
Goode, A.P., Carey, T.S., Jordan, J.M., 2013. Low back pain and lumbar spine osteoarthritis: how are they related? Curr Rheumatol Rep 15, 305.
Goode, A.P., Cleveland, R.J., Schwartz, T.A., Nelson, A.E., Kraus, V.B., Hillstrom, H.J., Hannan, M.T., Flowers, P., Renner, J.B., Jordan, J.M., Golightly, Y.M., 2019. Relationship of joint hypermobility with low Back pain and lumbar spine osteoarthritis. BMC Musculoskelet Disord 20, 158.
Goode, A.P., Nelson, A.E., Kraus, V.B., Renner, J.B., Jordan, J.M., 2017. Biomarkers reflect differences in osteoarthritis phenotypes of the lumbar spine: the Johnston County Osteoarthritis Project. Osteoarthritis Cartilage 25, 1672-1679.
Goto, T., Matsui, Y., Fernandes, R.J., Hanson, D.A., Kubo, T., Yukata, K., Michigami, T., Komori, T., Fujita, T., Yang, L., Eyre, D.R., Yasui, N., 2006. Sp1 family of transcription factors regulates the human alpha2 (XI) collagen gene (COL11A2) in Saos-2 osteoblastic cells. J Bone Miner Res 21, 661-673.
Grafe, I., Alexander, S., Peterson, J.R., Snider, T.N., Levi, B., Lee, B., Mishina, Y., 2018. TGF-β Family Signaling in Mesenchymal Differentiation. Cold Spring Harb Perspect Biol 10.
Grandel, H., Draper, B.W., Schulte-Merker, S., 2000. dackel acts in the ectoderm of the zebrafish pectoral fin bud to maintain AER signaling. Development 127, 4169-4178.
Graw, S., Chappell, K., Washam, C.L., Gies, A., Bird, J., Robeson, M.S., Byrum, S.D., 2021. Multi-omics data integration considerations and study design for biological systems and disease. Mol Omics 17, 170-185.

Gray, R.S., Wilm, T.P., Smith, J., Bagnat, M., Dale, R.M., Topczewski, J., Johnson, S.L., Solnica-Krezel, L., 2014. Loss of col8a1a function during zebrafish embryogenesis results in congenital vertebral malformations. Developmental Biology 386, 72-85.
Grotmol, S., Kryvi, H., Nordvik, K., Totland, G.K., 2003. Notochord segmentation may lay down the pathway for the development of the vertebral bodies in the Atlantic salmon. Anat Embryol (Berl) 207, 263-272.
Grotmol, S., Nordvik, K., Kryvi, H., Totland, G.K., 2005. A segmental pattern of alkaline phosphatase activity within the notochord coincides with the initial formation of the vertebral bodies. J Anat 206, 427-436.
Grundberg, E., Brandstrom, H., Lam, K.C., Gurd, S., Ge, B., Harmsen, E., Kindmark, A., Ljunggren, O., Mallmin, H., Nilsson, O., Pastinen, T., 2008. Systematic assessment of the human osteoblast transcriptome in resting and induced primary cells. Physiol Genomics 33, 301-311.
Gudmann, N.S., Karsdal, M.A., 2016. Chapter 10 - Type X Collagen. In: Biochemistry of Collagens, Laminins and Elastin: Structure, Function and Biomarkers. Eds MA Karsdal, Academic Press, 73-76.
Gudmann, N.S., Karsdal, M.A., 2016. Chapter 10 - Type X Collagen. Biochemistry of Collagens, Laminins and Elastin Structure, Function and Biomarkers, Pages 73-76.
Guntur, A.R., Rosen, C.J., 2013. IGF-1 regulation of key signaling pathways in bone. Bonekey Rep 2, 437.
Guo, L., Ikegawa, S., Shukunami, C., 2018. Emergence of Zebrafish as a Model System for Understanding Human Scoliosis. Zebrafish, Medaka, and Other Small Fishes: New Model Animals in Biology, Medicine, and Beyond, 217-234.
Gupta, T., Mullins, M.C., 2010. Dissection of organs from the adult zebrafish. J Vis Exp.
Guss, J.D., Horsfield, M.W., Fontenele, F.F., Sandoval, T.N., Luna, M., Apoorva, F., Lima, S.F., Bicalho, R.C., Singh, A., Ley, R.E., van der Meulen, M.C., Goldring, S.R., Hernandez, C.J., 2017. Alterations to the Gut Microbiome Impair Bone Strength and Tissue Material Properties. J Bone Miner Res 32, 1343-1353.
Haines, R.W., 1942. Eudiarthrodial joints in fishes. J Anat 77, 12-19.
Hall, B.K., 2015. Bones and Cartilage Developmental and Evolutionary Skeletal Biology. Developmental and Evolutionary Skeletal Biology.
Hammond, C.L., Moro, E., 2012. Using transgenic reporters to visualize bone and cartilage signaling during development in vivo. Front Endocrinol (Lausanne) 3, 91.
Hammond, C.L., Schulte-Merker, S., 2009. Two populations of endochondral osteoblasts with differential sensitivity to Hedgehog signalling. Development 136, 3991-4000.
Hartmann, C., Tabin, C.J., 2000. Dual roles of Wnt signaling during chondrogenesis in the chicken limb. Development 127, 3141-3159.
Haseeb, A., Kc, R., Angelozzi, M., de Charleroy, C., Rux, D., Tower, R.J., Yao, L., Pellegrino da Silva, R., Pacifici, M., Qin, L., Lefebvre, V., 2021. SOX9 keeps growth plates and articular cartilage healthy by inhibiting chondrocyte dedifferentiation/osteoblastic redifferentiation. Proceedings of the National Academy of Sciences 118, e2019152118.
Hasegawa, A., Yonezawa, T., Taniguchi, N., Otabe, K., Akasaki, Y., Matsukawa, T., Saito, M., Neo, M., Marmorstein, L.Y., Lotz, M.K., 2017. Role of Fibulin 3 in Aging-Related Joint Changes and Osteoarthritis Pathogenesis in Human and Mouse Knee Cartilage. Arthritis Rheumatol 69, 576-585.
Hashimoto, S., Creighton-Achermann, L., Takahashi, K., Amiel, D., Coutts, R.D., Lotz, M., 2002. Development and regulation of osteophyte formation during experimental osteoarthritis. Osteoarthritis Cartilage 10, 180-187.

Hayes, A.J., Reynolds, S., Nowell, M.A., Meakin, L.B., Habicher, J., Ledin, J., Bashford, A., Caterson, B., Hammond, C.L., 2013. Spinal deformity in aged zebrafish is accompanied by degenerative changes to their vertebrae that resemble osteoarthritis. PLoS One 8, e75787.
He, Y., Siebuhr, A.S., Brandt-Hansen, N.U., Wang, J., Su, D., Zheng, Q., Simonsen, O., Petersen, K.K., Arendt-Nielsen, L., Eskehave, T., Hoeck, H.C., Karsdal, M.A., Bay-Jensen, A.C., 2014. Type X collagen levels are elevated in serum from human osteoarthritis patients and associated with biomarkers of cartilage degradation and inflammation. BMC Musculoskelet Disord 15, 309.
Hellemans, J., Coucke, P.J., Giedion, A., De Paepe, A., Kramer, P., Beemer, F., Mortier, G.R., 2003. Homozygous mutations in IHH cause acrocapitofemoral dysplasia, an autosomal recessive disorder with cone-shaped epiphyses in hands and hips. Am J Hum Genet 72, 1040-1046.
Henke, E., Nandigama, R., Ergün, S., 2019. Extracellular Matrix in the Tumor Microenvironment and Its Impact on Cancer Therapy. Front Mol Biosci 6, 160.
Henrotin, Y., 2022. Osteoarthritis in year 2021: biochemical markers. Osteoarthritis Cartilage 30, 237-248.
Henrotin, Y., Gharbi, M., Mazzucchelli, G., Dubuc, J.E., De Pauw, E., Deberg, M., 2012. Fibulin 3 peptides Fib3-1 and Fib3-2 are potential biomarkers of osteoarthritis. Arthritis Rheum 64, 2260-2267.
Hill, T.P., Später, D., Taketo, M.M., Birchmeier, W., Hartmann, C., 2005. Canonical Wnt/beta-catenin signaling prevents osteoblasts from differentiating into chondrocytes. Dev Cell 8, 727-738.
Hirasawa, T., Kuratani, S., 2015. Evolution of the vertebrate skeleton: morphology, embryology, and development. Zoological Lett 1, 2.
Holmes, G., O'Rourke, C., Motch Perrine, S.M., Lu, N., van Bakel, H., Richtsmeier, J.T., Jabs, E.W., 2018. Midface and upper airway dysgenesis in FGFR2-related craniosynostosis involves multiple tissue-specific and cell cycle effects. Development 145.
Holzschuh, J., Wada, N., Wada, C., Schaffer, A., Javidan, Y., Tallafuss, A., Bally-Cuif, L., Schilling, T.F., 2005. Requirements for endoderm and BMP signaling in sensory neurogenesis in zebrafish. Development 132, 3731-3742.
Howe, K., Clark, M.D., Torroja, C.F., et al., 2013. The zebrafish reference genome sequence and its relationship to the human genome. Nature 496, 498-503.
Hsu, W.B., Hsu, W.H., Hung, J.S., Shen, W.J., Hsu, R.W., 2018. Transcriptome analysis of osteoblasts in an ovariectomized mouse model in response to physical exercise. Bone Joint Res 7, 601-608.
Hu, D., Marcucio, R.S., Helms, J.A., 2003. A zone of frontonasal ectoderm regulates patterning and growth in the face. Development 130, 1749-1758.
Hu, H., Hilton, M.J., Tu, X., Yu, K., Ornitz, D.M., Long, F., 2005. Sequential roles of Hedgehog and Wnt signaling in osteoblast development. Development 132, 49-60.
Hu, Z., Chen, B., Zhao, Q., 2019. Hedgehog signaling regulates osteoblast differentiation in zebrafish larvae through modulation of autophagy. Biol Open 8.
Huang, W., Chung, U.I., Kronenberg, H.M., de Crombrugghe, B., 2001. The chondrogenic transcription factor Sox9 is a target of signaling by the parathyroid hormone-related peptide in the growth plate of endochondral bones. Proc Natl Acad Sci U S A 98, 160-165.
Huang, W., Yang, S., Shao, J., Li, Y.P., 2007. Signaling and transcriptional regulation in osteoblast commitment and differentiation. Front Biosci 12, 3068-3092.
Huitema, L.F., Apschner, A., Logister, I., Spoorendonk, K.M., Bussmann, J., Hammond, C.L., Schulte-Merker, S., 2012. Entpd5 is essential for skeletal mineralization and regulates phosphate homeostasis in zebrafish. Proc Natl Acad Sci U S A 109, 21372-21377.

Hung, I.H., Yu, K., Lavine, K.J., Ornitz, D.M., 2007. FGF9 regulates early hypertrophic chondrocyte differentiation and skeletal vascularization in the developing stylopod. Dev Biol 307, 300-313.
Hur, M., Gistelinck, C.A., Huber, P., Lee, J., Thompson, M.H., Monstad-Rios, A.T., Watson, C.J., McMenamin, S.K., Willaert, A., Parichy, D.M., Coucke, P., Kwon, R.Y., 2017. MicroCT-based phenomics in the zebrafish skeleton reveals virtues of deep phenotyping in a distributed organ system. eLife 6.
Huse, M., Chen, Y.G., Massagué, J., Kuriyan, J., 1999. Crystal structure of the cytoplasmic domain of the type I TGF beta receptor in complex with FKBP12. Cell 96, 425-436.
Huysseune, A., 2000. Chapter 18 - Skeletal System, The Laboratory Fish Handbook of Experimental Animals. Academic Press, pp. 307-317.
Hwang, W.Y., Fu, Y., Reyon, D., Maeder, M.L., Tsai, S.Q., Sander, J.D., Peterson, R.T., Yeh, J.R., Joung, J.K., 2013. Efficient genome editing in zebrafish using a CRISPR-Cas system. Nat Biotechnol 31, 227-229.
Ikeda, T., Kawaguchi, H., Kamekura, S., Ogata, N., Mori, Y., Nakamura, K., Ikegawa, S., Chung, U.I., 2005. Distinct roles of Sox5, Sox6, and Sox9 in different stages of chondrogenic differentiation. J Bone Miner Metab 23, 337-340.
Ikegawa, S., Nishimura, G., Nagai, T., Hasegawa, T., Ohashi, H., Nakamura, Y., 1998. Mutation of the type X collagen gene (COL10A1) causes spondylometaphyseal dysplasia. Am J Hum Genet 63, 1659-1662.
Inada, M., Yasui, T., Nomura, S., Miyake, S., Deguchi, K., Himeno, M., Sato, M., Yamagiwa, H., Kimura, T., Yasui, N., Ochi, T., Endo, N., Kitamura, Y., Kishimoto, T., Komori, T., 1999. Maturational disturbance of chondrocytes in Cbfa1-deficient mice. Dev Dyn 214, 279-290.
Ingham, P.W., McMahon, A.P., 2001. Hedgehog signaling in animal development: paradigms and principles. Genes Dev 15, 3059-3087.
Inohaya, K., Takano, Y., Kudo, A., 2007. The teleost intervertebral region acts as a growth center of the centrum: in vivo visualization of osteoblasts and their progenitors in transgenic fish. Dev Dyn 236, 3031-3046.
Ishikawa, M., Williams, G., Forcinito, P., Petrie, R.J., Saito, K., Fukumoto, S., Yamada, Y., 2019. Pannexin 3 ER Ca. Sci Rep 9, 18759.
Ishikawa, M., Yamada, Y., 2017. The Role of Pannexin 3 in Bone Biology. J Dent Res 96, 372-379.
Israel, D.I., Nove, J., Kerns, K.M., Kaufman, R.J., Rosen, V., Cox, K.A., Wozney, J.M., 1996. Heterodimeric bone morphogenetic proteins show enhanced activity in vitro and in vivo. Growth Factors 13, 291-300.
Issack, P.S., DiCesare, P.E., 2003. Recent advances toward the clinical application of bone morphogenetic proteins in bone and cartilage repair. Am J Orthop (Belle Mead NJ) 32, 429-436.
Jacenko, O., LuValle, P.A., Olsen, B.R., 1993. Spondylometaphyseal dysplasia in mice carrying a dominant negative mutation in a matrix protein specific for cartilage-to-bone transition. Nature 365, 56-61.
Jacenko, O., Roberts, D.W., Campbell, M.R., McManus, P.M., Gress, C.J., Tao, Z., 2002. Linking hematopoiesis to endochondral skeletogenesis through analysis of mice transgenic for collagen X. Am J Pathol 160, 2019-2034.
Jacenko, O.a.C.D., 1998. Unraveling the consequences of collagen X mutations. J Cells Materials 8, 123--134.
James, M.J., Järvinen, E., Wang, X.P., Thesleff, I., 2006. Different roles of Runx2 during early neural crest-derived bone and tooth development. J Bone Miner Res 21, 1034-1044.
James, S.L., Abate, D., Hassen Abate, K., et al., 2018. Global, regional, and national incidence, prevalence, and years lived with disability for 354 diseases and injuries for 195

countries and territories, 1990-2017: a systematic analysis for the Global Burden of Disease Study 2017. (GBD 2017 Disease and Injury Incidence and Prevalence). Lancet 392, 1789-1858.
Jeong, J., Mao, J., Tenzen, T., Kottmann, A.H., McMahon, A.P., 2004. Hedgehog signaling in the neural crest cells regulates the patterning and growth of facial primordia. Genes Dev 18, 937-951.
Jiang, S., Yan, F.F., Hu, J.Y., Mohammed, A., Cheng, H.W., 2021. -Based Probiotic Improves Skeletal Health and Immunity in Broiler Chickens Exposed to Heat Stress. Animals (Basel) 11.
Jing, Y., Jing, J., Ye, L., Liu, X., Harris, S.E., Hinton, R.J., Feng, J.Q., 2017. Chondrogenesis and osteogenesis are one continuous developmental and lineage defined biological process. Sci Rep 7, 10020.
Jiramongkolchai, P., Owens, P., Hong, C.C., 2016. Emerging roles of the bone morphogenetic protein pathway in cancer: potential therapeutic target for kinase inhibition. Biochem Soc Trans 44, 1117-1134.
Johansson, N., Saarialho-Kere, U., Airola, K., Herva, R., Nissinen, L., Westermarck, J., Vuorio, E., Heino, J., Kähäri, V.M., 1997. Collagenase-3 (MMP-13) is expressed by hypertrophic chondrocytes, periosteal cells, and osteoblasts during human fetal bone development. Dev Dyn 208, 387-397.
Jorgenson, E., Makki, N., Shen, L., Chen, D.C., Tian, C., Eckalbar, W.L., Hinds, D., Ahituv, N., Avins, A., 2015. A genome-wide association study identifies four novel susceptibility loci underlying inguinal hernia. Nat Commun 6, 10130.
Jsbrand, I., Kramer, M., 2016. Chapter 17 - TGFβ and Signaling through Receptor Serine/Threonine Protein Kinases. Signal Transduction (Third Edition), 887-933.
Kague, E., Gallagher, M., Burke, S., Parsons, M., Franz-Odendaal, T., Fisher, S., 2012. Skeletogenic fate of zebrafish cranial and trunk neural crest. PLoS One 7, e47394.
Kague, E., Roy, P., Asselin, G., Hu, G., Simonet, J., Stanley, A., Albertson, C., Fisher, S., 2016. Osterix/Sp7 limits cranial bone initiation sites and is required for formation of sutures. Dev Biol 413, 160-172.
Kague, E., Turci, F., Newman, E., Yang, Y., Brown, K.R., Aglan, M.S., Otaify, G.A., Temtamy, S.A., Ruiz-Perez, V.L., Cross, S., Royall, C.P., Witten, P.E., Hammond, C.L., 2021. 3D assessment of intervertebral disc degeneration in zebrafish identifies changes in bone density that prime disc disease. Bone Res 9, 39.
Kahil, K., Varsano, N., Sorrentino, A., Pereiro, E., Rez, P., Weiner, S., Addadi, L., 2020. Cellular pathways of calcium transport and concentration toward mineral formation in sea urchin larvae. Proc Natl Acad Sci U S A 117, 30957-30965.
Kamiya, N., Kobayashi, T., Mochida, Y., Yu, P.B., Yamauchi, M., Kronenberg, H.M., Mishina, Y., 2010. Wnt inhibitors Dkk1 and Sost are downstream targets of BMP signaling through the type IA receptor (BMPRIA) in osteoblasts. J Bone Miner Res 25, 200-210.
Kamiya, N., Mishina, Y., 2011. New insights on the roles of BMP signaling in bone-A review of recent mouse genetic studies. Biofactors 37, 75-82.
Kamiya, N., Ye, L., Kobayashi, T., Mochida, Y., Yamauchi, M., Kronenberg, H.M., Feng, J.Q., Mishina, Y., 2008. BMP signaling negatively regulates bone mass through sclerostin by inhibiting the canonical Wnt pathway. Development 135, 3801-3811.
Kanehisa, M., Sato, Y., Kawashima, M., 2022. KEGG mapping tools for uncovering hidden features in biological data. Protein Sci 31, 47-53.
Kapoor, M., Martel-Pelletier, J., Lajeunesse, D., Pelletier, J.P., Fahmi, H., 2011. Role of proinflammatory cytokines in the pathophysiology of osteoarthritis. Nat Rev Rheumatol 7, 33-42.

Karaplis, A., 2008. Chapter 3- Embryonic development of bone and regulation of intramembranous and endochondral bone formation in Principles of Bone Biology (Third Edition). Principles of Bone Biology I, 53-84.
Karsdal, M.A., Nielsen, M.J., Sand, J.M., Henriksen, K., Genovese, F., Bay-Jensen, A.C., Smith, V., Adamkewicz, J.I., Christiansen, C., Leeming, D.J., 2013. Extracellular matrix remodeling: the common denominator in connective tissue diseases. Possibilities for evaluation and current understanding of the matrix as more than a passive architecture, but a key player in tissue failure. Assay Drug Dev Technol 11, 70-92.
Karsenty, G., Wagner, E.F., 2002. Reaching a genetic and molecular understanding of skeletal development. Dev Cell 2, 389-406.
Kevorkian, L., Young, D.A., Darrah, C., Donell, S.T., Shepstone, L., Porter, S., Brockbank, S.M., Edwards, D.R., Parker, A.E., Clark, I.M., 2004. Expression profiling of metalloproteinases and their inhibitors in cartilage. Arthritis Rheum 50, 131-141.
Kiernan, C., Knuth, C., Farrell, E., 2018. Chapter 6 - Endochondral Ossification : Recapitulating Bone Development for Bone Defect Repair, in: Martin J. Stoddart, A.M.C., ... Oliver F.W. Gardner (Ed.), Developmental Biology and Musculoskeletal Tissue EngineeringPrinciples and Applications. Academic Press, pp. 125-148.
Kim, H.J., Rice, D.P., Kettunen, P.J., Thesleff, I., 1998. FGF-, BMP- and Shh-mediated signalling pathways in the regulation of cranial suture morphogenesis and calvarial bone development. Development 125, 1241-1251.
Kim, I.S., Otto, F., Zabel, B., Mundlos, S., 1999. Regulation of chondrocyte differentiation by Cbfa1. Mech Dev 80, 159-170.
Kim, J.H., Liu, X., Wang, J., Chen, X., Zhang, H., Kim, S.H., Cui, J., Li, R., Zhang, W., Kong, Y., Zhang, J., Shui, W., Lamplot, J., Rogers, M.R., Zhao, C., Wang, N., Rajan, P., Tomal, J., Statz, J., Wu, N., Luu, H.H., Haydon, R.C., He, T.C., 2013a. Wnt signaling in bone formation and its therapeutic potential for bone diseases. Ther Adv Musculoskelet Dis 5, 13-31.
Kim, J.M., Lin, C., Stavre, Z., Greenblatt, M.B., Shim, J.H., 2020. Osteoblast-Osteoclast Communication and Bone Homeostasis. Cells 9.
Kim, M., Choe, S., 2011. BMPs and their clinical potentials. BMB Rep 44, 619-634.
Kim, M., Yu, Y., Moon, J.H., Koh, I., Lee, J.H., 2018. Differential Expression Profiling of Long Noncoding RNA and mRNA during Osteoblast Differentiation in Mouse. Int J Genomics 2018, 7691794.
Kim, Y.-I., Lee, S., Jung, S.-H., Kim, H.-T., Choi, J.-H., Lee, M.-S., You, K.-H., Yeo, S.-Y., Yoo, K.-W., Kwak, S., Lee, J.N., Park, R., Choe, S.-K., Kim, C.-H., 2013b. Establishment of a bone-specific col10a1:GFP transgenic zebrafish. Mol Cells 36, 145-150.
Kim, Y.I., Lee, S., Jung, S.H., Kim, H.T., Choi, J.H., Lee, M.S., You, K.H., Yeo, S.Y., Yoo, K.W., Kwak, S., Lee, J.N., Park, R., Choe, S.K., Kim, C.H., 2013c. Establishment of a bone-specific col10a1:GFP transgenic zebrafish. Molecules and cells 36, 145-150.
Kimmel, C.B., Ballard, W.W., Kimmel, S.R., Ullmann, B., Schilling, T.F., 1995. Stages of embryonic development of the zebrafish. Dev Dyn 203, 253-310.
Kimmel, C.B., Miller, C.T., Kruze, G., Ullmann, B., BreMiller, R.A., Larison, K.D., Snyder, H.C., 1998. The shaping of pharyngeal cartilages during early development of the zebrafish. Dev Biol 203, 245-263.
Kimmel, C.B., Miller, C.T., Moens, C.B., 2001. Specification and morphogenesis of the zebrafish larval head skeleton. Dev Biol 233, 239-257.
Klenotic, P.A., Munier, F.L., Marmorstein, L.Y., Anand-Apte, B., 2004a. Tissue inhibitor of metalloproteinases-3 (TIMP-3) is a binding partner of epithelial growth factor-containing fibulin-like extracellular matrix protein 1 (EFEMP1). Implications for macular degenerations. J Biol Chem 279, 30469-30473.

Klenotic, P.A., Munier, F.L., Marmorstein, L.Y., Anand-Apte, B., 2004b. Tissue Inhibitor of Metalloproteinases-3 (TIMP-3) Is a Binding Partner of Epithelial Growth Factor-containing Fibulin-like Extracellular Matrix Protein 1 (EFEMP1): Implications for macular degenerations. Journal of Biological Chemistry 279, 30469-30473.
Kluge, M., Mann, K., Dziadek, M., Timpl, R., 1990. Characterization of a novel calcium-binding 90-kDa glycoprotein (BM-90) shared by basement membranes and serum. Eur J Biochem 193, 651-659.
Knopf, F., Hammond, C., Chekuru, A., Kurth, T., Hans, S., Weber, C.W., Mahatma, G., Fisher, S., Brand, M., Schulte-Merker, S., Weidinger, G., 2011. Bone regenerates via dedifferentiation of osteoblasts in the zebrafish fin. Dev Cell 20, 713-724.
Knupp, C., Squire, J.M., 2005. Molecular packing in network-forming collagens. Adv Protein Chem 70, 375-403.
Ko Min, J., 2016. Genetic Syndromes Associated with Craniosynostosis. J Korean Neurosurg Soc 59, 187-191.
Kobayashi, N., Kostka, G., Garbe, J.H., Keene, D.R., Bächinger, H.P., Hanisch, F.G., Markova, D., Tsuda, T., Timpl, R., Chu, M.L., Sasaki, T., 2007. A comparative analysis of the fibulin protein family. Biochemical characterization, binding interactions, and tissue localization. J Biol Chem 282, 11805-11816.
Kobayashi, T., Kronenberg, H., 2005. Minireview: transcriptional regulation in development of bone. Endocrinology 146, 1012-1017.
Kojima, H., Urano, Y., Kikuchi, K., Higuchi, T., Hirata, Y., Nagano, T., 1999. Fluorescent Indicators for Imaging Nitric Oxide Production. Angew Chem Int Ed Engl 38, 3209-3212.
Komori, T., 2010. Regulation of bone development and extracellular matrix protein genes by RUNX2. Cell Tissue Res 339, 189-195.
Komori, T., 2011. Signaling networks in RUNX2-dependent bone development. J Cell Biochem 112, 750-755.
Komori, T., 2017. Roles of Runx2 in Skeletal Development. Adv Exp Med Biol 962, 83-93.
Komori, T., Yagi, H., Nomura, S., Yamaguchi, A., Sasaki, K., Deguchi, K., Shimizu, Y., Bronson, R.T., Gao, Y.H., Inada, M., Sato, M., Okamoto, R., Kitamura, Y., Yoshiki, S., Kishimoto, T., 1997. Targeted disruption of Cbfa1 results in a complete lack of bone formation owing to maturational arrest of osteoblasts. Cell 89, 755-764.
Koosha, E., Eames, B.F., 2022. Two Modulators of Skeletal Development: BMPs and Proteoglycans. J Dev Biol 10.
Kornak, U., Mundlos, S., 2003. Genetic disorders of the skeleton: a developmental approach. Am J Hum Genet 73, 447-474.
Kostka, G., Giltay, R., Bloch, W., Addicks, K., Timpl, R., Fassler, R., Chu, M.L., 2001. Perinatal lethality and endothelial cell abnormalities in several vessel compartments of fibulin-1-deficient mice. Mol Cell Biol 21, 7025-7034.
Kostoulas, G., Lang, A., Nagase, H., Baici, A., 1999. Stimulation of angiogenesis through cathepsin B inactivation of the tissue inhibitors of matrix metalloproteinases. FEBS Lett 455, 286-290.
Kozhemyakina, E., Lassar, A.B., Zelzer, E., 2015. A pathway to bone: signaling molecules and transcription factors involved in chondrocyte development and maturation. Development 142, 817-831.
Kronenberg, H.M., 2003. Developmental regulation of the growth plate. Nature 423, 332-336.
Kurihara, Y., Kurihara, H., Suzuki, H., Kodama, T., Maemura, K., Nagai, R., Oda, H., Kuwaki, T., Cao, W.H., Kamada, N., 1994. Elevated blood pressure and craniofacial abnormalities in mice deficient in endothelin-1. Nature 368, 703-710.
Kuyinu, E.L., Narayanan, G., Nair, L.S., Laurencin, C.T., 2016. Animal models of osteoarthritis: classification, update, and measurement of outcomes. J Orthop Surg Res 11, 19.

Kwan, A.P., Cummings, C.E., Chapman, J.A., Grant, M.E., 1991. Macromolecular organization of chicken type X collagen in vitro. J Cell Biol 114, 597-604.
Kwan, K.M., Pang, M.K., Zhou, S., Cowan, S.K., Kong, R.Y., Pfordte, T., Olsen, B.R., Sillence, D.O., Tam, P.P., Cheah, K.S., 1997. Abnormal compartmentalization of cartilage matrix components in mice lacking collagen X: implications for function. The Journal of cell biology 136, 459-471.
Kwon, R.Y., Watson, C.J., Karasik, D., 2019. Using zebrafish to study skeletal genomics. Bone 126, 37-50.
Laplante, B.L., DePalma, M.J., 2012. Spine osteoarthritis. PM R 4, S28-36.
Lapunzina, P., Aglan, M., Temtamy, S., Caparrós-Martín, J.A., Valencia, M., Letón, R., Martínez-Glez, V., Elhossini, R., Amr, K., Vilaboa, N., Ruiz-Perez, V.L., 2010. Identification of a frameshift mutation in Osterix in a patient with recessive osteogenesis imperfecta. Am J Hum Genet 87, 110-114.
Lawenius, L., Colldén, H., Horkeby, K., Wu, J., Grahnemo, L., Vandenput, L., Ohlsson, C., Sjögren, K., 2022. A probiotic mix partially protects against castration-induced bone loss in male mice. J Endocrinol 254, 91-101.
Lawrence, E.A., Kague, E., Aggleton, J.A., Harniman, R.L., Roddy, K.A., Hammond, C.L., 2018a. The mechanical impact of. Philos Trans R Soc Lond B Biol Sci 373.
Lawrence, E.A., Kague, E., Aggleton, J.A., Harniman, R.L., Roddy, K.A., Hammond, C.L., 2018b. The mechanical impact of col11a2 loss on joints; col11a2 mutant zebrafish show changes to joint development and function, which leads to early-onset osteoarthritis. Philos Trans R Soc Lond B Biol Sci 373.
Lazarus, J.E., Hegde, A., Andrade, A.C., Nilsson, O., Baron, J., 2007. Fibroblast growth factor expression in the postnatal growth plate. Bone 40, 577-586.
Le Pabic, P., Dranow, D.B., Hoyle, D.J., Schilling, T.F., 2022a. Zebrafish endochondral growth zones as they relate to human bone size, shape and disease. Front Endocrinol (Lausanne) 13, 1060187.
Le Pabic, P., Dranow, D.B., Hoyle, D.J., Schilling, T.F., 2022b. Zebrafish endochondral growth zones as they relate to human bone size, shape and disease. Frontiers in Endocrinology 13.
Le Pabic, P., Ng, C., Schilling, T.F., 2014. Fat-Dachsous signaling coordinates cartilage differentiation and polarity during craniofacial development. PLoS Genet 10, e1004726.
Lee, J.S., Burke, A.B., 2021. Biology of Bone and Cartilage Grafting." in A*esthetic Surgery of the Facial Skeleton-E-Book Aesthetic Surgery of the Facial Skeleton-E-Book* pp. 88-94.
Lefebvre, V., Dvir-Ginzberg, M., 2017. SOX9 and the many facets of its regulation in the chondrocyte lineage. Connect Tissue Res 58, 2-14.
Lehmann, K., Seemann, P., Silan, F., Goecke, T.O., Irgang, S., Kjaer, K.W., Kjaergaard, S., Mahoney, M.J., Morlot, S., Reissner, C., Kerr, B., Wilkie, A.O., Mundlos, S., 2007. A new subtype of brachydactyly type B caused by point mutations in the bone morphogenetic protein antagonist NOGGIN. Am J Hum Genet 81, 388-396.
Lenton, K.A., Nacamuli, R.P., Wan, D.C., Helms, J.A., Longaker, M.T., 2005. Cranial suture biology. Curr Top Dev Biol 66, 287-328.
Lepiller, S., Laurens, V., Bouchot, A., Herbomel, P., Solary, E., Chluba, J., 2007. Imaging of nitric oxide in a living vertebrate using a diamino-fluorescein probe. Free Radic Biol Med 43, 619-627.
Lettice, L., Hecksher-Sørensen, J., Hill, R., 2001. The role of Bapx1 (Nkx3.2) in the development and evolution of the axial skeleton. J Anat 199, 181-187.
Lettice, L.A., Purdie, L.A., Carlson, G.J., Kilanowski, F., Dorin, J., Hill, R.E., 1999. The mouse bagpipe gene controls development of axial skeleton, skull, and spleen. Proc Natl Acad Sci U S A 96, 9695-9700.

Leung, P.C.K., Peng, C., 2003. Activin Receptor Signaling. Encyclopedia of Hormones, p.17-23.
Leung, V.Y., Gao, B., Leung, K.K., Melhado, I.G., Wynn, S.L., Au, T.Y., Dung, N.W., Lau, J.Y., Mak, A.C., Chan, D., Cheah, K.S., 2011. SOX9 governs differentiation stage-specific gene expression in growth plate chondrocytes via direct concomitant transactivation and repression. PLoS Genet 7, e1002356.
Levasseur, R., Lacombe, D., de Vernejoul, M.C., 2005. LRP5 mutations in osteoporosis-pseudoglioma syndrome and high-bone-mass disorders. Joint Bone Spine 72, 207-214.
Levi, G., Narboux-Nême, N., Cohen-Solal, M., 2022. Genes in the Development and Maintenance of the Vertebrate Skeleton: Implications for Human Pathologies. Cells 11.
Li, N., Felber, K., Elks, P., Croucher, P., Roehl, H.H., 2009. Tracking gene expression during zebrafish osteoblast differentiation. Dev Dyn 238, 459-466.
Li, X., Ionescu, A.M., Schwarz, E.M., Zhang, X., Drissi, H., Puzas, J.E., Rosier, R.N., Zuscik, M.J., O'Keefe, R.J., 2003. Smad6 is induced by BMP-2 and modulates chondrocyte differentiation. J Orthop Res 21, 908-913.
Liedtke, D., Orth, M., Meissler, M., Geuer, S., Knaup, S., Köblitz, I., Klopocki, E., 2019. ECM alterations in Fndc3a (Fibronectin Domain Containing Protein 3A) deficient zebrafish cause temporal fin development and regeneration defects. Sci Rep 9, 13383.
Lin, C.-H., Hu, H.-J., Hwang, P.-P., 2017. Molecular Physiology of the Hypocalcemic Action of Fibroblast Growth Factor 23 in Zebrafish (Danio rerio). Endocrinology 158, 1347-1358.
Lin, P.M., Chen, C.T., Torzilli, P.A., 2004. Increased stromelysin-1 (MMP-3), proteoglycan degradation (3B3- and 7D4) and collagen damage in cyclically load-injured articular cartilage. Osteoarthritis Cartilage 12, 485-496.
Lin, X., Patil, S., Gao, Y.G., Qian, A., 2020. The Bone Extracellular Matrix in Bone Formation and Regeneration. Frontiers in pharmacology 11, 757.
Lin, Z., Gao, C., Ning, Y., He, X., Wu, W., Chen, Y.G., 2008. The pseudoreceptor BMP and activin membrane-bound inhibitor positively modulates Wnt/beta-catenin signaling. J Biol Chem 283, 33053-33058.
Ling, I.T., Rochard, L., Liao, E.C., 2017. Distinct requirements of wls, wnt9a, wnt5b and gpc4 in regulating chondrocyte maturation and timing of endochondral ossification. Dev Biol 421, 219-232.
Lister, J.A., 2002. Development of pigment cells in the zebrafish embryo. Microsc Res Tech 58, 435-441.
Liu, D.D., Zhang, C.Y., Liu, Y., Li, J., Wang, Y.X., Zheng, S.G., 2022. RUNX2 Regulates Osteoblast Differentiation via the BMP4 Signaling Pathway. J Dent Res 101, 1227-1237.
Liu, G., Cooley, M.A., Jarnicki, A.G., Borghuis, T., Nair, P.M., Tjin, G., Hsu, A.C., Haw, T.J., Fricker, M., Harrison, C.L., Jones, B., Hansbro, N.G., Wark, P.A., Horvat, J.C., Argraves, W.S., Oliver, B.G., Knight, D.A., Burgess, J.K., Hansbro, P.M., 2019. Fibulin-1c regulates transforming growth factor-β activation in pulmonary tissue fibrosis. JCI Insight 5.
Liu, Q., Li, M., Wang, S., Xiao, Z., Xiong, Y., Wang, G., 2020. Recent Advances of Osterix Transcription Factor in Osteoblast Differentiation and Bone Formation. Front Cell Dev Biol 8, 601224.
Liu, Z., Xu, J., Colvin, J.S., Ornitz, D.M., 2002. Coordination of chondrogenesis and osteogenesis by fibroblast growth factor 18. Genes Dev 16, 859-869.
Livingstone, I., Uversky, V.N., Furniss, D., Wiberg, A., 2020. The Pathophysiological Significance of Fibulin-3. Biomolecules 10.
Lleras Forero, L., Narayanan, R., Huitema, L.F., VanBergen, M., Apschner, A., Peterson-Maduro, J., Logister, I., Valentin, G., Morelli, L.G., Oates, A.C., Schulte-Merker, S., 2018. Segmentation of the zebrafish axial skeleton relies on notochord sheath cells and not on the segmentation clock. Elife 7.

Lleras-Forero, L., Winkler, C., Schulte-Merker, S., 2020. Zebrafish and medaka as models for biomedical research of bone diseases. Dev Biol 457, 191-205.
Loeser, R.F., Goldring, S.R., Scanzello, C.R., Goldring, M.B., 2012. Osteoarthritis: a disease of the joint as an organ. Arthritis Rheum 64, 1697-1707.
Lombardi, G., Ziemann, E., Banfi, G., Corbetta, S., 2020. Physical Activity-Dependent Regulation of Parathyroid Hormone and Calcium-Phosphorous Metabolism. Int J Mol Sci 21.
Long, F., 2012. Building strong bones: molecular regulation of the osteoblast lineage. Nature Reviews Molecular Cell Biology 13, 27-38.
Long, F., Ornitz, D.M., 2013. Development of the endochondral skeleton. Cold Spring Harb Perspect Biol 5, a008334.
Long, J.T.a.L.A.a.L.Y.a.R.Y.a.M.A.J.a.N.T.a.G.W.a.S.D.a.R.D.a.W., 2022. Hypertrophic chondrocytes serve as a reservoir for marrow-associated skeletal stem and progenitor cells, osteoblasts, and adipocytes during skeletal development. eLife 11, e76932 , citation = eLife 72022;76911 e76932.
Lories, R.J., Luyten, F.P., 2011. The bone-cartilage unit in osteoarthritis. Nat Rev Rheumatol 7, 43-49.
Lotz, M., Martel-Pelletier, J., Christiansen, C., Brandi, M.L., Bruyère, O., Chapurlat, R., Collette, J., Cooper, C., Giacovelli, G., Kanis, J.A., Karsdal, M.A., Kraus, V., Lems, W.F., Meulenbelt, I., Pelletier, J.P., Raynauld, J.P., Reiter-Niesert, S., Rizzoli, R., Sandell, L.J., Van Spil, W.E., Reginster, J.Y., 2013. Value of biomarkers in osteoarthritis: current status and perspectives. Ann Rheum Dis 72, 1756-1763.
Love, M.I., Huber, W., Anders, S., 2014. Moderated estimation of fold change and dispersion for RNA-seq data with DESeq2. Genome Biol 15, 550.
Lovely, C.B., Swartz, M.E., McCarthy, N., Norrie, J.L., Eberhart, J.K., 2016. Bmp signaling mediates endoderm pouch morphogenesis by regulating Fgf signaling in zebrafish. Development 143, 2000-2011.
Lowery, J.W., Rosen, V., 2018. The BMP Pathway and Its Inhibitors in the Skeleton. Physiol Rev 98, 2431-2452.
Lu, P., Takai, K., Weaver, V.M., Werb, Z., 2011. Extracellular matrix degradation and remodeling in development and disease. Cold Spring Harb Perspect Biol 3.
Lu, Y., Ren, X., Wang, Y., Bardai, G., Sturm, M., Dai, Y., Riess, O., Zhang, Y., Li, H., Li, T., Zhai, N., Zhang, J., Rauch, F., Han, J., 2018. Novel WNT1 mutations in children with osteogenesis imperfecta: Clinical and functional characterization. Bone 114, 144-149.
Luo, G., Ducy, P., McKee, M.D., Pinero, G.J., Loyer, E., Behringer, R.R., Karsenty, G., 1997. Spontaneous calcification of arteries and cartilage in mice lacking matrix GLA protein. Nature 386, 78-81.
Lyu, Z., Hu, Y., Guo, Y., Liu, D., 2023. Modulation of bone remodeling by the gut microbiota: a new therapy for osteoporosis. Bone Res 11, 31.
Ma, X., Wang, Y.W., Zhang, M.Q., Gazdar, A.F., 2013. DNA methylation data analysis and its application to cancer research. Epigenomics 5, 301-316.
Mackie, E.J., Ahmed, Y.A., Tatarczuch, L., Chen, K.S., Mirams, M., 2008. Endochondral ossification: how cartilage is converted into bone in the developing skeleton. Int J Biochem Cell Biol 40, 46-62.
Maeda, Y., Nakamura, E., Nguyen, M.T., Suva, L.J., Swain, F.L., Razzaque, M.S., Mackem, S., Lanske, B., 2007. Indian Hedgehog produced by postnatal chondrocytes is essential for maintaining a growth plate and trabecular bone. Proc Natl Acad Sci U S A 104, 6382-6387.
Maes, C., Kobayashi, T., Selig, M.K., Torrekens, S., Roth, S.I., Mackem, S., Carmeliet, G., Kronenberg, H.M., 2010. Osteoblast precursors, but not mature osteoblasts, move into developing and fractured bones along with invading blood vessels. Dev Cell 19, 329-344.

Maes, C., Kronenberg M., H., 2016. Chapter 60 - Bone Development and Remodeling, Endocrinology: Adult and Pediatric, 7th ed, pp. 1038-1062.e1038.
Mahajan, D., Kancharla, S., Kolli, P., Sharma, A.K., Singh, S., Kumar, S., Mohanty, A.K., Jena, M.K., 2021. Role of Fibulins in Embryonic Stage Development and Their Involvement in Various Diseases. Biomolecules 11.
Malaval, L., Wade-Guéye, N.M., Boudiffa, M., Fei, J., Zirngibl, R., Chen, F., Laroche, N., Roux, J.P., Burt-Pichat, B., Duboeuf, F., Boivin, G., Jurdic, P., Lafage-Proust, M.H., Amédée, J., Vico, L., Rossant, J., Aubin, J.E., 2008. Bone sialoprotein plays a functional role in bone formation and osteoclastogenesis. J Exp Med 205, 1145-1153.
Mallo, M., Wellik, D.M., Deschamps, J., 2010. Hox genes and regional patterning of the vertebrate body plan. Dev Biol 344, 7-15.
Mansell, J.P., Bailey, A.J., 1998. Abnormal cancellous bone collagen metabolism in osteoarthritis. J Clin Invest 101, 1596-1603.
Mansell, J.P., Tarlton, J.F., Bailey, A.J., 1997. Biochemical evidence for altered subchondral bone collagen metabolism in osteoarthritis of the hip. Br J Rheumatol 36, 16-19.
Mansour, A., Mezour, M.A., Badran, Z., Tamimi, F., 2017. Extracellular Matrices for Bone Regeneration: A Literature Review. Tissue Eng Part A 23, 1436-1451.
Maridas, E.D., Feigenson, M., Renthal, E.N., Chim, M.S., Gamer, W.L., Rosen, V., 2019. Principles of bone biology. Principles of bone biology.
Marie, P.J., 2008. Transcription factors controlling osteoblastogenesis. Arch Biochem Biophys 473, 98-105.
Marmorstein, L., 2004. Association of EFEMP1 with malattia leventinese and age-related macular degeneration: a mini-review. Ophthalmic Genet 25, 219-226.
Marmorstein, L.Y., McLaughlin, P.J., Peachey, N.S., Sasaki, T., Marmorstein, A.D., 2007. Formation and progression of sub-retinal pigment epithelium deposits in Efemp1 mutation knock-in mice: a model for the early pathogenic course of macular degeneration. Hum Mol Genet 16, 2423-2432.
Martini, F.H., Nath, J.L., Bartholomew, E.F., 2018. Fundamentals of Anatomy & Physiology. Pearson Education, Limited, 1304.
Massagué, J., Seoane, J., Wotton, D., 2005. Smad transcription factors. Genes Dev 19, 2783-2810.
Matsubara, T., Kida, K., Yamaguchi, A., Hata, K., Ichida, F., Meguro, H., Aburatani, H., Nishimura, R., Yoneda, T., 2008. BMP2 regulates Osterix through Msx2 and Runx2 during osteoblast differentiation. J Biol Chem 283, 29119-29125.
Maynard, R.L., Downes, N., 2019a. Chapter 3 - Introduction to the Skeleton : Bone, Cartilage and Joints. In: Anatomy and Histology of the Laboratory Rat in Toxicology and Biomedical Research; Ed. P. Gonzalez, Academic Press, Elsevier, London, UK, 11-22.
Maynard, R.L., Downes, N., 2019b. Chapter 3 - Introduction to the Skeleton : Bone, Cartilage and Joints, Anatomy and Histology of the Laboratory Rat in Toxicology and Biomedical Research. Academic Press, United Kingdom, pp. 11-22.
Mayne, R., 1989. Cartilage collagens. What Is Their Function, and Are They Involved in Articular Disease? . Arthritis & Rheumatology 32, 241-246.
Mbalaviele, G., Sheikh, S., Stains, J.P., Salazar, V.S., Cheng, S.L., Chen, D., Civitelli, R., 2005. Beta-catenin and BMP-2 synergize to promote osteoblast differentiation and new bone formation. J Cell Biochem 94, 403-418.
McIntosh, I., Abbott, M.H., Francomano, C.A., 1995. Concentration of mutations causing Schmid metaphyseal chondrodysplasia in the C-terminal noncollagenous domain of type X collagen. Hum Mutat 5, 121-125.

McIntosh, I., Abbott, M.H., Warman, M.L., Olsen, B.R., Francomano, C.A., 1994. Additional mutations of type X collagen confirm COL10A1 as the Schmid metaphyseal chondrodysplasia locus. Hum Mol Genet 3, 303-307.
McKee, T.J., Perlman, G., Morris, M., Komarova, S.V., 2019. Extracellular matrix composition of connective tissues: a systematic review and meta-analysis. Sci Rep 9, 10542.
McLaughlin, P.J., Bakall, B., Choi, J., Liu, Z., Sasaki, T., Davis, E.C., Marmorstein, A.D., Marmorstein, L.Y., 2007. Lack of fibulin-3 causes early aging and herniation, but not macular degeneration in mice. Hum Mol Genet 16, 3059-3070.
Mecham, R.P., 2012. Overview of extracellular matrix. Curr Protoc Cell Biol Chapter 10, 10 11 11-10 11 16.
Medeiros, D.M., Crump, J.G., 2012. New perspectives on pharyngeal dorsoventral patterning in development and evolution of the vertebrate jaw. Dev Biol 371, 121-135.
Mercader, N., Fischer, S., Neumann, C.J., 2006. Prdm1 acts downstream of a sequential RA, Wnt and Fgf signaling cascade during zebrafish forelimb induction. Development 133, 2805-2815.
Michigami, T., Ozono, K., 2019. Roles of Phosphate in Skeleton. Front Endocrinol (Lausanne) 10, 180.
Miller, C.T., Schilling, T.F., Lee, K., Parker, J., Kimmel, C.B., 2000. sucker encodes a zebrafish Endothelin-1 required for ventral pharyngeal arch development. Development 127, 3815-3828.
Miller, C.T., Yelon, D., Stainier, D.Y., Kimmel, C.B., 2003. Two endothelin 1 effectors, hand2 and bapx1, pattern ventral pharyngeal cartilage and the jaw joint. Development 130, 1353-1365.
Minina, E., Kreschel, C., Naski, M.C., Ornitz, D.M., Vortkamp, A., 2002. Interaction of FGF, Ihh/Pthlh, and BMP signaling integrates chondrocyte proliferation and hypertrophic differentiation. Dev Cell 3, 439-449.
Minina, E., Wenzel, H.M., Kreschel, C., Karp, S., Gaffield, W., McMahon, A.P., Vortkamp, A., 2001. BMP and Ihh/PTHrP signaling interact to coordinate chondrocyte proliferation and differentiation. Development 128, 4523-4534.
Miosge, N., Götz, W., Sasaki, T., Chu, M.L., Timpl, R., Herken, R., 1996. The extracellular matrix proteins fibulin-1 and fibulin-2 in the early human embryo. Histochem J 28, 109-116.
Miron, R.J., Zhang, Y.F., 2012. Osteoinduction: a review of old concepts with new standards. J Dent Res 91, 736-744.
Mitchell, R.E., Huitema, L.F., Skinner, R.E., Brunt, L.H., Severn, C., Schulte-Merker, S., Hammond, C.L., 2013. New tools for studying osteoarthritis genetics in zebrafish. Osteoarthritis Cartilage 21, 269-278.
Miyake, T., Cameron, A.M., Hall, B.K., 1997. Stage-specific expression patterns of alkaline phosphatase during development of the first arch skeleton in inbred C57BL/6 mouse embryos. J Anat 190 ( Pt 2), 239-260.
Miyazono, K., Shimanuki, T., 2008. Bone Morphogenetic Protein Receptors and Actions. Principles of Bone Biology, p.1177-1196.
Mohamed, A.M., 2008. An overview of bone cells and their regulating factors of differentiation. Malays J Med Sci 15, 4-12.
Mohedas, A.H., Xing, X., Armstrong, K.A., Bullock, A.N., Cuny, G.D., Yu, P.B., 2013. Development of an ALK2-biased BMP type I receptor kinase inhibitor. ACS Chem Biol 8, 1291-1302.
Montero, A., Okada, Y., Tomita, M., Ito, M., Tsurukami, H., Nakamura, T., Doetschman, T., Coffin, J.D., Hurley, M.M., 2000. Disruption of the fibroblast growth factor-2 gene results in decreased bone mass and bone formation. J Clin Invest 105, 1085-1093.

Moriarity, B.S., Otto, G.M., Rahrmann, E.P., Rathe, S.K., Wolf, N.K., Weg, M.T., Manlove, L.A., LaRue, R.S., Temiz, N.A., Molyneux, S.D., Choi, K., Holly, K.J., Sarver, A.L., Scott, M.C., Forster, C.L., Modiano, J.F., Khanna, C., Hewitt, S.M., Khokha, R., Yang, Y., Gorlick, R., Dyer, M.A., Largaespada, D.A., 2015. A Sleeping Beauty forward genetic screen identifies new genes and pathways driving osteosarcoma development and metastasis. Nat Genet 47, 615-624.
Mork, L., Crump, G., 2015. Zebrafish Craniofacial Development: A Window into Early Patterning. Curr Top Dev Biol 115, 235-269.
Mouw, J.K., Ou, G., Weaver, V.M., 2014. Extracellular matrix assembly: a multiscale deconstruction. Nat Rev Mol Cell Biol 15, 771-785.
Mueller, M.B., Tuan, R.S., 2008. Functional characterization of hypertrophy in chondrogenesis of human mesenchymal stem cells. Arthritis Rheum 58, 1377-1388.
Muller, M., Dalcq, J., Aceto, J., Larbuisson, A., Pasque, V., Nourizadeh-Lilladadi, R., Aleström, P., Martial, J.A., 2010. The function of the Egr1 transcription factor in cartilage formation and adaptation to microgravity in zebrafish, Danio rerio. Journal of Applied Ichthyology 26, 239-244.
Murchison, N.D., Price, B.A., Conner, D.A., Keene, D.R., Olson, E.N., Tabin, C.J., Schweitzer, R., 2007. Regulation of tendon differentiation by scleraxis distinguishes force-transmitting tendons from muscle-anchoring tendons. Development 134, 2697-2708.
Murray, K.J., Le Grande, M.R., Ortega de Mues, A., Azari, M.F., 2017. Characterisation of the correlation between standing lordosis and degenerative joint disease in the lower lumbar spine in women and men: a radiographic study. BMC Musculoskelet Disord 18, 330.
Murshed, M., 2018. Mechanism of Bone Mineralization. Cold Spring Harb Perspect Med 8.
Musumeci, G., Aiello, F.C., Szychlinska, M.A., Di Rosa, M., Castrogiovanni, P., Mobasheri, A., 2015. Osteoarthritis in the XXIst century: risk factors and behaviours that influence disease onset and progression. Int J Mol Sci 16, 6093-6112.
Myers, K., Ateshian, G.A., 2014. Interstitial growth and remodeling of biological tissues: tissue composition as state variables. J Mech Behav Biomed Mater 29, 544-556.
Nakamura, I., Takahashi, N., Jimi, E., Udagawa, N., Suda, T., 2012. Regulation of osteoclast function. Mod Rheumatol 22, 167-177.
Nakamura, T., Naruse, M., Chiba, Y., Komori, T., Sasaki, K., Iwamoto, M., Fukumoto, S., 2015. Novel hedgehog agonists promote osteoblast differentiation in mesenchymal stem cells. J Cell Physiol 230, 922-929.
Nakashima, K., Zhou, X., Kunkel, G., Zhang, Z., Deng, J.M., Behringer, R.R., de Crombrugghe, B., 2002. The novel zinc finger-containing transcription factor osterix is required for osteoblast differentiation and bone formation. Cell 108, 17-29.
Naomi, R., Ridzuan, P.M., Bahari, H., 2021. Current Insights into Collagen Type I. Polymers (Basel) 13.
Naumann, A., Dennis, J.E., Awadallah, A., Carrino, D.A., Mansour, J.M., Kastenbauer, E., Caplan, A.I., 2002. Immunochemical and mechanical characterization of cartilage subtypes in rabbit. J Histochem Cytochem 50, 1049-1058.
Neuhauss, S.C., Solnica-Krezel, L., Schier, A.F., Zwartkruis, F., Stemple, D.L., Malicki, J., Abdelilah, S., Stainier, D.Y., Driever, W., 1996. Mutations affecting craniofacial development in zebrafish. Development 123, 357-367.
Newfeld, S.J., Wisotzkey, R.G., Kumar, S., 1999. Molecular evolution of a developmental pathway: phylogenetic analyses of transforming growth factor-beta family ligands, receptors and Smad signal transducers. Genetics 152, 783-795.
Nie, C.-H., Wan, S.-M., Chen, Y.-L., Huysseune, A., Wu, Y.-M., Zhou, J.-J., Hilsdorf, A.W.S., Wang, W.-M., Witten, P.E., Lin, Q., Gao, Z.-X., 2022. Single-cell transcriptomes and

runx2b−/− mutants reveal the genetic signatures of intermuscular bone formation in zebrafish. National Science Review 9.
Nie, C.H., Zhang, N.A., Chen, Y.L., Chen, Z.X., Wang, G.Y., Li, Q., Gao, Z.X., 2021. A comparative genomic database of skeletogenesis genes: from fish to mammals. Comparative biochemistry and physiology. Part D, Genomics & proteomics 38, 100796.
Ninomiya, Y., Gordon, M., Van der, R.M., Schmid, T., Linsenmayer, T., Olsen, R.B., 1986. The developmentally regulated type X collagen gene contains a long open reading frame without introns. Journal of Biological Chemistry 261, 5041-5050.
Niu, P., Zhong, Z., Wang, M., Huang, G., Xu, S., Hou, Y., Yan, Y., Wang, H., 2017. Zinc finger transcription factor Sp7/Osterix acts on bone formation and regulates col10a1a expression in zebrafish. Sci Bull (Beijing) 62, 174-184.
Noden, D.M., 1991. Cell movements and control of patterned tissue assembly during craniofacial development. J Craniofac Genet Dev Biol 11, 192-213.
Nuesslein-Volhard, C.D., Ralf 2002. Zebrafish Practical Approach Series. Oxford University Press.
Oh, C.D., Lu, Y., Liang, S., Mori-Akiyama, Y., Chen, D., de Crombrugghe, B., Yasuda, H., 2014. SOX9 regulates multiple genes in chondrocytes, including genes encoding ECM proteins, ECM modification enzymes, receptors, and transporters. PLoS One 9, e107577.
Oh, J.H., Park, S.Y., de Crombrugghe, B., Kim, J.E., 2012. Chondrocyte-specific ablation of Osterix leads to impaired endochondral ossification. Biochem Biophys Res Commun 418, 634-640.
Oh, S.K., Shin, J.O., Baek, J.I., Lee, J., Bae, J.W., Ankamerddy, H., Kim, M.J., Huh, T.L., Ryoo, Z.Y., Kim, U.K., Bok, J., Lee, K.Y., 2015. Pannexin 3 is required for normal progression of skeletal development in vertebrates. FASEB J 29, 4473-4484.
Ohba, S., 2016. Hedgehog Signaling in Endochondral Ossification. J Dev Biol 4.
Ohba, S., 2020. Hedgehog Signaling in Skeletal Development: Roles of Indian Hedgehog and the Mode of Its Action. Int J Mol Sci 21.
Ohbayashi, N., Shibayama, M., Kurotaki, Y., Imanishi, M., Fujimori, T., Itoh, N., Takada, S., 2002. FGF18 is required for normal cell proliferation and differentiation during osteogenesis and chondrogenesis. Genes Dev 16, 870-879.
Ohlebusch, B., Borst, A., Frankenbach, T., Klopocki, E., Jakob, F., Liedtke, D., Graser, S., 2020. Investigation of alpl expression and Tnap-activity in zebrafish implies conserved functions during skeletal and neuronal development. Sci Rep 10, 13321.
Olczyk, P., Mencner, Ł., Komosinska-Vassev, K., 2014. The role of the extracellular matrix components in cutaneous wound healing. Biomed Res Int 2014, 747584.
Olsen, B.R., 1995. Mutations in collagen genes resulting in metaphyseal and epiphyseal dysplasias. Bone 17, 45S-49S.
Opperman, L.A., 2000. Cranial sutures as intramembranous bone growth sites. Dev Dyn 219, 472-485.
Ornitz, D.M., Marie, P.J., 2015. Fibroblast growth factor signaling in skeletal development and disease. Genes Dev 29, 1463-1486.
Otto, F., Thornell, A.P., Crompton, T., Denzel, A., Gilmour, K.C., Rosewell, I.R., Stamp, G.W., Beddington, R.S., Mundlos, S., Olsen, B.R., Selby, P.B., Owen, M.J., 1997. Cbfa1, a candidate gene for cleidocranial dysplasia syndrome, is essential for osteoblast differentiation and bone development. Cell 89, 765-771.
Paiva, K.B.S., Granjeiro, J.M., 2017. Matrix Metalloproteinases in Bone Resorption, Remodeling, and Repair. Prog Mol Biol Transl Sci 148, 203-303.
Pal, C.P., Singh, P., Chaturvedi, S., Pruthi, K.K., Vij, A., 2016. Epidemiology of knee osteoarthritis in India and related factors. Indian J Orthop 50, 518-522.

Papke, C.L., Yanagisawa, H., 2014. Fibulin-4 and fibulin-5 in elastogenesis and beyond: Insights from mouse and human studies. Matrix Biol 37, 142-149.
Parvizi, J., Kim K., G., 2010. Chapter 39 - Cartilage in High Yield Orthopaedics. High Yield Orthopaedics, 80-81.
Patra, C., Diehl, F., Ferrazzi, F., van Amerongen, M.J., Novoyatleva, T., Schaefer, L., Mühlfeld, C., Jungblut, B., Engel, F.B., 2011. Nephronectin regulates atrioventricular canal differentiation via Bmp4-Has2 signaling in zebrafish. Development 138, 4499-4509.
Paudel, S., Gjorcheska, S., Bump, P., Barske, L., 2022. Patterning of cartilaginous condensations in the developing facial skeleton. Dev Biol.
Pazzaglia, U.E., Reguzzoni, M., Casati, L., Minini, A., Salvi, A.G., Sibilia, V., 2019. Long bone human anlage longitudinal and circumferential growth in the fetal period and comparison with the growth plate cartilage of the postnatal age. Microsc Res Tech 82, 190-198.
Phimphilai, M., Zhao, Z., Boules, H., Roca, H., Franceschi, R.T., 2006. BMP signaling is required for RUNX2-dependent induction of the osteoblast phenotype. J Bone Miner Res 21, 637-646.
Pineault, K.M., Wellik, D.M., 2014. Hox genes and limb musculoskeletal development. Curr Osteoporos Rep 12, 420-427.
Pinto, J.P., Conceição, N.M., Viegas, C.S., Leite, R.B., Hurst, L.D., Kelsh, R.N., Cancela, M.L., 2005. Identification of a new pebp2alphaA2 isoform from zebrafish runx2 capable of inducing osteocalcin gene expression in vitro. J Bone Miner Res 20, 1440-1453.
Pirraco, R.P., Marques, A.P., Reis, R.L., 2010. Cell interactions in bone tissue engineering. J Cell Mol Med 14, 93-102.
Pogoda, H.M., Riedl-Quinkertz, I., Lohr, H., Waxman, J.S., Dale, R.M., Topczewski, J., Schulte-Merker, S., Hammerschmidt, M., 2018a. Direct activation of chordoblasts by retinoic acid is required for segmented centra mineralization during zebrafish spine development. Development 145.
Pogoda, H.M., Riedl-Quinkertz, I., Löhr, H., Waxman, J.S., Dale, R.M., Topczewski, J., Schulte-Merker, S., Hammerschmidt, M., 2018b. Direct activation of chordoblasts by retinoic acid is required for segmented centra mineralization during zebrafish spine development. Development 145.
Prince, V.E., Joly, L., Ekker, M., Ho, R.K., 1998. Zebrafish hox genes: genomic organization and modified colinear expression patterns in the trunk. Development 125, 407-420.
Provot, S., Schipani, E., Wu Y., J., Kronenberg, H., 2013. Chapter 6 - Development of the Skeleton. Osteoporosis (Fourth Edition), Eds: Academic Press.
Purushothaman, R., Cox, T.C., Maga, A.M., Cunningham, M.L., 2011. Facial suture synostosis of newborn Fgfr1(P250R/+) and Fgfr2(S252W/+) mouse models of Pfeiffer and Apert syndromes. Birth Defects Res A Clin Mol Teratol 91, 603-609.
Qi, H., Aguiar, D.J., Williams, S.M., La Pean, A., Pan, W., Verfaillie, C.M., 2003. Identification of genes responsible for osteoblast differentiation from human mesodermal progenitor cells. Proc Natl Acad Sci U S A 100, 3305-3310.
Quiroz, Y., Lopez, M., Mavropoulos, A., Motte, P., Martial, J.A., Hammerschmidt, M., Muller, M., 2012. The HMG-Box Transcription Factor Sox4b Is Required for Pituitary Expression of gata2a and Specification of Thyrotrope and Gonadotrope Cells in Zebrafish. Mol Endocrinol 26, 1014-1027.
Rakar, J., Lonnqvist, S., Sommar, P., Junker, J., Kratz, G., 2012. Interpreted gene expression of human dermal fibroblasts after adipo-, chondro- and osteogenic phenotype shifts. Differentiation 84, 305-313.

Raterman, S.T., Metz, J.R., Wagener, F.A.D.T., Von den Hoff, J.W., 2020. Zebrafish Models of Craniofacial Malformations: Interactions of Environmental Factors. Front Cell Dev Biol 8, 600926.
Rawlinson, S.C., McKay, I.J., Ghuman, M., Wellmann, C., Ryan, P., Prajaneh, S., Zaman, G., Hughes, F.J., Kingsmill, V.J., 2009. Adult rat bones maintain distinct regionalized expression of markers associated with their development. PLoS One 4, e8358.
Reinhold, M.I., Naski, M.C., 2007. Direct interactions of Runx2 and canonical Wnt signaling induce FGF18. J Biol Chem 282, 3653-3663.
Remst, D.F., Blaney Davidson, E.N., van der Kraan, P.M., 2015. Unravelling osteoarthritis-related synovial fibrosis: a step closer to solving joint stiffness. Rheumatology (Oxford) 54, 1954-1963.
Rendenbach, C., Yorgan, T.A., Heckt, T., Otto, B., Baldauf, C., Jeschke, A., Streichert, T., David, J.P., Amling, M., Schinke, T., 2014. Effects of extracellular phosphate on gene expression in murine osteoblasts. Calcif Tissue Int 94, 474-483.
Renn, J., Buttner, A., To, T.T., Chan, S.J., Winkler, C., 2013. A col10a1:nlGFP transgenic line displays putative osteoblast precursors at the medaka notochordal sheath prior to mineralization. Dev Biol 381, 134-143.
Renn, J., Winkler, C., 2014. Osterix/Sp7 regulates biomineralization of otoliths and bone in medaka (Oryzias latipes). Matrix Biol 34, 193-204.
Renn, J.a.P.B.a.M.M., 2014. Detection of nitric oxide by diaminofluorescein visualizes the skeleton in living zebrafish. Journal of applied ichthyology = Zeitschrift für angewandte Ichthyology. , lccn = 00242411 30 ,.
Ricard-Blum, S., 2011. The collagen family. Cold Spring Harb Perspect Biol 3, a004978.
Rice, D.P., Aberg, T., Chan, Y., Tang, Z., Kettunen, P.J., Pakarinen, L., Maxson, R.E., Thesleff, I., 2000. Integration of FGF and TWIST in calvarial bone and suture development. Development 127, 1845-1855.
Rice, D.P., Rice, R., 2008. Locate, condense, differentiate, grow and confront: developmental mechanisms controlling intramembranous bone and suture formation and function. Front Oral Biol 12, 22-40.
Richmond, C.M., Savarirayan, R., Adam, M.P., Mirzaa, G.M., Pagon, R.A., Wallace, S.E., Bean, L.J.H., Gripp, K.W., Amemiya, A., et al., 1993. GeneReviews. GeneReviews.
Riddle, R.D., Johnson, R.L., Laufer, E., Tabin, C., 1993. Sonic hedgehog mediates the polarizing activity of the ZPA. Cell 75, 1401-1416.
Rigoglou, S., Papavassiliou, A.G., 2013. The NF-κB signalling pathway in osteoarthritis. Int J Biochem Cell Biol 45, 2580-2584.
Roark, E.F., Keene, D.R., Haudenschild, C.C., Godyna, S., Little, C.D., Argraves, W.S., 1995. The association of human fibulin-1 with elastic fibers: an immunohistological, ultrastructural, and RNA study. J Histochem Cytochem 43, 401-411.
Rodda, S.J., McMahon, A.P., 2006. Distinct roles for Hedgehog and canonical Wnt signaling in specification, differentiation and maintenance of osteoblast progenitors. Development 133, 3231-3244.
Roehl, H., Nüsslein-Volhard, C., 2001. Zebrafish pea3 and erm are general targets of FGF8 signaling. Curr Biol 11, 503-507.
Runhaar, J., Sanchez, C., Taralla, S., Henrotin, Y., Bierma-Zeinstra, S.M.A., 2016. Fibulin-3 fragments are prognostic biomarkers of osteoarthritis incidence in overweight and obese women. Osteoarthritis and Cartilage 24, 672-678.
Russell, M.W., Raeker, M.O., Geisler, S.B., Thomas, P.E., Simmons, T.A., Bernat, J.A., Thorsson, T., Innis, J.W., 2014. Functional analysis of candidate genes in 2q13 deletion syndrome implicates FBLN7 and TMEM87B deficiency in congenital heart defects and FBLN7 in craniofacial malformations. Hum Mol Genet 23, 4272-4284.

Rutkovskiy, A., Stenslokken, K.O., Vaage, I.J., 2016. Osteoblast Differentiation at a Glance. Med Sci Monit Basic Res 22, 95-106.
Sahebjam, S., Khokha, R., Mort, J.S., 2007. Increased collagen and aggrecan degradation with age in the joints of Timp3(-/-) mice. Arthritis Rheum 56, 905-909.
Saito, T., Fukai, A., Mabuchi, A., Ikeda, T., Yano, F., Ohba, S., Nishida, N., Akune, T., Yoshimura, N., Nakagawa, T., Nakamura, K., Tokunaga, K., Chung, U.I., Kawaguchi, H., 2010. Transcriptional regulation of endochondral ossification by HIF-2alpha during skeletal growth and osteoarthritis development. Nat Med 16, 678-686.
Salazar, V.S., Gamer, L.W., Rosen, V., 2016. BMP signalling in skeletal development, disease and repair. Nat Rev Endocrinol 12, 203-221.
Sanchez, C., Mazzucchelli, G., Lambert, C., Comblain, F., DePauw, E., Henrotin, Y., 2018. Comparison of secretome from osteoblasts derived from sclerotic versus non-sclerotic subchondral bone in OA: A pilot study. PLoS One 13, e0194591.
Sanford, L.P., Ormsby, I., Gittenberger-de Groot, A.C., Sariola, H., Friedman, R., Boivin, G.P., Cardell, E.L., Doetschman, T., 1997. TGFbeta2 knockout mice have multiple developmental defects that are non-overlapping with other TGFbeta knockout phenotypes. Development 124, 2659-2670.
Sanvitale, C.E., Kerr, G., Chaikuad, A., Ramel, M.C., Mohedas, A.H., Reichert, S., Wang, Y., Triffitt, J.T., Cuny, G.D., Yu, P.B., Hill, C.S., Bullock, A.N., 2013. A new class of small molecule inhibitor of BMP signaling. PLoS One 8, e62721.
Sarzi-Puttini, P., Atzeni, F., Fumagalli, M., Capsoni, F., Carrabba, M., 2005. Osteoarthritis of the spine. Semin Arthritis Rheum 34, 38-43.
Schepper, J.D., Irwin, R., Kang, J., Dagenais, K., Lemon, T., Shinouskis, A., Parameswaran, N., McCabe, L.R., 2017. Probiotics in Gut-Bone Signaling. Adv Exp Med Biol 1033, 225-247.
Schilling, T.F., Kimmel, C.B., 1994. Segment and cell type lineage restrictions during pharyngeal arch development in the zebrafish embryo. Development 120, 483-494.
Schilling, T.F., Kimmel, C.B., 1997. Musculoskeletal patterning in the pharyngeal segments of the zebrafish embryo. Development 124, 2945-2960.
Schilling, T.F., Piotrowski, T., Grandel, H., Brand, M., Heisenberg, C.P., Jiang, Y.J., Beuchle, D., Hammerschmidt, M., Kane, D.A., Mullins, M.C., van Eeden, F.J., Kelsh, R.N., Furutani-Seiki, M., Granato, M., Haffter, P., Odenthal, J., Warga, R.M., Trowe, T., Nüsslein-Volhard, C., 1996a. Jaw and branchial arch mutants in zebrafish I: branchial arches. Development 123, 329-344.
Schilling, T.F., Walker, C., Kimmel, C.B., 1996b. The chinless mutation and neural crest cell interactions in zebrafish jaw development. Development 122, 1417-1426.
Schlesinger, P.H., Blair, H.C., Beer Stolz, D., Riazanski, V., Ray, E.C., Tourkova, I.L., Nelson, D.J., 2020. Cellular and extracellular matrix of bone, with principles of synthesis and dependency of mineral deposition on cell membrane transport. Am J Physiol Cell Physiol 318, C111-C124.
Schmid, T.M., Linsenmayer, T.F., 1990. Immunoelectron microscopy of type X collagen: supramolecular forms within embryonic chick cartilage. Dev Biol 138, 53-62.
Seeman, E., 2008. Bone quality: the material and structural basis of bone strength. J Bone Miner Metab 26, 1-8.
Sehring, I., Mohammadi, H.F., Haffner-Luntzer, M., Ignatius, A., Huber-Lang, M., Weidinger, G., 2022. Zebrafish fin regeneration involves generic and regeneration-specific osteoblast injury responses. Elife 11.
Setiawati, R., Rahardjo, P., 2008. Bone Development and Growth in Osteogenesis and Bone Regeneration, in: H, Y. (Ed.). IntechOpen.

Sharif, F., de Bakker, M.A., Richardson, M.K., 2014. Osteoclast-like Cells in Early Zebrafish Embryos. Cell J 16, 211-224.
Shen, G., 2005. The role of type X collagen in facilitating and regulating endochondral ossification of articular cartilage. Orthod Craniofac Res 8, 11-17.
Shibata, S., Fukada, K., Suzuki, S., Yamashita, Y., 1997. Immunohistochemistry of collagen types II and X, and enzyme-histochemistry of alkaline phosphatase in the developing condylar cartilage of the fetal mouse mandible. J Anat 191 ( Pt 4), 561-570.
Shibata, S., Yokohama-Tamaki, T., 2008. An in situ hybridization study of Runx2, Osterix, and Sox9 in the anlagen of mouse mandibular condylar cartilage in the early stages of embryogenesis. J Anat 213, 274-283.
Simões, B., Conceição, N., Viegas, C.S.B., Pinto, J.P., Gavaia, P.J., Hurst, L.D., Kelsh, R.N., Cancela, M.L., 2006. Identification of a Promoter Element within the Zebrafish colXα1 Gene Responsive to Runx2 Isoforms Osf2/Cbfa1 and til-1 but not to pebp2αA2. Calcified Tissue International 79, 230-244.
Singh, U., Sun, T., Larsson, T., Elliott, R.W., Kostka, G., Fundele, R.H., 2006. Expression and functional analysis of fibulin-1 (Fbln1) during normal and abnormal placental development of the mouse. Placenta 27, 1014-1021.
Siomava, N., Diogo, R., 2018. Comparative anatomy of zebrafish paired and median fin muscles: basis for functional, developmental, and macroevolutionary studies. J Anat 232, 186-199.
Sjögren, K., Engdahl, C., Henning, P., Lerner, U.H., Tremaroli, V., Lagerquist, M.K., Bäckhed, F., Ohlsson, C., 2012. The gut microbiota regulates bone mass in mice. J Bone Miner Res 27, 1357-1367.
Smeeton, J., Askary, A., Crump, J.G., 2017. Building and maintaining joints by exquisite local control of cell fate. Wiley Interdiscip Rev Dev Biol 6.
Smith, A., Avaron, F., Guay, D., Padhi, B.K., Akimenko, M.A., 2006. Inhibition of BMP signaling during zebrafish fin regeneration disrupts fin growth and scleroblasts differentiation and function. Dev Biol 299, 438-454.
Sojan, J.M., Raman, R., Muller, M., Carnevali, O., Renn, J., 2022. Probiotics Enhance Bone Growth and Rescue BMP Inhibition: New Transgenic Zebrafish Lines to Study Bone Health. International journal of molecular sciences 23.
Song, H.D., Sun, X.J., Deng, M., Zhang, G.W., Zhou, Y., Wu, X.Y., Sheng, Y., Chen, Y., Ruan, Z., Jiang, C.L., Fan, H.Y., Zon, L.I., Kanki, J.P., Liu, T.X., Look, A.T., Chen, Z., 2004. Hematopoietic gene expression profile in zebrafish kidney marrow. Proc Natl Acad Sci U S A 101, 16240-16245.
Sousa, S., Afonso, N., Bensimon-Brito, A., Fonseca, M., Simões, M., Leon, J., Roehl, H., Cancela, M.L., Jacinto, A., 2011. Differentiated skeletal cells contribute to blastema formation during zebrafish fin regeneration. Development 138, 3897-3905.
Spence, S.G., Argraves, W.S., Walters, L., Hungerford, J.E., Little, C.D., 1992. Fibulin is localized at sites of epithelial-mesenchymal transitions in the early avian embryo. Dev Biol 151, 473-484.
Spoorendonk, K.M., Peterson-Maduro, J., Renn, J., Trowe, T., Kranenbarg, S., Winkler, C., Schulte-Merker, S., 2008. Retinoic acid and Cyp26b1 are critical regulators of osteogenesis in the axial skeleton. Development 135, 3765-3774.
Staal, Y.C.M., Meijer, J., van der Kris, R.J.C., de Bruijn, A.C., Boersma, A.Y., Gremmer, E.R., Zwart, E.P., Beekhof, P.K., Slob, W., van der Ven, L.T.M., 2018. Head skeleton malformations in zebrafish (Danio rerio) to assess adverse effects of mixtures of compounds. Archives of toxicology 92, 3549-3564.

Stewart, A.J., Roberts, S.J., Seawright, E., Davey, M.G., Fleming, R.H., Farquharson, C., 2006. The presence of PHOSPHO1 in matrix vesicles and its developmental expression prior to skeletal mineralization. Bone 39, 1000-1007.
Stewart, C., 2021. Incidence of osteoarthritis in Europe in 2019, by joint and gender (per 100,000 population). Statista Inc.
Stewart, S., Stankunas, K., 2012. Limited dedifferentiation provides replacement tissue during zebrafish fin regeneration. Dev Biol 365, 339-349.
Stickney, H.L., Barresi, M.J., Devoto, S.H., 2000. Somite development in zebrafish. Dev Dyn 219, 287-303.
Suniaga, S., Rolvien, T., Vom Scheidt, A., Fiedler, I.A.K., Bale, H.A., Huysseune, A., Witten, P.E., Amling, M., Busse, B., 2018. Increased mechanical loading through controlled swimming exercise induces bone formation and mineralization in adult zebrafish. Sci Rep 8, 3646.
Swaim, L.E., Connolly, L.E., Volkman, H.E., Humbert, O., Born, D.E., Ramakrishnan, L., 2006. Mycobacterium marinum infection of adult zebrafish causes caseating granulomatous tuberculosis and is moderated by adaptive immunity. Infect Immun 74, 6108-6117.
Swartz, M.E., Sheehan-Rooney, K., Dixon, M.J., Eberhart, J.K., 2011. Examination of a palatogenic gene program in zebrafish. Dev Dyn 240, 2204-2220.
Sztal, T.E., Stainier, D.Y.R., 2020. Transcriptional adaptation: a mechanism underlying genetic robustness. Development 147.
Taylor, J.S., Braasch, I., Frickey, T., Meyer, A., Van de Peer, Y., 2003. Genome duplication, a trait shared by 22000 species of ray-finned fish. Genome Res 13, 382-390.
Teven, C.M., Farina, E.M., Rivas, J., Reid, R.R., 2014. Fibroblast growth factor (FGF) signaling in development and skeletal diseases. Genes Dis 1, 199-213.
Thomas, J.T., Kwan, A.P.L., Grant, M.E., Boot-Handford, R.P., 1991. Isolation of cDNAs encoding the complete sequence of bovine type X collagen. Evidence for the condensed nature of mammalian type X collagen genes. Biochemical Journal 273, 141-148.
Thurner, P.J., Chen, C.G., Ionova-Martin, S., Sun, L., Harman, A., Porter, A., Ager, J.W., Ritchie, R.O., Alliston, T., 2010. Osteopontin deficiency increases bone fragility but preserves bone mass. Bone 46, 1564-1573.
Tian, Y., Wang, W., Lautrup, S., Zhao, H., Li, X., Law, P.W.N., Dinh, N.D., Fang, E.F., Cheung, H.H., Chan, W.Y., 2022. WRN promotes bone development and growth by unwinding SHOX-G-quadruplexes via its helicase activity in Werner Syndrome. Nat Commun 13, 5456.
Timpl, R., Sasaki, T., Kostka, G., Chu, M.L., 2003. Fibulins: a versatile family of extracellular matrix proteins. Nat Rev Mol Cell Biol 4, 479-489.
Tonelli, F., Bek, J.W., Besio, R., De Clercq, A., Leoni, L., Salmon, P., Coucke, P.J., Willaert, A., Forlino, A., 2020. Zebrafish: A Resourceful Vertebrate Model to Investigate Skeletal Disorders. Front Endocrinol (Lausanne) 11, 489.
Topczewska, J.M., Shoela, R.A., Tomaszewski, J.P., Mirmira, R.B., Gosain, A.K., 2016. The Morphogenesis of Cranial Sutures in Zebrafish. PLoS One 11, e0165775.
Troeberg, L., Nagase, H., 2012. Proteases involved in cartilage matrix degradation in osteoarthritis. Biochim Biophys Acta 1824, 133-145.
Tsumaki, N., Horiki, M., Murai, J., Yoshikawa, H., 2004. [Role of BMPs and Smads during endochondral bone formation]. Clin Calcium 14, 52-57.
Uchida, Y., Irie, K., Fukuhara, D., Kataoka, K., Hattori, T., Ono, M., Ekuni, D., Kubota, S., Morita, M., 2018. Commensal Microbiota Enhance Both Osteoclast and Osteoblast Activities. Molecules 23.

Uchino, M., Izumi, T., Tominaga, T., Wakita, R., Minehara, H., Sekiguchi, M., Itoman, M., 2000. Growth factor expression in the osteophytes of the human femoral head in osteoarthritis. Clin Orthop Relat Res, 119-125.
Ulsamer, A., Ortuño, M.J., Ruiz, S., Susperregui, A.R., Osses, N., Rosa, J.L., Ventura, F., 2008. BMP-2 induces Osterix expression through up-regulation of Dlx5 and its phosphorylation by p38. J Biol Chem 283, 3816-3826.
Umair, M., Ahmad, F., Bilal, M., Ahmad, W., Alfadhel, M., 2018. Clinical Genetics of Polydactyly: An Updated Review. Front Genet 9, 447.
Valenti, M.T., Marchetto, G., Mottes, M., Dalle Carbonare, L., 2020. Zebrafish: A Suitable Tool for the Study of Cell Signaling in Bone. Cells 9.
van Beuningen, H.M., Glansbeek, H.L., van der Kraan, P.M., van den Berg, W.B., 1998. Differential effects of local application of BMP-2 or TGF-beta 1 on both articular cartilage composition and osteophyte formation. Osteoarthritis Cartilage 6, 306-317.
van de Loo, F.A., Joosten, L.A., van Lent, P.L., Arntz, O.J., van den Berg, W.B., 1995. Role of interleukin-1, tumor necrosis factor alpha, and interleukin-6 in cartilage proteoglycan metabolism and destruction. Effect of in situ blocking in murine antigen- and zymosan-induced arthritis. Arthritis Rheum 38, 164-172.
van der Kraan, P.M., 2013. Relevance of zebrafish as an OA research model. Osteoarthritis Cartilage 21, 261-262.
van der Kraan, P.M., van den Berg, W.B., 2012. Chondrocyte hypertrophy and osteoarthritis: role in initiation and progression of cartilage degeneration? Osteoarthritis Cartilage 20, 223-232.
Vandewalle, P., Parmentier, E., Poulicek, M., Bussers, J.C., Chardon, M., 1998. Distinctive anatomical features of the branchial basket in four carapidae species (ophidiiformi, paracanthopterygii). Eur J Morphol 36, 153-164.
VanPutte, C., Regan, J., Russo, A., 2013. In: Seeley's Essentials of Anatomy & Physiology., Skeletal system: Bones and joints. , 8th ed. Mc Graw Hill, USA, pp. pp. 110-149.
Velleman, S.G., 2000. The role of the extracellular matrix in skeletal development. Poult Sci 79, 985-989.
Venkatesh, B., Lee, A.P., Ravi, V., Maurya, A.K., Lian, M.M., Swann, J.B., Ohta, Y., Flajnik, M.F., Sutoh, Y., Kasahara, M., Hoon, S., Gangu, V., Roy, S.W., Irimia, M., Korzh, V., Kondrychyn, I., Lim, Z.W., Tay, B.H., Tohari, S., Kong, K.W., Ho, S., Lorente-Galdos, B., Quilez, J., Marques-Bonet, T., Raney, B.J., Ingham, P.W., Tay, A., Hillier, L.W., Minx, P., Boehm, T., Wilson, R.K., Brenner, S., Warren, W.C., 2014. Elephant shark genome provides unique insights into gnathostome evolution. Nature 505, 174-179.
Verreijdt, L., Vandervennet, E., Sire, J.Y., Huysseune, A., 2002. Developmental differences between cranial bones in the zebrafish (Danio rerio): some preliminary light and TEM observations. Connect Tissue Res 43, 109-112.
Vimalraj, S., Yuvashree, R., Hariprabu, G., Subramanian, R., Murali, P., Veeraiyan, D.N., Thangavelu, L., 2021. Zebrafish as a potential biomaterial testing platform for bone tissue engineering application: A special note on chitosan based bioactive materials. Int J Biol Macromol 175, 379-395.
Visconti, R.P., Barth, J.L., Keeley, F.W., Little, C.D., 2003. Codistribution analysis of elastin and related fibrillar proteins in early vertebrate development. Matrix Biol 22, 109-121.
Vogel, B.E., Hedgecock, E.M., 2001. Hemicentin, a conserved extracellular member of the immunoglobulin superfamily, organizes epithelial and other cell attachments into oriented line-shaped junctions. Development 128, 883-894.
von der Mark, K., Frischholz, S., Aigner, T., Beier, F., Belke, J., Erdmann, S., Burkhardt, H., 1995. Upregulation of type X collagen expression in osteoarthritic cartilage. Acta Orthop Scand Suppl 266, 125-129.

Wada, N., Javidan, Y., Nelson, S., Carney, T.J., Kelsh, R.N., Schilling, T.F., 2005. Hedgehog signaling is required for cranial neural crest morphogenesis and chondrogenesis at the midline in the zebrafish skull. Development 132, 3977-3988.
Wakabayashi, T., Matsumine, A., Nakazora, S., Hasegawa, M., Iino, T., Ota, H., Sonoda, H., Sudo, A., Uchida, A., 2010. Fibulin-3 negatively regulates chondrocyte differentiation. Biochem Biophys Res Commun 391, 1116-1121.
Waldmann, L., Leyhr, J., Zhang, H., Öhman-Mägi, C., Allalou, A., Haitina, T., 2021. The broad role of Nkx3.2 in the development of the zebrafish axial skeleton. PLoS One 16, e0255953.
Walker, J.M., 1991. Musculoskeletal development: a review. Phys Ther 71, 878-889.
Walker, M.B., Kimmel, C.B., 2007. A two-color acid-free cartilage and bone stain for zebrafish larvae. Biotech Histochem 82, 23-28.
Wallace, I.J., Worthington, S., Felson, D.T., Jurmain, R.D., Wren, K.T., Maijanen, H., Woods, R.J., Lieberman, D.E., 2017. Knee osteoarthritis has doubled in prevalence since the mid-20th century. Proc Natl Acad Sci U S A 114, 9332-9336.
Wang, J.S., Kamath, T., Mazur, C.M., Mirzamohammadi, F., Rotter, D., Hojo, H., Castro, C.D., Tokavanich, N., Patel, R., Govea, N., Enishi, T., Wu, Y., da Silva Martins, J., Bruce, M., Brooks, D.J., Bouxsein, M.L., Tokarz, D., Lin, C.P., Abdul, A., Macosko, E.Z., Fiscaletti, M., Munns, C.F., Ryder, P., Kost-Alimova, M., Byrne, P., Cimini, B., Fujiwara, M., Kronenberg, H.M., Wein, M.N., 2021. Control of osteocyte dendrite formation by Sp7 and its target gene osteocrin. Nat Commun 12, 6271.
Wang, X., Manner, P.A., Horner, A., Shum, L., Tuan, R.S., Nuckolls, G.H., 2004. Regulation of MMP-13 expression by RUNX2 and FGF2 in osteoarthritic cartilage. Osteoarthritis Cartilage 12, 963-973.
Warman, M.L., Abbott, M., Apte, S.S., Hefferon, T., McIntosh, I., Cohn, D.H., Hecht, J.T., Olsen, B.R., Francomano, C.A., 1993. A type X collagen mutation causes Schmid metaphyseal chondrodysplasia. Nat Genet 5, 79-82.
Watson, C.J., Monstad-Rios, A.T., Bhimani, R.M., Gistelinck, C., Willaert, A., Coucke, P., Hsu, Y.H., Kwon, R.Y., 2020a. Phenomics-Based Quantification of CRISPR-Induced Mosaicism in Zebrafish. Cell Syst 10, 275-286.e275.
Watson, C.J., Monstad-Rios, A.T., Bhimani, R.M., Gistelinck, C., Willaert, A., Coucke, P., Hsu, Y.H., Kwon, R.Y., 2020b. Phenomics-Based Quantification of CRISPR-Induced Mosaicism in Zebrafish. Cell Syst 10, 275-286 e275.
Wattanachanya, L., Wang, L., Millard, S.M., Lu, W.-D., O'Carroll, D., Hsiao, E.C., Conklin, B.R., Nissenson, R.A., 2015. Assessing the osteoblast transcriptome in a model of enhanced bone formation due to constitutive Gs–G protein signaling in osteoblasts. Experimental Cell Research 333, 289-302.
Wehling, N., Palmer, G.D., Pilapil, C., Liu, F., Wells, J.W., Müller, P.E., Evans, C.H., Porter, R.M., 2009. Interleukin-1beta and tumor necrosis factor alpha inhibit chondrogenesis by human mesenchymal stem cells through NF-kappaB-dependent pathways. Arthritis Rheum 60, 801-812.
Wein, N.M., 2017. Parathyroid Hormone Signaling in Osteocytes. JBMR Plus 2, 22-30.
Weinberg, D.S., Liu, R.W., Xie, K.K., Morris, W.Z., Gebhart, J.J., Gordon, Z.L., 2017. Increased and decreased pelvic incidence, sagittal facet joint orientations are associated with lumbar spine osteoarthritis in a large cadaveric collection. Int Orthop 41, 1593-1600.
Westerfield, M., 2007. THE ZEBRAFISH BOOK, 5th Edition; A guide for the laboratory use of zebrafish (Danio rerio), Eugene, University of Oregon Press.
White, H.E., Goswami, A., Tucker, A.S., 2021. The Intertwined Evolution and Development of Sutures and Cranial Morphology. Front Cell Dev Biol 9, 653579.
Whyte, M.P., 2017. Hypophosphatasia: An overview For 2017. Bone 102, 15-25.

Wight, T.N., Potter-Perigo, S., 2011. The extracellular matrix: an active or passive player in fibrosis? Am J Physiol Gastrointest Liver Physiol 301, G950-955.
Wilkie, A.O., 1997. Craniosynostosis: genes and mechanisms. Hum Mol Genet 6, 1647-1656.
Williams, R.G., 2013. Thyroid hormone actions in cartilage and bone. Eur Thyroid J 2, 3-13.
Williams, S., Alkhatib, B., Serra, R., 2019. Development of the axial skeleton and intervertebral disc. Curr Top Dev Biol 133, 49-90.
Windhausen, T., Squifflet, S., Renn, J., Muller, M., 2015. BMP Signaling Regulates Bone Morphogenesis in Zebrafish through Promoting Osteoblast Function as Assessed by Their Nitric Oxide Production. Molecules 20, 7586-7601.
Witten, P.E., Hansen, A., Hall, B.K., 2001. Features of mono- and multinucleated bone resorbing cells of the zebrafish Danio rerio and their contribution to skeletal development, remodeling, and growth. J Morphol 250, 197-207.
Witten, P.E., Harris, M.P., Huysseune, A., Winkler, C., 2017. Small teleost fish provide new insights into human skeletal diseases. Methods Cell Biol 138, 321-346.
Witten, P.E., Huysseune, A., 2009. A comparative view on mechanisms and functions of skeletal remodelling in teleost fish, with special emphasis on osteoclasts and their function. Biol Rev Camb Philos Soc 84, 315-346.
Wojtas, M., Lausch, A.J., Sone, E.D., 2020. Glycosaminoglycans accelerate biomimetic collagen mineralization in a tissue-based in vitro model. Proc Natl Acad Sci U S A 117, 12636-12642.
Wopat, S., Bagwell, J., Sumigray, K.D., Dickson, A.L., Huitema, L.F.A., Poss, K.D., Schulte-Merker, S., Bagnat, M., 2018. Spine Patterning Is Guided by Segmentation of the Notochord Sheath. Cell Rep 22, 2026-2038.
Wu, H., Wang, S., Li, G., Yao, Y., Wang, N., Sun, X., Fang, L., Jiang, X., Zhao, J., Wang, Y., Xu, C., 2021. Characterization of a novel COL10A1 variant associated with Schmid-type metaphyseal chondrodysplasia and a literature review. Mol Genet Genomic Med 9, e1668.
Wu, J.J., Lark, M.W., Chun, L.E., Eyre, D.R., 1991. Sites of stromelysin cleavage in collagen types II, IX, X, and XI of cartilage. J Biol Chem 266, 5625-5628.
Wu, L.A., Wang, F., Donly, K.J., Baker, A., Wan, C., Luo, D., MacDougall, M., Chen, S., 2016a. Establishment of Immortalized BMP2/4 Double Knock-Out Osteoblastic Cells Is Essential for Study of Osteoblast Growth, Differentiation, and Osteogenesis. J Cell Physiol 231, 1189-1198.
Wu, M., Chen, G., Li, Y.P., 2016b. TGF-β and BMP signaling in osteoblast, skeletal development, and bone formation, homeostasis and disease. Bone Res 4, 16009.
Xie, Y., Zhou, S., Chen, H., Du, X., Chen, L., 2014. Recent research on the growth plate: Advances in fibroblast growth factor signaling in growth plate development and disorders. J Mol Endocrinol 53, T11-34.
Xu, G., Cui, Y., Wang, L., Zhang, J., Shen, A., Li, W., Bao, G., Sun, Y., Cui, Z., 2015. Temporospatial expression of fibulin-1 after acute spinal cord injury in rats. J Spinal Cord Med 38, 709-716.
Yadav, M.C., Simão, A.M., Narisawa, S., Huesa, C., McKee, M.D., Farquharson, C., Millán, J.L., 2011. Loss of skeletal mineralization by the simultaneous ablation of PHOSPHO1 and alkaline phosphatase function: a unified model of the mechanisms of initiation of skeletal calcification. J Bone Miner Res 26, 286-297.
Yagami, K., Suh, J.Y., Enomoto-Iwamoto, M., Koyama, E., Abrams, W.R., Shapiro, I.M., Pacifici, M., Iwamoto, M., 1999. Matrix GLA protein is a developmental regulator of chondrocyte mineralization and, when constitutively expressed, blocks endochondral and intramembranous ossification in the limb. J Cell Biol 147, 1097-1108.

Yagi, K., Tsuji, K., Nifuji, A., Shinomiya, K., Nakashima, K., DeCrombrugghe, B., Noda, M., 2003. Bone morphogenetic protein-2 enhances osterix gene expression in chondrocytes. J Cell Biochem 88, 1077-1083.
Yan, J., Herzog, J.W., Tsang, K., Brennan, C.A., Bower, M.A., Garrett, W.S., Sartor, B.R., Aliprantis, A.O., Charles, J.F., 2016. Gut microbiota induce IGF-1 and promote bone formation and growth. Proc Natl Acad Sci U S A 113, E7554-E7563.
Yan, Y., Wang, Q., 2021. BMP Signaling: Lighting up the Way for Embryonic Dorsoventral Patterning. Front Cell Dev Biol 9, 799772.
Yang, Y., 2012. Wnt signaling in development and disease. Cell Biosci 2, 14.
Yang, Y., Topol, L., Lee, H., Wu, J., 2003. Wnt5a and Wnt5b exhibit distinct activities in coordinating chondrocyte proliferation and differentiation. Development 130, 1003-1015.
Yelick, P.C., Schilling, T.F., 2002. Molecular dissection of craniofacial development using zebrafish. Crit Rev Oral Biol Med 13, 308-322.
Yoshida, C.A., Komori, H., Maruyama, Z., Miyazaki, T., Kawasaki, K., Furuichi, T., Fukuyama, R., Mori, M., Yamana, K., Nakamura, K., Liu, W., Toyosawa, S., Moriishi, T., Kawaguchi, H., Takada, K., Komori, T., 2012. SP7 inhibits osteoblast differentiation at a late stage in mice. PLoS One 7, e32364.
Yu, P.B., Hong, C.C., Sachidanandan, C., Babitt, J.L., Deng, D.Y., Hoyng, S.A., Lin, H.Y., Bloch, K.D., Peterson, R.T., 2008. Dorsomorphin inhibits BMP signals required for embryogenesis and iron metabolism. Nat Chem Biol 4, 33-41.
Yu, T., Graf, M., Renn, J., Schartl, M., Larionova, D., Huysseune, A., Witten, P.E., Winkler, C., 2017. A vertebrate-specific and essential role for osterix in osteogenesis revealed by gene knockout in the teleost medaka. Development 144, 265-271.
Yuan, X.L., Meng, H.Y., Wang, Y.C., Peng, J., Guo, Q.Y., Wang, A.Y., Lu, S.B., 2014. Bone-cartilage interface crosstalk in osteoarthritis: potential pathways and future therapeutic strategies. Osteoarthritis Cartilage 22, 1077-1089.
Yue, B., 2014. Biology of the extracellular matrix: an overview. J Glaucoma 23, S20-23.
Zaitune, C.R., Fonseca, T.L., Capelo, L.P., Freitas, F.R., Beber, E.H., Dora, J.M., Wang, C.C., Miranda-Rodrigues, M., Nonaka, K.O., Maia, A.L., Gouveia, C.H.A., 2019. Abnormal Thyroid Hormone Status Differentially Affects Bone Mass Accrual and Bone Strength in C3H/HeJ Mice: A Mouse Model of Type I Deiodinase Deficiency. Front Endocrinol (Lausanne) 10, 300.
Zappia, J., Tong, Q., Van der Cruyssen, R., Cornelis, F.M.F., Lambert, C., Pinto Coelho, T., Grisart, J., Kague, E., Lories, R.J., Muller, M., Elewaut, D., Hammond, C.L., Sanchez, C., Henrotin, Y., 2023. Osteomodulin downregulation is associated with osteoarthritis development. Bone Res 11, 49.
Zbasnik, N., Dolan, K., Buczkowski, S.A., Green, R.M., Hallgrímsson, B., Marcucio, R.S., Moon, A.M., Fish, J.L., 2022. Fgf8 dosage regulates jaw shape and symmetry through pharyngeal-cardiac tissue relationships. Dev Dyn 251, 1711-1727.
Zhang, D., Han, S., Pan, X., Li, H., Zhao, H., Gao, X., Wang, S., 2022. EFEMP1 binds to STEAP1 to promote osteosarcoma proliferation and invasion via the Wnt/β-catenin and TGF-β/Smad2/3 signal pathways. J Bone Oncol 37, 100458.
Zhang, H.Y., Timpl, R., Sasaki, T., Chu, M.L., Ekblom, P., 1996. Fibulin-1 and fibulin-2 expression during organogenesis in the developing mouse embryo. Dev Dyn 205, 348-364.
Zhang, R., Edwards, J.R., Ko, S.Y., Dong, S., Liu, H., Oyajobi, B.O., Papasian, C., Deng, H.W., Zhao, M., 2011. Transcriptional regulation of BMP2 expression by the PTH-CREB signaling pathway in osteoblasts. PLoS One 6, e20780.
Zhang, X., Duan, L., Zhang, Y., Zhao, H., Yang, X., Zhang, C., 2020. Correlation of Fibulin-2 expression with proliferation, migration and invasion of breast cancer cells. Oncol Lett 20, 1945-1951.

Zhang, Y., Ahmadpoor, X., Lin, H., 2023. Roles of Local Soluble Factors in Maintaining the Growth Plate: An Update. Genes (Basel) 14.
Zhang, Y., Marmorstein, L.Y., 2010. Focus on molecules: fibulin-3 (EFEMP1). Exp Eye Res 90, 374-375.
Zhao, H.J., Chang, H.M., Klausen, C., Zhu, H., Li, Y., Leung, P.C.K., 2020. Bone morphogenetic protein 2 induces the activation of WNT/β-catenin signaling and human trophoblast invasion through up-regulating BAMBI. Cell Signal 67, 109489.
Zheng, Q., Sebald, E., Zhou, G., Chen, Y., Wilcox, W., Lee, B., Krakow, D., 2005. Dysregulation of chondrogenesis in human cleidocranial dysplasia. Am J Hum Genet 77, 305-312.
Zheng, Q., Zhou, G., Morello, R., Chen, Y., Garcia-Rojas, X., Lee, B., 2003. Type X collagen gene regulation by Runx2 contributes directly to its hypertrophic chondrocyte-specific expression in vivo. J Cell Biol 162, 833-842.
Zhou, X., Cao, H., Yuan, Y., Wu, W., 2020. Biochemical Signals Mediate the Crosstalk between Cartilage and Bone in Osteoarthritis. Biomed Res Int 2020, 5720360.
Zhou, X., Zhang, Z., Feng, J.Q., Dusevich, V.M., Sinha, K., Zhang, H., Darnay, B.G., de Crombrugghe, B., 2010. Multiple functions of Osterix are required for bone growth and homeostasis in postnatal mice. Proc Natl Acad Sci U S A 107, 12919-12924.
Zong, Z., Tees, S., Miyanji, F., Fauth, C., Reilly, C., Lopez, E., Tredwell, S., Paul Goldberg, Y., Delaney, A., Eydoux, P., Van Allen, M., Lehman, A., 2015. BMPER variants associated with a novel, attenuated subtype of diaphanospondylodysostosis. J Hum Genet 60, 743-747.
Zou, L., Zou, X., Li, H., Mygind, T., Zeng, Y., Lü, N., Bünger, C., 2006. Molecular mechanism of osteochondroprogenitor fate determination during bone formation. Adv Exp Med Biol 585, 431-441.

## Summary

**Osteoblast differentiation has been studied using a variety of systems, ranging from osteosarcoma cell lines to differentiating mesenchymal stem cells to KO mice, resulting in the description of a set of transcription factors and regulatory pathways that are involved in this process. Small teleost model systems like zebrafish are increasingly used to study vertebrate skeletal development and zebrafish mutants and transgenic lines are very useful models for studying human pathologies such as osteoporosis, osteopetrosis and osteoarthritis.**

**Understanding osteoblast differentiation and their function in bone matrix deposition and mineralization is central to the comprehension of bone development and of various bone pathologies. It is, therefore, crucial to not only follow the expression of some landmark transcription factors or extracellular matrix (ECM) proteins, but to also investigate the status of signalling pathways and factors regulating these processes. This can only be achieved by assessing the entire transcriptome of these cells. Zebrafish larvae offer the unique opportunity to directly access osteoblasts from the entire body without specific dissection. The aims are to study the osteoblast transcriptome of developing zebrafish and to investigate the role of the *efemp1*, *fbln1*, and *col10a1a* genes, coding for ECM proteins, in zebrafish skeletal development.**

**To gain insights into the mechanisms of osteoblast differentiation in the early development stage, we isolated cells from the transgenic reporter line *Tg(sp7:sp7-GFP)* at 4 days post-fertilization. Based on their differential GFP fluorescence, we identified two subpopulations of which we conducted transcriptomic profiling. Our data revealed that these two subpopulations are clearly distinct and that they differentially express many genes involved in skeletal development. The expression profile of these two populations clearly identifies them as osteoblastic cells, at present we consider the low fluorescence P1 population as pre-osteoblastic cells and the highly fluorescent P2 population as intermediate, functional osteoblasts.**

**ECM proteins are of crucial importance for cartilage and bone tissues. Based on their differential expression profile in these subpopulations, we generated mutants of the ECM protein coding genes *col10a1a, fbln1* and *efemp1* to examine their functions. Our results show that mutation of *col10a1a* results in decreased mineralization, while mutation of *fbln1* results in increased mineralization and a missing operculum. Mutation of *efemp1* results in increased mineralization and reduced intervertebral space, providing a model for spinal osteoarthritis. Furthermore, we investigated the effects of two probiotics on bone matrix synthesis and mineralization. We discovered that probiotic treatment is able to promote bone formation and to prevent the effects of inhibiting BMP signalling, with *Bacillus subtilis* being the more potent.**

**Collectively, these insights provide valuable cues that may contribute to improve understanding the roles of ECM proteins and probiotics in development, growth, and health of the bone skeleton.**